

**STRATEGIES AND FUNCTIONAL CONSEQUENCES OF INHIBITING
PROTEIN-PROTEIN INTERACTIONS**

by

Laura Catherine Cesa

A dissertation submitted in partial fulfillment
of the requirements for the degree of
Doctor of Philosophy
(Chemical Biology)
in the University of Michigan
2016

Doctoral Committee:

Associate Professor Jason E. Gestwicki, Co-Chair
Professor Anna K. Mapp, Co-Chair
Assistant Professor Brent R. Martin
Assistant Professor Daniel R. Southworth
Professor John J. G. Tesmer

© Laura Catherine Cesa 2016

Dedication

To my parents

Acknowledgments

First and foremost, I need to thank my advisors, Professors Jason Gestwicki and Anna Mapp. My path to a PhD has not been linear, traditional, or easy, and I am forever indebted to these two fantastic scientists and mentors for sharing their wisdom and expertise with me. Thank you to Jason for giving me the opportunity to work in your lab and being a “Skype-visor” from afar for the past three years. Not many advisors would have accommodated such an unusual arrangement, and I’m so grateful that he gave me a chance. By both allowing me to struggle and find my own way while still providing support when needed, he has helped me grow into a better scientist and a better person. Thank you to Anna for graciously giving me a space in her lab and always pushing me to achieve goals I didn’t think were possible. Anna has known me since I was an REU student in her lab, and without that opportunity I can confidently say I wouldn’t be writing this thesis now. I could not have accomplished any of this work without both of their constant support and encouragement.

I am incredibly grateful to the members of the Gestwicki and Mapp labs, past and present, for being fantastic friends and colleagues throughout my time in graduate school. In the Gestwicki lab, thank you to Srikanth, Andrea, Matt, Leah, and Anne for welcoming me with open arms and teaching me everything they know. It truly was a privilege to learn from you. Thank you to Victoria, Jenny, Bryan, Zapporah, Sharan, Xiaokai, and Atta for making the lab such a great place to work in. Thank you to Tomoko, who continues to inspire me as a scientist and person, and who is sincerely missed. To the new crowd at UCSF – Sue Ann, Hao, Jennifer, Rebecca, Matt, and Izzy – thanks for being my “Skype-mates”, but nonetheless supportive, encouraging, and great friends. Special thanks to Kojo – I’m glad I was able to be your “host mom” and bring to Jason’s lab, much to the chagrin of the U of M. I am also incredibly grateful to the members of the Mapp lab for being great friends and neighbors, and for putting up with

all my talk of chaperones. It has been a joy working with and learning from each and every one of you in the lab, especially Ningkun, Amanda, Steve, Andy, Matt, Meg, Cassie, Rachel, Jean, and Omari. I'm looking forward to seeing what Stephen, Alli, Nick, Kevon, and Matt accomplish in the future. I have also had the privilege of working with several talented undergraduate and rotation students – Danielle, Che, and Jamie – I'm sure I learned more from you than you did from me. Finally, I need to acknowledge Dr. Chinmay Majmudar, for graciously mentoring me as an REU student, for teaching me everything he knows, and for being a great friend ever since.

I am incredibly grateful for all the members of the Program in Chemical Biology, especially Chris, Matt, Hong, Paul, Elin, and everyone in my cohort. Thank you for the camaraderie and friendship, for being there when science wasn't going my way, and for cheering me in my successes.

I have been fortunate enough to work with a number of excellent scientists on my thesis committee, Professors Brent Martin, Dan Southworth, and John Tesmer. I have always appreciated their honesty, support, and constructive criticism, providing feedback on my work along the way and pushing me to be a better scientist. Thank you especially to Dan for providing me with a "second home" and allowing me to sit in on your group meetings. I would also be remiss if I did not acknowledge the tireless efforts by Laura Howe and Traci Swan behind the scenes in the Program in Chemical Biology keeping me on track. Finally, I must acknowledge Cherie Dotson, coordinator extraordinaire behind the iREU, for starting me on the right track in science 7 years ago, and being a friendly face and mentor on campus ever since.

I would not be the person I am today without my experience at Grinnell College. Thank you to Professor Jim Lindberg for sticking around at Grinnell and guiding me along the path to chemistry degree. Thank you for sharing your immeasurable life experiences with me, honestly and candidly providing advice and support in my decision to pursue a PhD. I also cannot thank Professor Mark Levandoski enough for taking me on as an undergraduate researcher in his lab. Thank you for putting up with my naïveté and my

wacky ideas, and for always pushing me to achieve my goals. Thank you for making sure I never ran out of OR2 and for keeping my supply of iced animal crackers high. I would not be the scientist I am today without his support and friendship. Finally, thank you to the many Grinnellians I am lucky enough to call friends, Phil, Perri, Garrett, Tony, Alex, Aaron, Stephanie, Kate, Greg, and many others. Thank you for keeping me honest and reminding me to think of the world beyond the lab.

Thank you to the past and current members of Ann Arbor Masters Swimming, especially Matt, Matt, Tom, Anne, and Justin for pushing me in the pool and cutting me some slack when I had to miss practice because I was working late.

Finally, I am so incredibly thankful for the love and support of my family. Thank you to my parents for being my first and best teachers, for telling me that I can accomplish anything I put my mind to, for encouraging me when things got hard, and for reminding me that the most important thing in life is to be happy. Thank you to my siblings Dave and Anna for being my friends and cheerleaders when I needed them the most. I'm so lucky to have all of you. Thank you to my sister-in-law Gretchan for livening up our quiet household and for providing support and laughter. I have also been lucky to have such a supportive extended family, both my own and my in-laws.

Last, but certainly not least, I have to thank my husband Brian DeVree. I cannot fully express how much your love and friendship means to me. Thank you for being my ally, in science and in life. None of this would have been possible without you, truly. I am so lucky to have found you, and I can't wait to see what the future has in store for us. I love you.

Table of Contents

| | |
|--|------|
| Dedication | ii |
| Acknowledgments..... | iii |
| List of Figures | viii |
| List of Tables | xi |
| List of Abbreviations | xii |
| Abstract | xv |
| Chapter 1 Direct and Propagated Effects of Small Molecules on Protein-Protein | |
| Interaction Networks | 1 |
| 1.1 Abstract | 1 |
| 1.2 Introduction | 1 |
| 1.3 Lessons learned: Natural and synthetic examples of allosteric regulation of protein complexes | 5 |
| 1.4 Methods for finding modulators of protein-protein interactions | 13 |
| 1.5 Dissecting protein networks <i>in vitro</i> and in cells | 22 |
| 1.6 Conclusions and Outlook | 27 |
| 1.7 Thesis outline | 28 |
| Chapter 2 Inhibitors of Difficult Protein-Protein Interactions Identified by High- | |
| Throughput Screening of Multi-protein Complexes | 29 |
| 2.1 Abstract | 29 |
| 2.2 Introduction | 29 |
| 2.3 Results | 33 |
| 2.4 Discussion | 45 |
| 2.5 Conclusions | 48 |
| 2.6 Experimental procedures | 49 |

| | |
|---|-----|
| Chapter 3 XIAP is a non-canonical client of the Hsp70 molecular chaperone | 54 |
| 3.1 Abstract | 54 |
| 3.2 Introduction | 54 |
| 3.3 Results | 56 |
| 3.4 Discussion | 77 |
| 3.5 Conclusions | 81 |
| 3.6 Experimental procedures | 81 |
| Chapter 4 Identification of the Sub-Network of Client Proteins that are Dependent on the Molecular Chaperone Hsp70 | 87 |
| 4.1 Abstract | 87 |
| 4.2 Introduction | 87 |
| 4.3 Results | 89 |
| 4.4 Discussion | 101 |
| 4.5 Future directions | 104 |
| 4.6 Experimental Procedures | 107 |
| Chapter 5 Conclusions and Future Directions: Strategies for Targeting Protein Conformation and Dynamics | 111 |
| 5.1 Abstract | 111 |
| 5.2 Summary and conclusions | 111 |
| 5.3 Future directions | 114 |
| 5.4 Broader implications | 119 |
| 5.5 Concluding remarks | 122 |
| References | 123 |

List of Figures

| | |
|--|----|
| Figure 1.1 Common themes in multi-protein complex assembly..... | 2 |
| Figure 1.2 Some protein-protein interactions may be more amenable to inhibition than others..... | 4 |
| Figure 1.3 Mechanisms of small molecule inhibition of protein-protein interactions..... | 9 |
| Figure 1.4 Considerations for choosing the best approach for protein-protein interaction inhibitor discovery. | 14 |
| Figure 1.5 Schematic representation of how small molecules might propagate changes in protein-protein interaction networks..... | 22 |
| Figure 2.1 Schematic of the DnaK-DnaJ-GrpE-substrate system. | 31 |
| Figure 2.2 Characterization of the stimulatory effects of DnaJ, GrpE, and NRLLLTG peptide on ATP turnover..... | 33 |
| Figure 2.3 High-throughput screens identify selective inhibitors of individual multi-protein complexes. | 35 |
| Figure 2.4 Additional results from the parallel HTS campaigns. | 36 |
| Figure 2.5 Active compounds identified in the binary HTS experiments are selective for either DnaJ- or GrpE-stimulated ATPase activity. | 39 |
| Figure 2.6 Zaf binds the ADP-bound form of DnaK and enhances the apparent affinity of DnaK for substrates..... | 40 |
| Figure 2.7 Controls and characterization of Zaf activity in the DnaK-DnaJ-GrpE systems. | 41 |
| Figure 2.8 Tel binds DnaK _{NBD} by NMR. | 43 |
| Figure 2.9 Tel binds subdomain IB in DnaK to allosterically block GrpE activity..... | 44 |

| | |
|---|----|
| Figure 2.10 Characterization of Tel effects on binding of DnaK to GrpE and peptide substrate. | 45 |
| Figure 2.11 Zaf and Tel inhibit DnaK with distinct mechanisms are target different co-chaperone activities..... | 48 |
| Figure 3.1 JG-98 is cytotoxic with only mild effects on oncogenic kinases. | 57 |
| Figure 3.2 Inhibition of both apoptosis and necroptosis is necessary to prevent JG-98 cytotoxicity. | 58 |
| Figure 3.3 JG-98 induces cell death through a novel RIP1-dependent process..... | 61 |
| Figure 3.4 IAPs are selectively destabilized by Hsp70 inhibition. | 63 |
| Figure 3.5 JG-98 causes destabilization of IAPs in multiple cancer cell lines. | 65 |
| Figure 3.6 JG-98-induced degradation of XIAP is not proteasome-dependent..... | 66 |
| Figure 3.7 Hsp70-mediated degradation of XIAP is dependent on the BIR2 and RING domains. | 67 |
| Figure 3.8 Hsp70 binds XIAP <i>in vitro</i> and in cells..... | 69 |
| Figure 3.9 Additional biochemical analysis of the interaction between Hsp70 and XIAP (120-356). | 71 |
| Figure 3.10 Structure and binding of XIAP (120-356) mutants to Hsp70..... | 73 |
| Figure 3.11 Characterization of the non-canonical interaction between Hsp70 and XIAP (120-356). | 75 |
| Figure 3.12 Structural analysis of the Hsp70-XIAP (120-356) interaction. | 76 |
| Figure 3.13 Model for Hsp70's role in RIP1-dependent cell death pathways..... | 78 |
| Figure 3.14 JG-98 causes loss of XIAP in MCF-7 xenograft model..... | 79 |
| Figure 4.1 JG-98 allosterically inhibits the Hsp70-NEF interactions..... | 90 |
| Figure 4.2 JG-98 causes degradation of classic Hsp90 client proteins..... | 91 |
| Figure 4.3 JG-98 mediated cytotoxicity is dependent on binding to Hsp70..... | 92 |

| | |
|--|-----|
| Figure 4.4 JG-98 treatment results in qualitative proteome-wide changes in protein expression levels. | 94 |
| Figure 4.5 Hsp70 inhibition results in differential expression of 10% of the identified proteome. | 96 |
| Figure 4.6 Conformation selective Src inhibitors may affect downstream PPIs. | 105 |
| Figure 5.1 Interactions of a central protein with diverse binding partners mediate the assembly of multi-protein complexes. | 118 |
| Figure 5.2 Comparison of GPCR ligands and PPI inhibitors. | 120 |
| Figure 5.3 Inhibition of interactions between a single protein target and different binding partners can elicit different outcomes. | 121 |

List of Tables

| | |
|--|----|
| Table 1.1 Summary of protein-protein interaction inhibitors | 10 |
| Table 1.2 Summary of protein-protein interaction stabilizers | 12 |
| Table 3.1 Effects of apoptosis and necroptosis inhibitors on JG-98 EC ₅₀ (μM; fold change) in cancer cell lines | 60 |
| Table 3.2 Summary of Hsp70 and Hsp90 inhibitor cytotoxicity (EC ₅₀ ; μM) in cancer cells | 65 |
| Table 4.1 Identified proteins with decreased expression after JG-98 treatment | 97 |
| Table 4.2 Identified proteins with increased expression after JG-98 treatment | 98 |
| Table 4.3 Top GO terms in identified proteins with differential expression after JG-98 treatment | 99 |

List of Abbreviations

| | |
|---------|---|
| 17-DMAG | 17-dimethylaminoethylamino-17-demethoxygeldanamycin |
| ADP | Adenosine diphosphate |
| AFU | Arbitrary fluorescence units |
| AP-MS | Affinity purification mass spectrometry |
| ATP | Adenosine triphosphate |
| ATPase | Adenosine triphosphate hydrolase |
| BAG | Bcl2 associated anthanogene |
| BCA | Bicinchoninic acid |
| BIR | Baculoviral IAP repeat |
| CBP | CREB binding protein |
| CD | Circular dichroism |
| CE | Capillary electrophoresis |
| CMA | Chaperone mediated autophagy |
| Co-IP | Co-immunoprecipitation |
| CV | Coefficient of variation |
| DMSO | Dimethyl sulfoxide |
| DTT | Dithiothreitol |
| ELISA | Enzyme-linked immunosorbent assay |
| FAK | Focal adhesion kinase |
| FAM | 6-carboxyfluorescein |
| FCPIA | Flow cytometry protein interaction assay |
| FDR | False discovery rate |
| FITC | Fluorescein isothiocyanate |
| FP | Fluorescence polarization |
| FRET | Förster resonance energy transfer |
| GO | Gene ontology |

| | |
|----------|---|
| GPCR | G-protein coupled receptor |
| HEPES | 4-(2-hydroxyethyl)-1-piperazineethanesulfonic acid |
| HRP | Horseradish peroxidase |
| Hsp70 | Heat shock protein 70 kDa |
| Hsp90 | Heat shock protein 90 kDa |
| HSQC | Heteronuclear single quantum coherence spectroscopy |
| HTS | High-throughput screening |
| IAP | Inhibitor of apoptosis protein |
| IM-MS | Ion mobility mass spectrometry |
| ITC | Isothermal titration calorimetry |
| LC-MS | Liquid chromatography mass spectrometry |
| MES | 2-(N-morpholino)ethanesulfonic acid |
| MoA | Mechanism of action |
| MS | Mass spectrometry |
| MS/MS | Tandem mass spectrometry |
| MTT | 3-(4,5-dimethylthiazole-2-yl)-2,5-diphenyltetrazolium bromide |
| Myr | Myricetin |
| NBD | Nucleotide binding domain |
| NEF | Nucleotide exchange factor |
| Ni-NTA | Nickel nitrilotriacetic acid |
| NMR | Nuclear magnetic resonance |
| NOE | Nuclear Overhauser effect |
| PaBr | Pancuronium bromide |
| PAGE | Polyacrylamide gel electrophoresis |
| PBS | Phosphate-buffered saline |
| PolyQ-AR | Poly-glutamine expanded androgen receptor |
| PPI | Protein-protein interaction |
| PVDF | Polyvinylidene difluoride |
| Q-TOF | Quadrupole time-of-flight |
| RING | Really interesting new gene |
| RIPA | Radioimmunoprecipitation assay |

| | |
|----------|---|
| RT | Room temperature |
| SA | Surface area |
| SBD | Substrate binding domain |
| SDS | Sodium dodecyl sulfate |
| SEC-MALS | Size exclusion chromatography with multi-angle light scattering |
| SEM | Standard error of the mean |
| SILAC | Stable isotope labeling with amino acids in cell culture |
| TBS | Tris-buffered saline |
| TCEP | Tris(2-carboxyethyl)phosphine |
| TMB | 3,3',5,5'-tetramethylbenzidine |
| Tel | Telmisartan |
| TPR | Tetratricopeptide repeat |
| TROSY | Transverse relaxation optimized spectroscopy |
| WST-1 | 2-(4-iodophenyl)-3-(4-nitrophenyl)-5-(2,4-disulfophenyl)-2H-tetrazolium |
| WT | Wild type |
| XIAP | X-linked inhibitor of apoptosis protein |
| Zaf | Zafirlukast |

Abstract

Networks of protein-protein interactions (PPIs) are essential in all aspects of cellular biology. At the nodes of these networks are multi-protein complexes that are often composed of dynamic, exchangeable modules assembled around a central enzyme. In this thesis, I have used the molecular chaperone heat shock protein 70 (Hsp70) as a model to develop ways of creating inhibitors of PPIs that tune the assembly and function of multi-protein complexes. Hsp70 is an ATPase and master regulator of protein homeostasis that interacts with co-chaperones, including nucleotide exchange factors (NEFs) and J-proteins. There is interest in creating chemical inhibitors that selectively interrupt PPIs between Hsp70 and its co-chaperones, as these molecules would be powerful chemical probes for validating Hsp70 as a target in cancer and other diseases. In this dissertation, I first review how advances in chemical screening methodologies, structural and computational biology, and proteomics have paved the way for the discovery of potent PPI inhibitors, even for difficult targets such as Hsp70 complexes. In Chapter 2, I develop a new high throughput screening (HTS) method in which Hsp70 is combined with co-chaperones and the ATPase activity of the combination is measured. I use this method to identify new inhibitors of Hsp70, characterizing their binding sites and molecular mechanism by NMR, mutagenesis and biochemical approaches. Importantly, I found that this HTS method reveals inhibitors of multiple PPIs within the Hsp70 system, including the interactions with NEFs and J proteins. This approach allowed me to find that Hsp70-NEF complexes control the stability of inhibitor of apoptosis (IAP) protein family members. In Chapter 3, I characterize IAPs as new “clients” of the Hsp70 system and explore the physical interaction between these proteins. That work establishes IAPs as the first sensitive, selective biomarkers suitable for use in pre-clinical studies of Hsp70 inhibitors. Finally, I show how inhibiting the Hsp70-NEF interaction has effects throughout the broader PPI network in Chapter 4. Together, these findings not only have important implications for Hsp70 drug discovery, but they also illustrate, more broadly,

how small molecules can be used to re-shape multi-protein complexes and propagate changes throughout PPI networks.

Chapter 1

Direct and Propagated Effects of Small Molecules on Protein-Protein Interaction Networks

1.1 Abstract

Networks of protein–protein interactions (PPIs) link all aspects of cellular biology. Dysfunction in the assembly or dynamics of PPI networks is a hallmark of human disease, and as such, there is growing interest in the discovery of small molecules that either promote or inhibit PPIs. PPIs were once considered undruggable because the surfaces buried in these interactions are often large and shallow. Despite these challenges, recent advances in chemical screening methodologies, combined with improvements in structural and computational biology have made some of these targets more tractable. In this chapter, I highlight developments that have opened the door to potent chemical modulators. I focus on how allostery is being used to produce surprisingly robust changes in PPIs, even for the most challenging targets. I also discuss how interfering with one PPI can propagate changes through the broader web of interactions. Through this analysis, it is becoming clear that a combination of direct and propagated effects on PPI networks is ultimately how small molecules re-shape biology.

1.2 Introduction

Multi-protein complexes are often assembled around a central enzyme, such as a kinase, phosphatase, protease, or nuclease. Interactions of the “core” enzyme with adaptor and scaffolding proteins often direct it to specific subcellular locations and/or regulating its enzymatic activity.^{1–3} For instance, protein A might trap a given conformer of the enzyme to favor a specific outcome, while interactions between the enzyme and a different partner, protein B, might change the activity (Figure 1.1). Many non-enzymes also control access of substrates to the core enzyme, shaping its selectivity. For example,

protein A might bind a specific substrate for the enzyme and thereby accelerate turnover by increasing its local availability.

The assembly of multi-protein complexes is often mediated by a combination of strong and weak interactions between the individual protein components. Weak interactions are used to provide facile exchange of components.⁴ Expanding beyond these immediate binding partners, multi-protein complexes often serve as “hubs” in a larger protein–protein interaction (PPI) network.⁵ These ancillary interactions link the core and its partners to the broader cellular systems through a physical web of PPIs. It is becoming clear that chemical perturbations of a single node within the PPI network can have implications far beyond the immediate neighborhood.⁶

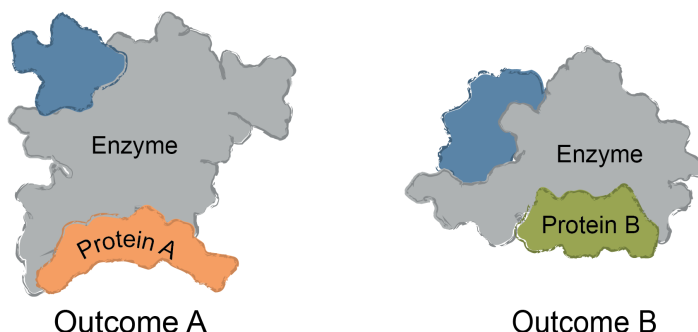


Figure 1.1 Common themes in multi-protein complex assembly. Multi-protein complexes are typically assembled around a core enzyme, while interactions with adaptor, scaffolding, and other partner proteins affect the overall function of the complex. Binding to ligands or macromolecules can trap one conformer of the complex. For example, binding to Protein A might alter the conformation of the enzyme to impact turnover or selectivity. Likewise, binding to Protein B (rather than Protein A) might be favored by a small molecule, changing the function and composition of the complex.

1.2.1 Protein-protein interactions as drug targets

Multi-protein complexes play critical roles in nearly all normal cellular functions, including gene expression, cell division, protein homeostasis, and signaling.^{7,8} Conversely, dysfunction in the assembly, localization, or dynamics of multi-protein complexes is associated with many diseases, including cancer, autoimmune disorders, and neurodegeneration. In some diseases, a complex may be aberrantly active; for example, in acute leukemia the *MLL* gene is translocated, resulting in fusion proteins between an N-terminal fragment of *MLL* and over 50 different target proteins.⁹ In other

diseases, the function of a multi-protein complex may be disrupted, such as occurs in some p53 mutations.¹⁰ While targeting the enzymatic components of multi-protein complexes has traditionally been the norm in drug discovery and in chemical biology, it is increasingly appreciated that PPIs could offer several advantages as targets.^{11–13} For instance, this approach might allow disruption of some aspects of signaling cascades without completely shutting them down.¹⁴ Also, PPI interfaces tend to be more unique and varied than enzyme active sites, thus offering the possibility of greater selectivity.¹⁵ As such, there is significant biological and therapeutic interest in developing chemical modulators of PPIs.¹⁴ Here, modulator is a term used to include both compounds that promote PPIs and those that inhibit PPIs. Such tools, provided they meet established criteria for chemical probes,¹⁶ are highly useful in revealing how specific PPIs are involved in normal function and pathobiology, as well as serving as starting points for therapies.¹⁷

PPIs have typically been challenging to disrupt with small molecules and, until relatively recently, these contacts have been classified as undruggable. It has become better appreciated that some PPIs may be more amenable to inhibition than others. For example, PPIs with relatively weak affinity and large surface areas (SAs) tend to be more challenging, while PPIs that rely on a few, closely spaced amino acids to bind with high affinity are relatively easier to inhibit.^{12,18–20} This point is demonstrated by the fact that of all known PPI modulators, the majority (> 60%) target PPIs with affinity better than 1 μM and total buried SA less than 1800 \AA^2 (Figure 1.2). Another key observation is that, across many systems, orthosteric competitors are ideal for inhibiting the types of PPIs that are characterized by low SAs and tight affinity. For other types of PPIs, allosteric inhibitors tend to be more successful because they can exploit distal pockets that might have more favorable binding properties. Indeed, it is often the lack of defined binding pockets that makes it challenging to target small molecules to the PPIs that involve large, complex surfaces. In such cases, the free energy of binding is typically a summation of many low-affinity contacts, making it hard to design an effective competitor with low molecular weight.²¹

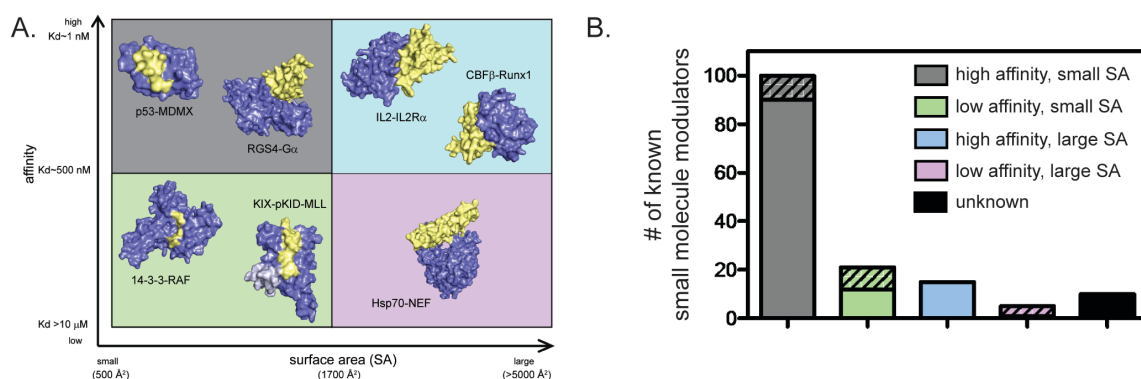


Figure 1.2 Some protein-protein interactions may be more amenable to inhibition than others. (A) PPIs categorized according to the apparent affinity of the interaction and the surface area (SA) buried by assembly. Application of arbitrary criteria for affinity (greater or less than 1 μM) and buried SA (greater or less than 1800 Å²) generates four quadrants. Examples of each class are shown. High affinity, small SA: p53-MDM2 (3DAC), RGS4-Gα (1AGR); high affinity, large SA: IL-2-IL-2Rα (1Z92), CBFβ-Runx1 (1E50); low affinity, small SA: GACKIX-pKID-MLL (2LXT), 14-3-3-RAF (3IQJ); low affinity, large SA: Hsp70-BAG1 (1HX1). (B) Known inhibitors of PPIs were collected from 2P2IDB and TIMBAL databases and plotted according to the affinity (reported in PDBbind²²) and buried SA (calculated by InterProSurf²³) of the target PPI. Inhibitors published since a similar analysis in 2012²⁴ are represented by hatched bars to highlight the most recent development and trends. Small molecules targeting PPIs with high affinity and small buried SA represent 66% of all known inhibitors, although 56% of newly identified inhibitors target more difficult classes of PPIs.

1.2.2 Allosteric inhibitors can offer greater control over downstream response

Two (or more) chemical inhibitors that act on the same target can produce different cellular responses because of the way that they alter local PPI networks. Extensive work on allosteric modulation of G-protein coupled receptors (GPCRs) and kinases has provided a blueprint for how this might be accomplished in other systems.²⁵

1.2.2.1 Allosteric modulation of GPCRs

GPCRs signal through a series of well-characterized downstream PPIs.²⁶ Allosteric and biased compounds offer an opportunity to have greater control over signaling by “fine-tuning” the response, illustrating the nuanced ways in which small molecules modulate the output of these systems.²⁷ A key observation from these examples is that binding of distinct ligands, even to the same site, can produce dramatically different effects on downstream signaling.²⁸ For example, propranolol binds the β2 adrenergic receptor, although it is an inverse agonist for adenylyl cyclase signaling and an agonist for extracellular signal-regulated kinase activity.

1.2.2.2 Allosteric inhibition of kinases

The field of kinase inhibitors may also provide another illustrative example. Kinase inhibitors fall into four general categories, the two most important of which are: type I and type II. Type I compounds bind directly to the ATP binding site in the kinase domain. Type II inhibitors, on the other hand, interact preferentially with the inactive conformation via binding to an allosteric site.²⁹ While both type I and type II inhibitors block enzymatic activity, they appear to have distinct effects on downstream PPIs between the kinases and their effectors. Why is this categorization important? For the sake of this analysis, type I and type II inhibitors might be expected to have different effects on the interactions between the kinase and its downstream effectors, such as 14-3-3 proteins, which link it to broader PPI networks. Thus, the effects of the inhibitors on cells might reflect both the inhibition of the kinase itself, but also the changes in PPIs.

1.2.3 Strategies for targeting PPIs with small molecules

In this chapter, I discuss how small molecules might be discovered and developed to take advantage of allosteric networks within multi-protein complexes. In the first section, I describe lessons learned from natural PPI modulators. I also review examples of synthetic molecules that have been discovered by serendipity to control PPIs through interesting mechanisms. In the second section, I survey a number of promising high-throughput screening (HTS) approaches that are geared toward the purposeful discovery of PPI modulators with similar mechanisms. Finally, in the third section, I speculate on which new methods and ideas might be needed to take full advantage of future opportunities. The over-arching theme is that small molecules have both proximal (or direct) effects on PPIs (*e.g.*, they block or favor specific PPIs), while also having less well-appreciated effects on downstream interactions within PPI networks.

1.3 Lessons learned: Natural and synthetic examples of allosteric regulation of protein complexes

Allostery, in which binding of a ligand at one site affects protein conformation at a distant site, enables small molecules to produce dramatic effects on protein structure and function, even at a distance.^{30,31} Classic work in this area was performed on the

hemoglobin system, revealing that action at one binding site can propagate conformational changes that impact other sites more than 25 Å away.³² This theme has been observed countless times in biology, with allosteric control observed for both small molecule- and protein-mediated interactions. To name just one example, the activity of the histone deacetylase enzyme HDAC3 requires recruitment to a co-repressor SMRT complex.^{33,34} However, when expressed in bacteria, recombinant HDAC3 and SMRT do not interact, leading to speculation that an assembly factor was missing.³⁵ It was subsequently found that the deacetylase activation domain (DAD) of SMRT undergoes substantial structural rearrangement upon binding to HDAC3 and that an inositol tetraphosphate molecule was essential for this transition.³⁶ The inositol molecule stabilizes the HDAC3–SMRT complex through conformational transitions involving both protein–protein and protein–small molecule contacts. What can be learned from these natural examples? In the HDAC3–SMRT case, a cascade of conformational changes occurs following the small molecule interaction. Thus, the small molecule needs to not only bind its target protein, but also alter the conformer of the target in the right way to enable subsequent binding to the downstream partner(s). In a broader sense, it seems possible that whenever a protein is bound by a small molecule, a specific subset of conformers is captured and those conformers might have important implications for what happens next.

1.3.1 Small molecules trap specific protein conformers

One illustrative example of these concepts is the case of the retinoic acid receptor (RAR). In this system, gene expression is repressed when RAR is bound to a co-repressor, while gene expression is activated when RAR recruits a co-activator.³⁷ The key structural feature is a switch between an extended β -strand and α -helix in RAR, which occurs in a region that is important for binding to both co-repressors and co-activators.³⁸ Chemical agonists of RAR promote co-activator binding by stabilizing the correct, permissive conformation,³⁹ while inverse agonists convert the α -helix to an extended β -strand, promoting binding to co-repressors. Finally, neutral antagonists stabilize a conformer in which neither co-activators nor co-repressors are bound.⁴⁰ Thus, depending on the chemical cue that is encountered (*e.g.*, agonist, neutral antagonist, *etc.*), there are dramatic and important changes in PPIs that dictate downstream signals.³⁸ Such systems

can be considered pharmacological “switches,” in which the local PPI network is re-wired by the small molecule.

Another useful example is the scaffolding protein family 14-3-3. These versatile adaptor proteins bind to hundreds of individual partners through a conserved amphipathic binding groove.^{41,42} 14-3-3 proteins are able to adopt many distinct conformations that allow them to interact with different binding partners.⁴³ Inhibitors exploit this property. For example, the natural product fusicoccin A promotes 14-3-3 complex assembly with some partners,^{44,45} while the pyridoxal-phosphate derivative FOBISIN101 inhibits interactions with other partners.⁴⁶ In these cases, the compound produces a specific cellular effect because it traps a conformation of the 14-3-3 protein and alters its PPI interfaces.⁴⁷

Another example includes the case in which small molecules have been found to tune the activity of the molecular chaperone, Hsp70. Dihydropyrimidines were identified that bind at the interface between Hsp70 and its PPI partner, Hsp40. Members of the dihydropyrimidine scaffold remodel the PPI surface, such that some analogs strengthen the Hsp70–Hsp40 complex, while others inhibit it.⁴⁸ Similar concepts have been proposed for the transcriptional co-activator proteins, including the master co-activator CBP and components of the Mediator complex, in which allosterically coupled binding interfaces mediate interactions with transcriptional activators.^{49–51} The theme in these systems is that the small molecule does not just alter enzyme activity – it impacts the way in which the protein partners recognize the target. Thus, I suggest that one of the most important features of a small molecule is how it traps a specific ensemble of protein conformers. The ultimate biological output of a small molecule will be a product of the changes in both enzyme activity and its effects on PPIs networks.

1.3.2 Inhibition of protein-protein interactions

1.3.2.1 Orthosteric inhibitors of PPIs

Significant progress has been made toward identifying orthosteric inhibitors of PPIs over the past 15–20 years.^{12,17,19,20} Classic success stories include inhibitors of p53–MDM2⁵² and inhibitors of BCL2/BCL-X_L⁵³ and IAPs.⁵⁴ In these cases, a molecule binds at the

surface and directly prevents the most important “hotspot” side chains from interacting (Figure 1.3). In addition, the search for orthosteric inhibitors has revealed important features of the dynamics of PPI surfaces. For example, Tilley and coworkers reported the discovery of a small molecule that inhibits binding between the cytokine IL-2 and the IL-2 α receptor (IL-2R α).⁵⁵ Subsequent structural analysis suggested that this compound binds to IL-2 in a region that is critical for productive binding to IL-2R α . Importantly, the unliganded IL-2R α binding interface on IL-2 is dynamic and samples many distinct conformations. Binding of the small molecule restricts the total number of conformations sampled by IL-2, effectively “trapping” the protein in a conformation distinct from either the apo or IL-2R α bound structures. Furthermore, the adaptive protein interface was more amenable to inhibitor discovery via disulfide tethering than an IL-2 subsite that is more conformationally restricted.⁵⁶ Many protein–protein interfaces are similarly adaptive, and while thought to be relatively flat and featureless, such binding interfaces can nonetheless sample conformations that allow for the formation of a small molecule binding pocket (Figure 1.3).^{57,58} Why is it worth considering classic and adaptive orthosteric inhibitors as different classes? While both types ultimately inhibit the PPI by occluding the site of interaction, medicinal chemistry efforts to optimize them will depend on their mechanism. For example, classic orthosteric inhibitors do not induce substantial conformational rearrangement of the binding site, and therefore the ligand free structure of the protein can be used to guide the synthesis of new analogs. On the other hand, adaptive inhibitors require a conformation of their protein target that is distinct from the apo structure. Thus, structure-guided medicinal chemistry campaigns must be undertaken with this in mind.

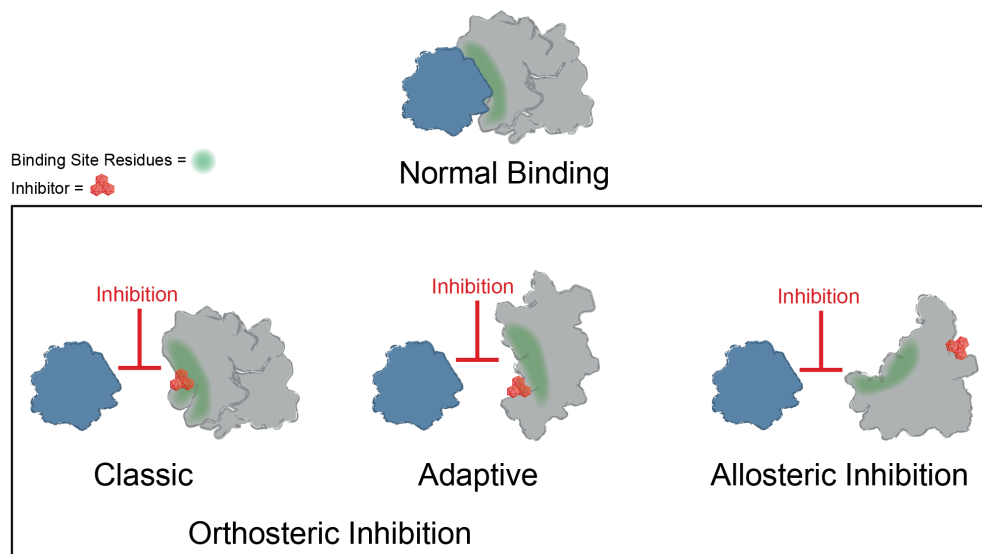


Figure 1.3 Mechanisms of small molecule inhibition of protein-protein interactions. Several different binding modes for small molecule inhibitors of PPIs are shown. Orthosteric inhibitor directly competes with one partner for binding. Orthosteric inhibitor taking advantage of an adaptive protein interface stabilizes a protein conformer such that the interaction surface is no longer amenable to binding. An allosteric inhibitor binds a site distal from the PPI interface, resulting in structural rearrangement in the target protein.

1.3.2.2 Allosteric PPI inhibition

Binding of small molecules at allosteric sites can also produce robust inhibition of PPIs (Figure 1.3). The interaction between Runx1 and CBF β mediates formation of the heterodimeric transcription factor CBF.⁵⁹ In some cases of acute myeloid leukemia, CBF β is fused to the smooth muscle myosin protein, favoring formation of the CBF β -Runx1 complex and resulting in dysfunction in CBF transcription.^{60–62} Thus, inhibition of CBF heterodimer formation represents an attractive therapeutic strategy. Unfortunately, this interface is relatively large and featureless, characteristic of the difficult PPIs described previously. While attempts to discover orthosteric inhibitors of CBF β -Runx1 binding have been unsuccessful, a combination of computational and NMR screens identified a class of 2-aminothiazoles that bind to an allosteric site on CBF β distinct from the Runx1 binding interface and block CBF β -Runx1 complex formation *in vitro* and in HEK293 cells.⁶³ Importantly, NMR chemical shift perturbations revealed that compound binding at the allosteric site produces changes in CBF β conformation and/or dynamics at the heterodimerization site. Similarly, irreversible binding of a small molecule at an allosteric site on the regulator of G-protein signaling protein 4 (RGS4) produces more

robust inhibition of binding to $G\alpha_o$ than covalent modification within the binding interface.⁶⁴ Temperature-accelerated molecular dynamics and NMR spectroscopy revealed how small molecule binding at an allosteric site on RGS4 is transmitted to the G-protein binding site in order to destabilize the PPI and block its GTPase accelerating activity.⁶⁵

Together, these studies suggest that allostery is a powerful approach for PPI inhibition and that it is particularly advantageous in circumventing the difficulties associated with challenging PPI interfaces, namely those with weak affinity and/or large SAs. This idea is illustrated in Table 1.1, in which the chemical structure of a subset of PPI inhibitors is listed next to the method used for their discovery, their mechanism of inhibition, and the class of the targeted PPI. This summary emphasizes the idea that allostery is a common property exploited by inhibitors of difficult targets and that certain discovery methods appear to be geared toward finding such molecules (as discussed below).

Table 1.1 Summary of protein-protein interaction inhibitors.

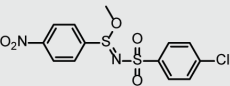
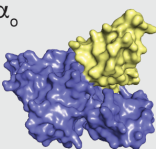
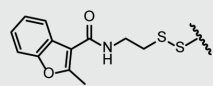
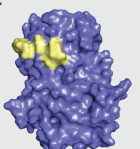
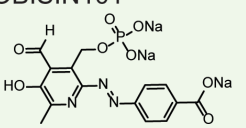
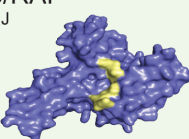
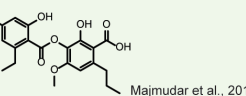

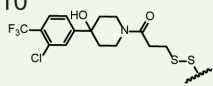
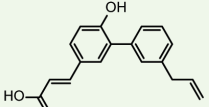
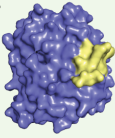
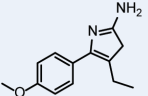
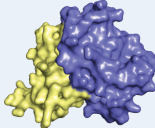
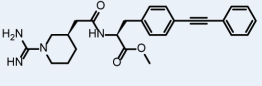
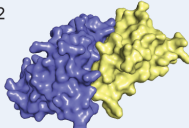
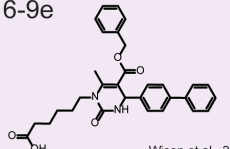
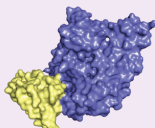
| Compound | PPI interface | Mechanism | Discovery method |
|---|--|-------------|------------------|
| CCG-4986  <small>Roman et al., 2007</small> | RGS4/$G\alpha_o$ PDB: 1AGR  | allosteric | FCPIA |
| 1F8  <small>Sadowsky et al., 2011</small> | PDK1/PIF PDB: 4RRV  | adaptive | Tethering |
| FOBISIN101  <small>Zhao et al., 2011</small> | 14-3-3/RAF PDB: 3IQJ  | orthosteric | FP |
| sekikaic acid  <small>Majmudar et al., 2012</small> | GACKIX/MLL PDB: 2LXT  | allosteric | FP |
| 1-10  <small>Wang et al., 2013</small> | | adaptive | Tethering |

Table 1.1 Continued

| Compound | PPI interface | Mechanism | Discovery method |
|---|--|-------------|---------------------|
| <p>honokiol</p>  <p>Scheepstra et al., 2014</p> | <p>RXR/TIF2 PDB: 4OC7</p>  | allosteric | NMR |
| <p>2-aminothiazole</p>  <p>Gorczyński et al., 2007</p> | <p>CBFβ/Runx1 PDB: 1E50</p>  | allosteric | NMR |
|  <p>Tilley et al., 1997</p> | <p>IL-2/IL-2Rα PDB: 1Z92</p>  | adaptive | Medicinal chemistry |
| <p>116-9e</p>  <p>Wisen et al., 2010</p> | <p>Hsp70/DnaJ PDB: 2QWN</p>  | orthosteric | Gray-box |

High affinity, small SA (gray); low affinity, small SA (green); high affinity, large SA (blue); low affinity, large SA (purple).

1.3.3 Promoting protein complex assembly

Small molecules can also be used to stabilize (rather than inhibit) PPIs, as described for the HDAC3–SMRT complex.³⁶ In some cases, such potentiation can be therapeutically beneficial. Natural PPI stabilizers have been identified that nicely illustrate this idea.⁶⁶ The immunosuppressant cyclosporin A acts as a “molecular glue” between the peptidyl-prolyl *cis-trans* isomerase cyclophilin A and the protein phosphatase calcineurin.⁶⁷ Similarly, FK506 stabilizes the interaction between the peptidyl-prolyl isomerase FKBP and calcineurin.⁶⁸ Another immunosuppressant, rapamycin, uses a similar approach to inhibit mTOR kinase.⁶⁹ An example critical in plant development is the hormone auxin, which binds to TIR1 F-box proteins and stabilizes their interactions with Aux/IAA transcriptional repressor proteins.⁷⁰ Finally, acyl-homoserine lactone (AHL) molecules are used by photobacteria in quorum sensing-mediated bioluminescence. AHL binding facilitates dimerization of LuxR-type transcription factors, increasing their DNA binding capacity and expression of target genes.^{71,72} Importantly, in all cases, ternary complex

formation is essential for function; that is, in the absence of small molecule, protein complex formation is negligible.

A number of synthetic stabilizers of PPIs have also been identified in recent years. For example, the murine double minute proteins MDM2 and MDMX are often overexpressed in cancer and negatively regulate p53-dependent gene expression.^{73,74} The tumor suppressor p53 controls pro-apoptotic and growth suppressing genes, and thus activation of p53-dependent transcription could have utility in cancer therapy.⁷⁵ However, inhibition of either the p53–MDM2 or p53–MDMX interaction alone was not sufficient to fully restore p53 signaling, and simultaneous inhibition of both PPIs is necessary for full activity.^{76,77} Unfortunately, structural differences in the p53 binding sites of MDM2 and MDMX have hindered development of dual antagonists.⁷⁸ Graves and coworkers at Roche Research Center instead identified a class of small molecules that inhibit both p53–MDM2 and p53–MDMX binding by inducing MDM2–MDMX protein dimerization, occluding the p53 binding site.⁷⁹ While most reported examples of PPI stabilizers bind directly to the protein–protein interface, establishing contacts with both binding partners (those discussed in this chapter are summarized in Table 1.2),⁶⁶ it is reasonable to speculate that small molecules might also be identified to stabilize specific PPIs through allosteric regulation, in which compound binding at a distal site would modulate the protein interface such that binding affinity is increased.

Table 1.2 Summary of protein-protein interaction stabilizers

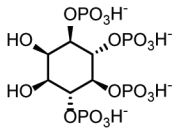
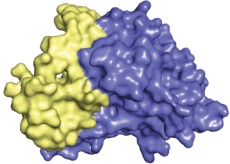
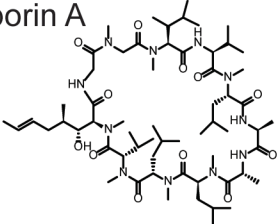
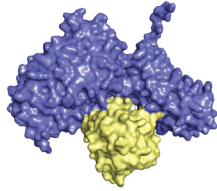
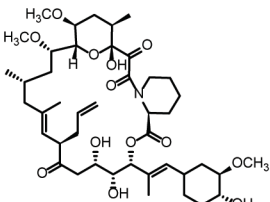
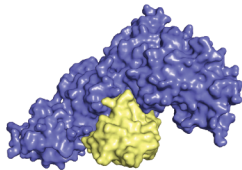
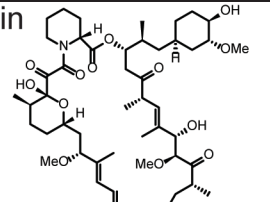
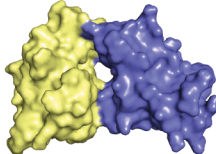
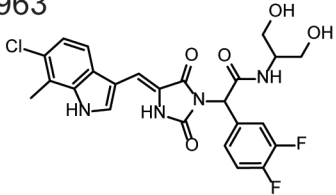
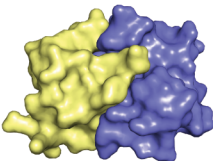
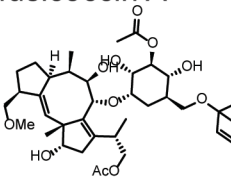
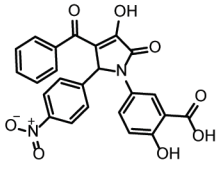
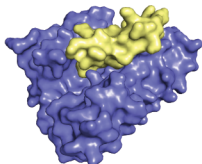
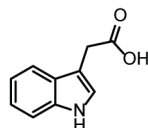
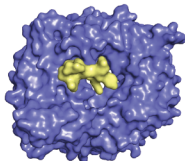
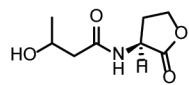
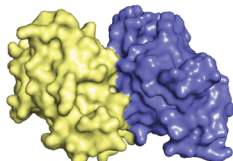
| Compound | PPI Interface |
|---|--|
| <p>inositol tetrakisphosphate</p>  <p style="text-align: right;">Watson et al., 2012</p> | <p>HDAC3/SMRT PDB: 4A69</p>  |
| <p>cyclosporin A</p>  <p style="text-align: right;">Huai et al., 2002</p> | <p>Cyclophilin A/calcineurin PDB: 1M63</p>  |

Table 1.2 Continued

| Compound | PPI Interface | |
|--|--|--|
| <div>FK506</div> <div></div> <div>Griffith et al., 1995</div> | <div>FKBP12/calcineurin</div> <div>PDB: 1TCO</div> <div></div> | |
| <div>rapamycin</div> <div></div> <div>Brown et al., 1994</div> | <div>FKBP12/mTOR</div> <div>PDB: 1FAP</div> <div></div> | |
| <div>RO-5963</div> <div></div> <div>Graves et al., 2012</div> | <div>MDM2/MDMX</div> <div>PDB: 2VJE</div> <div></div> | |
| <div>fusicoccin A</div> <div></div> <div>Wurtele et al., 2003</div> | <div>pyrrolinone</div> <div></div> <div>Rose et al., 2010</div> | <div>14-3-3/PMA2</div> <div>PDB: 3M51</div> <div></div> |
| <div>indole-3-acetic acid</div> <div></div> <div>Delker et al., 2008</div> | <div>TIR1/Aux/IAA</div> <div>PDB: 2P1N</div> <div></div> | |
| <div>acyl homoserine lactone</div> <div></div> <div>Churchill & Chen et al., 2011</div> | <div>LuxR dimer</div> <div>PDB: 2UV0</div> <div></div> | |

1.4 Methods for finding modulators of protein-protein interactions

Recent reviews have discussed the specific need for new methods in finding modulators of PPIs.^{19,80} One identified challenge is that many traditional HTS methods rely on the measurement of direct binding between two protein partners. Such methods may not be

suitable for finding potent inhibitors of some categories of PPIs, such as weaker ones. Another challenge is that very few methods are available that provide insight into the effects of a small molecule on broader PPI networks. This is particularly important for PPI inhibitor campaigns because screens must be specifically geared toward the discovery of molecules with the most suitable features, such as disrupting a subset of PPIs or favoring others.⁸¹ In other words, you get what you screen for.

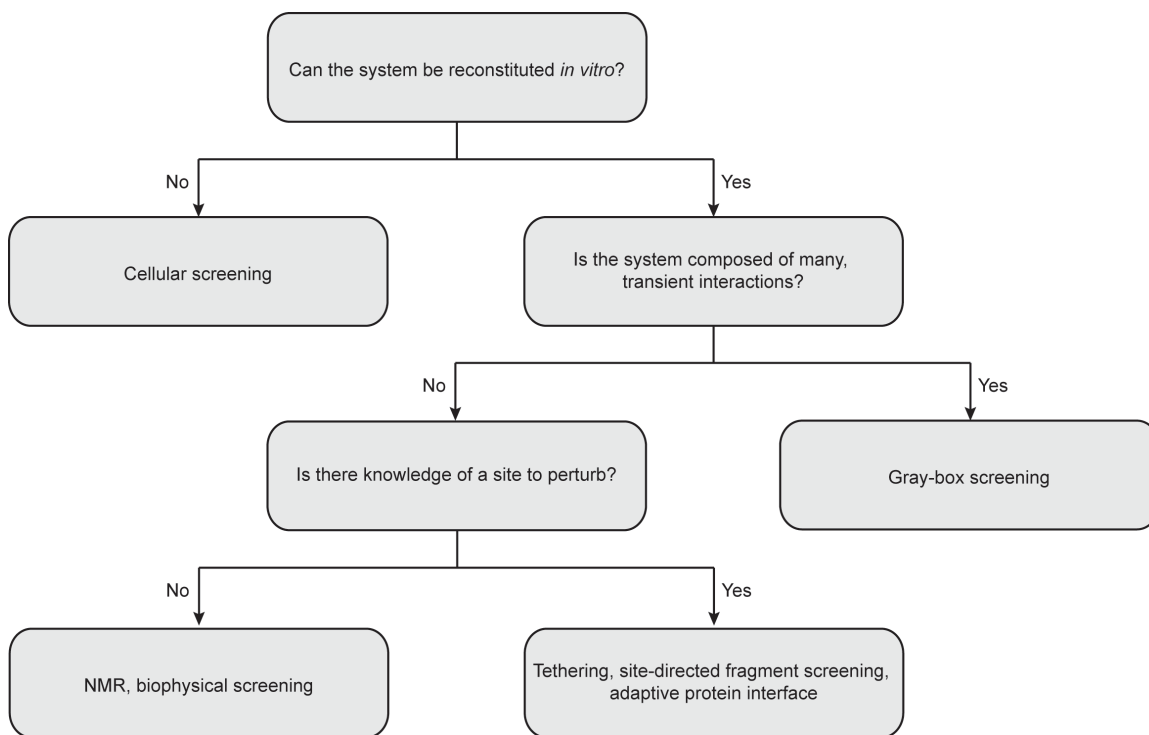


Figure 1.4 Considerations for choosing the best approach for protein-protein interaction inhibitor discovery. Central questions to consider include if the multi-protein complex can be reconstituted *in vitro* with recombinant proteins, how strong the interactions between individual components, and if there is any precedent for sites to perturb. It is important to note that some approaches might be best used in tandem and that more than one platform might be best for different systems.

Due to the inherent complexity of multi-protein systems, it is difficult to provide a “one-size fits all” approach for future work, as a given HTS campaign must necessarily be geared for the complex of interest (Figure 1.4). For instance, many biophysical methods demand little advance knowledge of the complexities of a given system and require only purified recombinant protein. In addition, these approaches can quickly provide valuable information on protein and ligand-binding sites, allosteric networks, and druggable interfaces. On the other hand, cellular screening methods are well suited for multi-protein complexes composed of transient interactions that cannot be reconstituted *in vitro*. In this

section, I highlight several successful approaches to discovering PPI modulators and comment on needs for the future. This overview is not meant to be an exhaustive list of all HTS methods, but is rather meant to provide a general roadmap for the design of screening campaigns.

1.4.1 Biophysical methods

Some PPIs are difficult to directly measure, although assays based on fluorescence polarization (FP), surface plasmon resonance (SPR), fluorescence energy transfer (FRET), bioluminescence energy transfer (BRET), differential scanning fluorimetry (DSF), hydrogen-deuterium exchange, AlphaLisa, and NMR spectroscopy have been developed and each has its strengths.^{82,83}

1.4.1.1 Flow cytometry protein interaction assay

FP is typically effective when the PPI involves a small SA;⁸⁴ however, many PPIs occur over large, flat surfaces that lack such a discrete binding site. In these instances, a flow cytometry-based protein interaction assay (FCPIA) has proven to be a powerful, versatile alternative for PPI inhibitor discovery. In this method, one partner is biotinylated and attached to avidin beads, while the other partner is labeled with a fluorophore. A flow cytometer is used to measure bead-associated fluorescence, providing a quantitative measurement of protein binding.^{85–87} FCPIA was used to discover inhibitors of the high-affinity interaction between a regulator of G-protein signaling protein RGS4 and $G\alpha_o$ ($K_D \sim 4$ nM).⁸⁸ Importantly, RGS4 accelerates GTPase activity of $G\alpha_o$, and inhibitors of the PPI also block GTPase stimulation. FCPIA has also been used to identify inhibitors of weaker PPIs, including that between Hsp70 and the BAG family of nucleotide exchange factors ($K_D \sim 1$ μ M).^{89,90}

1.4.1.2 Capillary electrophoresis

Another technique used to study protein complexes is capillary electrophoresis (CE). This method allows for separation of complexes from their individual components based on their size and charge. Labeling one or more of the individual protein partners enables sensitive detection of bound:free ratios.^{91,92} CE has been used to identify inhibitors of a

number of macromolecular complexes, including those between SH2 domains and short phosphorylated peptides⁹³ and Hsp70–BAG.⁸⁹ One advantage of CE is that it allows for easy detection of aggregators, a common problem in PPI inhibitor screens. Finally, both CE and FCPIA are compatible with multi-color fluorescent labeling, which facilitates the ready detection of ternary and higher order complexes in 384-well plate format.

1.4.1.3 NMR spectroscopy

NMR spectroscopy-based strategies are particularly useful for the detection of ligand binding to protein interfaces, even that those that involve modest affinity (*e.g.*, high micromolar or millimolar dissociation constants).⁹⁴ Furthermore, these experiments often illuminate the ligand-binding modes by chemical shift perturbations. This approach has been particularly powerful for fragment-based screens. Protein-observed NMR screening requires homogenous ¹⁵N or ¹³C isotopically labeled protein that has high solubility and stability even at high concentrations.⁹⁵ Isotopic labeling can be costly, and data acquisition for NMR spectra is often time-consuming. One alternative is ligand-based NMR screening and another is protein-observed fluorine NMR spectroscopy (PrOF NMR), an attractive approach with high sensitivity and rapid data collection. The ¹⁹F nucleus is highly responsive in NMR experiments and accounts for 100% of naturally occurring fluorine, eliminating the need for isotopic labeling.⁹⁶ Native tyrosine residues are replaced with singly labeled fluorinated tyrosine, allowing for sensitive detection of protein conformation in simplified 1D-NMR spectra. This approach is particularly useful in the discovery of inhibitors of PPIs due to the enrichment of aromatic amino acids at PPI interfaces and has been used to characterize ligand binding to the transcriptional co-activation domain CBP/p300 GACKIX⁹⁷ and bromodomains in BRD4, BrdT, and BPTF.⁹⁸ In addition, genetic incorporation of trifluoromethyl-phenylalanine was used to probe protein–ligand interactions within the thioesterase domain of fatty acid synthase.⁹⁹ Recently, a full PrOF NMR fragment screen was used to discover several new small molecule ligands for distinct binding sites on CBP/p300 GACKIX, confirming the druggability of this dynamic protein interface.¹⁰⁰

Another emerging approach to get around the typical size limits of NMR spectroscopy is to label methyl groups on amino acid side chains. Methyl groups frequently reside in the hydrophobic interior of proteins and are sensitive reporters of protein structure and dynamics.¹⁰¹ NOEs can be used to determine spatial proximity of methyl groups, reporting on tertiary and quaternary protein structure.^{102,103} Furthermore, methyl groups located at the end of side chains undergo slower relaxation kinetics, facilitating the acquisition of NMR spectra for large proteins with high sensitivity and resolution.^{104,105} Researchers at Abbott Laboratories adapted this approach to screen a series of protein targets using selective ¹³C labeling of methyl groups in valine, leucine, and isoleucine side chains, demonstrating the utility of this strategy in HTS for target proteins up to 110 kDa in size.¹⁰⁶

1.4.2 Site-directed fragment-based screening

Covalent disulfide trapping, or Tethering, can be used in HTS to facilitate discovery of PPI inhibitors. In this method, fragment molecules containing disulfide moieties covalently modify a natural or engineered cysteine. The relative strength of the interaction is typically measured by competition with DTT or similar thiol modification reagent, permitting the selection of fragments that have the best affinity for the site.^{107,108} Binding is typically explored by crystallography, SPR or mass spectrometry. Tethering is a particularly powerful technique because it is site-directed. Indeed, Tethering screens have demonstrated that adaptive, conformationally flexible regions of protein–protein interfaces are often more amenable to inhibitors.^{109–111} Tethering was recently used to successfully define the role of an allosteric site in activation of the PDK1 kinase. Engineered cysteines lining the rim of the PDK1-interacting fragment (PIF) pocket on PDK1 were screened for disulfide capture against a library of fragment molecules.¹¹² Interestingly, tethered fragments at a single site resulted in both activation and inhibition of PDK1, and the allosteric effect was unrelated to binding potency. Rather, fragment binding at a single allosteric site elicited subtle changes in the active conformation of PDK1, leading to potentiation or inhibition of kinase activity. Another recent example identified inhibitors of a specific cysteine mutant of Ras.¹¹³

Fragments identified from Tethering screens can be powerful chemical probes for dissecting allosteric networks in flexible proteins. For example, the GACKIX domain of the transcriptional co-activator protein CBP/p300 displays considerable structural plasticity.¹¹⁴ A recent Tethering screen yielded a small molecule (1-10) that has a remarkable effect on the overall thermal stability of GACKIX and was used as an aid in crystallization in order to obtain the first X-ray crystal structure of GACKIX at 2 Å resolution.¹¹⁵ More recently, 1-10 was used in conjunction with kinetic and computational analyses to reveal the mechanism of allostery between two activator-binding sites in GACKIX. Binding of one ligand does not affect the association kinetics for the second partner, but rather decreases the rate of dissociation of the complex.¹¹⁶ These results suggest that cooperativity between the two activator-binding sites is achieved by increasing the energy barrier for dissociation, effectively stabilizing the GACKIX ternary complex.¹¹⁷ In other words, inhibition of activator binding is mediated by favoring the unbound binary complex.

1.4.3 Adaptive protein interfaces

One screening approach is to take advantage of the conformational plasticity of PPIs. Protein surfaces that mediate contacts with a variety of other proteins are typically flexible, allowing them to adapt to each partner. For example, the GACKIX domain of the transcriptional co-activator CBP/p300 is an important regulatory node of gene expression and mediates binding to diverse transcriptional activators via two allosterically coupled binding sites.^{50,114,118} Majmudar and coworkers reasoned that small molecules could take advantage of this intrinsic motion to trap specific states.¹¹⁹ GACKIX was screened with the activator MLL bound in the deeper and more conformationally flexible binding site, and this approach identified two natural products, sekikaic acid and lobaric acid. These compounds bind to a dynamic site on CBP/p300 GACKIX and allosterically inhibit interactions at the distal binding site with good specificity. In this case, knowledge of the adaptive, local PPI network was used to establish a screening paradigm that favored discovery of the desired probe.

Another recent example focused on nuclear receptors and their co-activator proteins. The retinoid X receptor (RXR) contains a dynamic protein interface, termed activation

function 2 (AF2) that mediates interactions with co-activator proteins.^{120,121} Sheepstra and coworkers used a combination of NMR spectroscopy and molecular docking to identify a natural product honokiol that targets both sides of the adaptive AF2 domain.¹²² They used rational design to “split” the two functions of honokiol, generating a potent RXR agonist with one and an antagonist with the other. The first ligand inhibits the RXR-coactivator PPI by binding at an allosteric site, while the second ligand binds directly to the ligand-binding site on RXR to favor interactions with the co-activator. Like the example of the CBP/p300, this approach exploits the inherent conformational flexibility of the AF2 domain and demonstrates how binding of small molecules at the same protein interface can differentially modulate specific PPIs.

Another interesting example involves the adaptor protein 14-3-3 introduced earlier. Binding between 14-3-3 and the plant proton pump PMA2 was monitored by SPR, and a small compound library was screened for stabilizers of the interaction.¹²³ This campaign identified small molecules that promote the PPI between 14-3-3 and PMA2 by binding to a flexible groove on 14-3-3 and making contacts with both partners. Synthetic optimization of the pyrrolinone scaffold in one of these molecules resulted in the development of a derivative that further stabilized the 14-3-3–PMA2 interaction.¹²⁴ This example is interesting because the screening method was designed such that the two partners were near their half-maximal concentrations, which likely facilitated the discovery of the “hits”. Most screening campaigns involve saturating concentrations of the two interacting partners; not surprisingly, inhibitors are more commonly observed under these conditions.

These successful HTS campaigns demonstrate how a conformationally dynamic protein can be targeted with small molecules to specifically modulate the assembly and disassembly of multi-protein complexes. A key design feature of these screens is that structural knowledge of the system was used to guide the screen and favor identification of compounds with the desired mechanism.

1.4.4 “Gray-box” screening

In many cases, weak binding affinity between a protein and its binding partner can complicate the design of an effective screening assay. In these cases, it can be useful to screen the functional output of the interaction, rather than the physical interaction itself. A method referred to as “gray-box” screening¹²⁵ was developed specifically for this purpose. The name of this method comes from the term “black box” screens, which is applied to phenotypic assays. While screens in whole cells or organisms are powerful, it is often difficult to find the target. Likewise, biochemical screens against purified proteins, such as kinases or proteases, are clean, but they often ignore the impact of PPIs and non-enzyme partners. Gray-box screens are designed to include not just the enzyme, but also its binding partners, and the physical target of an inhibitor is therefore not obvious until follow-up mechanistic studies have been performed. In the first example of this approach, the ATPase, Hsp70, was mixed with its co-chaperones, including Hsp40. These co-chaperones act as catalysts of Hsp70’s ATPase activity,^{126–128} so the readout of the screen was largely a result of the PPIs and not the enzyme activity *per se*. Thus, the functional consequence of the interactions, measured as elevated turnover, can be used as a surrogate for binding.^{129,130} This type of approach has identified many specific chemical modulators of PPIs between Hsp70 and co-chaperones, ATPase activity, and chaperone function.^{48,131,132} Indeed, I discuss in Chapter 2 a screen against all possible binary and ternary complexes in the prokaryotic Hsp70 system which identified inhibitors that were specific for given co-chaperones, each taking advantage of previously unexplored allosteric networks to inhibit Hsp70 activity.¹³³ Such diverse inhibitors are likely to be powerful tools and could enable the definition of Hsp70 PPI networks in a cellular environment. Gray-box screening has also been used to identify inhibitors of the interactions between G α proteins and regulators of G-protein signaling (RGS) proteins, which act as GTPase activating proteins (GAPs). In this case, GTPase activity was used as a surrogate for RGS-G α binding, and this screen identified several molecules capable of targeting the specific interactions between different RGS proteins and G α_i .¹³⁴ In another example, the progesterone receptor (PR) was reconstituted with Hsp90 chaperone complexes, and compounds were screened for their ability to inhibit refolding of PR, a

physiological substrate of Hsp90.¹³⁵ Overall, gray-box screening is particularly well suited to finding inhibitors of challenging PPIs.

1.4.5 Screening in cells

Some PPI networks cannot be readily replicated *in vitro*, demanding the use of cell-based screening platforms. However, even for a well-defined PPI, cell-based screens of the native network will likely yield modulators of up- and downstream interactions, required substantial deconvolution. To circumvent these challenges, enzyme fragment complementation can be used, allowing for a specific PPI to be screened in the cellular environment such that the functional output of the assay is dependent solely on the PPI of interest.¹³⁶ In this approach, protein fragments derived from enzymes such as luciferase, β -galactosidase, or dihydrofolate reductase are fused to putative interacting partners. The inactive fragments can reassemble into a functional complex upon interaction of the protein partners. Reconstituted enzymatic activity is used to quantify protein binding, even between transiently interacting partners.

The split luciferase assay can be used to detect PPIs in cells¹³⁷ and can be expanded to include a Cre-recombinase-mediated cassette exchange¹³⁸ allowing for inducible gene expression. The recombinase-enhanced bimolecular luciferase complementation platform (ReBiL) allows for the detection and analysis of even weak PPIs in living cells in real time. This platform enabled the detection of the transient PPI between the E2 ubiquitin-conjugating enzyme UBE2T and its partner E3 ubiquitin ligase FANCL.¹³⁹ This complex has a low micromolar dissociation constant and cocrystallization required the creation of a fusion protein between UBE2T and FANCL.^{140,141} This complex has previously eluded detection in living mammalian cells, although the ReBiL platform was able to readily detect the interaction. Furthermore, this assay was used to evaluate several reported small molecule and peptide antagonists of p53–MDM2 and p53–MDM4 interactions.¹³⁹ In particular, SAH peptides did not disrupt complex formation between p53 and either MDM2 or MDM4; rather, their previously reported cellular activity could be contributed to p53-independent cell membrane disruption. Importantly, ReBiL was readily adapted to 1536-well format, making it a powerful, high-throughput technique for the detection of even weak or transient protein complex formation in real time in living cells.

1.5 Dissecting protein networks *in vitro* and in cells

While the previous sections focused on methods for discovering modulators of PPIs, it is also critical to understand the impact of the molecules on broader PPI networks. A key tool here continues to be mass spectrometry. Many groups have developed methods for measuring and quantifying PPI networks in cells.¹⁴² What has been less well explored is how small molecules affect these systems. This is somewhat surprising, and a more concerted effort to study how compounds change PPI networks will provide significant insight. Inhibiting a single protein target with a small molecule affects not only the direct interactions between the target and its partners, but also propagates changes throughout the entire protein network (Figure 1.5). In addition, the shape of the ligand and the accompanying conformer of the bound protein target dictate how changes are transmitted throughout the overall protein network, both in the extent of modulation and which “arms” of the network are affected. One might envision that some inhibitors might act on the same target, but produce different outcomes because of their unique pattern of affected PPIs (Figure 1.5).

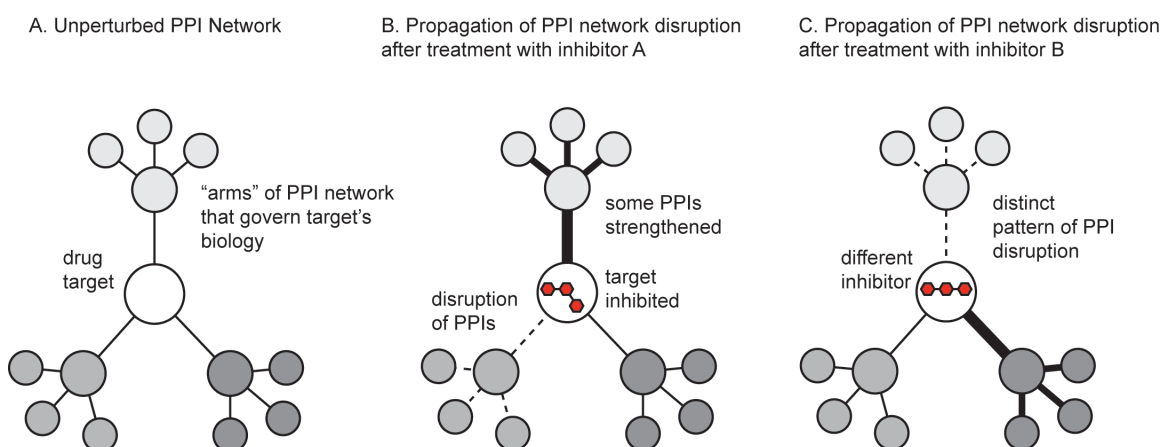


Figure 1.5 Schematic representation of how small molecules might propagate changes in protein-protein interaction networks. (A) A theoretical drug target interacts with multiple proteins, which connect it to the broader PPI network. (B) Treatment with an inhibitor might weaken some PPIs (dotted lines) and strengthen others (dark lines). The ultimate response to the inhibitor is manifested by both the direct effect on its target and the new state of the perturbed PPI network. (C) A different inhibitor, even acting on the same target, might generate a non-overlapping phenotype by trapping the target in a state that perturbs the network in distinct ways.

1.5.1 Mass spectrometry can detect changes in protein structure

Proteins and other macromolecules exist in an ensemble of conformational states, and binding to other macromolecules or ligands can have profound effects on their

dynamics.^{143,144} Each member of the structural ensemble has the potential to bind different partners or perform specific tasks.¹⁴⁵ As discussed, many small molecules trap particular protein conformations and these states can propagate important downstream effects.¹⁴⁶ Thus, one powerful method is to explore time-dependent perturbations in protein structure using mass spectrometry (MS).^{147,148} Pioneering efforts in native MS and nanoflow electrospray ionization (nESI) have revolutionized the study of large protein complexes with its increased sensitivity and preservation of weak non-covalent interactions.¹⁴⁹ Because detection occurs in the gas phase, this technique effectively captures a “snapshot” of a binding equilibrium that exists in solution. Furthermore, multiple protein partners can be detected simultaneously within the context of the larger assembly without the need to isolate specific complexes.¹⁵⁰ nESI is therefore particularly suited to the study of multi-protein complexes in real time. Recently, it has been used to quantify the assembly of complexes between the molecular chaperones Hsp90, Hsp70 and the co-chaperones FKBP52 and HOP,¹⁵¹ as well as polydispersed oligomers of small heat shock proteins.¹⁵²

Ion mobility-mass spectrometry (IM-MS) is a technique that separates macromolecules in the gas phase, analogous to electrophoresis in solution. Measurement of ion migration, or drift time, can be used to generate information on the collisional cross section of a protein of interest, which can in turn be used to infer changes in the folded conformation of a protein upon ligand or macromolecule binding.¹⁵³ The introduction of collision-induced unfolding measurements enable IM-MS to report on more subtle changes in protein tertiary structure induced by ligand binding.^{154,155} This development has been useful for evaluating different binding modes of similar ligands, in particular the subtle differences in kinase structure upon binding to type I and type II inhibitors.¹⁵⁶ This approach was sensitive enough to cluster several well-characterized type I and type II Abl kinase inhibitors based on their preferred protein structure and has the potential to be adapted to a larger screen of a chemical library for evaluation of ligand-induced changes in protein conformation.

1.5.2 Small molecules produce diverse cellular outcomes through the same target

It is important to consider that small molecule modulators of PPIs are often not simple, functional “on-off switches”. Rather, compounds can have sundry effects on function because the immediate PPIs are linked to the broader network. To illustrate this complexity, it is worth considering the example of Hsp70 inhibitors. Hsp70 is a molecular chaperone that regulates protein quality control through a conserved mechanism of ATP hydrolysis and substrate binding. Many classes of Hsp70 inhibitors have been identified and each of these inhibits nucleotide turnover *in vitro*.^{157,158} Thus, one might assume that each of these compounds have similar downstream effects on Hsp70’s functions in cells. However, this assumption turns out to be incorrect because each category of inhibitor has a unique impact on Hsp70 PPIs. Efforts by multiple groups have provided Hsp70 “inhibitors” that either compete with ATP or inhibit interactions with specific classes of co-chaperones.¹⁵⁹ In each case, the compound blocks steady-state ATPase activity *in vitro*, yet the cellular effects are not equivalent. For example, rhodacyanines that inhibit PPIs between Hsp70 and its nucleotide exchange factors¹⁶⁰ lead to dramatic degradation of the polyglutamine expanded androgen receptor (polyQ-AR),¹⁶¹ a well-established Hsp70 client, while molecules that inhibit ATP binding¹⁶² lead to substantial increases in accumulation of polyQ-AR.¹⁶³ Therefore, two classes of molecules with equivalent ability to inhibit ATPase activity have opposing effects on polyQ-AR levels, although the exact mechanisms that link these events to cellular outcome are not yet clear. Nonetheless, molecules targeting the same protein can produce distinct outcomes, likely due to differences in the way that the target, in this case Hsp70, engages with downstream partners. An increased understanding of how protein networks are linked to disease may eventually allow for a more rational approach to drug discovery and improved screening paradigms that more correctly predict outcomes. In many ways, these observations mirror what is observed in GPCR agonists/antagonists.

1.5.3 Methods for detecting small molecule-induced changes in local and global protein networks

1.5.3.1 Affinity purification and quantitative mass spectrometry

Emerging large-scale PPI maps have been instrumental in defining the protein interactome in mammalian cells.^{164,165} Advances in quantitative mass spectrometry, including its combination with affinity purification (AP-MS), have allowed for dynamic profiling of PPIs at near physiological conditions.¹⁶⁶ In this technique, a protein of interest (bait) is expressed with an epitope tag, which is used to purify the bait protein from cell lysate along with its interacting protein partners (prey).¹⁶⁷ Commonly used tags include the short FLAG tag or the tandem affinity purification (TAP) tag. The TAP approach requires two affinity tags separated by a protease cleavage site.¹⁶⁸ Purification of the bait and prey proteins from cell lysate occurs over two steps, and this strategy can decrease the identification of false positive proteins in subsequent analysis. Tandem mass spectrometry is then used for identification and quantitation of the isolated proteins. This powerful approach allows for rapid sequencing and identification of thousands of individual peptides, including characterization of post-translational modifications.^{169,170} Furthermore, mass spectrometry is readily adapted to quantify protein abundance in the original sample, which can provide insight into the dynamics of protein complex assembly (and disassembly) in response to pharmacological manipulation.¹⁷¹ It is important to note that the lack of detection in an AP-MS experiment does not imply a lack of interaction between the bait protein and a prey protein of interest. The stringency of washing conditions can disrupt transient PPIs, which can complicate analysis.¹⁶⁶

Despite these limitations, many groups have nonetheless successfully used AP-MS to identify and characterize protein complexes in living cells in response to pharmacological manipulation. In *Saccharomyces cerevisiae*, polyglutamine (polyQ) fragments form cytosolic aggregates, and this process is regulated by molecular chaperones.¹⁷² The dihydropyrimidine 115-7c promotes binding of Hsp70 to Hsp40 and polyQ, increasing polyQ solubility. AP-MS revealed changes in proteins bound to polyQ fragments as a function of polyQ length, aggregation time, and 115-7c treatment.¹⁷³ In a similar study, Thompson and coworkers used AP-MS to study acute changes in the interaction network associated with turnover of microtubule-associated protein tau.¹⁷⁴ Several proteins, including Hsp70 and Hsp90 had differential association with tau following treatment with

an inducer of tau degradation. In both examples, MS was a powerful tool for dissecting the dynamic changes in multi-protein complexes in response to pharmacological disruption of PPIs.

1.5.3.2 Covalent chemical crosslinking

A major hurdle to AP-MS is the difficulty in identifying partners with low affinity and/or low abundance. Several groups have developed creative solutions to this challenging problem, including crosslinking. Examples of synthetic crosslinkers include activated diesters linked by a cyclic quaternary diamine. The diamine is cleavable by collision-induced dissociation and facilitates identification of crosslinked peptides.¹⁷⁵ Another crosslinking method is the use of genetically encoded photoactivatable amino acids, such as *p*-benzoyl-L-phenylalanine (Bpa), which are used to covalently and site-specifically capture PPIs in their native environment.^{176,177} This approach has been successfully adapted to both stable, high-affinity PPIs as well as more transient, moderate- to low-affinity PPIs within the transcriptional machinery. Photoactivation of Bpa encoded in the transcriptional activator Gal4 captured its stable interaction with the suppressor protein Gal80.¹⁷⁸ Interactions of transcriptional activators with co-activator proteins are typically much more transient.¹⁷⁹ For example, the Swi/Snf chromatin-modifying complex is a proposed binding target for the viral activator VP16, although the specific interactions had evaded detection with traditional methods.¹⁸⁰ Photo-crosslinking of Bpa confirmed that VP16 makes direct contacts with both Snf2 and Snf5 during transcription initiation.¹⁸¹ Because this approach is site-directed, it can be combined with mass spectrometry to localize interaction “hot spots” for specific PPIs and to identify and characterize novel binding partners for a protein of interest.¹⁸²

1.5.3.3 Proximity biotinylation

A recently reported proximity biotinylation approach, BioID is a complementary method for mapping specific PPIs within large multi-protein complexes. This strategy is particularly advantageous because it does not require that complexes be maintained across numerous purification steps and therefore has the potential to identify more transient PPIs compared to traditional AP-MS techniques.¹⁸³ In this method, the bait

protein is fused to a mutated prokaryotic biotin ligase BirA. This enzyme covalently links acceptor proteins with biotin via an activated intermediate (biotinoyl-5'-AMP). However, the mutant enzyme dissociates rapidly from the activated biotinoyl-5'-AMP, creating a “cloud” of activated biotin surrounding the bait protein.¹⁸⁴ The activated biotin can then covalently modify exposed lysine residues on the prey proteins, which can include direct partners as well as neighboring proteins. Alternatively, specific prey proteins can be fused with an acceptor peptide for the biotin ligase.¹⁸⁵ Rather than subsequent affinity purification with the tagged bait protein, prey proteins are enriched with streptavidin purification and identified by mass spectrometry. This approach has been successfully adapted to the *in vivo* characterization of a number of diverse, dynamic protein complexes, including the chromatin-associated mediator complex,¹⁸⁶ members of the nuclear lamina¹⁸³ and nuclear pore complexes,¹⁸⁷ and components of the inner membrane complex in *Toxoplasma gondii*, among others.¹⁸⁸ These complementary approaches, including AP-MS, protein crosslinking, and proximity biotinylation can be used in tandem to create a full picture of a protein complex in living cells, as each approach has the potential to identify novel interactions.

1.6 Conclusions and Outlook

Multi-protein complexes are the “hubs” of the cellular PPI networks and attractive drug targets for a variety of diseases. I have illustrated in this chapter several “success stories” of small molecules that target PPIs. Often, the development of new methodology was required to identify these PPI modulators. Indeed, creative HTS strategies are beginning to expand the toolbox of available approaches, although there is no algorithm or “road map” for a successful screen. Rather, each campaign must be designed individually, taking into account the affinity of the interactions, the topology of the interaction surfaces, and the interplay between different components of the system. For instance, a phenotypic or gray-box screen has the best chance of success for finding small molecules that can perturb protein networks. However, these strategies require significant knowledge of the structure and function of individual PPIs within a greater protein complex, highlighting the importance of basic research in order to be able to ask the right questions.

1.7 Thesis outline

Although great strides have been made in targeting PPIs with small molecules, several fundamental questions remain; namely, can we selectively modulate some PPIs and not others within a larger protein network? Can we use such inhibitors to reveal biological functions of a given protein complex? Finally, can small molecules be used to “tune” protein networks in a predictable way? In this dissertation, I address several of these key questions. In Chapter 2, I outline a novel, robust HTS strategy for finding inhibitors of specific PPIs within the Hsp70 chaperone complex. In Chapter 3, I use an inhibitor of the Hsp70–BAG interaction to elucidate the role of this complex in pro-survival signaling. This probe allowed me to discover that the inhibitor of apoptosis proteins (IAPs) are a previously unexplored class of Hsp70 client proteins. In Chapter 4, I describe initial efforts to study the effect of inhibitors on more global protein networks, using protein kinases and the Hsp70 system as illustrative examples. Finally in Chapter 5, I discuss the implications of this work and describe future strategies for targeting PPIs, both for the development of tool compounds as well as potential therapeutics.

Notes

This chapter is adapted from Cesa, L. C. *et al.* “Direct and Propagated Effects of Small Molecules on Protein-Protein Interaction Networks” **2015** *Frontiers in Bioengineering and Biotechnology* 3: 119. Laura C. Cesa, Anna K. Mapp, and Jason E. Gestwicki contributed to these ideas.

Chapter 2

Inhibitors of Difficult Protein-Protein Interactions Identified by High-Throughput Screening of Multi-protein Complexes

2.1 Abstract

Multi-protein complexes are important in all aspects of cellular function, and there is interest in finding inhibitors of individual protein–protein interactions (PPIs) within these complexes. As discussed in Chapter 1, PPIs with weak affinities and/or large interfaces have traditionally been more resistant to the discovery of inhibitors, partly because it is more challenging to develop high-throughput screening (HTS) methods that permit direct measurements of these physical interactions. In this chapter, we explore whether the functional consequences of altering a weak PPI might be used to assess binding of a small molecule modulator. As a model, we used the bacterial ATPase DnaK and its partners DnaJ and GrpE. Both DnaJ and GrpE bind DnaK and catalytically accelerate its ATP cycling, so we used stimulated nucleotide turnover to indirectly report on the status of these PPIs. In pilot screens, we identified compounds that blocked activation of DnaK by either DnaJ or GrpE. Interestingly, at least one of these molecules selectively blocked binding of DnaK to DnaJ, while another compound disrupted allostery between DnaK and GrpE without altering the physical interaction. These findings suggest that the activity of a reconstituted multi-protein complex might be used in some cases to identify allosteric inhibitors of specific, challenging PPIs within a larger protein network.

2.2 Introduction

Multi-protein complexes are critical to cellular functions.^{7,8,189,190} These complexes are typically assembled from a combination of enzymes and non-enzymes: the enzymes, such as demethylases, proteases, or ATPases, often conduct the work associated with the system, while the non-enzymes regulate this activity, either by dictating subcellular location, guiding the selection of binding partners, or controlling enzyme turnover rates.

Thus, the protein–protein interactions (PPIs) between enzymes and non-enzymes are critical for the overall function of the complexes and inhibitors of these PPIs are important chemical probes.^{13,24} More recently, there has also been renewed interest in targeting PPIs in the treatment of disease.^{12,14,19,20}

2.2.1 PPIs are challenging drug targets

As discussed in Chapter I, while there has been tremendous progress in the general area of PPI inhibitors, it has become clear that some types of PPIs are more challenging to target than others.^{21,191} In particular, PPIs involving weak ($K_D > 200$ nM) interactions that occur over large contact surfaces ($> 2,500$ Å²) tend to be more difficult to inhibit.²¹ One challenge in finding inhibitors of weak interactions is that it is difficult to develop robust, high-throughput screening (HTS) methodology to directly measure the physical interactions between transient partners. Accordingly, many research groups have been interested in exploring new HTS platforms that are specifically designed for use against these types of challenging PPIs.^{129,130} These methods, such as fragment-based screens and high content screening (HCS), are promising to open the number of “druggable” PPIs to include even the challenging targets.^{21,191}

2.2.2 The prokaryotic Hsp70 multi-protein complex as a model system

Despite the advances described in Chapter 1, major challenges remain, particularly in targeting those PPIs involving weak interactions. These observations have driven us to use the *Escherichia coli* chaperone complex, which is composed of an enzyme (DnaK) and multiple non-enzymes (DnaJ, GrpE, and peptide substrate), as a model system.¹⁹² DnaK is a member of the highly conserved heat shock protein 70 kDa (Hsp70) family of molecular chaperones, which are important in protein quality control.^{193,194} Like other Hsp70s, DnaK is an ATP-driven enzyme that has a nucleotide-binding domain (NBD) and a substrate-binding domain (SBD) (Figure 2.1). ATP is hydrolyzed in the NBD, while the SBD binds to hydrophobic segments of polypeptides, such as those exposed in misfolded proteins.^{195,196} Allosteric communication between the two domains modulates the affinity of DnaK for peptides; DnaK binds peptide substrates loosely in the ATP-bound state, while it binds tightly in the ADP-bound form.^{197,198} A

major role of DnaK's non-enzyme partners, DnaJ and GrpE, is to regulate this ATP cycling. Specifically, DnaJ and peptide substrates stimulate the rate of nucleotide hydrolysis in DnaK,^{127,199} while GrpE accelerates release of ADP and peptide.¹²⁶ Together, the components of the DnaK-DnaJ-GrpE-peptide complex work together to coordinate ATP hydrolysis and regulate dynamic binding to misfolded proteins.

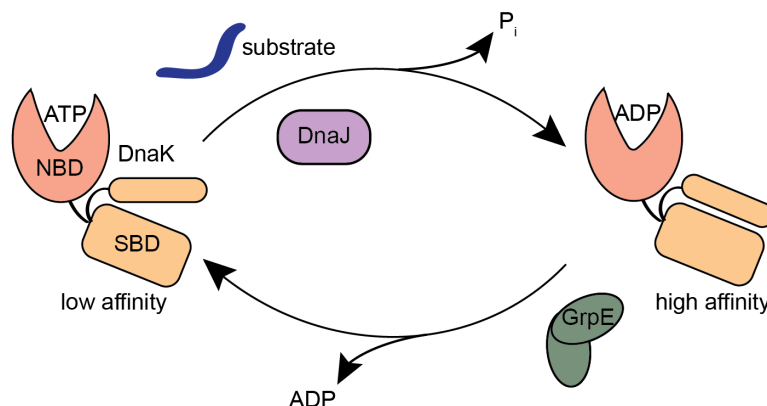


Figure 2.1 Schematic of the DnaK-DnaJ-GrpE-substrate system. Nucleotide hydrolysis by DnaK is stimulated by DnaJ and peptide substrate, while GrpE stimulates ADP and peptide substrate release. ATP-bound DnaK has low affinity for substrates, and ATP hydrolysis triggers the ADP-bound, high affinity conformation.

Each of the components of the DnaK-DnaJ-GrpE-peptide complex is thought to play an important role in chaperone functions *in vivo*, and this system is highly conserved in mammals.¹⁹² Thus, inhibitors of the individual PPIs are expected to be powerful chemical probes, and these molecules may even find use in the treatment of bacterial infections, cancer, and neurodegenerative diseases.¹⁵⁷ However, DnaJ and peptides each bind DnaK with weak, micromolar affinities,^{128,200} while GrpE binds DnaK over a large and topologically complex surface ($\sim 2800 \text{ \AA}^2$).¹²⁶ These partners interact with DnaK transiently (*e.g.*, fast on-fast off), acting as catalysts rather than stable binding partners. As evidence of this mechanism, sub-stoichiometric amounts of DnaJ are sufficient to convert DnaK from its ATP- to ADP-bound state under single turnover conditions.²⁰¹ Further, structural studies on DnaK-DnaJ have provided insight into the possible mechanism of this transient interaction, as the protein-protein contact surface is shallow and almost entirely electrostatic,¹²⁸ suggesting that the two proteins form dynamic complexes that are able to form and dissociate rapidly. In *E. coli*, the levels of DnaK are

approximately 10-fold greater than the concentration of DnaJ or GrpE, suggesting that this weak interaction is physiologically relevant.

2.2.3 Enzymatic activity of reconstituted protein complexes can be used as a surrogate for binding in HTS

As discussed above, it has proven especially challenging to find inhibitors of weak, transient PPIs, such as those between DnaK-DnaJ, not only because of these interactions are difficult to detect, but also for practical concerns including the high concentration of sample required for stringent binding screens.^{24,202} In this chapter, we hypothesized that we could use the enzymatic activities of the reconstituted DnaK-DnaJ, DnaK-GrpE, and DnaK-peptide complexes as a surrogate for the physical, bimolecular interactions. We considered this approach potentially feasible because, despite their moderate to weak affinities for DnaK, each of the non-enzyme partners (DnaJ, GrpE, and peptide substrates) produce dramatic effects on ATP cycling, enhancing steady-state hydrolysis by approximately 10-fold, 2-fold and 3-fold, respectively.^{127,203} Thus, even though they bind transiently, these non-enzyme “catalysts” produce potent effects on nucleotide turnover.

We measured phosphate release from eight distinct, reconstituted *E. coli* DnaK complexes and screened a pilot chemical library for possible inhibitors. Strikingly, we found that both the identity of the non-enzyme (*e.g.*, DnaJ or GrpE) and its stoichiometry relative to DnaK (*e.g.*, maximal or half-maximal) affected the number and types of inhibitors that were identified. At least one of these molecules had the characteristics of a direct inhibitor of the DnaK interaction with DnaJ, while another molecule operated at an allosteric site in DnaK to block stimulation by GrpE. These results suggest that PPI inhibitors with distinct mechanisms-of-action can be identified via screening reconstituted multi-protein complexes *in vitro*. This approach should contribute to a growing arsenal of HTS methods for finding inhibitors of challenging PPIs.

2.3 Results

We reasoned that one way to screen for inhibitors of weak PPIs might be to monitor the functional consequences of the interactions (*e.g.*, ATP hydrolysis), rather than measuring the physical binding events themselves. This approach, termed “gray-box screening” is particularly well suited for weak contacts, such as the one between DnaK and DnaJ, because these interactions are technically challenging to directly measure using typical, HTS-compatible formats, such as flow cytometry, FP, AlphaLisa, or surface plasmon resonance (SPR).^{83,204} Yet, the transient PPIs between DnaK and DnaJ provide robust and readily measured changes in enzymatic turnover.^{127,199}

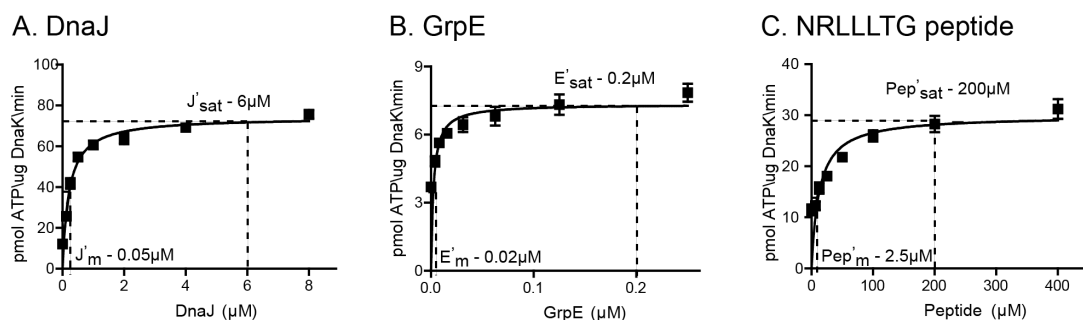


Figure 2.2 Characterization of the stimulatory effects of DnaJ, GrpE, and NRLLLTG peptide on ATP turnover. Stimulation of DnaK's ATPase activity by (A) DnaJ, (B) GrpE, and (C) NRLLLTG peptide was measured by malachite green. Results are the representative averages of triplicates of three independent experiments, and error is SEM. Data were fit to the Michaelis-Menten equation. The saturation (sat) and half-maximal (M) values are shown. DnaK = 0.4 μM.

2.3.1 Design of HTS campaigns to identify inhibitors of the DnaK-DnaJ-GrpE-peptide system

A series of small-scale pilot screens was performed to better understand the potential feasibility of the PPI surrogate approach. We first expressed and purified *E. coli* DnaK, DnaJ and GrpE and synthesized a model peptide substrate with the sequence NRLLLTG.²⁰⁵ Using an adaptation of a malachite green assay for detecting release of inorganic phosphate,²⁰⁶ we confirmed that DnaJ, GrpE and the NRLLLTG peptide all stimulated the steady state ATPase activity of DnaK. During these experiments, we also determined the levels of each partner that was required to maximally and half-maximally promote hydrolysis (Figure 2.2). For example, DnaJ stimulated the ATPase activity of DnaK (0.4 μM) with a half-maximal concentration of 0.05 μM and reached full

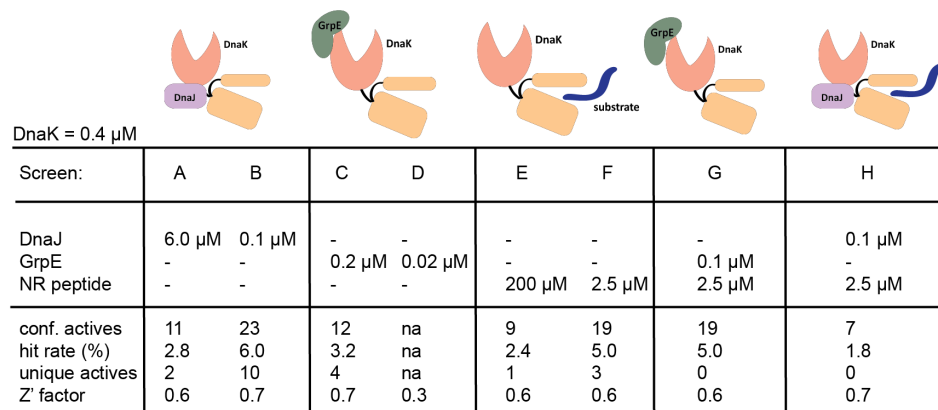
stimulation at $\sim 6\ \mu\text{M}$, values consistent with published values.^{127,203} We then reconstituted DnaK with each of these partners to establish a series of 8 different screening targets (screens A-H) (Figure 2.3A). All of the screens used the same amount of DnaK ($0.4\ \mu\text{M}$) and varied only in the identity and relative stoichiometry of the non-enzyme binding partner. In selecting this series of targets, we focused on exploring the effects of molar ratio by either saturating the levels of the partners (screens A, C, and E) or using half-maximal amounts (screens B, D, and F) (Figure 2.3A). We hypothesized that high levels of non-enzyme partner might yield better signal:noise and Z' values, while half-maximal levels might facilitate discovery of PPI inhibitors by decreasing competition between the test molecules and the partner proteins. In addition to the binary complexes, we also assembled ternary complexes of DnaK-DnaJ-peptide (screen G) and DnaK-GrpE-peptide (screen H). Screen G was included because DnaJ and peptide are known to use synergistic allosteric pathways to stimulate ATP hydrolysis,²⁰⁷ while screen H was included because GrpE alone has a relatively modest effect on ATPase activity, and we suspected that the signal:noise in the DnaK-GrpE screens (screens C and D) may not be sufficient to achieve good screening parameters.

2.3.2 Parallel chemical screens yield inhibitors of distinct DnaK complexes

The series of reconstituted targets was screened against a pilot library of ~ 300 molecules.¹²⁹ This library was composed of commercially available compounds and was assembled at the University of Michigan's Center for Chemical Genomics. Guided by previous observations,¹³² we specifically selected a library enriched in plant natural products because these molecules are expected to yield relatively high "hit rates" (up to 3% or 4% in some DnaK screens),¹³² allowing us to rapidly and cost effectively test the performance of this HTS approach on a relatively small number of compounds. On each plate, 12 wells were assigned to a positive control (*e.g.*, lacking only the enzyme, DnaK) and 12 wells served as negative controls (1% DMSO). Active molecules were defined as those that reduced the signal by at least three standard deviations from the negative controls with intrinsic fluorescence values less than 500 AFUs. Compounds that met these criteria were then subjected to dose-response in triplicate and were considered "confirmed actives" if they had IC_{50} values less than $75\ \mu\text{M}$ (Figure 2.3A). Of the eight

screens, only the DnaK-GrpE screen with low GrpE levels (screen D) failed to give a Z' factor greater than the 0.5 cutoff due to a poor signal:noise; thus, it was removed from subsequent analyses.

A. Results of parallel HTS pilot screens against reconstituted complexes



B. DnaK-DnaJ and DnaK-GrpE screens against an expanded chemical collection

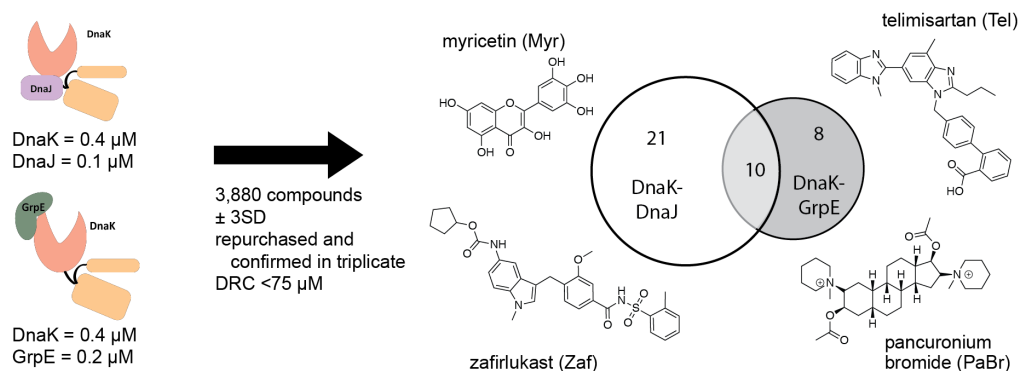
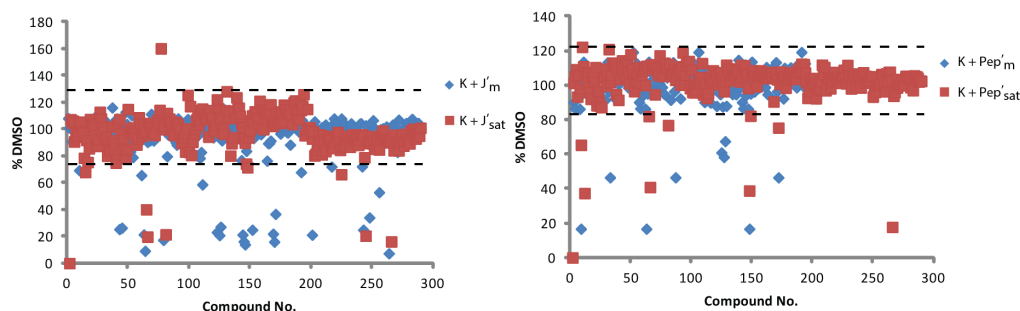


Figure 2.3 High-throughput screens identify selective inhibitors of individual multi-protein complexes. (A) Results of eight parallel, pilot HTS campaigns. The indicated non-enzyme partner was added at an amount that either saturated steady-state ATP hydrolysis or at the half-maximal amount ($K_{M,app}$). Confirmed actives = repeated in triplicate, dose response < 75 μ M. Unique actives = compounds found with a specific non-enzyme but not others. (B) Comparison of the actives from screening 3,880 molecules against the DnaK-DnaJ and DnaK-GrpE combinations in 384-well plates. In these screens, DnaJ was used at $K_{M,app}$ and GrpE at saturation. The chemical structures of representative unique actives are shown.

A. Samples of the screening results



B. Structures of selective DnaK-DnaJ and DnaK-GrpE inhibitors from the primary HTS

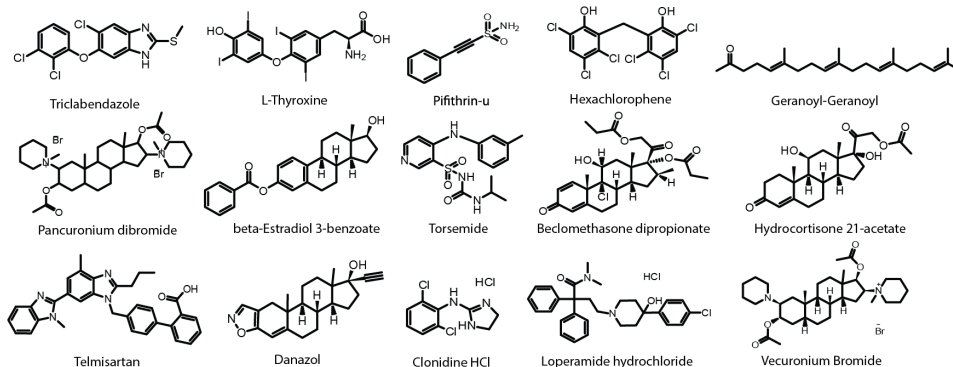


Figure 2.4 Additional results from the parallel HTS campaigns. (A) Representative examples of the primary, raw screening results, highlighting the effects of saturating non-enzyme partner. (B) Chemical structures of the molecules re-purchased and confirmed as inhibitors of DnaK-DnaJ or DnaK-GrpE.

2.3.2.1 Varying the identity and stoichiometry of the non-enzyme enables the discovery of unique inhibitors

From the pilot screening results, a number of observations were made. First, seven compounds were inhibitors of all reconstituted complexes, regardless of their composition. The broad activity of these molecules suggests that they may be competitive inhibitors of ATP binding in DnaK or that they interfere with the assay (*e.g.*, strong aggregators). More interesting were the compounds that acted on only specific multi-protein complexes, but not others (“unique actives”) (Figure 2.3A and B). For example, 10 compounds were identified as active in only the DnaK-DnaJ screen (screen B), but not the screens involving GrpE or peptide (screens C, E, and F). Likewise, 4 compounds were inhibitors in the DnaK-GrpE screen (screen C), but not in the screens involving any of the other non-enzymes. These results suggest that the combination of components chosen for the screen may favor discovery of molecules exclusive for that pair. This is an

interesting result because the same enzyme, DnaK, is used in all of the parallel pilot screens. We speculate that conformational changes, which occur as a consequence of the individual PPIs, might create new opportunities for inhibitor binding. For example, the ADP-bound form of DnaK is not heavily populated in the absence of DnaJ, because the rate-limiting step, ATP hydrolysis, is slow.²⁰⁸ Thus, molecules that bind the ADP-bound state of DnaK might only become potent when this state becomes significantly populated by the DnaJ-DnaK interaction. Another observation was that screens of ternary combinations did not reveal new compounds that were not already found in the relevant binary complexes (Figure 2.3B), although this result may be influenced by the small size of the pilot library.

We also found that “saturating” the amount of non-enzyme (especially DnaJ or peptide) tended to suppress the identification of inhibitors, consistent with the idea that half-maximal levels are more permissive to inhibitor discovery (Figure 2.3A and Figure 2.4A). For example, dropping the level of DnaJ to its half-maximal concentration (0.05 μ M) increased the number of confirmed actives from 11 to 23 (Figure 2.3A). This observation is interesting because HTS campaigns, at least in our experience, typically start with the goal of optimizing the signal:noise in order to obtain the best possible screening statistics (*e.g.*, Z' factor, *etc.*). Thus, maximizing the signal in a PPI assay may, in some cases, create a disadvantage for the discovery of inhibitors. Together, these studies provided insights into the design principles and implementation strategies for screens against reconstituted multi-protein complexes.

2.3.2.2 HTS hits are selective inhibitors of specific PPIs

Next, we wanted to explore this HTS concept in studies of larger and more diverse chemical collections. In these studies, we focused on the DnaK-DnaJ (screen B) and DnaK-GrpE (screen C) combinations for rescreening against an expanded collection of \sim 3880 known bioactive molecules, including the MS2000 and NCC libraries. These compounds were screened at \sim 50 μ M in 384-well plate format using a quinaldine red-based modification of the malachite green assay.²⁰⁹ The Z' factors from these screens were between 0.6 and 0.7, and CV values were between 6% and 9% (Figure 2.3A). The

primary actives were subject to the same triage criteria as in the pilot screens, yielding 31 confirmed hits against DnaK-DnaJ and 18 against DnaK-GrpE. Of these compounds, 10 were common to both DnaJ and GrpE, leaving 21 unique hits for DnaK-DnaJ and 8 for DnaK-GrpE (Figure 2.3B). The unique inhibitors of DnaK-DnaJ included myricetin (Myr) and zafirlukast (Zaf), which were previously identified as inhibitors of DnaK-DnaJ.^{130,132} In addition, these screens revealed a number of additional molecules, including pancuronium bromide (PaBr) and telmisartan (Tel), which appeared as actives in the DnaK-GrpE screen but not the DnaK-DnaJ screen (Figure 2.3B).

Using repurchased compounds, we confirmed that Myr and Zaf are only inhibitors of the DnaK-DnaJ combination (Figure 2.5A), while Tel and PaBr were only inhibitors of the DnaK-GrpE combination (Figure 2.5B). For example, Zaf inhibited DnaJ-stimulated ATPase activity ($IC_{50} = 37 \pm 1 \mu M$) but did not have a measurable effect on GrpE-stimulation ($IC_{50} > 200 \mu M$). Because PaBr is weakly soluble and the activity of Myr has already been reported,¹³² we selected Zaf and Tel as test molecules for further characterization. Specifically, we measured the activity of these molecules against each of the possible binary combinations (DnaK-DnaJ, DnaK-GrpE, and DnaK-peptide) and against DnaK's intrinsic ATPase activity. In these studies, we varied the levels of each non-enzyme and tested if compounds could interfere with the individual stimulatory activities. These results showed that Zaf is able to suppress the activity of DnaK-DnaJ, but that it had weak or no activity against DnaK-GrpE or DnaK alone (Figure 2.5C). In contrast, Tel had little activity against DnaK alone or the complexes containing DnaJ or peptide but it significantly inhibited the DnaK-GrpE combination (Figure 2.5D).

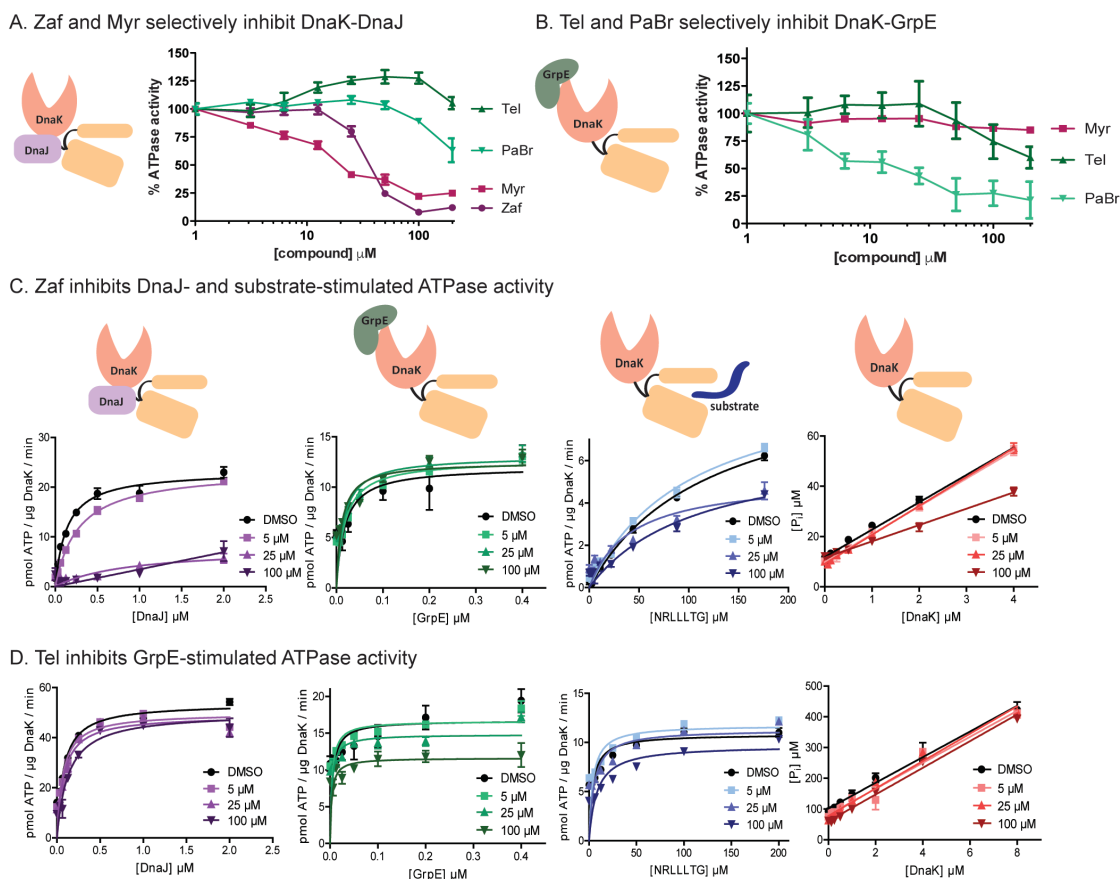


Figure 2.5 Active compounds identified in the binary HTS experiments are selective for either DnaJ- or GrpE-stimulated ATPase activity. (A) Zaf and Myr inhibit ATPase activity of the DnaK-DnaJ complex. Results are the representative averages of triplicates of three independent experiments. Error bars represent SEM. (B) Tel and PaBr inhibit the DnaK-GrpE complex. (C, D) The ATPase activity of either DnaK alone or DnaK stimulated by DnaJ, GrpE, or peptide substrate (NRLLLTG) was measured at three concentrations of Zaf (C) or Tel (D). Zaf has activity against the DnaK-DnaJ and DnaK-substrate combinations, with weak activity against the DnaK alone or DnaK-GrpE combinations. Conversely, Tel inhibited the DnaK-GrpE pair but had weak activity against the others. All experiments are representative averages of triplicate of three independent experiments, and the error bars represent SEM. Curves were fit to the Michaelis-Menten equation.

We next wanted to explore the mechanisms-of-action of Zaf and Tel to begin defining the general ways that the compounds might interfere with the functions of the DnaK multi-protein systems. Specifically, we were interested in whether these molecules might directly compete with non-enzyme partners for binding to DnaK (“orthosteric” inhibitors) or whether they might impact the communication between DnaK and the non-enzymes without disrupting the PPI itself (*e.g.*, by binding to an important allosteric site).

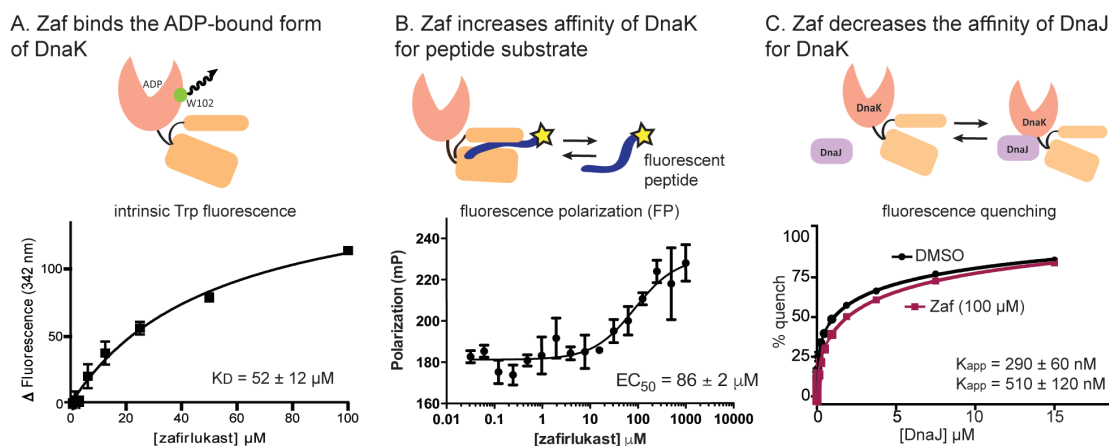


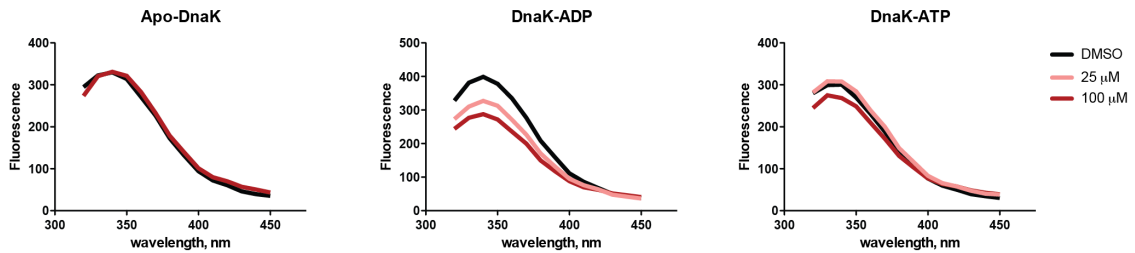
Figure 2.6 Zaf binds the ADP-bound form of DnaK and enhances the apparent affinity of DnaK for substrates. (A) Intrinsic Trp fluorescence of DnaK in the presence of ADP (1 mM) and Zaf. Zaf had no effect on Trp fluorescence in the ATP-bound states ($p = 0.06$) (Figure 2.5). Results are the representative averages of triplicates of three independent experiments, and the error bars represent SEM. (B) Zaf enhances the apparent affinity of DnaK for a model peptide substrate (FITC-HLA), as measured by fluorescence polarization (FP). (C) Zaf partially inhibits binding of DnaJ to DnaK. DnaK and DnaJ were labeled with a fluorescence quench pair, as described in Section 2.6. Zaf weakened the interaction by ~ 2 -fold ($p = 0.07$). Binding curves were fit to the Langmuir binding equation; does-response curves were fit to the Hill equation.

2.3.3 Zafirlukast preferentially binds ADP-DnaK and enhances DnaK's affinity for substrate

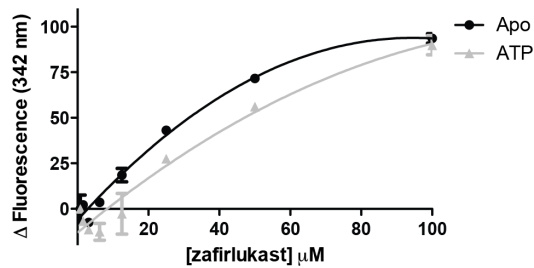
To explore the mechanism by which Zaf inhibits the DnaK-DnaJ combination, we first tested whether it interacted with DnaK using intrinsic tryptophan fluorescence. DnaK has a single tryptophan located at the NBD-SBD interface (Figure 2.6A), and this residue is commonly used to probe structural changes in DnaK.²¹⁰ When DnaK (5 μM) was incubated with 25 or 100 μM concentration of Zaf, the fluorescence intensity at 342 nm decreased by $\sim 25\%$ and the peak shifted by ~ 2 nm (Figure 2.7A), suggesting that Zaf binds to DnaK. Using this approach, dose-dependent changes in tryptophan fluorescence were measured, and we found that the apparent affinity (K_D) was dependent on nucleotide: Zaf bound DnaK with a K_D of 52 ± 12 μM in the presence of ADP (Figure 2.6A), but its K_D was greater than 100 μM for apo- or ATP-bound DnaK (Figure 2.7B). The ADP-bound form of DnaK is known to have a better affinity for peptide substrates.¹⁹⁶ Thus, to test whether Zaf could stabilize the “tight binding” form of DnaK, we measured the affinity of DnaK for a fluorescent 10-mer peptide derived from the MHC class I antigen HLA-B2702 (FITC-HLA). We first confirmed that FITC-HLA binds to DnaK

with low micromolar affinity using a fluorescence polarization (FP) assay (Figure 2.7D). This affinity is similar to what had been previously found for binding of FITC-HLA to human Hsp70.²¹¹ Addition of Zaf enhanced the apparent affinity of DnaK for FITC-HLA (Figure 2.6B), suggesting that it stabilizes the tight-binding form of DnaK.

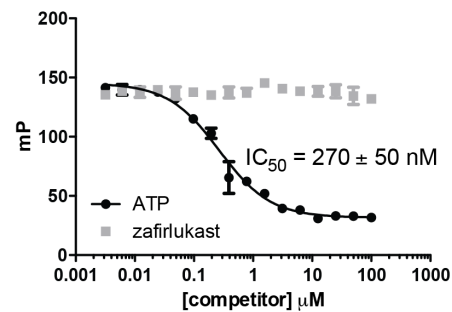
A. Tryptophan fluorescence spectra



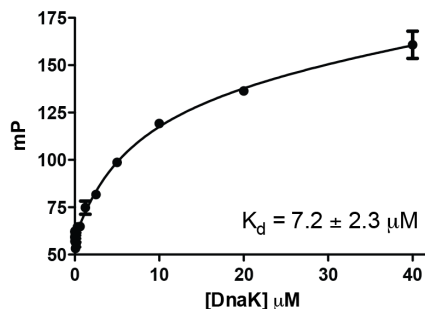
B. Zaf binds weakly to apo- and ATP-DnaK



C. Zaf does not compete with a fluorescent ATP analog



D. DnaK binding to FITC-HLA peptide



E NRLLLTG peptide and tau compete for binding of FITC-HLA to DnaK

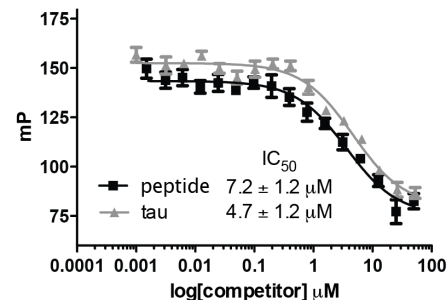


Figure 2.7 Controls and characterization of Zaf activity in the DnaK-DnaJ-GrpE systems. (A) Raw tryptophan fluorescence spectra of Zaf binding to DnaK in the apo, ADP-, and ATP-bound forms. Nucleotide was added at 1 mM. Signal for Zaf alone was subtracted. (B) Zaf binds very weakly to the ATP-bound form of DnaK, as measured by tryptophan fluorescence (see Figure 2.4A for the ADP results). (C) Zaf does not compete with a fluorescent nucleotide for binding to DnaK. ATP is shown as a positive control. (D) DnaK binds to the FITC-HLA peptide, similar to what was previously reported for human Hsp72. (E) As positive controls, both NRLLLTG peptide and human tau compete for binding with the FITC-HLA peptide, showing that binding occurs in the SBD. Results are the representative averages of triplicates of three independent experiments, and error bars represent SEM. Binding data were fit to the Langmuir binding equation; inhibition data were fit to the Hill equation.

To better understand the relationship between Zaf and nucleotide binding, we performed additional FP studies with a fluorescent nucleotide analogue (FAM-ATP). In this assay, Zaf was unable to compete with FAM-ATP for binding to DnaK (Figure 2.7C), suggesting that it binds outside the ATP-binding cleft to stabilize the ADP-bound state. Finally, we tested whether Zaf might block binding of labeled DnaJ to DnaK, using a fluorescence-quenching assay.¹³² In this platform, Zaf slightly weakened binding of DnaJ to DnaK by ~1.8-fold (Figure 2.6C). Although this effect did not reach statistical significance, it was nonetheless reproducible, suggesting that Zaf might partially block this PPI. Together, these studies suggest that Zaf binds the ADP-bound form of DnaK, stabilizes binding to peptides, and partially inhibits physical interactions with DnaJ.

2.3.4 Telmisartan interacts with the IB subdomain of DnaK and allosterically inhibits nucleotide affinity

To elucidate the mechanism of Tel inhibition, we first tested whether the molecule might bind to DnaK using the tryptophan fluorescence assay described above. Unfortunately, Tel interfered with the Trp fluorescence signature, preventing interpretation of the data (not shown). However, a recent mutagenesis study suggested a pocket in DnaK that might be involved in Tel-mediated inhibition of GrpE function.²¹² Specifically, it was recently found that mutations in the IB and IIB subdomains of DnaK, including Phe67, Arg71, Phe91 and Lys263, suppresses the ability of GrpE to stimulate DnaK's ATPase activity. Because the behavior of these mutants was similar to what was seen with Tel addition, we hypothesized that the compound might also bind in this region. To test this model, we used induced fit docking to generate a model of Tel bound to the putative binding pocket in the NBD of DnaK (see Section 2.6). This simulation suggested that Tel might bind between the IB and IIB subdomains, and in the two best, low energy orientations, Tel was predicted to make hydrophobic contacts with a series of residues (Figure 2.8A). To test this prediction, we titrated Tel into a sample of ¹⁵N DnaK_{NBD} (residues 1–388) and performed the TROSY-HSQC NMR experiment (Figure 2.8B). Analysis of the results suggested a number of strong (two standard deviations, 2σ) and intermediate (at least one standard deviation, 1σ) chemical shift perturbations. Mapping these chemical shifts onto the DnaK_{NBD} crystal structure (PDB id 1DKG) supported the

idea that Tel binds to the 1B subdomain of the chaperone (Figure 2.8B and C). Residues with the largest change in chemical shift were found in the site predicted by computational docking to bind Tel. Additional residues were clustered in surface-exposed regions of the NBD, which could arise from allosteric interactions. We did not observe any binding of Tel to either DnaJ or GrpE by isothermal calorimetry (ITC) ($K_D > 100 \mu\text{M}$) (Figure 2.10D). Together with the NMR data, the results suggest that Tel binds to DnaK in the NBD, but not to either of the co-chaperones.

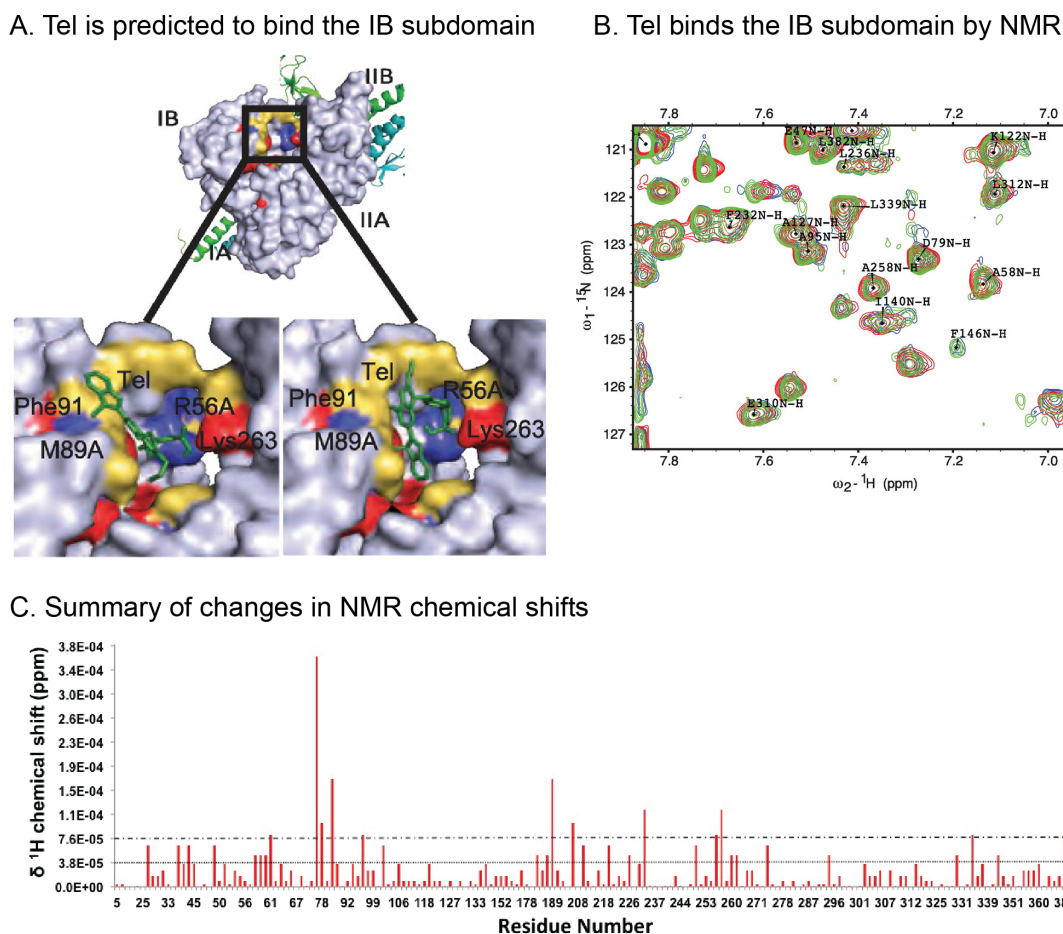
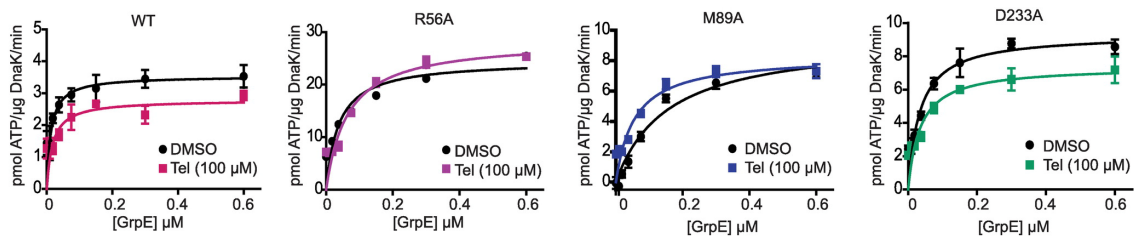


Figure 2.8 Tel binds DnaK_{NBD} by NMR. (A) Results of docking Tel to the IB subdomain, showing the two lowest energy conformations (see Section 2.6 for details). GrpE is removed from the structure (PDB id 1DKG) for clarity. (B) Titration of Tel into the nucleotide-binding domain of DnaK (^{15}N DnaK_{NBD}) provided NMR chemical shifts that support the binding of Tel to DnaK. Red = $> 2\sigma$ shift; yellow = $> 1\sigma$ shift; green = $< 1\sigma$ shift; gray = unassigned or overlapped. (C) Quantification of the changes in the proton NMR chemical shifts after Tel treatment. The dotted line represents the standard deviation of all the changes (σ); the dashed line represents 2σ .

A. Point mutants in DnaK support the Tel-binding site



B. Overlay of Tel-sensitive residues with DnaK_{NBD}-GrpE crystal structure

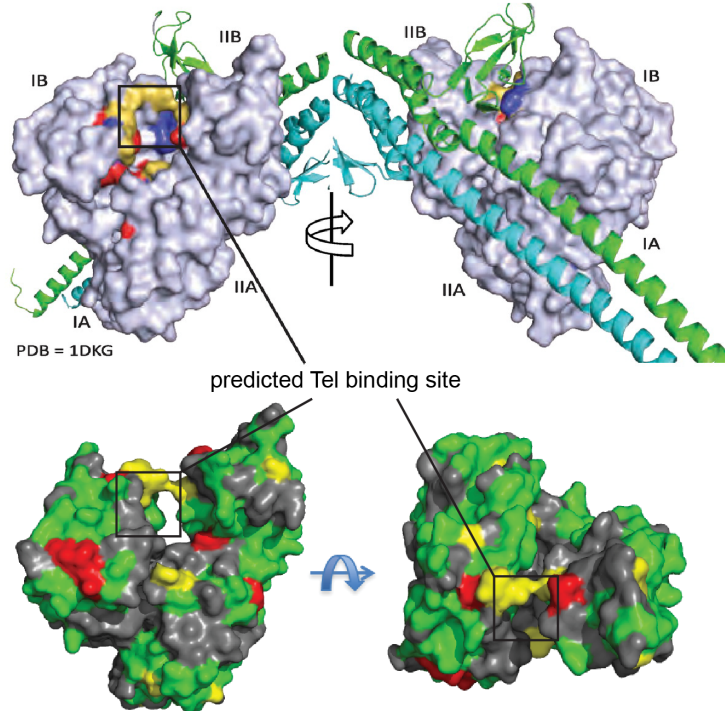


Figure 2.9 Tel binds subdomain IB in DnaK to allosterically block GrpE activity. (A) Mutation of residues in the predicted docking site supports the proposed Tel-binding site. Tel inhibits GrpE stimulation of wild type and a control mutant (D233A), but mutations near the proposed binding site (R56A and M89A) were resistant. Results of the ATPase assays are the average of triplicates, and error bars represent SEM. (B) Overlay of Tel-sensitive residues on the co-crystal structure of DnaK's NBD in complex with GrpE. Red = mutations that block GrpE stimulation. Blue = mutations that block Tel activity. Yellow = residues predicted to bind Tel by docking.

To further explore the binding site suggested by the docking and NMR studies, we mutated some of the nearby residues (Arg56 and Met89) in the pocket and an unrelated residue, Asp233,²¹² and measured the ability of Tel to block GrpE-stimulation of these mutants using ATPase assays. These studies showed that both R56A and M89A were resistant to Tel, while the control mutant (D233A) was identical to wild type (~ 1.5-fold increase in K_M) (Figure 2.9A). Together, these results suggest that Tel might bind in a

pocket between the IB and IIB subdomains of DnaK. Interestingly, this predicted binding site does not overlap with the surface of DnaK that is normally bound to GrpE¹²⁶ (Figure 2.9B), suggesting that Tel acts through an allosteric mechanism. In fact, Tel had no effect on the physical interaction between DnaK and GrpE, as measured by the fluorescence-quenching assay (Figure 2.10A). Together, these data suggest that Tel may interrupt allosteric conformational changes that occur in DnaK upon binding of GrpE, without blocking their physical interaction.

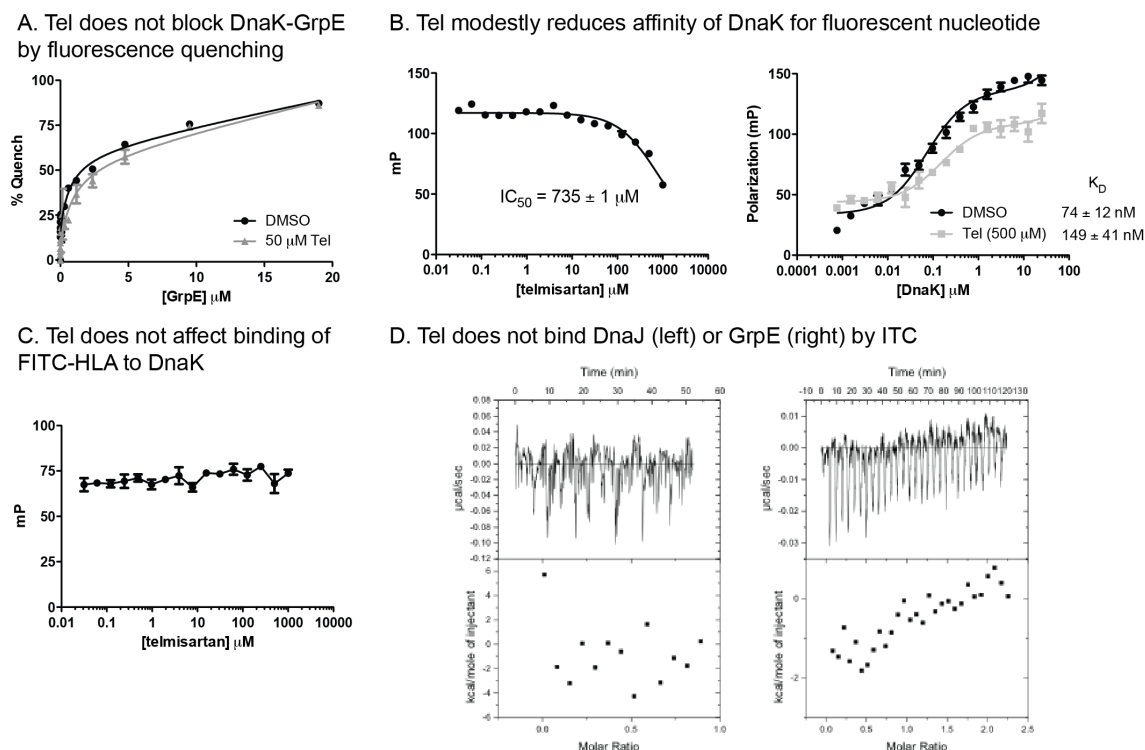


Figure 2.10 Characterization of Tel effects on binding of DnaK to GrpE and peptide substrate. (A) Labeled DnaK binding to GrpE was measured as in Figure 2.6B. Tel did not have any effect on the apparent affinity ($p = 0.33$). (B) Tel inhibits binding of fluorescent nucleotide (FAM-ATP) to DnaK, as measured by FP. (C) Tel did not inhibit binding of DnaK to FITC-HLA peptide. All results are representative averages of three independent experiments, and error bars represent SEM. Binding data were fit to the Langmuir binding equation; inhibition data were fit to the Hill equation. (D) Tel did not bind to either DnaJ or GrpE, as measured by ITC.

2.4 Discussion

There is growing interest in targeting PPIs and an emerging realization that not all PPIs are equally amenable to HTS-based methods. We performed pilot screens using eight different combinations of DnaK with its various non-enzyme partners to explore whether stimulated enzymatic activity might be used as a surrogate for transient or challenging

PPIs. An interesting observation from the pilot screens was that changing the identity of the non-enzyme component (*e.g.*, switching DnaJ for GrpE) allowed discovery of “unique actives” (*e.g.*, those some compounds that inhibit one combination and not others). On first glance, this finding is counterintuitive, because the same enzyme, DnaK, was used in all of the screens. Why might changing the identity of the non-enzyme favor discovery of unique actives? It would seem unlikely that these compounds could be competitive with nucleotide, because such molecules would be expected to be inhibitors of all the combinations. Rather, our follow-up studies on Zaf and Tel (see Figures 2.6 through 2.10) suggest that the molecules identified using this HTS approach may be more likely to disrupt specific PPIs or PPI-induced conformational changes. Another theoretical way that unique actives might emerge from these types of screens is through the action of the compounds on the non-enzyme (*e.g.*, DnaJ or GrpE) itself. It is important to note that we cannot fully discount the possibility that Tel or Zaf might weakly bind to GrpE or DnaJ, although we were unable to measure such an interaction. However, it seems logical that such mechanisms will be identified in screens of larger chemical collections.

2.4.1 Chemical screens yield molecules with distinct inhibitory mechanisms

Following the pilot screens, we examined ~ 3,800 compounds for their ability to inhibit ATPase activity of either the DnaK-DnaJ or DnaK-GrpE complexes. These studies confirmed the results of the pilot screens and led to the identification of a number of molecules that targeted one complex without influencing the other. To understand what types of mechanisms these molecules might have, we explored the activity of Zaf and Tel in a series of secondary assays. These assays were designed to reveal effects on PPIs and the biochemical activities of the DnaK systems.

Interestingly, we found that Zaf only inhibited the ATPase activity of the DnaK-DnaJ combination and that it weakened the physical interaction between DnaK and DnaJ (see Figure 2.6). Also, this molecule bound the ADP-bound form of DnaK and stabilized substrate-DnaK complexes. Based on these findings, a likely mechanism is that DnaJ first promotes ATP hydrolysis in DnaK, followed by binding of Zaf to ADP-DnaK, which

traps this nucleotide state. This “dead-end” complex appears to have a weak ability to rebound to DnaJ, but a strong ability to remain bound to peptide substrates. It is known that DnaJ binds poorly to DnaK in the ADP-bound form.¹⁹⁶ Thus, the effects of Zaf on the DnaK-DnaJ interaction are likely due to trapping of the “dead-end” ADP-bound complex. Interestingly, stabilization of the ADP-bound form of Hsp70s reduces accumulation of proteotoxic proteins in cellular and animal models of neurodegenerative disease,^{161,213} so this step in the ATPase cycle appears to be especially important in protein quality control. Molecules with a mechanism-of-action (MoA) similar to Zaf might be useful in those settings and, more importantly, this HTS approach might be a good platform for identifying compounds with this MoA.

In contrast to Zaf, Tel was identified as an inhibitor of the DnaK-GrpE combination, with little effect on the DnaJ-DnaK or other combinations. Interestingly, Tel appeared to block GrpE activity without impacting the physical interaction between these partners. Rather, NMR, mutagenesis, and modeling results suggest that Tel might bind between the IB and IIB subdomains, on the opposite face of DnaK than the one involved in GrpE binding (see Figure 2.9). How might binding in this region impact GrpE function without impacting its affinity for DnaK? GrpE normally rotates the IIB subdomain relative to IB and opens the nucleotide-binding cleft.²¹⁴ Thus, one possibility is that Tel might interfere with the conformational transitions needed to couple GrpE binding with its effects on ADP release, perhaps by limiting mobility of the IIB subdomain. Tel also had a mild (2-fold) effect on FAM-ATP binding (see Figure 2.10B), but it is not yet clear how this reduced nucleotide affinity might relate to its inhibition of GrpE stimulation.

2.4.2 Inhibitory mechanisms provide insight into allosteric networks in DnaK

Although both Tel and Zaf were identified as inhibitors of DnaK’s ATPase activity in the primary HTS experiments, the subsequent mechanistic studies showed that they had very different mechanisms. For example, while Zaf dramatically enhanced binding of DnaK to FITC-HLA in the FP assay and had no effect on nucleotide affinity, Tel had no effect on FITC-HLA binding (Figure 2.10C) and interfered with binding to FAM-ATP (Figure

2.10B). Thus, although both Tel and Zaf might be considered “inhibitors” of DnaK, they have distinct mechanisms and target different co-chaperone activities (Figure 2.11).

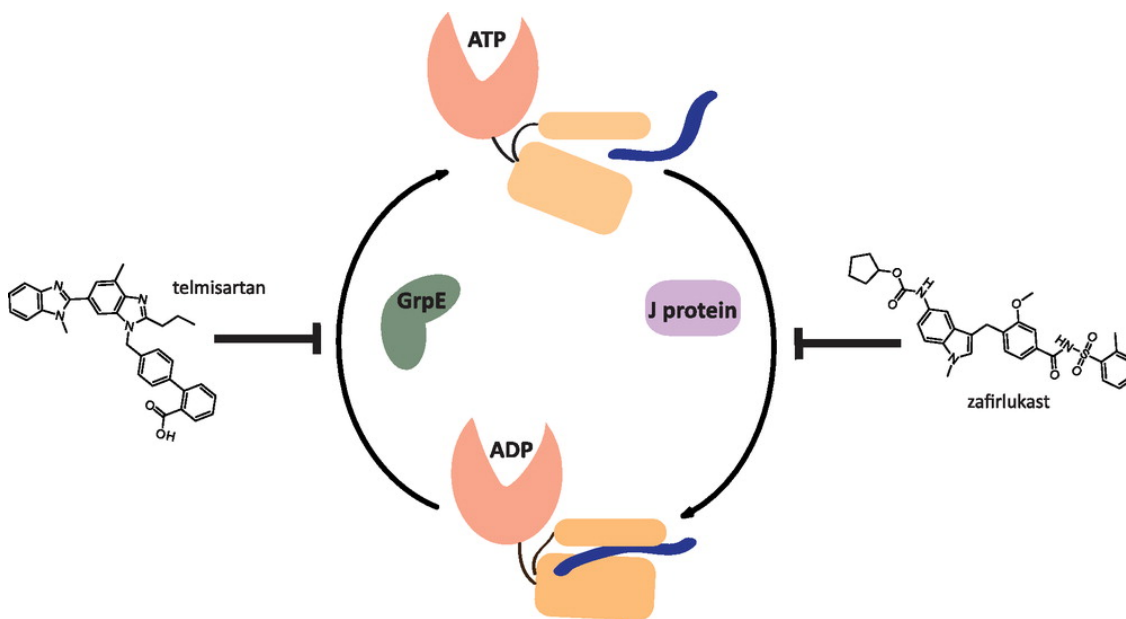


Figure 2.11 Zaf and Tel inhibit DnaK with distinct mechanisms and target different co-chaperone activities. Zaf partially inhibits the interaction between DnaK and DnaJ by binding to the ADP-bound state of DnaK. Tel interferes with conformational changes that couple GrpE binding with nucleotide release.

It is worth noting that these HTS “hits” are unlikely to be selective for the DnaK system in cells. In fact, both Zaf and Tel are already FDA-approved drugs with previously known targets: Zaf is a leukotriene receptor antagonist used in the treatment of asthma,²¹⁵ while Tel is an angiotensin II receptor antagonist and selective modulator of peroxisome proliferator-activated receptor gamma (PPAR- γ).²¹⁶ Although we did not consider Zaf or Tel to be particularly strong leads for further development, they are nonetheless useful probes of previously unexplored allosteric networks in DnaK and may provide a blueprint for the rational design of future inhibitors.

2.5 Conclusions

A growing number of studies have reported potent inhibitors of PPIs, including both small molecules and protein mimics that either directly¹² or allosterically²¹⁷ inhibit the formation of protein complexes. These molecules have great promise as chemical probes for better understanding the biology and “druggability” of multi-protein complexes. Against this backdrop, the studies described in this chapter provide an HTS approach that

appears to be particularly well suited for finding orthosteric and/or allosteric inhibitors of challenging PPIs, especially those in which the interaction produces a measurable change in enzyme turnover rates. Moreover, this modular approach allows for the discovery of inhibitors of specific PPIs within the context of a larger multi-protein system.

2.6 Experimental procedures

2.6.1 Reagents and general methods

Myricetin (Myr) was purchased from Sigma (St. Louis, MO), zafirlukast (Zaf) from Cayman Chemical (Ann Arbor, MI), pancuronium bromide (PaBr) from Santa Cruz Biotechnology (Santa Cruz, CA), and telmisartan (Tel) from AK Scientific (Union City, CA). The identities and purities (> 90%) of all compounds were confirmed by NMR and mass spectrometry. Alexa Fluor 488 was purchased from Invitrogen, and BHQ-10 carboxylic acid was obtained from Biosearch Technologies. All other biological reagents were obtained from Sigma (St. Louis, MO) unless otherwise noted. All spectroscopic measurements were obtained using a SpectraMax M5 microplate reader (Molecular Devices).

2.6.2 Peptide synthesis

The peptide FITC-HLA (RENLRIRLY) was synthesized on Wang resin using microwave-assisted DIC/HOBt solid-phase peptide synthesis. It was capped with two β -alanine residues and labeled on resin via the N-terminus with fluorescein-5-isothiocyanate (Anaspec). Crude TFA-cleaved peptide (> 90% purity) was extracted with ether and stored in DMSO as a concentrated stock at -20°C until use. The NR peptide (NRLLLTG) was synthesized on Wang resin, cleaved with TFA, precipitated with ether, and purified with reverse-phase HPLC using 0.1% TFA/ CH_3CN solvent system (> 95% purity). The masses of the peptides were verified using electrospray ionization mass spectrometry.

2.6.3 Protein expression and purification

DnaK, DnaJ, and GrpE were expressed and purified as previously described,¹³⁰ using a His column and subsequent cleavage of the His tag by TEV protease. DnaK was further purified using an ATP column, while both DnaJ and GrpE were subjected to final purification on a Superdex 200 gel filtration column (GE Healthcare). All proteins were concentrated and stored in 25 mM HEPES buffer containing 10 mM KCl and 5 mM MgCl₂ (pH 7.5) until use. Protein purities were estimated at greater than 90% by SDS-PAGE. The BCA (bicinchoninic acid) assay kit (Thermo Fisher Scientific Inc.) was used to measure total protein concentration and the activity of the purified proteins was verified with the described ATPase assays.

2.6.4 High-throughput screening

The high-throughput screening methodology was developed following previously published protocols.^{129,130} The libraries used were a natural product library,¹³² the NCC collection of ~500 bioactive molecules and the MicroSource MS2000 library containing ~2000 bioactives. The quinaldine red (QR) reagent was prepared fresh for each experiment by mixing stock solutions of 0.05% QR, 2% polyvinyl alcohol, 6% ammonium heptamolybdate tetrahydrate in 6 M HCl, and water in a 2:1:1:2 ratio. DnaK at 0.4 μ M and the indicated concentrations of co-chaperones (DnaJ, GrpE, or NRLLLTG) were diluted into assay buffer (100 mM Tris-HCl, 20 mM KCl, 6 mM MgCl₂, 0.01% Triton-X, pH 7.4), and 5 μ L of this solution was added to each well of a white, opaque, low-volume 384-well plate (Greiner Bio-One). To this solution was added 200 nL of compound stocks (2 μ M) or DMSO to each well for a final screening concentration of ~55 μ M. ATP (1 mM) was added to begin the reaction, followed by incubation for 3 hr at 37 °C. QR reagent (15 μ L) was added, and the reaction was quenched with 2 μ L of 32% sodium citrate after 2 min. Following incubation at 37 °C for 15 min, the fluorescence intensity (excitation 430 nm, emission 530 nm) was measured on a PHERAstar plate reader. Standard curves were obtained using stock solutions of dibasic potassium phosphate. Z' scores were calculated using no DnaK solutions as the positive control (100% “inhibited”) and DMSO-treated samples as the negative control (0% inhibited).

2.6.5 ATPase assays

ATPase assays were performed as described.^{129,130} Stock solutions of DnaK, DnaJ, or GrpE were made in assay buffer (100 mM Tris-HCl, 20 mM KCl, 6 mM MgCl₂, pH 7.4). Unless otherwise noted, the DnaK concentration was 0.6 μM, while DnaJ and GrpE concentrations are indicated. If applicable, stock solutions of compound were made in DMSO and then diluted into 15 μL of assay buffer and protein in clear, flat-bottom 96-well plates (Thermo Fisher Scientific Inc.) to the final concentrations noted. Absorbance was measured at 620 nm. Data were fit to the Michaelis–Menten equation ($Y = V_{\max}X/[K_m + X]$) in GraphPad PRISM.

2.6.6 Tryptophan fluorescence

Tryptophan fluorescence was measured as previously described.^{129,130} DnaK was diluted to 5 μM in storage buffer containing 1 mM of nucleotide and Zaf at the indicated concentrations, with a total volume of 25 μL in black, flat-bottom 96-well plates (Costar). The mixture was incubated for 30 min at 37 °C in the dark, and either the emission spectrum between 300 and 450 nm or emission at 340 nm (excitation 290 nm) was measured. Binding data were fit to a form of the Langmuir isotherm ($Y = B_{\max}X/[K_D + X]$).

2.6.7 Fluorescence quenching

DnaK and DnaJ/GrpE were labeled with Alexa Fluor 488 and BHQ-10 carboxylic acid, respectively, and their binding affinity was measured by FRET as previously described.^{129,130} Briefly, compound was diluted to the final indicated assay concentration from a concentrated DMSO stock into 20 μL of assay buffer (50 mM HEPES, 75 mM NaCl, pH 7.2) containing 50 nM labeled DnaK, labeled DnaJ at the noted concentrations, and 1 mM ATP. Following incubation for 1 hr at 37 °C, fluorescence at 525 nm (excitation 480 nm, cutoff 515 nm) was measured. The compounds did not affect either the fluorescence of Alexa-labeled DnaK or the absorbance spectra of BHQ-10 labeled partner. Binding data were fit to the Langmuir isotherm, as described above. Statistical significance was determined using an unpaired *t* test.

2.6.8 Fluorescence polarization

Binding of fluorescent peptide (FITC-HLA) to DnaK was carried out using the method of Ricci and Williams,²¹¹ with minor modifications. In a black, round-bottom, low-volume 384-well plate (Corning), 5 μ M DnaK, and 1 mM ATP in 10 μ L of assay buffer (25 mM HEPES, 150 mM KCl, pH 7.2) were incubated with the indicated compound concentrations or a solvent control for 30 min at RT. A stock of FITC-HLA was diluted to 25 nM into each well, for a total volume of 20 μ L. The plate was incubated in the dark for 10 min at RT before the fluorescence polarization (excitation 494 nm, emission 519 nm) was read. The dose-response data was fit to the Hill equation ($Y = E_{\max}/[1 + (EC_{50}/X)^{n_H}]$), providing EC50 values.

We also measured binding of a fluorescent ATP analogue, N⁶-(6-Amino)hexyl-ATP-5-FAM (FAM-ATP) (Axxora LLC), to DnaK using a fluorescence polarization binding assay. An aqueous stock of FAM-ATP was diluted to 20 nM in assay buffer (100 mM Tris-HCl, 20 mM KCl, 6 mM MgCl₂, pH 7.4) and titrated with DnaK in a black, round-bottom, low-volume, 384-well plate (Corning) in a total volume of 20 μ L. The plate was incubated in the dark for 10 min at RT before the fluorescence polarization (excitation 485 nm, emission 535 nm) was read. Binding data were fit to the Langmuir equation as described above. Competition data were fit to the Hill equation.

2.6.9 Docking

We used AutoDock 4 to simulate binding of Tel to DnaKNBD. First, GrpE was removed from the crystal structure (PDB id 1DKG). For the computations, we used published parameters.²¹⁸ The grid box was located between the IB and IIB subdomains, near the top of the nucleotide-binding cleft, with 0.2 Å resolution. Docked conformations were evaluated using PyMOL. The calculations were performed on an Apple MacBook5.1 running Mac OS X 10.6.8.

2.6.10 Isothermal titration calorimetry

Isothermal calorimetric titrations were performed on a VP-ITC MicroCalorimeter (MicroCal, Inc.) at 25 °C. DnaJ or GrpE were diluted into buffer containing 25 mM HEPES (pH 7.5), 5 mM MgCl₂, 10 mM KCl, 5 mM TCEP, and 0.5% DMSO to a final concentration of 10 μM. Protein samples were extensively dialyzed and added into the calorimetric cell (cell volume = 1.43 mL). DnaJ and GrpE were individually titrated with 100 μM Tel in 30 × 10 μL increments. Injections were performed at 2 μL/s. Data were analyzed using Microcal Origin (v2.9).

2.6.11 NMR

Binding of Tel to DnaK_{NBD} was measured by 2D HSQC-TROSY NMR on a Varian/Agilent 800 MHz NMR system, using methods that were previously described.²¹⁸ Briefly, small aliquots of compound solution (100 mM in DMSO) were added to ¹⁵N-labeled DnaK_{NBD}(1–388) (100 μM) in NMR buffer (25 mM Tris, 10 mM MgCl₂, 5 mM KCl, 10% ²H₂O, 0.01% sodium azide, pH 7.1, 5 mM ADP, 10 mM potassium phosphate). Identical aliquots of DMSO without compound were added to the protein sample in NMR control experiments. Residues were selected as significantly affected if the compound-induced chemical shift, correcting for the shift with DMSO alone, were above one standard deviation (1σ; see Figure 2.6).

Notes

This chapter is adapted from Cesa, L. C. *et al.* “Inhibitors of Difficult Protein-Protein Interactions Identified by High-Throughput Screening of Multi-protein Complexes” **2013** *ACS Chemical Biology* 8(9): 1988-1997. Laura C. Cesa, Srikanth Patury, Tomoko Komiyama, and Jason E. Gestwicki designed the experiments. Laura C. Cesa, Srikanth Patury, and Tomoko Komiyama conducted the experiments. Atta Ahmad and Erik R. P. Zuiderweg performed the NMR. We acknowledge the expert assistance of Lyra Chang, Steven Vander Roest, and Thomas McQuade.

Chapter 3

XIAP is a non-canonical client of the Hsp70 molecular chaperone

3.1 Abstract

Proteins must achieve a proper three-dimensional structure in order to function appropriately. In cancer, many proteins harbor mutations that render them susceptible to misfolding and/or high turnover. Overexpression of molecular chaperones allows the cancer cell to cope with the proteotoxic stress induced by these mutations, and as a result, molecular chaperones are key players in tumor growth and important drug targets for cancer therapy. In particular, there has been significant interest in the development of both Hsp70 and Hsp90 inhibitors for the treatment of a variety of cancers. The development of Hsp90 inhibitors has coincided with the discovery of Hsp90-specific client proteins that are degraded in response to Hsp90 inhibition. However, no specific Hsp70 client proteins have been identified in cancer cells. In this chapter, we use an allosteric inhibitor of the interaction between Hsp70 and nucleotide exchange factors to show that the inhibitor of apoptosis protein family (IAPs) is a previously unexplored class of Hsp70 substrates, and that IAPs are degraded by Hsp70 but not Hsp90 inhibition. Supporting this, we have characterized the interaction between one IAP family member, XIAP, and Hsp70. XIAP interacts with Hsp70 at a non-canonical binding site and is degraded independent of the proteasome. These results have important implications for Hsp70 drug discovery by establishing that IAPs can be used as biomarkers for Hsp70 target engagement in cells and our understanding of Hsp70-client interactions at the molecular level.

3.2 Introduction

Molecular chaperones are key players in cancer cell survival; overexpression of Hsp70 and Hsp90 in particular has been linked to poor prognosis and resistance to chemotherapeutics.^{219,220} Hsp70 and Hsp90 assist in protein folding and prevent

misfolding and aggregation. Inhibition of Hsp90 causes degradation of “client” proteins, a group of oncoproteins including kinases, transcription factors, and E3 ubiquitin ligases.^{221,222} Knowledge of specific proteins degraded by Hsp90 has provided a benchmark for the development of Hsp90 inhibitors for use in the clinic. While it is thought that Hsp70 inhibitors will have similar effects on its client proteins, to date, no specific Hsp70 clients have been identified.²²³

3.2.1 The Hsp70 complex as a drug target for cancer therapy

Hsp70 is regulated through an allosteric mechanism that couples ATP hydrolysis in nucleotide binding domain (NBD) with affinity for clients in the substrate binding domain (SBD). In its ATP-bound state, Hsp70 has a low affinity for substrates, but upon ATP hydrolysis, it adopts a high affinity conformation.^{197,198} Traditionally, Hsp70 substrate peptides are defined as short stretches of 4-5 hydrophobic amino acids that bind to Hsp70 in an extended conformation.^{195,196,224} While Hsp70 binding sites are typically buried in the hydrophobic interior of the folded client protein, Hsp70 has been shown to interact with proteins that are in partially folded conformations and to induce global unfolding in select substrates.^{225–227} However, Hsp70 does not accomplish these diverse tasks alone, but rather works in concert with a team of co-chaperone proteins. J proteins increase the rate of nucleotide turnover, while nucleotide exchange factors (NEFs) promote release of ADP following ATP hydrolysis.^{128,228} In addition, other types of co-chaperones, including the tetratricopeptide repeat (TPR) domain containing proteins link Hsp70 with the larger network of molecular chaperones and the protein quality control machinery.²²⁹

Because Hsp70 is essential for survival in both healthy and stressed cells, it is important to understand how to inhibit Hsp70 to achieve cell death in cancer cells while not affecting healthy cells. Our group has recently identified and characterized analogs of the rhodacyanine dye MKT-077 as selective Hsp70 inhibitors. These compounds bind to an allosteric site on Hsp70 only in the ADP-bound conformation,²¹⁸ similar to the inhibitor zafirlukast identified in Chapter 2. The BAG family of NEFs binds to Hsp70 in the apo conformation,⁹⁰ and MKT-077 analogs therefore inhibit interactions between Hsp70 and

the BAGs.¹⁶⁰ In addition, both Hsp70 and the BAG3 co-chaperone have been shown to play essential roles in tumor progression, as knockdown of either protein resulted in upregulation of senescence genes and downregulation of genes involved in tumor growth, invasion, and metastasis.²³⁰ Our group has shown that inhibition of the Hsp70-BAG3 interaction with the MKT-077 analog JG-98 was anti-proliferative in a variety of cancer cell lines, while it was markedly less cytotoxic in healthy mouse fibroblasts, validating this PPI as a potential therapeutic target.¹⁶⁰ Finally, treatment with JG-98 and other MKT-077 analogs causes destabilization of a number of substrate proteins, including FoxM1, tau, and polyQ-AR.^{160,161,213} Therefore, we hypothesized that we could use JG-98 as a tool compound to uncover new roles for Hsp70, particularly in complex with BAG3, in cancer signaling.

3.2.2 IAPs are involved in multiple pro-survival signaling pathways

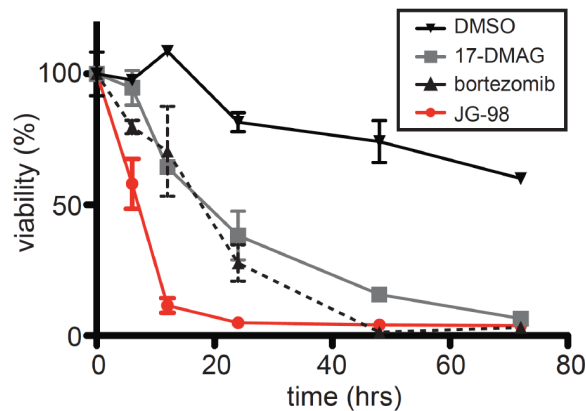
In this chapter, we demonstrate that the inhibitor of apoptosis proteins (IAPs) are destabilized in response to treatment with an allosteric inhibitor of Hsp70. IAPs are important mediators of cell survival signaling and are overexpressed in many cancers.²³¹ IAPs are defined to contain at least one baculoviral IAP repeat (BIR) domain.^{232–234} The cellular IAPs c-IAP1, c-IAP2, and XIAP each contain three BIR domains, which allow them to bind to caspases and prevent apoptotic signaling cascades.²³⁵ IAPs can also trigger pro-survival signaling pathways through activation of NF- κ B and E3 ligase activity of their C-terminal RING finger motif.^{236–238} In this chapter, we show that the IAPs are a class of specific Hsp70 client proteins and that XIAP interacts with Hsp70 through a non-canonical binding mechanism. These results suggest that IAPs could be used as biomarkers of Hsp70 target engagement for drug discovery.

3.3 Results

Cancer cells have evolved to rely on overexpression of molecular chaperones in order to cope with their extreme proteotoxic stress. In particular, Hsp70 has generally been thought to inhibit apoptosis by protecting “client” proteins, like the oncoproteins Raf-1 and AKT1 from degradation.^{239–241} This model is largely based on the activity of Hsp90, however.^{242–244} Treatment with Hsp90 inhibitors causes client release and ultimately their

degradation.^{245,246} However, it is not clear if Hsp70 plays a strictly “Hsp90-like” role in cancer cells, or if it is involved in unique pathways. In this chapter, we use a recently reported allosteric inhibitor of Hsp70-NEF interactions to probe the role of Hsp70 in pro-survival signaling.

A. JG-98 rapidly kills MDA-MB-231 breast cancer cells



B. Loss of clients occurs after the onset of cell death

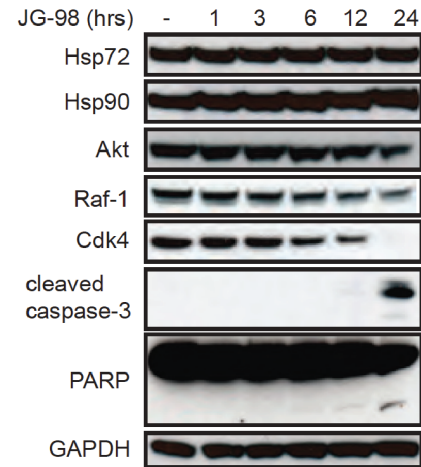


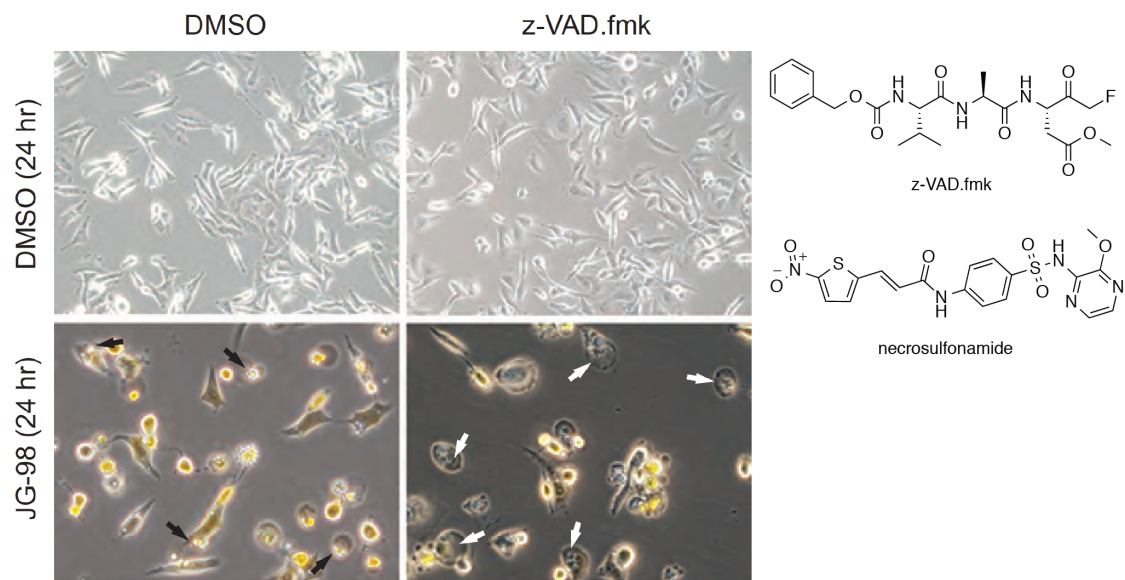
Figure 3.1 JG-98 is cytotoxic with only mild effects on oncogenic kinases. (A) JG-98 (5 μ M) kills MDA-MB-231 cancer cells with relatively rapid kinetics compared to 17-DMAG (5 μ M) or bortezomib (40 nM), as monitored by MTT assays. Results are the average of two independent experiments performed in quintuplicates. The error bars represent SEM. (B) Chaperone clients are degraded relatively late after treatment with JG-98 (10 μ M), after onset of cell loss. Results are representative of experiments performed in duplicate.

3.3.1 Inhibition of Hsp70 causes rapid cell death and destabilization of pro-survival kinases

In order to understand the mechanistic role of Hsp70 in cancer cells, we first measured the kinetics of the anti-proliferative effects of an allosteric Hsp70 inhibitor JG-98 and compared it to the effects of other proteostasis modulators, including the Hsp90 inhibitor 17-DMAG and the proteasome inhibitor bortezomib. Strikingly, we found that the first signs of cell death in MDA-MB-231 cells occurred within 10 hours of treatment with JG-98, whereas 17-DMAG and bortezomib exhibited markedly slower kinetics, with induction of cell death occurring after around 24 hours of treatment (Figure 3.1A). To understand this effect in greater detail, we measured the stability of several oncogenic client proteins. Hsp90 inhibitors are known to destabilize ~200 oncogenic clients, leading

to apoptosis.²⁴⁷ We found that treatment with the Hsp70 inhibitor JG-98 resulted in modest degradation of a few of the most sensitive Hsp90 clients, including Raf-1, AKT1, and CDK4 (Figure 3.1B).

A. JG-98 induces necrosis when apoptosis is blocked



B. JG-98 cytotoxicity is suppressed when both apoptosis and necroptosis are blocked

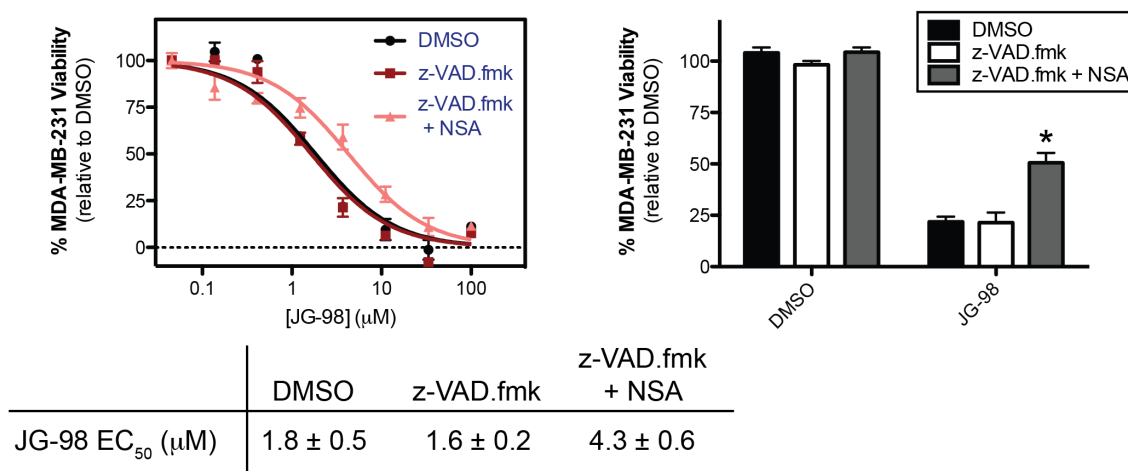


Figure 3.2 Inhibition of both apoptosis and necroptosis is necessary to prevent JG-98 cytotoxicity. (A) Cells were pretreated with z-VAD.fmk (40 μM) for 1 hour prior to addition of JG-98 (10 μM) and visualized using an Olympus IX83 inverted microscope. Black arrows indicate apoptotic cells; black arrows indicate necroptotic cells. (B) Cells were treated as in panel A and MTT assays were performed after 24 hours. Results are the average of three independent experiments performed in triplicate, and error bars are SEM. *p < 0.05.

However, destabilization of client proteins occurred many hours after the onset of cell death, in contrast with treatment with Hsp90 inhibitors, in which cell death and client degradation occur in unison.^{248,249} In addition, JG-98 did not induce a stress response, as indicated by the constant levels of Hsp70 and Hsp90. These results indicate that the mechanism of cell death in response to Hsp70 inhibitors cannot be explained with simply “Hsp90-like” effects.

3.3.2 JG-98 induces necrosis when apoptosis is blocked

In order to understand the mechanism of JG-98 cytotoxicity, we first verified that MDA-MB-231 cells underwent apoptosis in response to treatment, as judged by morphological assessment and cleavage of apoptotic executors (caspase-3 and PARP) (Figures 3.1B and 3.2A). However, despite caspase-3 activation by JG-98, inhibition of caspases with z-VAD.fmk was not sufficient to prevent cell death induced by the Hsp70 inhibitor (Figure 3.2B). In fact, we observed that cells pre-treated with the pan-caspase inhibitor displayed morphological features consistent with necrotic cell death, including a swollen cytoplasm and the development of cytoplasmic granules (Figure 3.2A). Furthermore, we also found that pre-treatment with necrosulfonamide (NSA) alone, a necroptosis inhibitor did not prevent cell death induced by JG-98 (Sharan R. Srinivasan, Ph. D. thesis). However, the combination of both the caspase inhibitor and the necroptosis inhibitor was able to prevent JG-98-mediated cell death (Figure 3.2B).

To explore this phenomenon more broadly, we tested the cytotoxicity of JG-98 in combination with z-VAD.fmk or z-VAD.fmk plus NSA in a small panel of cancer cell lines derived from a variety of tissues. The apoptosis inhibitor z-VAD.fmk was unable to protect against JG-98 cytotoxicity in cells derived from breast (MDA-MB-231, MCF-7, SK-BR-3, T-47D), peripheral blood (Jurkat), lung (A549), or colon (HT-29) (Table 3.1). However, cervical derived tumor cells (HeLa) were partially protected from JG-98 cytotoxicity by z-VAD.fmk alone (EC_{50} increased 2-fold). These results suggest that not all cell types share the same reliance on cell death pathways. Furthermore, the combination of z-VAD.fmk and NSA was required to block cell death in MDA-MB-231, MCF-7, SK-BR-3, and Jurkat cells. Finally, this combination was unable to prevent JG-

98-mediated cell death in T-47D, A549, and HT-29 cells, and in A549 and HT-29 cells, the effect of JG-98 may have been mildly exacerbated. Hsp70 is known to be involved in lysosomal cell death,²⁵⁰ so JG-98 may activate alternative cell death pathways in some cell types.

Table 3.1 Effects of apoptosis and necroptosis inhibitors on JG-98 EC₅₀ (μM; fold change) in cancer cell lines

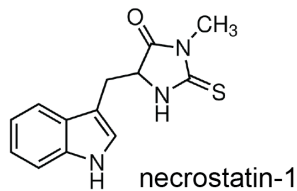
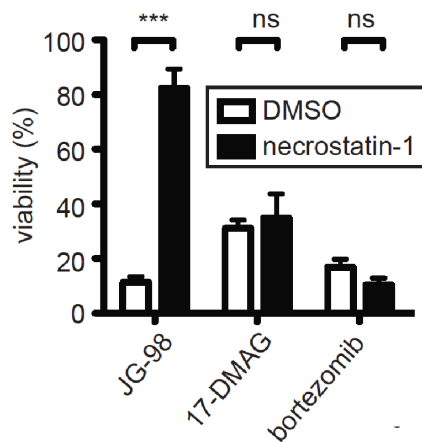
| Tissue | Cell line | DMSO | z-VAD.fmk | z-VAD.fmk+NSA |
|----------|------------|-----------|--|--|
| Breast | MDA-MB-231 | 1.8 ± 0.5 | 1.6 ± 0.2 (1.0) ^{ns} | 4.3 ± 0.6 (2.3)** |
| | MCF-7 | 1.1 ± 0.2 | 1.3 ± 0.2 (1.0) ^{ns} | 2.8 ± 0.6 (1.4)* |
| | SK-BR-3 | 2.0 ± 0.3 | 2.2 ± 0.3 (1.0) ^{ns} | 2.9 ± 0.5 (1.3)* |
| | T-47D | 9.7 ± 1.0 | 10 ± 1 (1.1) ^{ns} | 8.6 ± 1.8 (1.1) ^{ns} |
| Leukemia | Jurkat | 8.0 ± 0.4 | 8.8 ± 1.0 (1.1) ^{ns} | 14 ± 2 (1.8)* |
| Cervix | HeLa | 5.0 ± 0.6 | 14 ± 5 (2.0)* | 15 ± 3 (2.3)* |
| Lung | A549 | 34 ± 7 | 32 ± 8 (1.0) ^{ns} | 13 ± 2 (0.7)* |
| Colon | HT-29 | 12 ± 2 | 11 ± 1 (1.0) ^{ns} | 1.7 ± 0.3 (0.1)** |

*p < 0.05; **p < 0.01; ns = not significant

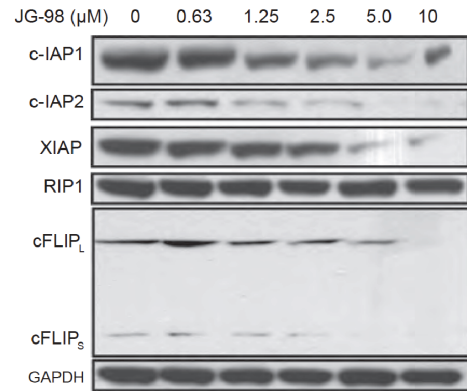
3.3.3 JG-98 activity is dependent on RIP1 and causes destabilization of IAPs

The kinase RIP1 is an important regulator of both apoptotic and necroptotic signaling cascades and is also involved in NF-κB pro-survival signaling.^{251–253} Because JG-98 seemed to initiate both apoptotic and necroptotic cell death, we determined if its effect was dependent on RIP1 kinase activity. Indeed, pretreatment with the RIP1 inhibitor necrostatin-1 almost completely blocked cell death with the Hsp70 inhibitor JG-98 (Figure 3.3A). Neither 17-DMAG nor bortezomib cytotoxicity was prevented by necrostatin-1.

A. JG-98 activity is suppressed by necrostatin-1



B. JG-98 causes loss of IAPs and cFLIP



C. JG-98 causes RIP1 oligomerization

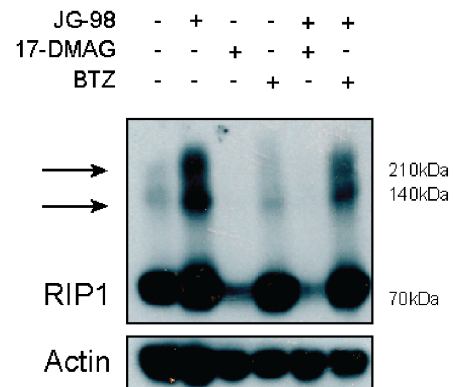


Figure 3.3 JG-98 induces cell death through a novel RIP1-dependent process. (A) JG-98 cytotoxicity prior to addition of compounds. Viability was determined by three independent MTT assays performed in quintuplicate. Error bars represent SEM. *** $p < 0.001$, ns = not significant. (B) JG-98 induces degradation of RIP1 modulators, but does not affect RIP1 levels. MDA-MB-231 cells were treated for 24 hours. Results represent three independent experiments. (C) JG-98 causes RIP1 oligomerization. MDA-MB-231 cells were treated with JG-98 (10 μM), 17-DMAG (10 μM), or bortezomib (40 nM) for 24 hours. Results are representative of two independent experiments.

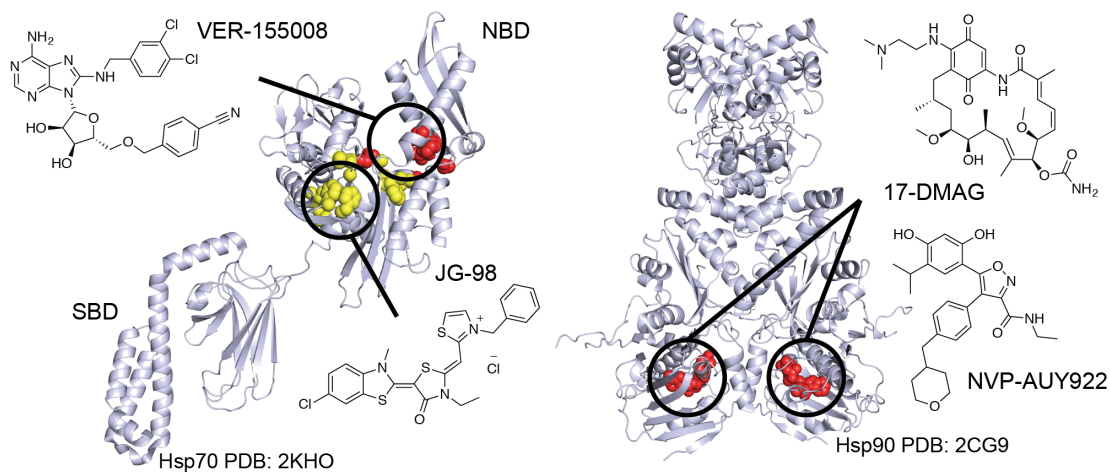
RIP1 is constitutively ubiquitinated by the E3 ligases XIAP, c-IAP1, c-IAP2, and cFLIP_{SL}.²⁵⁴ RIP1 ubiquitination is linked not only to its turnover, but also to non-degradation pathways that modulate its activity.²⁵⁵ In addition, RIP1 ubiquitination is believed to protect against necroptosis.²⁵⁶ In order to understand how Hsp70 might modulate RIP1 function, we treated MDA-MB-231 cells with JG-98 and examined levels of RIP1 and the IAPs. Treatment with JG-98 caused a striking loss in XIAP, c-IAP1/2, and cFLIP_{LS} levels (Figure 3.3B). Furthermore, although total RIP1 levels did not change, JG-98 did induce an apparent oligomerization in RIP1, which was not observed with either 17-DMAG or bortezomib (Figure 3.3C). In fact, 17-DMAG caused RIP1

degradation, consistent with literature precedent.²⁵⁷ RIP1 has been shown to interact with itself and with the related kinase RIP3 to form dimers, oligomers, and even amyloid-like fibrils. These fibrils are thought to form a functional signaling complex to trigger necroptosis.²⁵⁸ It is tempting to speculate that Hsp70 inhibition might trigger both degradation of the RIP1 E3 ligases and oligomerization of RIP1 itself to induce cell death, although the exact mechanism of Hsp70-mediate RIP1 oligomerization or fibril formation remains to be tested.

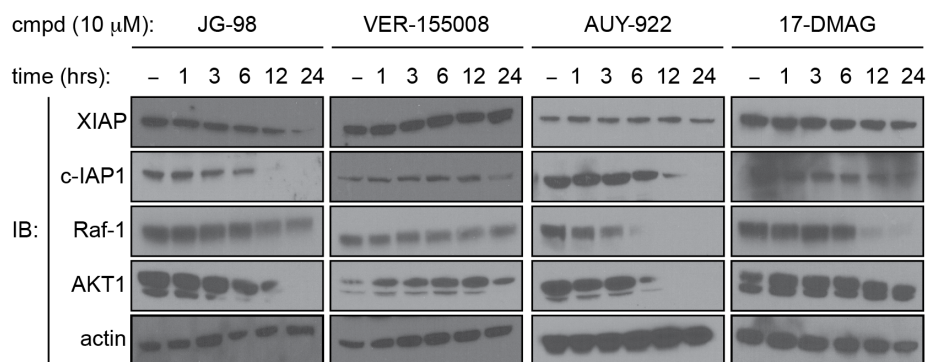
3.3.4 Hsp70 inhibition results in rapid degradation of IAPs

We have shown above that inhibition of Hsp70 triggers cell death in cancer cells through a mechanism dependent on RIP1 kinase. Specifically, Hsp70 inhibition resulted in striking destabilization of the E3 ubiquitin ligases of RIP1, the IAPs. Therefore, we hypothesized that IAPs are specific clients of Hsp70. While it is well known that classic Hsp90 client proteins like kinases and transcription factors are also Hsp70 clients,^{239,240} we wanted to determine if the reverse was true. Are IAPs clients of Hsp90 as well, or are they specifically regulated by Hsp70? In order to answer this question, we examined the kinetics of degradation of the IAPs XIAP and c-IAP1 and compared them to degradation of the traditional Hsp90 clients Raf-1 and AKT1 after treatment with both Hsp70 and Hsp90 inhibitors. Hsp70 inhibitors included the ATP-competitive inhibitor VER-155008²⁴¹ and the allosteric inhibitor JG-98²⁵⁹, and Hsp90 inhibitors included the ATP-competitive inhibitor NVP-AUY922²⁶⁰ and the geldanamycin analog 17-DMAG^{261,262} (Figure 3.4A).

A. Structures of Hsp70 and Hsp90 inhibitors and binding sites



B. Loss of IAPs occurs after Hsp70 inhibition, but not Hsp90 inhibition



C. Quantitation of protein levels after inhibitor treatment

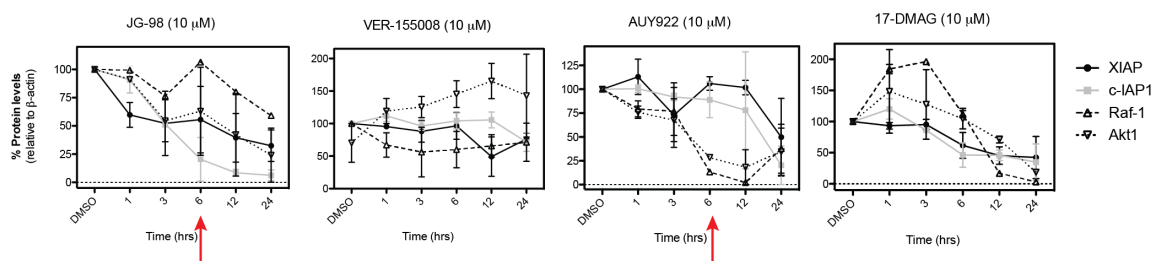


Figure 3.4 IAPs are selectively destabilized by Hsp70 inhibition. (A) Crystal structures of human Hsp70 (left, PDBid 2KHO) and yeast Hsp90 (right, PDBid 2CG9). Specific amino acids comprising the binding sites of Hsp70 inhibitors (VER-155008, JG-98) and Hsp90 inhibitors (NVP-AUY922, 17-DMAG) are highlighted. Orthosteric (ATP) binding sites are shown in red; allosteric sites are shown in yellow. (B) Destabilization of IAPs occurs after treatment with Hsp70 inhibitors. MDA-MB-231 cells were treated with 10 μ M JG-98, VER-155008, NVP-AUY922, or 17-DMAG for the indicated time points. Degradation of Hsp90 clients after Hsp90 inhibition is shown as a control. The blots shown are representative of at least two independent experiments. (C) Quantification of protein levels of the blots shown in (B). Degradation of IAPs occurs after 6 hour treatment with Hsp70 inhibitors, while Hsp90 clients are degraded after 6 hour treatment with Hsp90 inhibitors (red arrows). Results shown are averages of at least two independent experiments, and error bars represent SEM.

From these initial experiments, several interesting observations were made. Consistent with our previous results, inhibition of Hsp70 resulted in rapid destabilization of the IAPs, although degradation was more pronounced with the allosteric inhibitor JG-98 versus the ATP-competitive VER-155008 (Figure 3.4B, panels 1 and 2). This indicates that the mode of inhibition may play a role in the kinetics of destabilization of Hsp70 clients or that these effects may be client-specific. Furthermore, loss of the IAPs coincided with the kinetics of JG-98-mediated cell death, with degradation occurring between 3 and 6 hours. This result sharply contrasts with the delay in Hsp90 client destabilization. There is also a marked difference in the destabilization profile of Hsp90 clients Raf-1 and AKT in response to Hsp70 inhibition (Figure 3.4B, panel 1). This effect is particularly strong in the first 6 hours of treatment with JG-98, after which time nearly 75% degradation of c-IAP1 and 50% degradation of XIAP is observed, while Raf-1 and AKT1 levels remained constant (Figure 3.4C, panel 1, red arrows). This effect is reversed after treatment with Hsp90 inhibitors, particularly AUY922. In this case, Hsp90 clients are destabilized very rapidly upon treatment with AUY922, while the IAPs are not rapidly degraded (Figure 3.4B, panel 3); again, after 6 hours of treatment, Raf-1 and AKT1 levels are down nearly 90% of the DMSO control, while XIAP and c-IAP1 levels remain constant (Figure 3.4C, panel 3, red arrows). Notably, this pattern of client destabilization is consistent across multiple cell lines, including MCF-7 and HeLa cells. However, this effect is specific to cancer cells, as we observed only mild degradation of IAPs in IMR90 fibroblast cells (Figure 3.5).

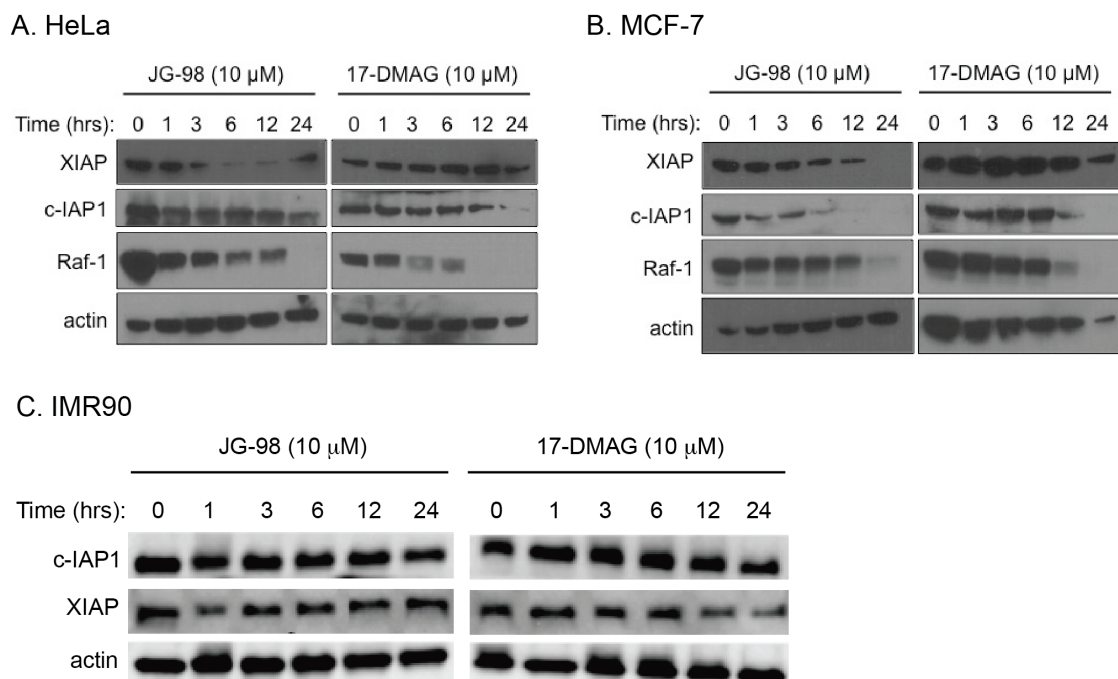


Figure 3.5 JG-98 causes destabilization of IAPs in multiple cancer cell lines. (A) HeLa, (B) MCF-7, and (C) IMR90 cells were treated with 10 μ M JG-98 or 17-DMAG for the indicated time points. Results shown are representative of at least two independent experiments.

It is important to note that while degradation of IAPs and Hsp90 clients at later time points of exposure with 17-DMAG was observed (Figure 3.4B and C, panel 4), this compound is markedly cytotoxic under these conditions (Table 3.2), and these effects are therefore likely nonspecific. Taken together, these data support a mechanism in which the IAPs are specifically regulated by Hsp70 and are thus rapidly and selectively destabilized upon Hsp70 inhibition.

Table 3.2 Summary of Hsp70 and Hsp90 inhibitor cytotoxicity (EC_{50} ; μ M) in cancer cells

| | JG-98 | 17-DMAG |
|------------|-----------------|-----------------|
| MDA-MB-231 | 1.8 ± 1.0 | 11 ± 4 |
| MCF-7 | 0.78 ± 0.28 | 0.37 ± 0.16 |
| HeLa | 2.1 ± 0.8 | 11 ± 5 |

Cells were treated with the indicated compounds for 24 hours, viability measured by MTT assay.

Because JG-98 analogs have previously been shown to promote ubiquitination and proteasomal degradation of FoxM1, tau, and polyQ-AR,^{161,213} we hypothesized that degradation of IAPs triggered by JG-98 would also be proteasome-dependent. We therefore pre-treated MDA-MB-231 cells with the proteasome inhibitor lactacystin²⁶³

prior to exposure to JG-98; strikingly, degradation of XIAP both in the presence and absence of lactacystin was observed (Figure 3.6), suggesting that degradation occurs independent of the proteasome.

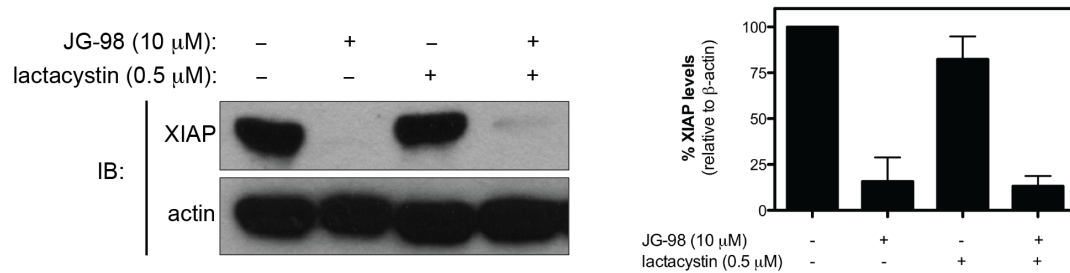


Figure 3.6 JG-98-induced degradation of XIAP is not proteasome-dependent. MDA-MB-231 cells were pretreated with 0.5 μ M lactacystin for 1 hour before addition of 10 μ M JG-98 for 24 hours. Blots shown (left) are representative of three independent experiments, and protein quantification (right) is shown as averages of three biological replicates. Error bars are SEM.

3.3.5 XIAP BIR2 and RING domains are essential for Hsp70-mediated degradation

Hsp70 inhibition leads to proteasome-independent degradation of XIAP. In order to understand the mechanism of recognition and degradation of XIAP by Hsp70, series of XIAP deletion mutations were designed, corresponding to the deletion of each individual domain, as well as truncations containing two and three BIR domains, respectively (Figure 3.7A). After treatment with JG-98 for 24 hours, most XIAP deletion mutants were degraded. Strikingly, however, the Δ RING mutation accumulated in response to JG-98 treatment (Figure 3.7B). In addition, we did not observe degradation for a mutant lacking the BIR2 domain and attenuated degradation for the Δ BIR1 mutation (Figure 3.7B). Together, these data suggest that both the RING and BIR domains are essential for Hsp70-mediated degradation of XIAP.

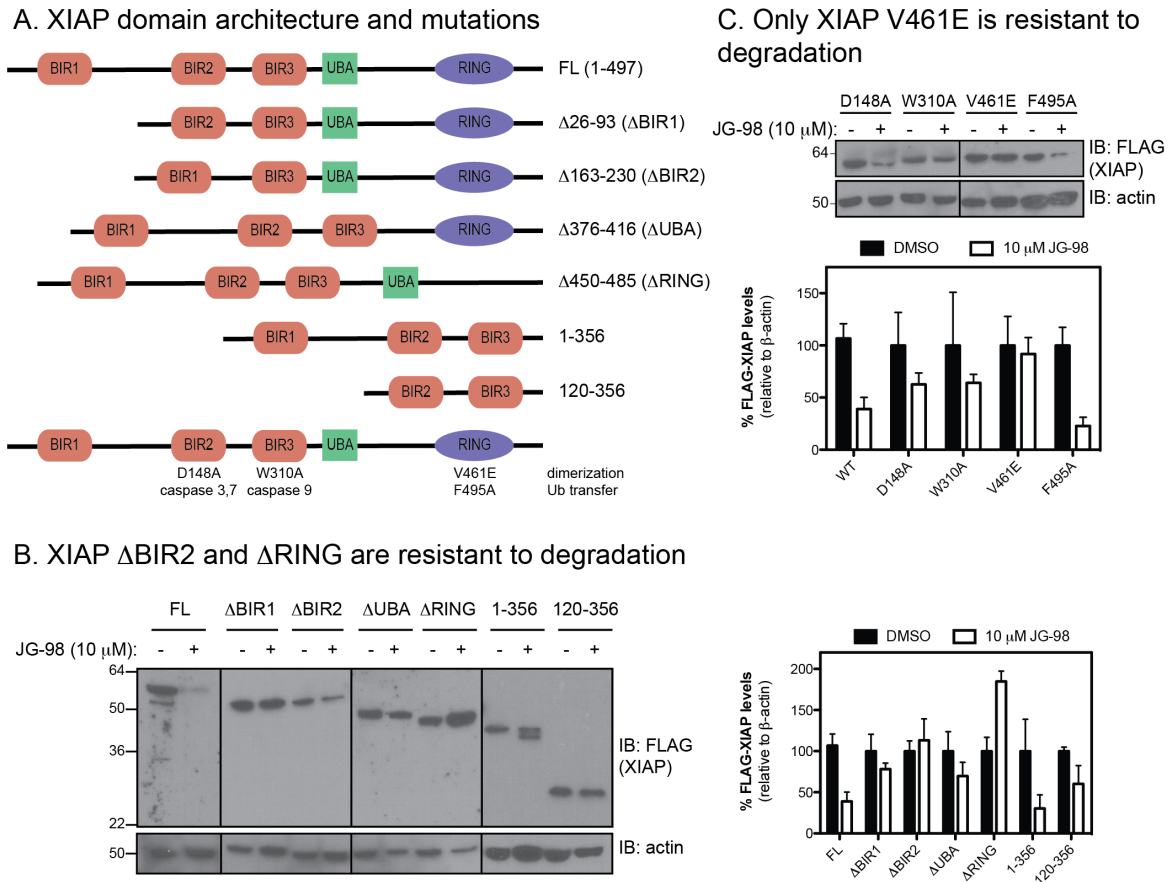


Figure 3.7 Hsp70-mediated degradation of XIAP is dependent on the BIR2 and RING domains. (A) Domain architecture of XIAP. Point and deletion mutations are shown. (B) XIAP Δ BIR2 is not degraded and Δ RING is accumulated in response to Hsp70 inhibition. HeLa cells overexpressing the indicated FLAG-tagged XIAP deletion mutations were treated with 10 μ M JG-98 for 24 hours. Blots are representative of at least two independent experiments and quantification is the average of at least two biological replicates. Error bars represent SEM. (C) XIAP V461E is resistant to degradation by Hsp70 inhibition. HeLa cells overexpressing the indicated FLAG-tagged XIAP point mutations were treated with 10 μ M JG-98 for 24 hours. Blots are representative of two independent experiments and quantification is the average of two biological replicates. Error bars represent SEM.

3.3.5.1 RING dimerization is essential for Hsp70-mediated degradation

The RING domain of XIAP is important in mediating homodimerization and heterodimerization with the c-IAPs, as well as in promoting autoubiquitination.²³⁶ In order to determine if these functions of the RING domain play a role in Hsp70-mediated degradation, we made point mutations in XIAP that have previously been shown to block degradation and ubiquitin transfer (V461E and F495A, respectively)^{264,265} (Figure 3.7A). XIAP F495A was degraded in response to JG-98 treatment, whereas XIAP V461E was completely resistant to degradation (Figure 3.7C), suggesting that dimerization of the

RING domain is essential for degradation of XIAP following Hsp70 inhibition, whereas ubiquitin transfer is not.

3.3.5.2 Caspase binding is dispensable in XIAP destabilization

We next determined if the function of the BIR domains are essential for Hsp70-mediated degradation of XIAP. Through its BIR2 and BIR3 domains, XIAP interacts with caspases 3, 7, and 9.²³⁴ We overexpressed point mutations that have been previously shown to block caspase 3 and 7 and caspase 9 binding (D148A and W310A, respectively),²⁶⁶ and after treatment with JG-98 for 24 hours, we observed degradation of both the D148A and W310A mutants, although the effect was slightly attenuated for W310A (Figure 3.7C). These results suggest that functional caspase 9 binding may be important for Hsp70 recognition of XIAP, while binding to caspases 3 and 7 is dispensable for XIAP's Hsp70-mediated degradation.

3.3.6 Hsp70 and XIAP form a complex in cells

Given that dimerization of the RING domain of XIAP was essential for Hsp70-mediated degradation, while caspase binding was not, we next determined if Hsp70 directly interacts with XIAP to regulate its stability. We hypothesized that Hsp70 and XIAP form a complex in cells. Indeed, endogenous Hsp70 was immunoprecipitated with XIAP from MCF-7 cell lysate (Figure 3.8A). However, we were unable to pull down XIAP with an Hsp70 immunoprecipitation. We speculate that this is due to the relatively greater number of interacting partners of Hsp70 than XIAP.

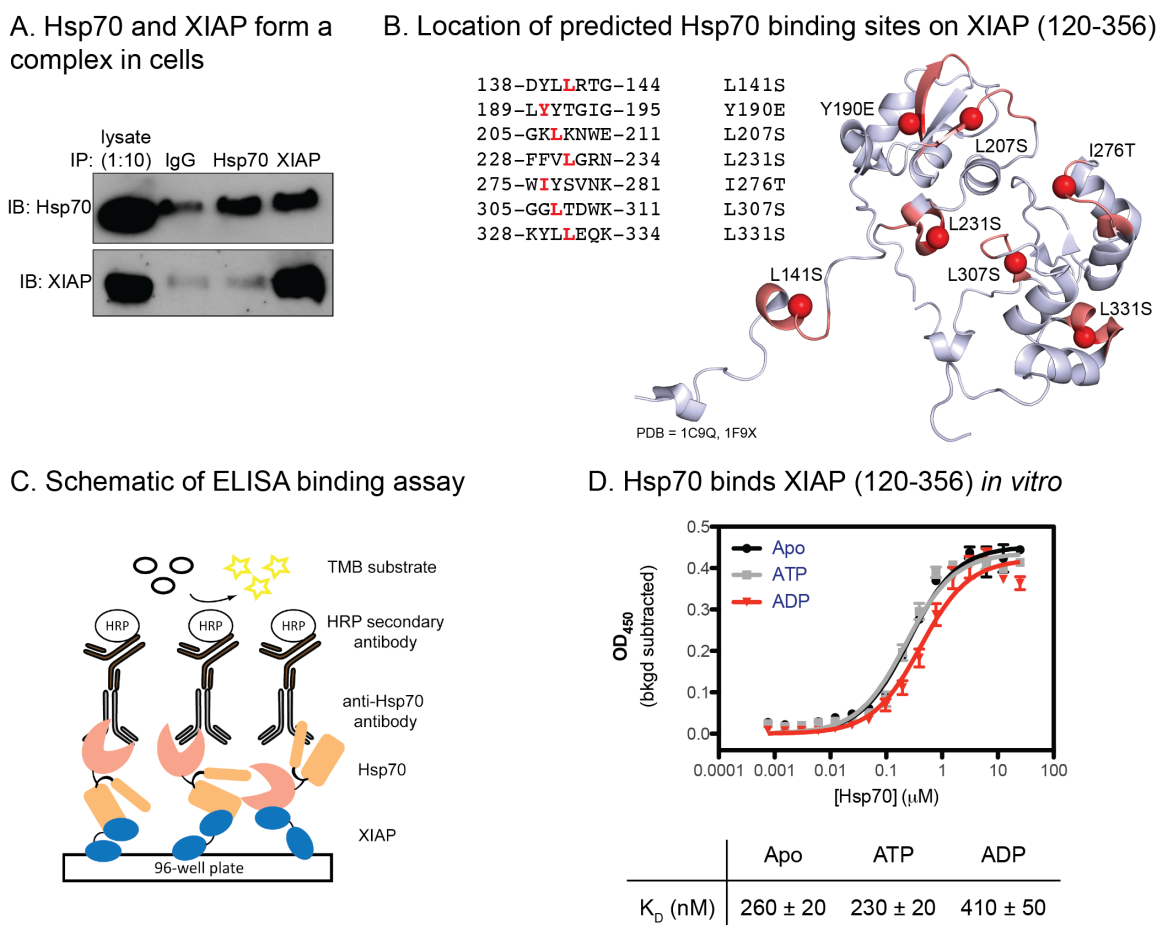


Figure 3.8 Hsp70 binds XIAP *in vitro* and in cells. (A) XIAP is co-immunoprecipitated with Hsp70. Endogenous protein from MCF-7 cell extracts was immunoprecipitated with Hsp70 and XIAP antibodies. Blots are representative of three independent biological replicates. (B) Predicted Hsp70 binding sites on XIAP BIR2 and BIR3 (PDBid 1C9Q, 1F9X) are shown in red. Individual point mutations are shown on the sequences of the predicted Hsp70 binding sites. (C) Schematic of ELISA protein interaction assay. (D) XIAP (120-356) has a slight preference for binding apo and ATP-bound Hsp70, as measured by ELISA. Results are representative averages of triplicate of three independent experiments, and error bars are SEM. Binding data were fit to the Langmuir binding isotherm.

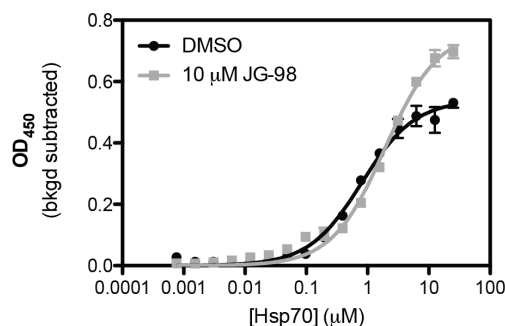
3.3.7 Hsp70 binds XIAP (120-356) *in vitro*

Using a prediction algorithm for chaperone binding sites,²²⁴ we determined XIAP contains seven predicted binding sites for the prokaryotic Hsp70 chaperone, all located within the BIR2 and BIR3 domains, consistent with the cellular degradation and immunoprecipitation data (Figure 3.8B). The cellular data suggests that Hsp70 forms a complex with the BIR2 and BIR3 domains of XIAP to regulate its stability and mediate its degradation in response to Hsp70 inhibition with JG-98. To further characterize this interaction *in vitro*, the minimal region of XIAP (120-356) predicted to interact with

Hsp70 was expressed and purified. In order to measure binding to Hsp70, a modified ELISA protein-protein interaction assay was used in which XIAP (120-356) was nonspecifically immobilized in a 96-well plate and incubated with full-length Hsp70 (Figure 3.8C). In this platform, we found that Hsp70 bound XIAP (120-356) with high nanomolar affinity ($K_D = 260 \pm 20$ nM) (Figure 3.8D). It is well-established that Hsp70 binds to client proteins more tightly when in the ADP-bound state; however, we found that ADP-bound Hsp70 bound to XIAP (120-356) with ~ 2 -fold weaker affinity ($K_D = 410 \pm 50$ nM) than apo or ATP-bound Hsp70. Given that JG-98 prefers binding to Hsp70 in the ADP-bound state,²¹⁸ we expected that JG-98 would likewise inhibit binding of Hsp70 to XIAP (120-356); indeed the addition of 10 μ M JG-98 weakened the affinity of Hsp70 for XIAP (120-356) by ~ 2 -fold (Figure 3.9A).

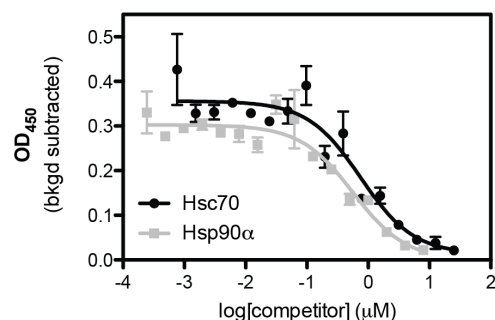
Our cell-based experiments demonstrate that XIAP is degraded more rapidly and effectively by treatment with Hsp70 inhibitors rather than Hsp90 inhibitors, suggesting that it may be an Hsp70-specific client protein. Therefore, we expected that XIAP would not bind to Hsp90. We measured the ability of Hsc70 and Hsp90 α to compete with Hsp70 for binding to XIAP (120-356) in the ELISA platform. Surprisingly, we found that both Hsc70 and Hsp90 α bound to XIAP with similar affinity (Figure 3.9B). This result suggests that binding to XIAP is not an exclusive predictor of a chaperone's ability to regulate its homeostasis. Furthermore, addition of a Smac mimetic²⁶⁷ blocked binding of Hsp70 to XIAP (120-356) (Figure 3.9C), suggesting that Smac or caspase binding to XIAP and Hsp70 recognition are mutually exclusive.

A. JG-98 partially blocks Hsp70-XIAP interaction



| | DMSO | JG-98 |
|------------|--------------|----------------|
| K_D (nM) | 800 ± 70 | 1930 ± 140 |

B. Hsc70 and Hsp90 compete for binding to XIAP



| | Hsc70 | Hsp90 |
|------------|---------------|---------------|
| K_i (nM) | 300 ± 200 | 230 ± 140 |

C. SM164 inhibits binding of XIAP to Hsp70

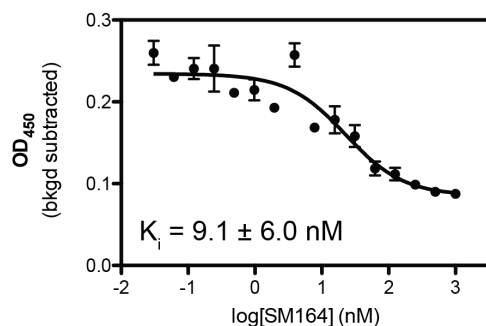


Figure 3.9 Additional biochemical analysis of the interaction between Hsp70 and XIAP (120-356). (A) JG-98 moderately decreases the affinity of Hsp70 for XIAP (120-356) by ELISA. (B) Hsc70 and Hsp90α compete with Hsp70 for binding to XIAP (120-356) by ELISA. (C) Binding of SM164 to XIAP (120-356) decreases affinity of XIAP for Hsp70 by ELISA. All experiments are representative averages of triplicate of three independent experiments, and error bars represent SEM. Binding data were fit to the Langmuir equation and inhibition data were fit to the Hill equation.

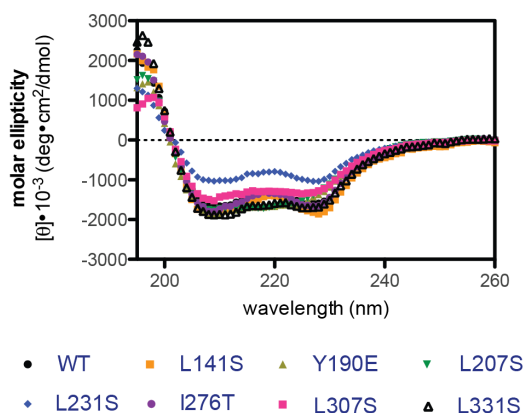
3.3.8 Hsp70 and XIAP (120-356) form a multimeric complex *in vitro*

XIAP contains seven predicted chaperone binding sites in its BIR2 and BIR3 domains. We wanted to determine which, if any, of the predicted sites are necessary for Hsp70 binding *in vitro*. We therefore purified XIAP (120-356) constructs bearing individual point mutations in each of the seven predicted binding sites (see Figure 3.8B). We verified that each of these mutants retained WT-like secondary structure, measured by circular dichroism (Figure 3.10A) and measured their affinity for Hsp70 by ELISA. Of these mutants, Y190E, L207S, L307S, and L331S all bound Hsp70 with reduced affinity, with dissociation constants ranging from 2-fold (Y190E and L331S) to greater than 10-

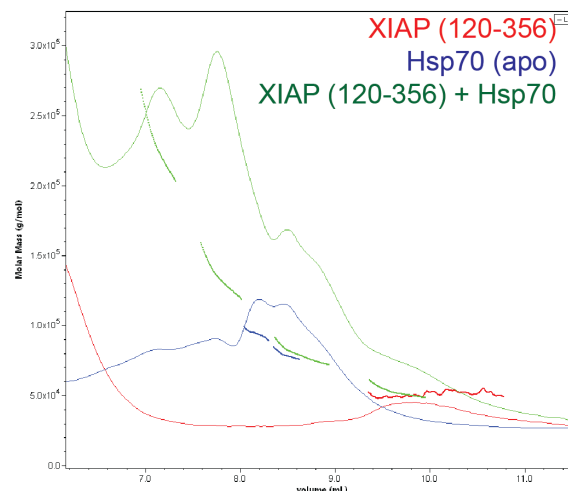
fold (L207S) weaker than the wild type protein (Figure 3.10C). However, none of these mutations completely abrogated Hsp70 binding, suggesting that Hsp70 may bind to multiple sites on XIAP (120-356). Furthermore, the lack of important “hot spot” residues is consistent with protein-protein interactions occurring over a large surface area, which is to be expected for the interaction between Hsp70 and XIAP.^{21,202} Indeed, Hsp70 and XIAP (120-356) were found to form a higher-order multimeric complex by size exclusion chromatography and multi-angle light scattering (SEC-MALS), approximately 200 kDa in size (Figure 3.10B).

XIAP (120-356) Y190E and L207S both bind to Hsp70 with weaker affinity than WT; these residues are proximally located along the central β sheet in BIR2 (Figure 3.8B). We hypothesized that these mutants would also be resistant to degradation in response to inhibition of Hsp70 with JG-98. We therefore transfected full-length XIAP Y190E, L207S, and the corresponding double mutant in HeLa cells and compared total FLAG-XIAP protein levels with and without JG-98 treatment. As expected, the Y190E mutant was not degraded upon Hsp70 inhibition, supporting the idea that this site is important for Hsp70 binding to XIAP (Figure 3.10D). Surprisingly, XIAP L207S and the double mutant were degraded in response to Hsp70 inhibition, similar to WT (compare Figure 3.7B and 3.10D), suggesting that Hsp70 recognition alone is not sufficient to induce XIAP degradation. Taken together, these results support a model in which Hsp70 may preferentially recognize specific binding sites on XIAP to form a multimeric complex and mediate its homeostasis in cells.

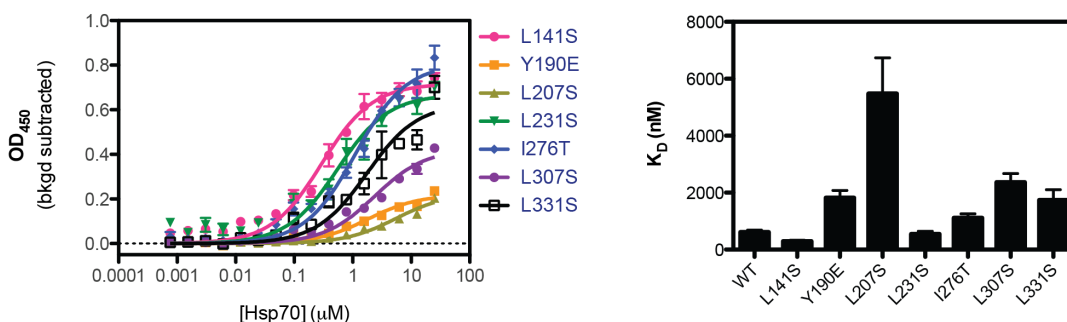
A. XIAP (120-356) mutants are well-folded



B. Hsp70 and XIAP (120-356) form a higher order complex by SEC-MALS



C. Binding of XIAP (120-356) mutants to Hsp70 in ELISA



D. XIAP Y190E is resistant to Hsp70-mediated degradation

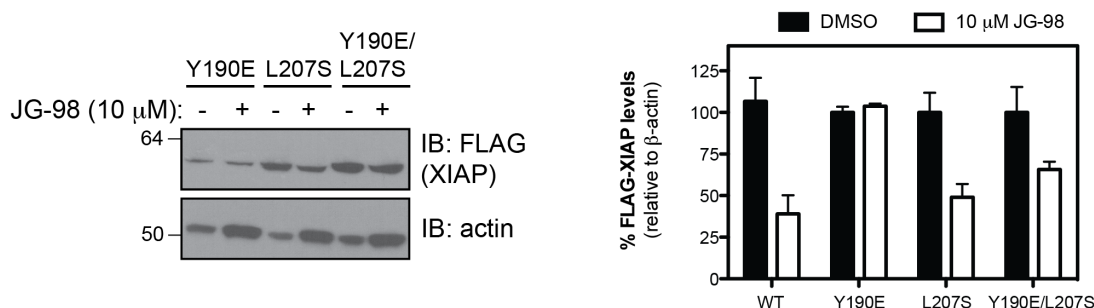
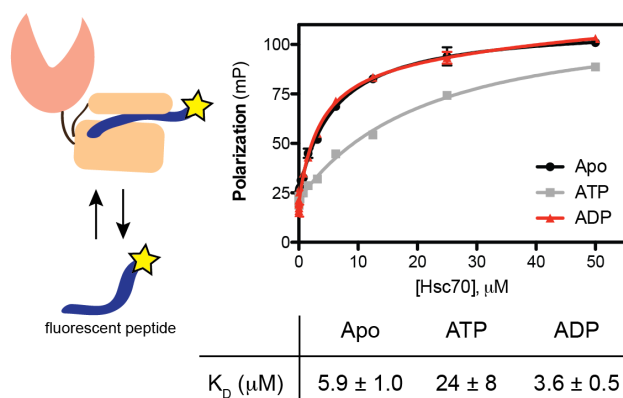


Figure 3.10 Structure and binding of XIAP (120-356) mutants to Hsp70. (A) CD spectra for XIAP (120-356) WT and mutant proteins. Each reported spectrum is the average of 6 scans, subtracting the signal acquired for buffer alone. (B) Size exclusion chromatography analysis of XIAP (120-356) – Hsp70 complex (absorbance at 280 nm versus elution volume). Approximate molecular weights calculated by multi-angle light scattering. (C) Binding of XIAP (120-356) point mutations to Hsp70, as measured by ELISA. Results are representative averages of triplicate of three independent experiments, and error bars are SEM. Binding data were fit to the Langmuir binding isotherm. (E) XIAP Y190E is resistant to Hsp70-mediated degradation. HeLa cells overexpressing the indicated XIAP point mutations were treated with JG-98 (10 μ M) for 24 hrs. Blots are representative of two independent experiments (left), and quantification is the averages of biological replicates (right). Error bars are SEM.

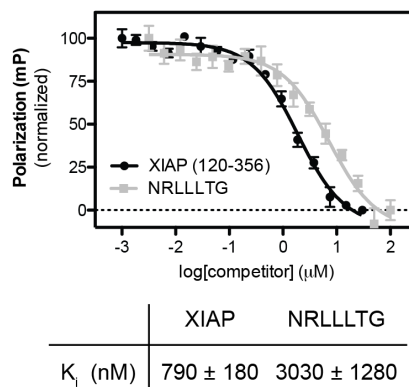
3.3.9 XIAP is a non-canonical client of Hsp70

Because XIAP binds Hsp70 *in vitro* and relies on Hsp70 for its stability in cells, we hypothesized that it would behave as a typical client protein. Canonical client binding is typically defined as an interaction with the Hsp70 SBD.^{268,269} In order to determine if XIAP (120-356) binds at a similar site, we first determined if it was able to compete with a fluorescent peptide substrate for binding to Hsc70 using a previously described fluorescence polarization assay.¹³³ In this platform, the tracer FAM-HLA binds to Hsc70 with low micromolar affinity dependent on the nucleotide state ($K_D = 3.6 \pm 0.5 \mu\text{M}$ for ADP-bound Hsp70) (Figure 3.11A). XIAP (120-356) competed with FAM-HLA for binding to Hsc70 ($K_i = 790 \pm 180 \text{ nM}$), similar to the canonical NRLLLTG substrate peptide ($K_i = 3.0 \pm 1.3 \mu\text{M}$) (Figure 3.11B). These findings suggest that XIAP (120-356) likely binds to Hsp70 similarly to known client proteins. We next wanted to determine if the reverse was also true; do peptide substrates compete with XIAP for binding to Hsp70? In order to answer this question, we used our ELISA protein-protein interaction assay. Surprisingly, we found that although XIAP (120-356) was able to compete with itself for binding to Hsp70 ($\text{IC}_{50} = 6.9 \pm 1.4 \mu\text{M}$), the NR peptide was not (Figure 3.11C). Even more strikingly, we observed a Hill slope (n_H) > 1 for XIAP competition, which would be expected for the multimeric complex suggested by SEC-MALS.

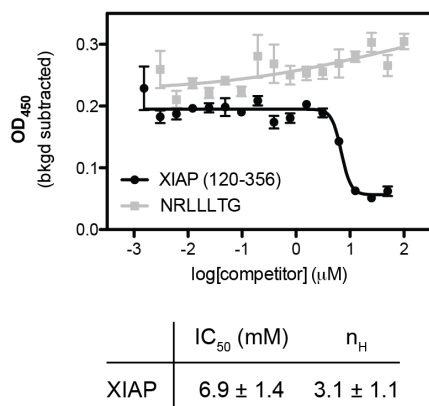
A. FAM-HLA tracer binds Hsc70 in FP



B. XIAP (120-356) and NRLLLTG compete with FAM-HLA tracer in FP



C. NRLLLTG does not compete with XIAP (120-356) in ELISA



D. Both Hsc70_{NBD} and Hsc70_{SBD} compete for XIAP binding in ELISA

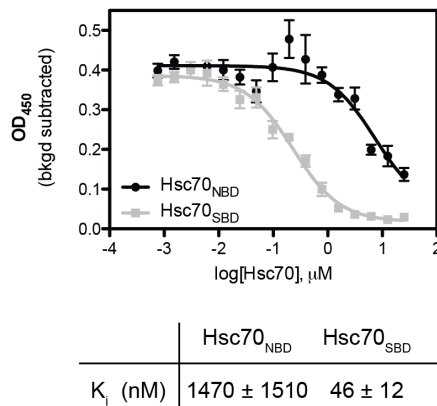


Figure 3.11 Characterization of the non-canonical interaction between Hsp70 and XIAP (120-356). (A) Client tracer (FAM-HLA) binds preferentially to ADP-bound Hsc70, as measured by fluorescence polarization. (B) XIAP (120-356) and NRLLLTG peptide compete with FAM-HLA peptide for binding to Hsc70 by fluorescence polarization. (C) NRLLLTG peptide does not compete with XIAP (120-356) for binding to Hsp70, as measured by ELISA. (D) Both Hsc70_{NBD} and Hsc70_{SBD} compete with full-length Hsp70 for binding to XIAP (120-356), as measured by ELISA. Results shown are representative averages of triplicate of three independent experiments, and error bars are SEM. Binding data were fit to the Langmuir binding isotherm, and competition data were fit to the Hill equation.

The above results suggest that XIAP is able to compete with some substrates, but not others for binding to Hsp70. It has previously been shown that the HLA peptide makes secondary binding contacts outside of the canonical substrate binding site on Hsp70,²⁷⁰ whereas NRLLLTG binds exclusively to the β -sheet SBD.²⁷¹ Because XIAP was able to compete with FAM-HLA, while the NR peptide was unable to compete with XIAP for binding to Hsp70, we hypothesized that XIAP also makes secondary contacts outside of

the SBD. We therefore determined if the isolated Hsc70 NBD or SBD were able to compete with FL Hsp70 for binding to XIAP (120-356) in the ELISA platform. We found that both Hsc70_{NBD} and Hsc70_{SBD} competed with FL Hsp70 for binding to XIAP (120-356), indicating that XIAP interacts with each domain, at least partially (Figure 3.11D). We performed TROSY-HSQC NMR with ¹³C, ¹⁵N – labeled Hsp70_{SBD} and observed chemical shift perturbations distinct from those induced by the canonical NRLLLTG peptide (Figure 3.12A and B), supporting our observations from the biochemical experiments that XIAP binds to Hsp70 in a manner distinct from that of a canonical client. Further evidence of the non-canonical interaction is given by the fact that XIAP (120-356) does not stimulate ATPase activity of the prokaryotic Hsp70, a well-known feature of peptide substrates like NRLLLTG (Figure 3.12D).¹⁹⁶

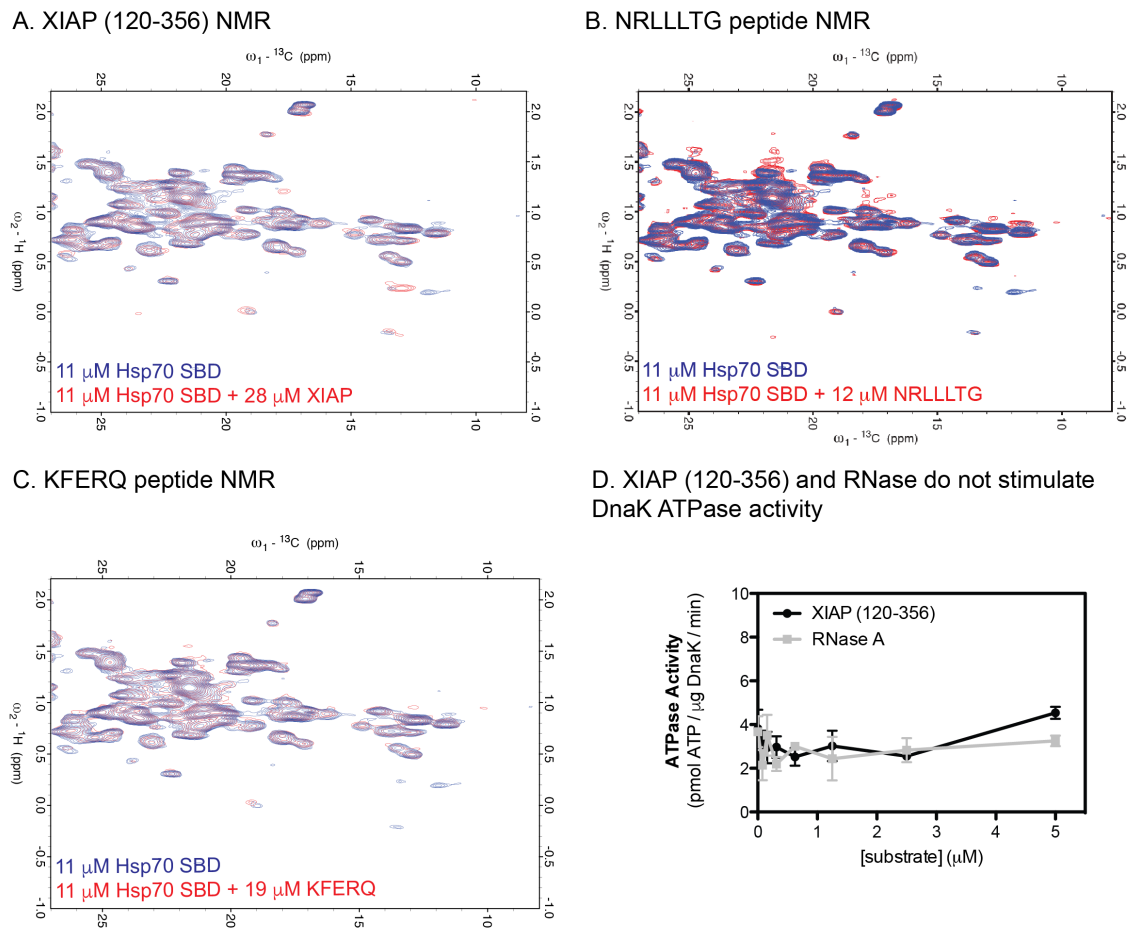


Figure 3.12 Structural analysis of the Hsp70-XIAP (120-356) interaction. TROSY-HSQC NMR spectra for ¹³C, ¹⁵N – labeled Hsc70_{SBD} (395-507) in complex with substrates (A) XIAP (120-356), (B) NRLLLTG peptide, and (C) KFERQ peptide. Spectra shown are Hsc70 alone (blue) and in complex with substrates (red). (D) XIAP (120-356) and RNase A do not stimulate ATPase activity of DnaK, as measured by malachite green. Results are averages of three independent experiments.

3.4 Discussion

There is growing interest in the development of Hsp70 inhibitors as a promising therapeutic strategy for the treatment of a variety of cancers.^{272,273} However, to date, no Hsp70-specific client proteins have been identified, and the field has suffered from a lack of biomarkers for Hsp70 engagement in cancer cells.²⁷⁴ In this chapter, we identified the IAPs as a potential new class of Hsp70 client proteins. We also explored if these proteins are chaperoned exclusively by Hsp70 and the mechanism of client recognition.

3.4.1 Hsp70 regulates RIP1-dependent cell death

The results presented in this chapter support a model in which inhibition of Hsp70-NEF interactions triggers cell death proceeding through RIP1 kinase (Figure 3.13). This pathway appears to involve both RIP1 oligomerization and the rapid destabilization of the E3 ligases of RIP1. In its normal function, Hsp70 is known to protect a number of client proteins from degradation, and it seems likely that Hsp70 may normally stabilize the IAPs and block RIP1 fibril formation to prevent RIP1-dependent cell death. While the mechanism of RIP1 oligomerization in response to Hsp70 inhibition remains to be tested, preliminary data suggests that Hsp70 is able to prevent against RIP1 aggregation in yeast (Greg Newby, Susan Lindquist laboratory, MIT, personal communication), supporting this hypothesis. When the interactions between Hsp70 and the BAG family of NEFs is inhibited, apoptosis is the predominant cell death pathway. However, necroptosis can be initiated when apoptosis is blocked. Only dual inhibition of both apoptotic and necroptotic signaling or inhibition of RIP1 kinase activity was sufficient to prevent cell death in response to JG-98 in most cell types tested, suggesting an unexpected role for Hsp70 as a hub of multiple cell survival systems. These results clearly differentiate Hsp70 from other proteostasis regulators, making it an attractive drug target in cancer.

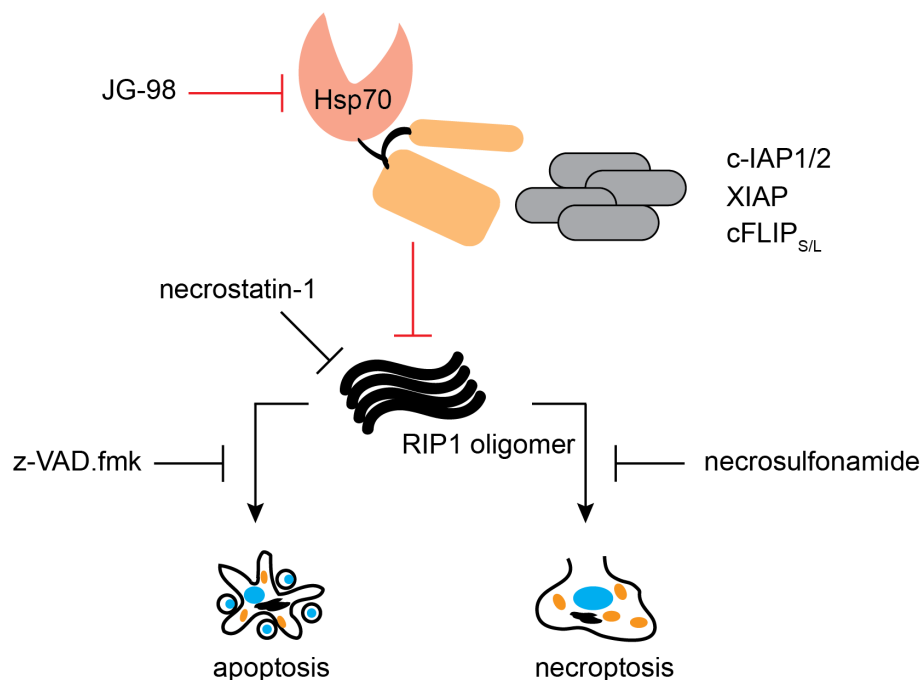


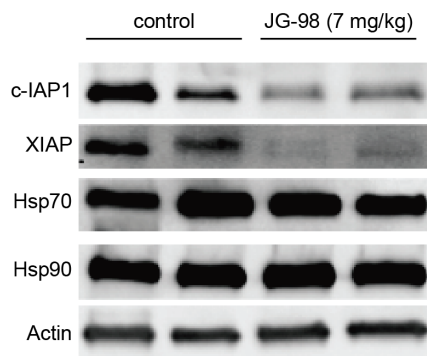
Figure 3.13 Model for Hsp70's role in RIP1-dependent cell death pathways. Hsp70 stabilizes the RIP1 E3 ligases, IAPs and FLIP and prevents formation of RIP1 oligomers. Inhibition of Hsp70-BAG interactions causes destabilization of the IAPs and RIP1 oligomerization, resulting in cell death through both apoptotic and necroptotic pathways.

3.4.2 IAPs are biomarkers for Hsp70 target engagement

By examining the kinetics of IAP destabilization following treatment with both Hsp70 inhibitors and Hsp90 inhibitors, we found that IAP degradation is both more rapid and more pronounced after treatment with Hsp70 inhibitors. This effect is particularly noticeable in the first 6 hours after treatment with the allosteric Hsp70 inhibitor JG-98, after which time we observed up to 75% loss of IAP protein levels, while levels of classic Hsp90 clients remained unchanged. In addition, treatment with Hsp90 inhibitors elicits only limited IAP degradation, while the classic Hsp90 biomarkers (Raf-1 and AKT1) are destabilized rapidly and dramatically. Our preliminary work has also suggested that IAP degradation occurs following treatment with a JG-98 analog causes degradation of the IAPs in a mouse xenograft model (Figure 3.14A). Therefore, we propose that the IAPs can be used as a biomarker for Hsp70 target engagement in cancer cells. Cellular potency and efficacy of newly developed Hsp70 inhibitors can be assessed by examining IAP levels in the first 6 hours of treatment, and along with cytotoxicity measurements, this

type of analysis should provide a good benchmark for success in Hsp70 inhibitor development.

A. Treatment with JG-98 causes loss of IAPs in mouse xenograft model



B. Loss of XIAP coincides with formation of high MW smearing

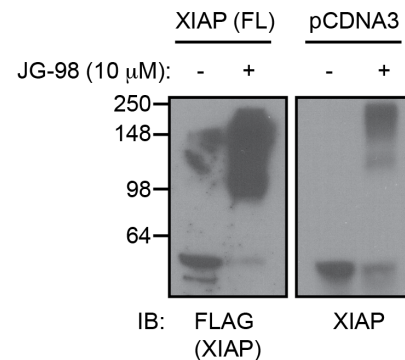


Figure 3.14 JG-98 causes loss of XIAP in MCF-7 xenograft model. (A) JG-98 treatment in mice with MCF-7 cells xenografted causes XIAP degradation. Protein levels were measured by Western blots for samples from two separate animals. (B) Degradation of XIAP coincides with high MW smearing pattern. HeLa cells transfected with either full length FLAG-tagged XIAP or empty vector were treated with 10 μ M JG-98 for 24 hours. JG-98 causes degradation of both overexpressed (left) and endogenous (right) XIAP. Results shown are representative of at three independent experiments.

Surprisingly, we did not observe proteasomal degradation of IAPs following treatment with JG-98, as co-treatment with a proteasome inhibitor did not block degradation. We did observe a high molecular weight smearing pattern along with degradation of both endogenous and overexpressed XIAP after the addition of JG-98 (Figure 3.14B). While such a smearing pattern would be consistent with poly-ubiquitination, we cannot rule out the formation of high molecular weight XIAP oligomers or protofibrils. However, given that the dimerization function of the RING domain was essential for Hsp70-mediated degradation of XIAP, we speculate that Hsp70 inhibition may induce heterodimerization with c-IAP and poly-ubiquitination of XIAP, which has been observed previously.^{275,276} XIAP has been shown to undergo lysosomal degradation by timosaponin AIII, and ubiquitination of XIAP was essential for its autophagic degradation.²⁷⁷ Therefore, it is likely that JG-98 may induce IAP degradation via chaperone-mediated autophagy (CMA), although this mechanism remains to be tested.

3.4.3 XIAP interacts with Hsp70 at a non-canonical binding site

Our cellular data suggested that the IAPs are specific substrates of Hsp70, and we explored the biochemical basis for the interaction between Hsp70 and XIAP *in vitro*. Strikingly we found that a minimal binding region of XIAP (120-356) bound Hsp70 in an atypical nucleotide-dependent manner, with XIAP (120-356) having weaker affinity for ADP-bound Hsp70 than ATP-bound Hsp70. Although we observed an interaction between XIAP (120-356) and both the NBD and SBD of Hsp70, the interaction with the SBD was distinct from that of a canonical peptide substrate by NMR. These data suggest that XIAP may interact with Hsp70 primarily through binding to the α -helical lid or unstructured C-terminal domain, with secondary contacts in the NBD and peptide binding groove of the SBD. The lid in particular has been shown to undergo significant structural rearrangement during nucleotide cycling, and can adopt intermediate conformations between the typical “open” and “closed” conformations when bound to a full-length client protein.^{278,279} Partial closing of the lid may explain the preference of XIAP to bind apo or ATP-bound Hsp70. Notably, the well-characterized CMA substrate peptide KFERQ does not bind the canonical binding groove (Figure 3.12C), and neither XIAP nor the CMA client RNase A stimulate ATP hydrolysis of DnaK (Figure 3.12D). Together, these data support our hypothesis that XIAP is a non-canonical Hsp70 CMA client.

In addition to the apparent non-canonical interaction, we noted from our mutagenesis data that no single mutation was sufficient to completely abrogate binding of XIAP to Hsp70. While it is possible that another site is necessary for recognition of XIAP by Hsp70, we hypothesize that XIAP harbors multiple Hsp70 binding sites. The observation of a ~200 kDa complex between XIAP and Hsp70 by SEC-MALS is inconsistent with 1:1 binding stoichiometry and rather suggests formation of a multimeric complex. Multiple DnaK molecules have been shown to bind denatured rhodanese to alter its conformational distribution, and binding of DnaK to hTRF1 resulted in global unfolding of the substrate.^{226,280} Given the emerging model that Hsp70 induces rapid expansion of client proteins, a multi-site binding model is expected.

3.5 Conclusions

In summary, Hsp70 is an important emerging drug target, but development of new Hsp70 inhibitors has been limited by the lack of a biomarker for Hsp70 target engagement.²⁷³ In this chapter, we used an allosteric inhibitor of Hsp70-BAG interactions to show that the IAPs are specific clients of Hsp70, and that their rapid destabilization can be used to report on the efficacy of Hsp70 inhibitors in cancer cells. Hsp70 inhibition leads to cell death dependent on RIP1 kinase. Furthermore, we have found that Hsp70 recognizes the client protein XIAP through a non-canonical, multi-site binding mechanism. These results have important implications not only for the future therapeutic development of Hsp70 inhibitors, but also offer important insights into our understanding of how Hsp70 recognizes full-length, native client proteins.

3.6 Experimental procedures

3.6.1 Reagents and general methods

Antibodies used are as follows: XIAP (Enzo Life Sciences ADI-AAM-050-E), c-IAP1 (Enzo Life Sciences ALX-803-335-C100), c-IAP2 (Cell Signaling Technology 3130), β -actin (AnaSpec AS-54591), FLAG (Sigma Aldrich F1804), Hsp70 (SantaCruz Biotechnology sc-137239 and sc-33575), Raf-1 (SantaCruz Biotechnology sc-133), AKT1 (Cell Signaling Technology 2967), GAPDH (SantaCruz Biotechnology sc-32233), Hsp90 (SantaCruz Biotechnology sc-7947), cleaved caspase 3 (Cell Signaling Technology 9664), RIP1 (BD Pharmingen 610459), CDK4 (BD Pharmingen 559693), FLIP (Alexis ALX-804-428), goat anti-mouse HRP (AnaSpec 28173), goat anti-rabbit HRP (AnaSpec 28177), and goat anti-rat HRP (SantaCruz Biotechnology sc-2006).

Inhibitors used are as follows: Necrostatin-1, bortezomib, VER-155008 (Sigma Aldrich), z-VAD.fmk (Enzo Life Sciences), necrosulfonamide (Millipore), lactacystin (Cayman Chemical), 17-DMAG (LC Laboratories), and NVP-AUY922 (ApexBio). JG-98 was synthesized according to previously described methods.²⁵⁹ All compounds were suspended in DMSO and the final solvent concentration was held at 1% in all assays.

All other biological reagents were purchased from Sigma Aldrich unless otherwise noted. All spectroscopic measurements were obtained with a SpectraMax M5 microplate reader (Molecular Devices). ATPase and fluorescence polarization assays were performed according to previously published methods.¹³³

3.6.2 Plasmids and site-directed mutagenesis

XIAP mutants were prepared using the QuikChange site-directed mutagenesis kit (Stratagene). The following mutants were engineered into the human *XIAP* (120-356) gene in pet28a vector: L141S, Y190E, L207S, L231S, I276T, L307S, and L331S. Wild type and mutant XIAP (120-356) constructs all contained additional C202A C213G mutations for stability. N-terminally FLAG-tagged, full length *XIAP* in pCMV6 was obtained from GeneArt (Invitrogen). The following point and deletion mutations were made in the full length *XIAP* gene: V80D, D148A, W310A, V461D, M382L F384L, F495A, Δ 26-93 (Δ BIR1), Δ 163-230 (Δ BIR2), Δ 265-330 (Δ BIR3), Δ 376-416 (Δ UBA), and Δ 450-485 (Δ RING).

3.6.3 Protein expression and purification

All His-tagged Hsp70 proteins (HSPA1A, HSPA8, Hsc70_{NBD} (1-383) and Hsc70_{SBD} (395-509)) were purified as previously described using batch purification with Ni-NTA resin (Novagen) and subsequent cleavage of the His tag with TEV protease.²¹² Hsp70, Hsc70, and Hsc70_{NBD} were further purified using an ATP column while Hsc70_{SBD} underwent gel filtration chromatography on a Superdex 75 16/60 column (GE Healthcare). His-tagged Hsp90 α was batch purified with Ni-NTA resin and anion exchange chromatography on a Source Q column (GE Healthcare). Fractions containing Hsp90 α were pooled and dialyzed overnight into 20 mM Tris buffer (pH 7.5) containing 50 mM KCl, 6 mM β -mercaptoethanol, and 10% glycerol. WT His-tagged XIAP (120-356) and its mutants were batch purified with Ni-NTA resin and eluted with 400 mM imidazole. DTT was added to 10 mM, and XIAP (120-356) was further purified by gel filtration chromatography on a Superdex 75 16/60 column (GE Healthcare) in 20 mM Tris buffer containing 200 mM NaCl, 50 μ M Zn acetate, and 1 mM DTT (pH 7.5). Fractions containing XIAP (120-356), as assessed by SDS-PAGE were pooled, concentrated, and

DTT was added to 10 mM before storing at -80°C. The BCA (bicinchoninic acid) assay kit (Thermo Fisher Scientific Inc.) was used to determine protein concentration, and protein purities were estimated at > 90% by SDS-PAGE and Q-TOF LC-MS (Agilent).

3.6.4 Tissue culture, viability assays, and transfections

MCF-7 and HeLa cells (ATCC) were maintained in DMEM (Invitrogen) supplemented with 10% fetal bovine serum and 1% penicillin-streptomycin. MDA-MB-231 cells (ATCC) were maintained in DMEM supplemented with 10% fetal bovine serum, 1% penicillin-streptomycin, and non-essential amino acids. If indicated, cell viability was determined using the MTT assay as previously described.²⁵⁹ XIAP pCMV6 plasmids were transfected using Lipofectamine 2000 (Invitrogen) according to the manufacturer's instructions. If indicated, cells were visualized using an Olympus IX83 inverted microscope. For each experiment, at least 10 individual frames were examined, and representative panels were chosen for presentation.

3.6.5 Western blotting

Cell extracts were prepared in chilled RIPA buffer (50 mM Tris pH 8, 150 mM NaCl, 1% Triton X-100, 0.5% Na deoxycholate, 0.1% SDS) unless otherwise indicated. Protein concentration was determined by the BCA assay and 20 µg of total protein was separated by SDS-PAGE on 10% Mini-PROTEAN TGX gel (Bio-Rad) and transferred to PVDF membrane (Thermo Fisher Scientific Inc). Membranes were blocked with 5% milk in TBS, 0.05% Tween for 1 hr at room temperature, incubated with primary antibodies overnight at 4°C, washed with TBS, 0.05% Tween, and incubated with the appropriate horseradish peroxidase conjugated secondary antibody for 1 hr at room temperature. Membranes were developed using chemiluminescence (ECL Prime, GE Healthcare).

3.6.6 Co-immunoprecipitation

Cell extracts were prepared in chilled lysis buffer (50 mM Tris pH 8, 150 mM NaCl, 1 mM ATP, 10 mM KCl, 5 mM Mg(OAc)₂, 1% NP-40) supplemented with protease inhibitor cocktail (Roche Applied Science). The total protein concentration was adjusted to 5 mg of protein in 1 mL of cell extract. PureProteome Protein G magnetic beads

(Millipore) were incubated with 6 μ g of the appropriate antibody or nonspecific mouse IgG (Santa Cruz Biotechnology) for 30 min at room temperature with mixing, followed by antibody crosslinking with bis(sulfosuccinimidyl) suberate (Thermo Scientific) for 1 hr at room temperature with mixing. The crosslinking reaction was quenched with 1 M Tris (pH 7.5) for 1 hour at room temperature with mixing. Meanwhile, equal 100 μ L samples of cell lysate were pre-cleared by incubation with 50 μ L of protein G beads for 1 hour at room temperature with mixing. Protein complexes were immunoprecipitated by incubation of the pre-cleared lysate (1 mg total protein per IP) with 50 μ L of antibody-crosslinked protein G beads for 1 hour at room temperature with mixing. The immunocomplexes were washed 3 times with 500 μ L of wash buffer (PBS pH 7.4, 0.1% Tween-20) and eluted with 0.1 M glycine (pH 2.6). Proteins were visualized by Western blot.

3.6.7 ELISA

Binding of human Hsp70 to XIAP (120-356) was measured using a protocol adapted from a previous report.¹⁷⁴ XIAP (120-356) was non-covalently immobilized in the wells of a clear, flat-bottom 96-well plate (Thermo Fisher Scientific Inc) by incubating 100 μ L of 100 nM XIAP (120-356) in immobilization buffer (20 mM MES, pH 5.2) overnight at 37°C. XIAP (120-356) was removed from the wells, and the wells were washed with 3 x 150 μ L of TBS supplemented with 0.05% Tween (TBS-T). Each wash was incubated, with gentle rocking, for 3 min at room temperature. Following washing, 30 μ L of Hsp70 was added at the indicated concentrations in binding buffer (25 mM HEPES pH 7.4, 40 mM KCl, 8 mM MgCl₂, 100 mM NaCl, 0.01% Tween), supplemented with 1 mM ATP and 1 mM DTT. The plates were incubated at room temperature for 24 hrs with gentle rocking. Solutions of Hsp70 were removed and each well was washed as before and blocked with 100 μ L of 5% milk in TBS-T for 5 min at room temperature. The plates were developed using 50 μ L each of Hsp70 primary antibody (1:5000 in TBS-T) and an HRP-conjugated secondary antibody (1:5000 in TBS-T), washing with TBS-T between each 1 hr incubation at room temperature. Binding was detected using the TMB substrate kit (Cell Signaling Technology), and absorbance was read at 450 nm. Data were analyzed

using GraphPad Prism software and fit to the Langmuir binding isotherm ($Y = B_{\max} X / (K_D + X)$).

3.6.8 Size exclusion chromatography and multi-angle light scattering

XIAP (120-356) and Hsp70 were separated by size exclusion chromatography on a Superose 6 column (GE Healthcare) in 20 mM Tris buffer (pH 7.5) containing 200 mM NaCl, 5 mM $MgCl_2$, 10 mM KCl, 50 μ M Zn acetate, 1 mM DTT. The average molecular weight of the complex was determined using a DAWN HELEOS II MALS detector and Optilab rEX differential refractive index detector with ASTRA VI software (Wyatt Technology Corporation). The molecular weight of a selected peak was calculated using the Raleigh ratio of the static light scattering and protein concentration.

3.6.9 Circular dichroism

CD spectra of XIAP (120-356) were acquired on a J-715 spectropolarimeter (Jasco Inc) using a 1 mM pathlength quartz cuvette, subtracting the CD signal acquired for buffer alone (10 mM sodium phosphate pH 7.6, 100 mM NaF, 50 μ M Zn acetate, 0.5 mM DTT). Data were converted to mean residue ellipticity ($\text{deg cm}^{-1} \text{dmol}^{-1}$) according to the equation $\Theta = \Psi / (1000nlc)$, where Ψ is the CD signal in degrees, n is the number of amides, l is the path length in centimeters, and c is the concentration in decimoles per cm^3 . Each spectrum reported is the average of 6 scans.

3.6.10 NMR

Binding of XIAP (120-356) to Hsc70_{SBD} was measured by 2D HSQC-TROSY NMR on a Varian/Agilent 800 MHz NMR system, using methods that were previously described.²¹⁸ Briefly, small aliquots of XIAP (120-356) (380 μ M in storage buffer) were added to ^{13}C , ^{15}N – labeled Hsc70_{SBD} (395-507) (11 μ M) in NMR buffer (25 mM Tris, 10 mM $MgCl_2$, 5 mM KCl, 10% $^2\text{H}_2\text{O}$, 0.01% sodium azide, pH 7.1, 5 mM ADP, 10 mM potassium phosphate). Identical aliquots of buffer without compound were added to the protein sample in NMR control experiments.

Notes

Portions of this chapter have been submitted or are in preparation for submission for publication as Srinivasan, S. R.; Cesa L.C. *et al.* “Hsp70 Regulates RIP1-Dependent Cell Death”, under review at *Nature Chemical Biology*, and Cesa, L. C. *et al.* “X-linked Inhibitor of Apoptosis Protein (XIAP) is a Non-Canonical Client of the Hsp70 Molecular Chaperone”, in preparation. Laura C. Cesa, Sharan R. Srinivasan, Hao Shao, Anna K. Mapp, and Jason E. Gestwicki designed the experiments. Laura C. Cesa, Sharan R. Srinivasan, Hao Shao, and Chetali Jain conducted the experiments. Erik R. P. Zuiderweg performed the NMR. The XIAP (120-356) pet28a vector and Hsp90 α pet151 vector were kind gifts from Dr. Jeanne Stuckey and Dr. Daniel Southworth, respectively. SM-164 was provided by Dr. Shaomeng Wang.

Chapter 4

Identification of the Sub-Network of Client Proteins that are Dependent on the Molecular Chaperone Hsp70

4.1 Abstract

Protein-protein interactions (PPIs) form the backbone of a larger protein network essential for nearly all cellular processes. Multi-protein complexes are hubs in this networks and connect diverse cellular processes through a physical web of individual protein interactions. Although targeting the enzymatic activity of the core components of these complexes has long been a major goal in drug discovery, inhibiting the individual PPIs may offer several therapeutic advantages. Chief among these is the idea that targeting PPIs may allow for greater specificity in the ability to target certain cellular pathways and not others. However, it is often not straightforward to understand how modulation of a single PPI within a larger multi-protein complex might affect binding (and/or activity) of other downstream partners. In other words, by trapping a specific conformation of a given protein target, can we “tune” the protein network such that interactions with certain binding partners are strengthened while others are inhibited? In this chapter, we use a small molecule inhibitor of the molecular chaperone Hsp70 to understand how stabilizing a particular Hsp70 nucleotide state affects binding to both co-chaperone and substrate proteins. We also describe preliminary efforts to characterize effects of small molecules on PPIs in another system with Src kinase. Knowledge of how small molecules are able to modulate protein networks will inform how we can use such inhibitors to achieve a desired therapeutic outcome.

4.2 Introduction

Multi-protein complexes are ubiquitous in biology and are essential for many cellular processes, including gene expression, protein homeostasis, cell signaling, and countless others.^{7,8} These large structures are assembled around a “core” enzyme, such as a kinase,

phosphatase, or GTPase. Interactions between the core enzyme and adaptor and scaffolding proteins or other non-enzymes modulate the function of the complex by dictating subcellular localization, regulating enzymatic activity, or controlling substrate binding.¹⁻³ The specific arrangement of these interchangeable modules is mediated by a combination of strong and weak interactions, giving rise to specificity in overall function while maintaining the transience necessary for regulatory signaling, in which binding partners trap certain conformations of the “core” enzyme and favor a specific outcome.⁴

4.2.1 Small molecules propagates changes in protein networks

As discussed in Chapter 1, it is increasingly appreciated that targeting the specific PPIs that comprise these systems could offer several advantages.¹¹⁻¹³ For instance, by targeting specific PPIs within a larger enzymatic complex, it is possible to “tune” the output of the system without completely blocking activity, and this idea is well-established for modulators of GPCRs and nuclear receptors.¹⁴ In addition, the potential for specificity exceeds that of targeting the enzymes themselves, which often feature conserved active sites and mechanisms of action.¹⁵

Interactions with immediate binding partners regulate the function of an enzyme and can also link the enzyme to a broader PPI network. In this chapter, we explore the effect of inhibiting a single protein target or “node” with a small molecule on both its direct interactions with binding partners and the function of the larger protein network.

4.2.2 The Hsp70 molecular chaperone complex as a model system

As a model system, we used the Hsp70 molecular chaperone complex (see Chapter 2). This system consists of the core enzyme Hsp70, an ATPase containing a nucleotide binding domain and a substrate binding domain connected by a short linker, and several families of co-chaperone proteins.¹⁹² Hsp70 is regulated by an allosteric mechanism whereby its affinity for substrates is dependent on its nucleotide state; the ATP-bound state adopts an “open” conformation with a characteristically low affinity for substrates, and ATP hydrolysis triggers a “closed” conformation with a higher affinity for bound substrates.^{197,198} Enzymatic activity of Hsp70 is regulated by a number of non-enzyme

binding partners. For example, J proteins increase the rate of ATP hydrolysis,^{127,199} while nucleotide exchange factors (NEFs) facilitate the release of ADP and allow Hsp70 to proceed through many iterative cycles of ATP binding and hydrolysis.¹²⁶ In addition, interactions with scaffolding proteins and other non-enzymes link Hsp70 with the larger network of molecular chaperones and protein quality control machinery; in particular, E3 ligases bind to Hsp70 and promote substrate ubiquitination and proteasomal degradation.^{281–283} Importantly for this work, Hsp70 also makes PPIs with client proteins. As discussed in Chapter 3, Hsp70 binds to a wide number of both folded and unfolded proteins. This interaction can be stabilizing in some cases, such that interactions with Hsp70 are required for the lifetime of the client.

In this chapter, we examined the effect of an allosteric inhibitor of Hsp70 on its network of substrate proteins using an unbiased proteomics approach. We found that treatment with an Hsp70 inhibitor resulted in destabilization of a number of “client” proteins in cells. Therefore, we used the pattern of protein degradation in response to Hsp70 inhibition to infer how inhibition of Hsp70 propagates changes throughout the larger network of Hsp70 substrates. This approach allowed us to define a subset of the proteome that relies on Hsp70 for stability.

4.3 Results

JG-98 is an allosteric inhibitor of Hsp70 that stabilizes the ADP-bound state of Hsp70 by binding in the NBD at a site distal to the nucleotide binding site.²¹⁸ The BAG family of NEFs prefer binding to apo-Hsp70,⁹⁰ and therefore JG-98 acts as an inhibitor of the PPI between Hsp70 and the BAGs (Figure 4.1). Importantly, JG-98 has little effect on other PPIs with Hsp70, including J proteins or TPR (tetratricopeptide repeat) domain containing proteins.²⁸⁴ It had previously been shown that inhibition of the Hsp70-BAG3 interaction led to destabilization and degradation of a number of known Hsp70 client proteins, including FoxM1, tau, and polyQ-AR.^{160,161,213} We hypothesized that we could use JG-98 to tune the Hsp70 PPI network such that interactions with BAGs were selectively disrupted while interactions with other co-chaperones were unaffected. We measured this pattern of PPI disruption, allowing us to identify a network of Hsp70-BAG

dependent client proteins using mass spectrometry and proteomics. In other words, we could disrupt a single PPI in the sub-network and then explore the functional implications on the Hsp70-client interactions.

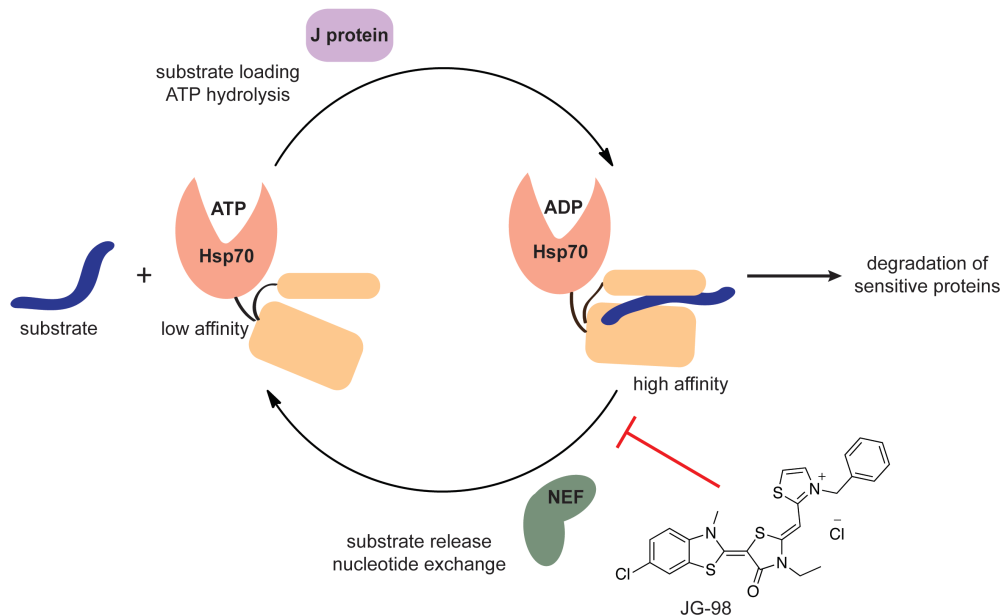
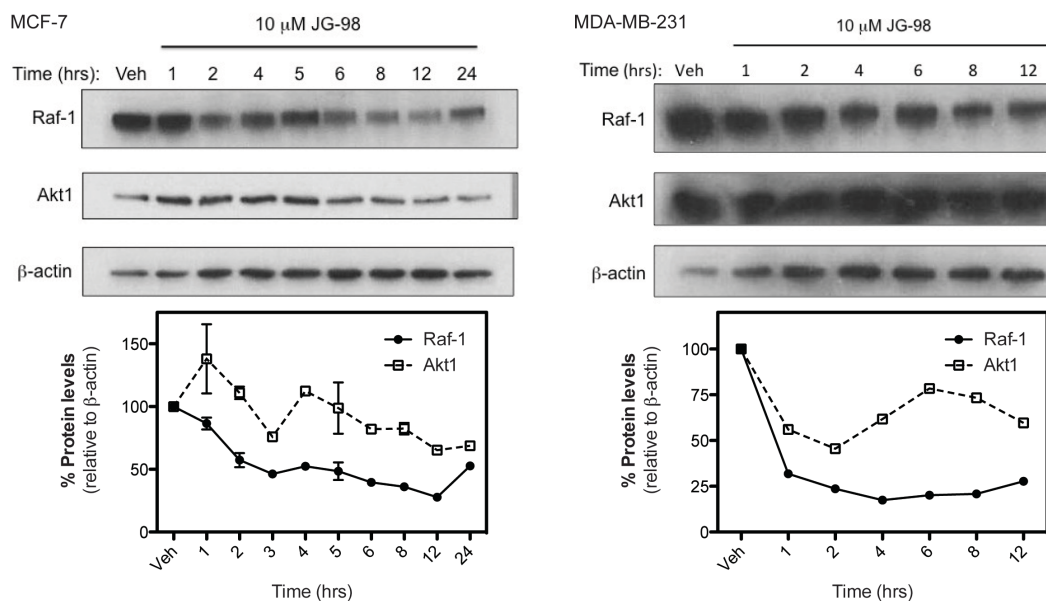


Figure 4.1 JG-98 allosterically inhibits the Hsp70-NEF interactions. Hsp70 hydrolyzes ATP to modulate its affinity for substrate proteins. J proteins stimulate ATP hydrolysis, while NEFs promote nucleotide release. JG-98 binds to Hsp70 at an allosteric site, stabilizing the ADP-bound conformation and inhibiting interactions with BAG NEFs. The ADP-bound state in turn has a higher affinity for substrate proteins, which we hypothesized would lead to degradation of bound substrates.

4.3.1 JG-98 causes rapid degradation of classic Hsp90 client proteins

In order to identify proteins sensitive to Hsp70 inhibition, we first wanted to determine the kinetics of degradation of known clients following treatment with JG-98. It is well known that Hsp90 clients like kinases, transcription factors, and E3 ubiquitin ligases are rapidly destabilized in cells following treatment with both Hsp90 and Hsp70 inhibitors.^{239,240} Indeed, in Chapter 3, we demonstrate that some Hsp90 clients are also sensitive to inhibition of Hsp70 with JG-98 in a number of breast cancer cell lines. Therefore, we treated MCF-7 and MDA-MB-231 cells with 10 μ M JG-98 over 24 hours and blotted for Hsp90 clients Raf-1 and AKT1. Degradation of these client proteins was more pronounced in MCF-7 cells, with Raf-1 degradation after 2 hours of JG-98 treatment and AKT1 degradation after 6 hours (Figure 4.2A). In MDA-MB-231 cells, degradation occurred after 4 and 6 hours, respectively (Figure 4.2A).

A. JG-98 induces rapid degradation of Hsp90 clients in breast cancer cell lines



B. 5 hour treatment with JG-98 is sufficient to cause Hsp90 client degradation

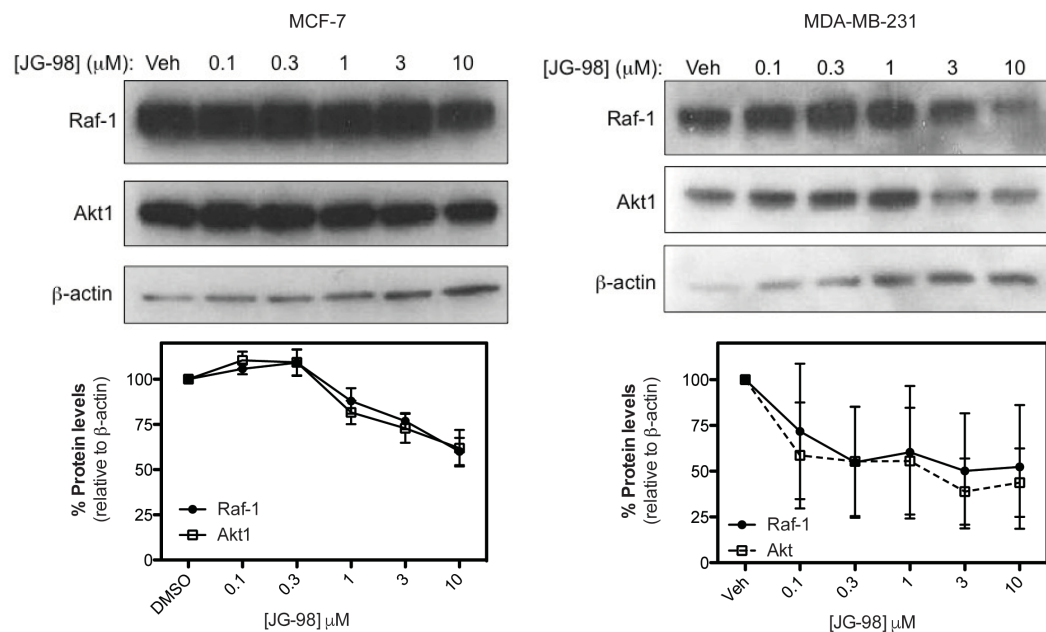
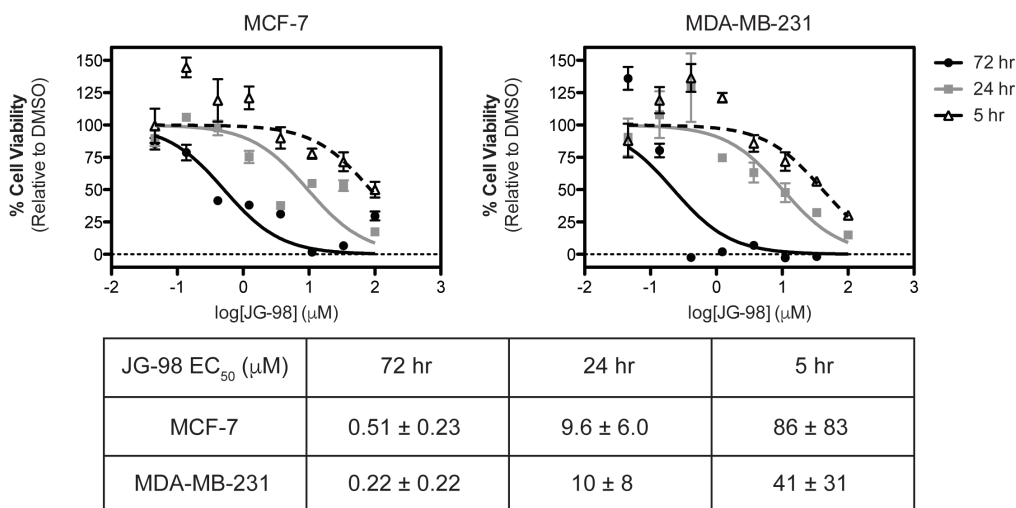


Figure 4.2 JG-98 causes degradation of classic Hsp90 client proteins. (A) JG-98 induces rapid degradation of Hsp90 clients Raf-1 and AKT1 in MCF-7 (left) and MDA-MB-231 (right) cells. Cells were treated with 10 μ M JG-98 for the indicated time points. (B) 5 hour JG-98 treatment is sufficient to induce degradation of Raf-1 and AKT1 in MCF-7 (left) and MDA-MB-231 (right) cells. Cells were treated with JG-98 at the indicated concentrations for 5 hrs. All blots shown are representative of two independent biological replicates, and protein levels were quantified across all biological replicates. Error bars are SEM.

A. 5 hour treatment with JG-98 is weakly cytotoxic in breast cancer cell lines



B. JG98-biotin binds Hsp70, but not Hsp90, by ELISA

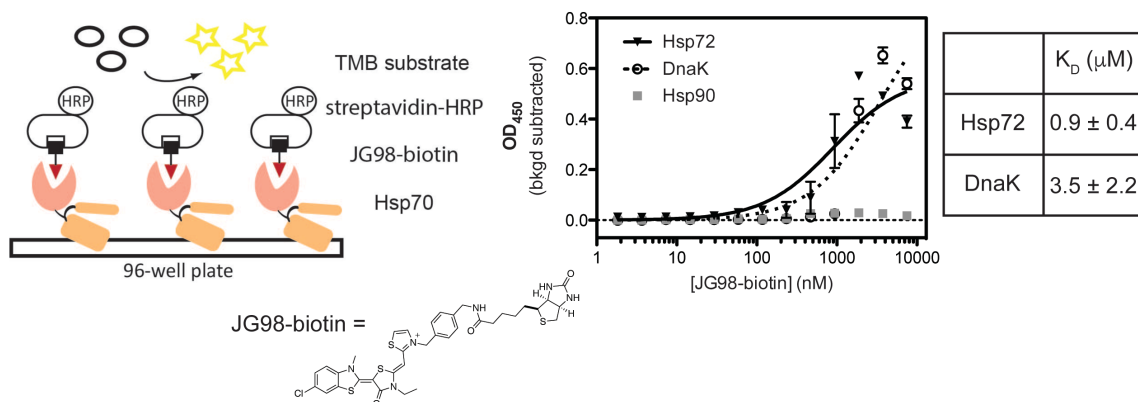


Figure 4.3 JG-98 mediated cytotoxicity is dependent on binding to Hsp70. A) JG-98 is weakly cytotoxic in 5 hour treatment window in MCF-7 (left) and MDA-MB-231 (right) cell lines. Cells were treated with JG-98 at the indicated concentrations for 5, 24, and 72 hrs. Viability was measured with the WST-1 reagent. (B) JG98-biotin binds to Hsp70, but not Hsp90. Affinity of biotinylated JG-98 for DnaK, Hsp72, and Hsp90α in an ELISA assay (left schematic). Protein was immobilized in the wells of a 96-well plate and incubated with JG98-biotin. Binding was detected with streptavidin-HRP. All results shown are representative averages of triplicate of three independent experiments, and error bars are SEM.

Given this window of JG-98 treatment after which Hsp90 clients became destabilized, we hypothesized that 5 hour treatment would be sufficient to induce degradation of both Raf-1 and AKT1 in both MCF-7 and MDA-MB-231 cells. At the same time, we wanted to pick a relatively early time point to minimize the opportunity of finding secondary effects. After 5 hour treatment with 10 μM JG-98, we observed at least 50% degradation of both client proteins in both cell lines (Figure 4.2B). These results suggest that this

treatment regime was indeed sufficient to cause measurable degradation of several known Hsp90 client proteins.

4.3.2 JG-98 is mildly cytotoxic after 5 hours

In order to simplify analysis of future proteomics data, we wanted to ensure that JG-98 is not inducing significant cell death under treatment conditions sufficient to induce degradation of classic Hsp90 clients. We therefore measured cell viability in both MCF-7 and MDA-MB-231 at 5 hours, 24 hours, and 72 hours following treatment with JG-98. While JG-98 was strongly anti-proliferative in both cell lines at 72 hours ($EC_{50} = 510 \pm 230$ nM and 220 ± 220 nM, respectively), it was less potent at 24 hours ($EC_{50} \sim 10$ μ M for both cell lines) (Figure 4.3A). At just 5 hours however, we did not observe significant loss of cell viability in either cell line at 10 μ M JG-98 ($EC_{50} > 40$ μ M) (Figure 4.3A). These results suggest a treatment and dosing regime in which the effects of JG-98 on client would primarily be due to its effect on the PPI between Hsp70 and BAG3, and not a secondary effect.

4.3.3 JG-98 binds Hsp70, but not Hsp90

While it is well established that inhibition of Hsp70 causes destabilization of canonical Hsp90 clients,^{239,240} we wanted to ensure that the effect of JG-98 on Raf-1 and AKT1 stability was due to its affinity for Hsp70, not because of any interaction with Hsp90. JG-98 has a very different chemical structure than known Hsp90 inhibitors, but this was still an important control. We therefore expressed and purified recombinant Hsp70 and Hsp90 from bacteria and measured their affinity for a biotinylated analog of JG-98 using a modified ELISA assay.²⁵⁹ In this platform, JG-98 bound the human stress inducible Hsp72 and its prokaryotic paralog DnaK with comparable affinity ($K_D = 0.9 \pm 0.4$ μ M and 3.5 ± 2.2 μ M, respectively) (Figure 4.3B). As expected, we did not observe significant binding to Hsp90 α ($K_D > 30$ μ M) (Figure 4.3B). These results that JG-98 induces degradation of Hsp90 clients primarily by binding to Hsp70.

4.3.4 Hsp70 inhibition results in qualitative proteomic changes

By examining changes in Raf-1 and AKT1 levels and measuring cell viability in response to JG-98 treatment, we identified a treatment regime in which Hsp90 clients were degraded but significant cell death had not yet occurred. We next wanted to determine the effect of this JG-98 treatment on global protein levels, using Western blotting of several known Hsp90 clients and silver staining of whole cell lysates as a qualitative assessment of the stability of the proteome after acute disruption of Hsp70 function. We grew large 10 mL cultures of MCF-7 and MDA-MB-231 cells and treated parallel cultures of each cell line with either 10 μ M JG-98 or 0.1% DMSO for 5 hours. Cell extracts were blotted for the Hsp90 client proteins Raf-1, AKT1, HER2, and CDK4. As expected, we observed degradation of all proteins under these treatment conditions, with more dramatic reductions in protein levels observed in MDA-MB-231 cell lysate (Figure 4.4A).

A. JG-98 causes degradation of multiple Hsp90 clients B. JG-98 treatment results in changes in global protein levels

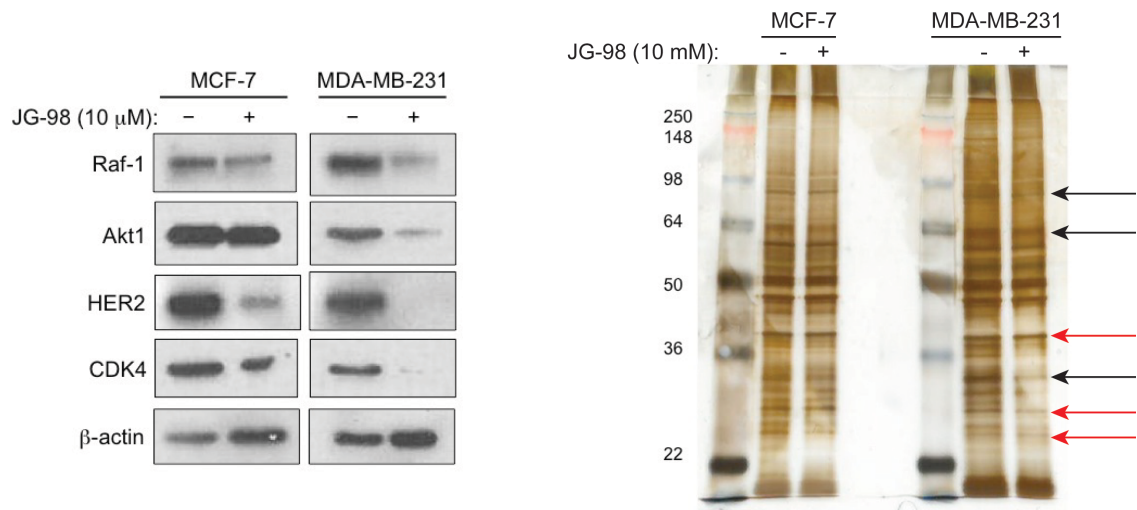


Figure 4.4 JG-98 treatment results in qualitative proteome-wide changes in protein expression levels. (A) JG-98 treatment results in degradation of multiple Hsp90 client proteins. MCF-7 (left) and MDA-MB-231 (right) cells were treated with 10 μ M JG-98 for 5 hrs. Cell extracts were blotted for Raf-1, AKT1, HER2, CDK4, and actin as a loading control. (B) JG-98 causes qualitative changes in global protein levels. MCF-7 (left) and MDA-MB-231 (right) cells were treated with 10 μ M JG-98 for 5 hrs. Cell extracts were separated by SDS-PAGE and silver stained. Black arrows indicate individual protein bands decreased in both cell lines; red arrows indicate protein bands decreased in only one cell line. All results shown are representative of two independent biological replicates.

We then wanted to qualitatively assess protein levels across the proteome in both cell lines after JG-98 treatment. This type of experiment could be performed in a number of different ways. We chose separate equal amounts of total protein by SDS-PAGE to see if

there were obvious changes in a subset of the proteome. Indeed, we observed several changes in both cell lines under these treatment conditions (Figure 4.4B). Interestingly, while some bands were decreased in response to JG-98 treatment in both cell lines (Figure 4.4B, black arrows), we also observed distinct changes in MCF-7 cells that were not present in MDA-MB-231 cells and vice versa (Figure 4.4B, red arrows). These results suggest that Hsp70 may play cell-type specific roles in protein quality control. For example, MDA-MB-231 is a triple negative breast cancer cell line, indicating that cells do not overexpress the estrogen receptor (ER), progesterone receptor (PR), or HER2.²⁸⁵ Conversely, MCF-7 cells are negative for only HER2 overexpression, but express both estrogen and progesterone receptors.²⁸⁶ Both ER and PR are members of the class of nuclear hormone receptors, a group of known Hsp90 clients.^{287,288} Hsp70 has been shown to collaborate with Hsp90 and a number of co-chaperones to stabilize the glucocorticoid receptor (GR),^{151,289,290} and differential effects of JG-98 on global protein levels in MCF-7 versus MDA-MB-231 may be due to variation in expression of both known Hsp90 clients and unknown Hsp70 clients in these cells.

4.3.5 Quantitative proteomics reveals a network of client proteins sensitive to Hsp70 inhibition

Given the promising qualitative assessment of changes in protein levels in response to JG-98 treatment, we hypothesized that this inhibitor would allow us to define a network of proteins, the levels of which are sensitive to inhibition of the interaction between Hsp70 and BAG3. While it is well known that Hsp90 clients are degraded in response to treatment with Hsp70 inhibitors,^{239,240} it is not known if the pool of Hsp70 clients is redundant with Hsp90 clients. In other words, are all Hsp70 clients also Hsp90 clients? Our results described in Chapter 3 suggest that this is not the case, as the inhibitor of apoptosis proteins (IAPs) are sensitive to Hsp70 inhibition, but not Hsp90 inhibition. We therefore wanted to define the global network of Hsp70 client proteins in more detail.

4.3.5.1 10% of identified proteins are differentially expressed in SILAC

Stable isotope labeling with amino acids in cell culture (SILAC) is a powerful tool to quantify changes in global protein levels under different conditions.^{291,292} We therefore

used this approach to identify which proteins are differentially expressed after inhibition of Hsp70 with JG-98 in MCF-7 cells.

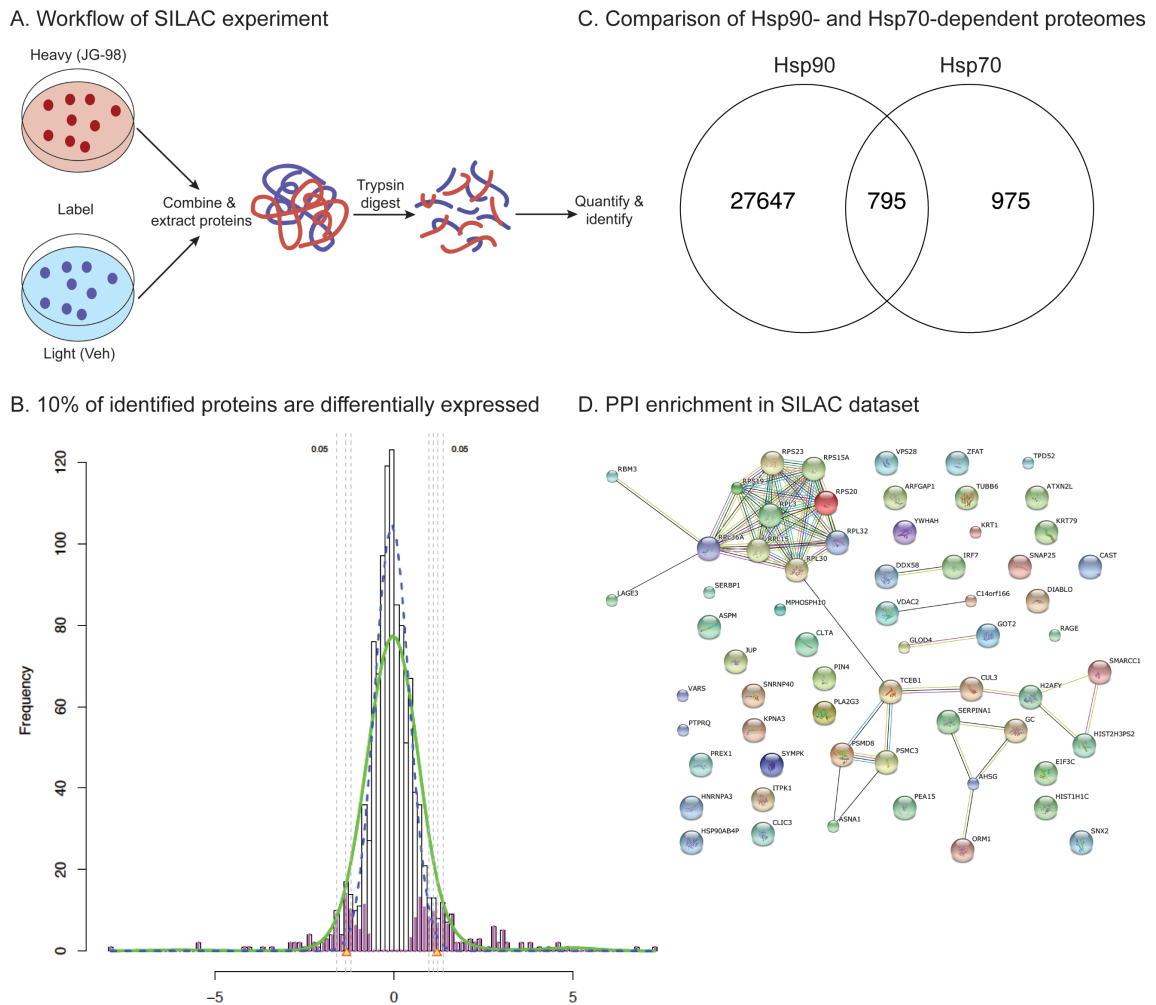


Figure 4.5 Hsp70 inhibition results in differential expression of 10% of the identified proteome. (A) Schematic of SILAC experimental workflow. Parallel cultures of heavy and light labeled MCF-7 cells were treated with either 10 μ M JG-98 or 0.1% DMSO for 5 hrs. Cell extracts were mixed in a 1:1 heavy:light ratio and subjected to in-gel tryptic digest. Proteins were identified by MS/MS and relative quantitation was obtained by comparing the intensity of light and heavy peaks of individual peptides. (B) Histogram of protein quantitation of ~1000 identified proteins with a probability cutoff of 0.9. With a FDR of 0.05% (dashed lines), ~100 proteins (10% of those identified) were differentially expressed. (C) Comparison of Hsp70-dependent proteome with Hsp90-dependent proteome identified in a similar analysis.²⁹³ Numbers represent individual peptides, not taking into account common peptides in protein groups. (D) Protein interaction map of proteins with decreased expression after JG-98 treatment, predicted by STRING.²⁹⁴ A total of 56 interactions were observed of 63 total proteins (p-value – 1.26×10^{-6}).

Parallel cultures were grown in media spiked with either $^{12}\text{C}_6$ (“light”) or $^{13}\text{C}_6$ (“heavy”) labeled arginine and lysine. The heavy culture was treated with 10 μ M JG-98, while the light culture was treated with 0.1% DMSO (Figure 4.5A). Cell extracts were mixed in a

1:1 heavy:light ratio, resolved by SDS-PAGE and digested with trypsin. Following additional separation by reverse phase liquid chromatography, proteins were identified using tandem mass spectrometry (MS/MS). By comparing the abundance of individual peptide ions of a given protein in the light versus heavy state, the absolute quantitation of protein levels in both cultures was determined. With a probability cutoff of 0.9, we identified ~1000 total proteins. Comparing the heavy:light ratio of all identified proteins and setting a false discovery rate (FDR) of 0.05% allowed us to determine that the levels approximately 10% of all identified proteins were changed by Hsp70 inhibition (Figure 4.5B). More specifically, ~60 proteins were found to have lower levels following JG-98 treatment (Table 4.1), while 35 proteins had higher levels under the same conditions (Table 4.2).

Table 4.1 Identified proteins with decreased expression after JG-98 treatment

| Expression ratio | Unique peptides | Gene name | Expression ratio | Unique peptides | Gene name |
|-------------------------|------------------------|------------------|-------------------------|------------------------|------------------|
| 0.46 | 2 | KPNA3 | 0.19 | 1 | TCEB1 |
| 0.37 | 3 | HIST1H1C | 0.19 | 1 | IRF7 |
| 0.10 | 3 | RPS19 | 0.28 | 4 | AHSG |
| 0.44 | 20 | RPL30 | 0.21 | 2 | H2AFY |
| 0.30 | 4 | ARFGAP1 | 0.12 | 3 | RPL36A |
| 0.46 | 6 | ASNA1 | 0.37 | 1 | SERBP1 |
| 0.02 | 1 | SNX2 | 0.42 | 2 | CLTA |
| 0.27 | 14 | CLIC3 | 0.13 | 3 | SNAP25 |
| 0.25 | 11 | SERPINA1 | 0.33 | 2 | RPS23 |
| 0.46 | 2 | JUP | 0.29 | 1 | VDAC2 |
| 0.23 | 2 | KRT1 | 0.22 | 2 | ASPM |
| 0.41 | 3 | KRT79 | 0.41 | 1 | SMARCC1 |
| 0.22 | 1 | HSP90AB4P | 0.34 | 1 | HIST2HPS2 |
| 0.23 | 14 | PSMC3 | 0.23 | 1 | PLA2G3 |
| 0.46 | 2 | CAST | 0.42 | 1 | DDX58 |
| 0.46 | 4 | VARS | 0.08 | 2 | ORM1 |
| 0.40 | 27 | RPL3 | 0.09 | 1 | GC |
| 0.44 | 9 | PSMD8 | 0.22 | 8 | C4B1 |
| 0.44 | 2 | HNRNPA3 | 0.46 | 2 | LAGE3 |
| 0.21 | 3 | PrLZ | 0.36 | 1 | MPHOSPH10 |
| 0.45 | 27 | RPS20 | 0.20 | 1 | VPS28 |
| 0.44 | 15 | RPL15 | 0.20 | 2 | GLOD4 |

Table 4.1 continued

| Expression ratio | Unique peptides | Gene name | Expression ratio | Unique peptides | Gene name |
|------------------|-----------------|-----------|------------------|-----------------|-----------|
| 0.42 | 17 | RPS15A | 0.40 | 2 | ITPK1 |
| 0.29 | 2 | YWHAH | 0.11 | 1 | SYMPK |
| 0.45 | 9 | RPL32 | 0.13 | 2 | ZFAT |
| 0.41 | 4 | PEA15 | 0.03 | 3 | PIN4 |
| 0.44 | 18 | PREX1 | 0.20 | 1 | SNRNP40 |
| 0.31 | 3 | EIF3C | 0.23 | 2 | ATXN2L |
| 0.44 | 13 | C14orf166 | 0.46 | 2 | RBM3 |
| 0.41 | 1 | TUBB6 | 0.20 | 1 | PTPRQ |
| 0.32 | 2 | GOT2 | 0.39 | 1 | CUL3 |
| 0.19 | 1 | TCEB1 | 0.51 | 2 | DIABLO |

Table 4.2 Identified proteins with increased expression after JG-98 treatment

| Expression ratio | Unique peptides | Gene name | Expression ratio | Unique peptides | Gene name |
|------------------|-----------------|-----------|------------------|-----------------|-----------|
| 7.90 | 4 | KPNA4 | 2.64 | 1 | DNPEP |
| 3.39 | 9 | EDF1 | 2.85 | 2 | SERPINB6 |
| 2.59 | 10 | S100P | 2.28 | 2 | NOMO2 |
| 2.92 | 4 | RPL22 | 2.86 | 1 | MED4 |
| 2.09 | 3 | NPLOC4 | 52.88 | 2 | STXBP3 |
| 2.58 | 5 | AIP | 2.09 | 1 | HIP1R |
| 2.19 | 4 | LSM1 | 3.53 | 1 | LRBA |
| 6.97 | 3 | HDGFRP2 | 3.99 | 1 | WDR77 |
| 3.28 | 2 | KPNA6 | 15.25 | 2 | PSMB6 |
| 2.98 | 3 | POTEF | 3.53 | 3 | IRS1 |
| 2.17 | 22 | CTTN | 3.07 | 2 | CREBBP |
| 2.28 | 6 | SAFB | 2.10 | 2 | H1FX |
| 3.34 | 4 | SF1 | 3.80 | 2 | PSMD5 |
| 3.01 | 4 | USP7 | 5.81 | 1 | UNC5D |
| 2.18 | 6 | ACIN1 | 15.22 | 1 | PPP1R13B |
| 2.29 | 3 | CBFA2T3 | 5.10 | 2 | FAH |
| 2.12 | 3 | SRP54 | 1.83 | 37 | HSPA9 |

It is important to note that this analysis did not identify either of the “control” proteins (Hsp90 clients Raf-1 and AKT1), likely because of the low expression levels of those proteins. Thus, this dataset is not intended to serve as a definitive list of Hsp70 clients. Moreover (as discussed in more detail below), this experiment requires additional biological and technical replicates. Despite these caveats, we were interested in understanding if any patterns would emerge. We therefore used gene ontology (GO)

enrichment analysis with the Database for Annotation, Visualization, and Integrated Discovery (DAVID) to identify specific categories of biological processes (GO terms) that are more prevalent in our dataset than others.^{295,296} From this analysis, the top GO terms enriched in our dataset included translation elongation, translation regulation, and RNA processing (Table 4.3). Importantly, the enriched processes also included apoptosis, macromolecular complex assembly, and protein ubiquitination, all of which are known to be broadly regulated by Hsp70.¹⁹⁴

Table 4.3 Top GO terms in identified proteins with differential expression after JG-98 treatment

| Cluster | Enrichment score |
|--|-------------------------|
| Translation elongation | 9.33 |
| RNA processing | 2.39 |
| Macromolecular complex assembly | 1.98 |
| RNA splicing | 1.79 |
| Glycolysis | 1.69 |
| tRNA aminoacylation | 1.48 |
| Chromatin assembly | 1.47 |
| Ubiquitin-protein ligase activity | 1.43 |
| Intracellular protein transport | 1.31 |
| Translational initiation | 1.08 |
| Response to insulin stimulus | 1.04 |
| Insulin-like growth factor receptor binding | 1.02 |
| Generation of precursor metabolites and energy | 0.88 |
| Transcription coactivator activity | 0.82 |
| Apoptosis | 0.66 |
| Phospholipid binding | 0.64 |
| Actin filament organization | 0.62 |
| Regulation of synaptic plasticity | 0.56 |
| Endopeptidase inhibitor activity | 0.50 |
| Regulation of neuron differentiation | 0.43 |
| (negative) regulation of apoptosis | 0.41 |
| Protein kinase binding | 0.40 |
| Cell cycle process | 0.36 |
| (positive) regulation of apoptosis | 0.32 |
| Transcription | 0.28 |
| Inflammatory response | 0.27 |
| Vesicle-mediated transport | 0.26 |
| Nucleotide binding | 0.23 |
| Transcription activator activity | 0.18 |
| Proteolysis | 0.07 |
| Calcium ion binding | 0.05 |

4.3.5.2 Hsp70 and Hsp90 regulated proteomes are partially overlapping

A major goal of our proteomic analysis was to determine if the group of proteins that rely on Hsp70 for their stability overlaps with the group of proteins that is sensitive to Hsp90 inhibition; are all Hsp70 clients also Hsp90 clients? Kuster and colleagues recently used geldanamycin, a well-characterized Hsp90 inhibitor, to identify the Hsp90 regulated proteome with SILAC.²⁹³ Their analysis revealed a network of approximately 1600 Hsp90 client proteins, particularly enriched in protein kinases, across a panel of four different cell lines. We compared the proteins identified in this study with those proteins that were differentially expressed in our experiment. Notably, while a number of proteins were identified in both the Hsp70 and Hsp90 regulated proteome, we also identified many proteins that were only sensitive to Hsp70 inhibition (Figure 4.5C). Perhaps unexpectedly, the Hsp90 regulated proteome also contained proteins unique to that dataset, indicating that Hsp90 may be involved in protein quality control pathways that are not also regulated by Hsp70. It is important to note that the protein counts listed in this comparison are over-inflated, as they do not take into account protein groups, *i.e.* proteins that share common peptides and are thus indistinguishable in the MS/MS analysis.

4.3.5.3 Inhibition of Hsp70-BAG3 PPI tunes the Hsp70 interactome

JG-98 inhibits the interaction between Hsp70 and BAG3,¹⁶⁰ and we hypothesized that blocking this PPI would tune the Hsp70 interactome such that some interactions were favored while others were disrupted. While we did not measure the “Hsp70-ome” directly, we instead used the relative expression of proteins identified in the MS/MS as a reporter of the pattern of Hsp70 PPIs that were strengthened or inhibited when the Hsp70-BAG3 interaction is blocked. We therefore determined if PPI networks were enriched in our SILAC dataset using the STRING database.²⁹⁴ From this analysis, we found that our dataset of proteins with decreased expression is enriched in PPIs (p-value = 1.26×10^{-6} , 56 observed interactions of 63 total proteins) (Figure 4.5D). Notably, the list of proteins with decreased expression following JG-98 treatment contained several components of the ribosome and proteasome complexes, which was expected given the observed enrichment of translation regulation and protein ubiquitination GO terms in the

dataset. Together, this analysis suggests that inhibition of the Hsp70-BAG3 PPI might favor interactions between Hsp70 and components of the ribosome or proteasome to trigger their degradation.

4.4 Discussion

While it has been previously established that classic Hsp90 client proteins, including the kinases Raf-1 and AKT1 are sensitive to both Hsp70 and Hsp90 inhibition,^{239,240} it was less understood if the pool of Hsp70 and Hsp90 client proteins were completely overlapping, or if there existed a network of Hsp70-specific client proteins. In Chapter 3, we demonstrated that the IAP family represents a class of unique Hsp70 clients. This finding is important, both for fundamental knowledge of biology, but also for biomarker discovery. Thus, we considered it important to understand the role that Hsp70 plays in protein quality control in the context of the whole proteome. By treating breast cancer cells that had been grown in media containing “heavy” amino acids (¹³C₆ – arginine and lysine) with JG-98, we were able to quantitatively assess the impact of Hsp70 inhibition on the whole proteome using SILAC.

4.4.1 Hsp70 client proteins are involved in translation regulation, protein degradation, and apoptosis

In this experiment, we found that approximately 10% of the identified proteome was sensitive to Hsp70 inhibition. Of these sensitive proteins, approximately 70% had lower levels of expression after JG-98 treatment, while the remaining 30% had higher levels of expression. This dataset was particularly enriched for proteins involved in regulation of protein translation and RNA processing, although we also observed a number of proteins responsible for protein ubiquitination and degradation as well as macromolecular complex assembly, processes in which Hsp70 is known to play a role.¹⁹⁴ Furthermore, we observed enrichment in proteins essential for apoptotic signaling, such as Smac/DIABLO, which is released from the mitochondria during apoptosis and binds to the IAPs to block their ability to inhibit caspases.^{297,298} Given our observations in Chapter 3 that Hsp70 plays a key role in IAP homeostasis, decreased Smac levels following

Hsp70 inhibition with JG-98 in our SILAC experiment provide further evidence for regulation of apoptotic signaling by Hsp70 in cancer cells.

4.4.2 Only a fraction of the proteome is sensitive to Hsp70 inhibition

Hsp70 is known to be a relatively promiscuous chaperone; nearly 100% of all cellular proteins are predicted to contain at least one Hsp70 binding site.²²⁴ These substrate peptides are defined as a stretch of 4-5 hydrophobic amino acids flanked by basic residues on either side.^{195,268,299} While such sequences would be expected to be buried in the interior of a protein in its native state, they would be exposed in a nascent, partially folded, or misfolded protein.³⁰⁰ Furthermore, given that Hsp70 has been shown to induce global unfolding in bound substrate proteins,^{226,280} it is unsurprising that Hsp70 has been linked to many protein quality control processes from folding of newly synthesized polypeptides to disaggregation of highly stable protein oligomers. Why then did we only observe sensitivity of 10% of the proteome to Hsp70 inhibition? It is possible that stabilization of the ADP-bound state of Hsp70 may strengthen its affinity for a number of co-chaperones that can specifically target some client proteins, but not others, for degradation. In addition, some proteins might fold faster than others, with the slow-folding clients becoming more dependent on Hsp70.

It has been hypothesized that with only 13 Hsp70 family members in eukaryotic cells but over 100 different co-chaperone proteins belonging to several diverse classes, that co-chaperones would provide a selectivity “filter” for specific substrates.^{301,302} Indeed, the interaction of Hsp70 with one J protein family member is essential for uncoating of clathrin-coating vesicles.^{303,304} In addition, it has been shown that JG-98 potentiates binding between Hsp70 and HOP (Hsp70-Hsp90 organizing protein) to induce degradation of polyQ-AR,^{161,305} and this may also be the case for other co-chaperones and substrates. Finally, previous work from our research group suggests that JG-98 may preferentially target mortalin, the mitochondrial isoform of Hsp70.²⁸⁴ While it is unknown the extent to which mortalin binding sites are predicted to differ from those of cytosolic Hsp70, binding sites for the ER resident Hsp70 BiP occurred less frequently than cytosolic Hsp70 binding sites.²²⁴ It is therefore tempting to speculate that mortalin may be

responsible for maintaining protein homeostasis in a smaller subset of the proteome than cytosolic Hsp70.

4.4.3 SILAC dataset lacks statistical power

It is important to note that the SILAC mass spectrometry data presented in this chapter represents only one biological replicate, and it is therefore difficult to draw firm conclusions about statistical significance of proteins that were found to be differentially expressed. In addition, we did not independently verify either degradation or accumulation of proteins identified in the SILAC experiment with Western blots. It remains a possibility that any proteins with differential expression in SILAC could represent false positives or contamination. Finally, we identified ~1000 total proteins by MS/MS analysis, which itself represents only a fraction of the total proteome. Mass spectrometry is biased toward identification of high abundance proteins, although advances in instrumentation and analysis have improved the detection of proteins with low abundance.³⁰⁶ We are unable to draw conclusions about specific putative client proteins without additional biological replicates and independent experimental verification of differentially expressed proteins.

4.4.4 Small molecules can be used to tune protein networks

In summary, we have used an inhibitor of Hsp70 to demonstrate that binding of a small molecule to a single protein target can have profound effects on the global protein network. Hsp70 forms the core of a multi-protein complex made of interactions with a variety of different co-chaperone proteins. JG-98 binds at an allosteric site on Hsp70 to lock it in the ADP-bound conformation, inhibiting its interaction with the BAG family of nucleotide exchange factors, while strengthening interactions with substrates. Here we show that JG-98 treatment in breast cancer cells results in differential expression of about 10% of the identified proteome, and this perturbation of the larger protein network suggests that certain proteins may rely preferentially on Hsp70 for their stability. Our work demonstrates that small molecules can effect changes in proteins distal from their primary target by modulating individual PPIs.

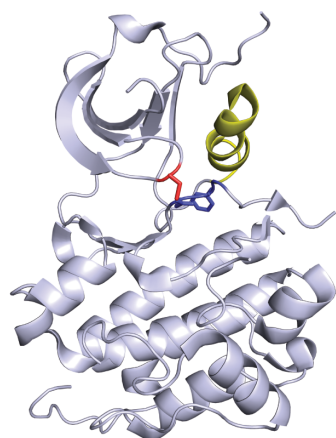
4.5 Future directions

We have shown in this chapter that small molecules can be used to tune protein networks by stabilizing a unique set of PPIs while inhibiting others. By inhibiting a single protein target, Hsp70, the small molecule inhibitor JG-98 alters individual PPIs within the “hub” multi-protein complex to affect a subset of the proteome that is dependent on Hsp70 for stability. Kinases also form the core of multi-protein complexes that trigger signaling pathways through a defined set of downstream PPIs.³⁰⁷ Because kinase inhibitors are well known to recognize specific kinase conformations, we hypothesized that we could use these compounds to modulate the kinase-dependent proteome. Such a system might allow us to more closely examine acute changes in a PPI network in response to a series of small molecules. Unlike the Hsp70 system, there are many available inhibitors with different characteristics and many of the PPIs are well-validated. Thus, kinases seemed like a good model in which to extend the ideas of this chapter.

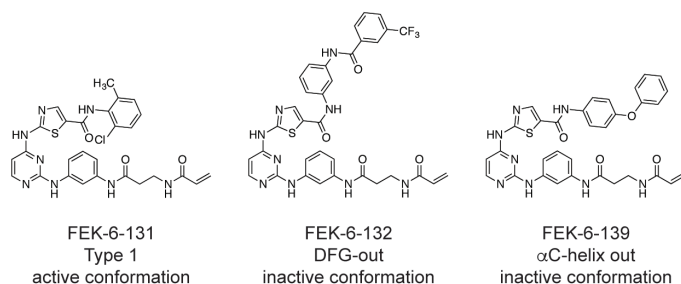
4.5.1 Design of irreversible inhibitors of Src kinase

Kinase inhibitors fall into four general categories, the two most important of which are type I and type II inhibitors. Type I inhibitors bind the orthosteric ATP-binding site, while type II inhibitors bind at an allosteric site to stabilize the closed or inactive conformation of the kinase.²⁹ We expect that, while both classes of inhibitors inhibit the enzymatic activity of the kinase, they might produce distinct patterns of PPI disruption throughout the broader protein network.

A. Structure of c-Src kinase domain



B. Dasatinib-based irreversible Src inhibitors



C. Src-FAK complex is not detected by co-immunoprecipitation

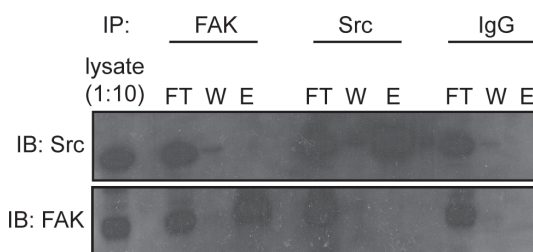


Figure 4.6 Conformation selective Src inhibitors may affect downstream PPIs. (A) Structure of the chicken c-Src kinase domain (PDB id = 3F6X). Catalytic Asp-Phe-Gly (DFG) motif is shown in blue, αC-helix is shown in yellow, and non-catalytic, non-conserved Cys-277 targeted by irreversible inhibitors is shown in red. (B) Structures of conformation-selective, irreversible dasatinib analog c-Src kinase inhibitors. All inhibitors were designed, synthesized, and characterized by Frank Kwarciński. (C) Co-immunoprecipitation does not detect a complex between Src and FAK in MDA-MB-231 cell lysate. Flow-through (FT), first wash (W), and elution (E) fractions of FAK, Src, and IgG IP conditions are shown. Blot is representative of two independent biological replicates.

Dasatinib is an FDA-approved inhibitor of several tyrosine kinases,³⁰⁸ including Src family kinases, which are important tyrosine kinases involved in a number of oncogenic signaling cascades (Figure 4.6A).^{309,310} Understanding how small molecules disrupt the network of c-Src PPIs could provide a blueprint for the development of therapeutic c-Src inhibitors. Dr. Matthew Soellner's research group at the University of Michigan recently developed a number of irreversible dasatinib analogs that target specific kinase conformations (Figure 4.6B).³¹¹ These compounds all target a non-catalytic, non-conserved cysteine in the active site of c-Src; FEK-6-131 is a type I inhibitor that stabilizes the active conformation, while FEK-6-132 and FEK-6-139 stabilize the inactive conformation. FEK-6-132 causes a conserved Asp-Phe-Gly (DFG) motif required for

catalysis to flip outward, resulting in inactivation. FEK-6-139, on the other hand, causes displacement of the α C-helix. Each of these inhibitors stabilizes a specific kinase conformation. Furthermore, irreversible binding should facilitate labeling of c-Src kinase in living cells, which in turn will enable the study of the effect of these inhibitors on downstream PPIs.

4.5.2 FAK may prefer binding to DFG-out conformation

Focal adhesion kinase (FAK) is a non-receptor tyrosine kinase activated by c-Src to trigger multiple downstream signaling pathways essential for cell growth, adhesion, and migration.³¹² A recent screening campaign identified an inhibitor of c-Src that stabilizes the DFG-out conformation.³¹³ Interestingly, this compound potentiated binding of FAK to c-Src, suggesting that FAK may prefer binding to c-Src in the DFG-out conformation. We therefore expected that the c-Src-FAK interaction would be a useful proof-of-concept that small molecules are able to effect distinct patterns of PPI disruption via binding to the same target.

4.5.3 Co-immunoprecipitation does not detect the Src-FAK complex

Previous work suggests that FAK may prefer binding to c-Src in the DFG-out, inactive conformation.³¹³ We hypothesized that labeling endogenous c-Src with the Type II (DFG-out) irreversible dasatinib analog would favor this interaction, while the interaction between FAK and Src labeled with either the Type I irreversible inhibitor or the analog that stabilizes the α C-helix-out inactive conformation would be disrupted. Therefore, we sought to capture the interaction between endogenous c-Src and FAK in living cells. MDA-MB-231 have high levels of endogenous c-Src expression (Matthew Soellner, unpublished data), and we thus prepared extracts from these cells and immunoprecipitated for both c-Src and FAK in order to detect the complex. Unfortunately, co-immunoprecipitation with either c-Src or FAK was not able to pull down the interacting partner in our hands (Figure 4.6C). Given that the interactions between many kinases and their substrates are transient ($K_D \sim 5 \mu\text{M}$), it is not surprising that the c-Src-FAK complex was not identified by co-IP, as this technique typically favors detection of PPIs with higher affinity ($K_D < 1 \mu\text{M}$).¹⁶⁶

Although we were unable to detect an interaction between c-Src and its substrate FAK, conformation-selective, irreversible c-Src inhibitors could nonetheless be useful probes of c-Src function. For example, given that it is often difficult to detect weak PPIs, such as those between kinases and their substrates, by co-IP, phosphorylation of downstream substrates could be used a surrogate for binding to infer changes in the local PPI network in response to c-Src inhibition. This idea will be discussed more in Chapter 5.

4.6 Experimental Procedures

4.6.1 Reagents and general methods

Antibodies used are as follows: Raf-1 (SantaCruz Biotechnology sc-133), Akt1 (Cell Signaling Technology 2967), HER2 (Cell Signaling Technology 4290), CDK4 (BD Pharmingen 559693), Src (Cell Signaling Technology 2123), FAK (Cell Signaling Technology 3285), β -actin (AnaSpec AS-54591), goat anti-mouse HRP (AnaSpec 28173), and goat anti-rabbit HRP (AnaSpec 28177). JG-98 and JG98-biotin were synthesized according to previously described methods.²⁵⁹ All other biological reagents were purchased from Sigma Aldrich unless otherwise noted. All spectroscopic measurements were made on a SpectraMax M5 multimode plate reader (Molecular Devices).

4.6.2 Tissue culture and viability assays

MCF-7 cells (ATCC) were maintained in DMEM (Invitrogen) supplemented with 10% fetal bovine serum and 1% penicillin-streptomycin. MDA-MB-231 cells (ATCC) were grown in DMEM supplemented with 10% fetal bovine serum, 1% penicillin-streptomycin, and non-essential amino acids. Cell viability assay was determined using the WST-1 reagent (Roche) according to the manufacturer's instructions.

4.6.3 Western blotting and silver stain

Cell extracts were prepared in chilled RIPA buffer (50 mM Tris pH 8, 150 mM NaCl, 1% Triton X-100, 0.5% Na deoxycholate, 0.1% SDS) unless otherwise indicated. Protein concentration was determined by the BCA assay and 5 μ g of total protein was separated

by SDS-PAGE on 10% Tris-glycine gel and transferred to PVDF membrane (Thermo Fisher Scientific Inc). Membranes were blocked with 5% milk in TBS, 0.05% Tween (TBS-T) for 1 hr at room temperature, incubated with primary antibodies overnight at 4°C, washed with TBS-T, and incubated with the appropriate horseradish peroxidase conjugated secondary antibody for 1 hr at room temperature. After a final wash with TBS-T, membranes were developed using chemiluminescence (ECL Prime, GE Healthcare). The silver stain (Sigma Aldrich) was performed according to the manufacturer's instructions.

4.6.4 Protein expression and purification

DnaK, Hsp72, and Hsp90 α were expressed and purified as previously described, using a His column and subsequent cleavage of the His tag by TEV protease.²¹² DnaK and Hsp72 were further purified on an ATP column. Both proteins were concentrated and stored in 25 mM HEPES buffer (pH 7.5) containing 10 mM KCl and 5 mM MgCl₂ until use. Hsp90 α was further purified by anion exchange on a Source Q column (GE Healthcare) and dialyzed overnight into 20 mM Tris buffer (pH 7.5) containing 50 mM KCl, 6 mM β -mercaptoethanol, and 10% glycerol. Protein purities were estimated at greater than 90% by SDS-PAGE. The BCA (bicinchoninic acid) assay kit (Thermo Fisher Scientific Inc) was used to determine protein concentration, and the activity of the purified proteins was verified with previously described ATPase assays (see Chapter 2 for details).¹³³

4.6.5 ELISA

Binding of Hsp72, DnaK, and Hsp90 α to JG98-biotin was determined using a modified ELISA assay as previously described.²⁵⁹ Hsp72, DnaK, or Hsp90 α was non-covalently immobilized in the wells of a clear, flat-bottom 96-well plate (Thermo Fisher Scientific Inc) by incubating 50 μ L of 0.06 mg/mL protein in immobilization buffer (20 mM MES, pH 5.2) overnight at 37°C. Non-immobilized protein was removed from the wells, and the wells were washed with 3 x 150 μ L of TBS supplemented with 0.05% Tween (TBS-T). Each wash was incubated, with gentle rocking, for 3 min at room temperature. Following washing, 25 μ L of JG98-biotin was added at the indicated concentrations in binding buffer (25 mM HEPES pH 7.4, 40 mM KCl, 8 mM MgCl₂, 100 mM NaCl,

0.01% Tween), supplemented with 1 mM ATP and 1 mM DTT. The plates were incubated at room temperature for 24 hrs with gentle rocking. Solutions of JG98-biotin were removed and each well was washed as before and blocked with 100 μ L of 3% bovine serum albumin in TBS-T for 5 min at room temperature. The plates were developed using 50 μ L of streptavidin-HRP, for 1 hr incubation at room temperature. After washing, binding was detected using the TMB substrate kit (Cell Signaling Technology), and absorbance was read at 450 nm. Data were analyzed using GraphPad Prism software and fit to the Langmuir binding isotherm ($Y = B_{\max}X/[K_D + X]$).

4.6.6 Proteomic analysis by SILAC MS/MS

The base culture medium DMEM (deficient in L -arginine, L -lysine, L -glutamine, and sodium pyruvate) was supplemented with 10% fetal bovine serum, 1% penicillin-streptomycin, L -glutamine, sodium pyruvate, and 100 μ g/mL of either $^{12}\text{C}_6$ (light) – or $^{13}\text{C}_6$ (heavy) – arginine and lysine. Parallel cultures of MCF-7 cells were propagated in either light or heavy media for at least eight cell divisions, and incorporation of the light and heavy amino acids was verified at > 97%. The heavy culture was treated with 10 μ M JG-98 for 5 hours, while the light culture received vehicle (0.1% DMSO) alone. Cell extracts were prepared in chilled lysis buffer (50 mM Tris pH 8, 8 M urea, 0.1% SDS). Protein quantitation was performed with the BCA assay, and cell extracts were mixed in a protein concentration ratio of 1:1 heavy:light. Proteins were resolved by SDS-PAGE and stained with Coomassie. Individual bands were excised and subjected to in-gel reduction, cysteine alkylation, and digestion with trypsin. Tryptic peptides were resolved by reverse-phase liquid chromatography and introduced directly into an Orbitrap XL Tandem Mass Spectrometer. Proteins were identified by searching the MS/MS data against the human protein database with added decoy (reverse) sequences using X!Tandem/Trans-Proteomic Pipeline (TPP). Positive protein identifications were those with probability ≥ 0.9 . SILAC ratios were calculated and differentially expressed proteins (0.05% FDR) were selected for further analysis.

4.6.7 Co-immunoprecipitation

MDA-MB-231 cell extracts were prepared in chilled lysis buffer (50 mM Tris pH 8, 150 mM NaCl, 1 mM ATP, 10 mM KCl, 5 mM Mg(OAc)₂, 1% NP-40) supplemented with protease inhibitor cocktail (Roche Applied Science). The total protein concentration was adjusted to 5 mg of protein in 1 mL of cell extract. PureProteome Protein G magnetic beads (Millipore) were incubated with 6 µg of Src (Cell Signaling Technology 2123) or FAK (Cell Signaling Technology 3285) primary antibodies or nonspecific mouse IgG (Santa Cruz Biotechnology sc-2025) for 30 min at room temperature with mixing, followed by antibody crosslinking with bis(sulfosuccinimidyl) suberate (Thermo Scientific) for 1 hr at room temperature with mixing. The crosslinking reaction was quenched with 1 M Tris (pH 7.5) for 1 hour at room temperature with mixing. Meanwhile, equal 100 µL samples of cell lysate were pre-cleared by incubation with 50 µL of protein G beads for 1 hour at room temperature with mixing. Protein complexes were immunoprecipitated by incubation of the pre-cleared lysate (1 mg total protein per IP) with 50 µL of antibody-crosslinked protein G beads for 1 hour at room temperature with mixing. The immunocomplexes were washed 3 times with 500 µL of wash buffer (PBS pH 7.4, 0.1% Tween-20) and eluted with 0.1 M glycine (pH 2.6). Proteins were visualized by Western blot.

Notes

This work is a collaboration of multiple research groups. JG-98 and JG98-biotin were synthesized by Xiaokai Li. The SILAC studies were performed at the Proteomic Resource Facility in the Department of Pathology at the University of Michigan by Venkatesha Basrur. Bioinformatic analysis of SILAC data was performed by Venkatesha Basrur and Damian Fermin. The irreversible Src kinase inhibitors were developed by Matthew Soellner's research group and synthesized and characterized by Frank Kwarcinski. The Hsp90α pet151 plasmid was a kind gift from Daniel Southworth

Chapter 5

Conclusions and Future Directions: Strategies for Targeting Protein Conformation and Dynamics

5.1 Abstract

Throughout this dissertation, I have described my efforts to target the Hsp70 molecular chaperone complex with small molecules in order to understand its biology in greater detail. Hsp70 regulates many diverse tasks in protein homeostasis by interacting with a variety of co-chaperone proteins that modulate its activities and shape its overall function. In Chapter 2, I developed a high-throughput screening (HTS) method to identify selective inhibitors of Hsp70's interactions with two classes of co-chaperones, J proteins and NEFs, in parallel. In probing the mechanisms of action (MoA) of these inhibitors, I uncovered binding sites and allosteric networks that can be exploited by future inhibitors. I applied one such allosteric inhibitor, JG-98, to evaluate Hsp70's role in pro-survival signaling, which led to the discovery of IAPs as a new class of Hsp70 client proteins in Chapter 3. These results suggest that Hsp70-NEF complexes are key regulators of cell survival and provide a novel biomarker. In addition to advancing our understanding of Hsp70 function, these results also provide a template for how multi-protein complexes might collaborate to carry out diverse cellular tasks. In this chapter, I expand on these broader possibilities. Specifically, I comment on possible future strategies for the discovery of new modulators of PPIs and describe how the assembly of multiple inhibitors targeting a single protein might be used to tune signaling in larger networks. I also speculate on how we might take advantage of these probes to achieve a desired functional outcome, especially in designing new, safer therapeutics.

5.2 Summary and conclusions

In the cell, protein structure, function, and signaling are regulated by individual protein-protein interactions. These interactions mediate the assembly of multi-protein complexes,

which are often constructed around a central “core” component, usually an enzyme. As discussed in Chapter 1, interactions of the core component with adaptor, scaffolding, and regulatory proteins then adjust the function of the enzyme by directing its subcellular localization or altering enzymatic activity.¹⁻³ More broadly, these multi-protein complexes form hubs of the larger protein interaction network in the cell, connecting signaling cascades through a physical web of PPIs.⁵ Targeting individual PPIs with small molecules has recently gained favor in drug discovery because such inhibitors have greater potential for and are also able to “tune” protein function, rather than completely blocking activity.¹⁴

While there have been great strides in PPI inhibitor discovery in recent years, there is still much work to be done. As discussed in Chapter 1, one of the biggest challenges has been targeting PPIs with large buried surface area and/or weak binding affinity. Therefore, a major goal of this dissertation was to understand how to tackle difficult PPIs. As a model, I focused on the heat shock protein 70 (Hsp70) system. Hsp70 forms the core of a multi-protein complex with its co-chaperones. While many of these co-chaperones, including the J proteins and NEFs, regulate the ATPase activity of Hsp70, other co-chaperones, such as TPR domain proteins, do not.¹⁹⁴ Because the activity of Hsp70 is driven by its interactions with co-chaperones, there was great interest in developing selective inhibitors of the PPIs. However, many of these interactions are weak and others occur over large surface areas.

5.2.1 Enzymatic activity can be used as a surrogate for binding in HTS

When I first joined the Gestwicki laboratory in 2011, Lyra Chang and Yoshi Miyata had recently completed the first HTS campaign against bacterial Hsp70 (*i.e.* DnaK) in complex with co-chaperones.^{129,130,132} They made the important discovery that while the physical PPIs were difficult to measure, the binding of co-chaperones to Hsp70 could be estimated by effects on ATPase activity. Concurrently, Anne Gillies, Jennifer Rauch, and Victoria Assimon were making strides in biochemically characterizing Hsp70's interactions with J proteins, NEFs, and TPR proteins, respectively.^{90,314,315} Together with Srikanth Patury and Tomoko Komiyama, I reasoned that because J proteins and NEFs

produce a diagnostic increase in Hsp70's ATPase activity, enzymatic activity could be used as a surrogate for co-chaperone binding in HTS. In Chapter 2, I describe how we used this approach to discover small molecules that bind to DnaK and inhibit its interactions with specific co-chaperones.¹³³ I found that zafirlukast binds specifically to ADP-bound Hsp70, blocking the physical interaction between the J protein and Hsp70 and inhibiting J protein-stimulated ATP hydrolysis. On the other hand, telmisartan did not alter the PPI between Hsp70 and its NEF, but rather inhibited NEF-stimulated ATPase activity by interfering with the conformational change in Hsp70 that couples NEF binding with nucleotide release. This work demonstrates that individual PPIs within a multi-protein complex can be selectively inhibited with small molecules, and this HTS approach is particularly well-suited for finding both orthosteric and allosteric inhibitors of challenging PPIs.

5.2.2 Hsp70 interacts with BAG co-chaperones to stabilize IAPs and regulate pro-survival signaling

To complement the screening approach, Yoshi Miyata and Xiaokai Li took advantage of an existing chemical scaffold, based on the rhodacyanine dye MKT-077, to build inhibitors of Hsp70.³¹⁶ They showed that MKT-077 binds to Hsp70 at an allosteric site and stabilizes Hsp70 in the ADP-bound conformation.²¹⁸ This compound had previously entered clinical trials due to its anti-proliferative activity in a number of cancer cell lines.^{317,318} Xiaokai and Hao Shao synthesized ~ 450 MKT-077 analogs and optimized this scaffold for Hsp70 binding, anti-proliferative activity, and various pharmacokinetic properties.^{259,319} Jennifer Rauch made the important discovery that one of the best analogs, JG-98, blocked the physical PPI between Hsp70 and the BAG family of NEFs.¹⁶⁰ Sharan Srinivasan and I reasoned that we could use JG-98 to probe the role of the Hsp70-BAG complex in pro-survival signaling in cancer cells. In Chapter 3, I demonstrate that JG-98 is strongly anti-proliferative in breast cancer cells and that the kinetics of degradation of classic Hsp90 clients does not correspond with the kinetics of cell death. Rather, JG-98's anti-proliferative activity is dependent on the protein kinase RIP1, a master regulator of both cell death and survival signaling pathways, and blocking the Hsp70-BAG PPI results in rapid destabilization of several members of the IAP family. Importantly, the

kinetics of IAP degradation are closely aligned with the induction of cell death after Hsp70 inhibition. I go on to show that the IAPs are specific, non-canonical clients of Hsp70. This work has provided important insight into the mechanism by which Hsp70 recognizes client proteins. Furthermore, because the IAPs are specific Hsp70 clients, their degradation can be used as a biomarker for Hsp70 target engagement in cells, which should aid in the future therapeutic development of Hsp70 inhibitors.

5.2.3 A network of client proteins rely on Hsp70 for stability

My findings in Chapter 3 provided a benchmark for how inhibition of the Hsp70-BAG PPI could be used to identify and characterize a specific class of Hsp70 client proteins. I then wanted to expand this approach to understand how inhibition of this PPI might propagate changes throughout the larger network of Hsp70-bound proteins, the Hsp70 “interactome”. Andrea Thompson found that another Hsp70 inhibitor, methylene blue, accelerates the clearance of the microtubule-associated protein tau, and she used quantitative mass spectrometry to understand how the tau-associated proteome changes when degradation is induced with methylene blue.¹⁷⁴ I was encouraged by Andrea’s findings and reasoned that I could use a similar approach to identify which proteins are destabilized by inhibition of the interaction between Hsp70 and BAG proteins. In Chapter 4, I show that approximately 10% of the proteome relies on Hsp70 for stability and that this subset of the proteome is enriched with proteins involved in protein translation, degradation, and apoptosis. These results demonstrate that small molecules can modulate the assembly of multi-protein complexes, in that inhibition of one “node” of a larger protein network can have profound implications on individual PPIs downstream of the original target.

5.3 Future directions

The results in this dissertation highlight the importance of PPIs as drug targets. Future efforts in targeting PPIs with small molecules should increase our understanding of how to modulate Hsp70 and other protein complexes.

5.3.1 New HTS methodology for the discovery of PPI inhibitors

In Chapter 2, I outline how the emergent properties of a PPI can be used in HTS instead of directly measuring the physical interaction with conventional biophysical methods.¹³³

In the case of Hsp70, binding of co-chaperone proteins results in stimulation of ATP turnover, and we used ATPase activity as the functional readout to identify inhibitors of specific PPIs. In the future, I propose that this method can easily be adapted to any system in which binding of one protein results in a measurable change in enzymatic activity of its partner. For example, many GTPases, phosphatases, and other enzymes have binding partners that might accelerate or inhibit turnover. One particularly interesting example might be the anticancer target Ras, a GTPase with well-validated binding partners.³²⁰

Going forward, the “next stage” of PPI inhibitor discovery might involve targeting aspects of protein structure and function that do not involve enzymatic activity. Specifically, I propose that next generation screens should focus on two things: targeting protein conformations (rather than activities) and modulating ternary and higher order protein complexes (rather than just dimer interfaces). Importantly, the development of new methodologies to study these aspects of PPIs will lead to new discoveries.

All proteins have dynamic motions and many will populate a number of discrete states. Thus, a single polypeptide sequence can adopt multiple conformations. For example, Hsp70 can be in the ATP- or ADP-bound conformation. Similarly, prion proteins are well known to have a healthy, normal conformer and a disease-associated conformer, typically with increased protease resistance.³²¹ As chemical biologists, we might be able to take advantage of conformational dynamics to discover small molecules that “capture” a single protein conformation. Indeed, this approach has been used in targeting transcriptional co-activator proteins. Transcriptional co-activators allows need to adopt distinct conformers to recognize many different transcriptional activators, which initiates the first step in gene.^{50,114,118} By screening for inhibitors with one activator bound to the GACKIX domain of CBP/p300, my colleagues in the Mapp laboratory discovered allosteric inhibitors of specific PPIs between GACKIX and activators.¹¹⁹ This approach

might be adapted to any multi-protein system, provided there is sufficient structural information on how partners influence the conformation of the core protein. For example, in the Hsp70 system, BAG proteins bind tightly to apo- and ATP-bound Hsp70.⁹⁰ One would expect that screening for inhibitors of Hsp70 in the presence of the BAGs would favor the discovery of small molecules that capture the ADP-bound conformation.

It is also important to consider individual protein conformers and PPIs in the context of the larger protein network, as discussed in Chapter 4. When an inhibitor traps a specific conformer, this change likely has implications for PPIs within the multi-protein complex and beyond. However, we still need better analytical tools for studying such changes. To be useful for this purpose, the method should be capable of being used in HTS (*e.g.* low volume, high sensitivity), and it should report on multiple PPIs at the same time. In Chapter 1, I introduced how FCPIA and CE rely on multi-color fluorescent labeling to detect the effect of small molecules on ternary and higher order complex formation. Similarly, mass spectrometry has gained favor for capturing a “snapshot” of protein binding equilibrium in larger networks,¹⁵⁰ and this method could also be readily adapted to study the effects of small molecules on the assembly of multi-protein complexes in real time.

5.3.2 Small molecules propagate changes in global PPI networks

When a molecule traps a conformer of a target protein, this change has effects throughout the web of cellular PPIs. In Chapter 4, I describe preliminary studies to characterize these effects in both the Hsp70 molecular chaperone and Src kinase PPI networks. These results illustrate how the PPI detection method must be adapted to the system of interest. For example, I identified a sub-network of Hsp70 client proteins by identifying which proteins were differentially expressed after Hsp70 inhibition. While I was able to use this information to infer which proteins might preferentially rely on Hsp70 for stability, it does not directly report on changes in the network of bound Hsp70 clients. In order to answer this question, I suggest a similar SILAC experiment with affinity purification for Hsp70, which would capture and identify Hsp70 interacting partners. This approach has

the advantage that it could characterize how Hsp70's interactions with both co-chaperones and substrates are altered by inhibitors.

On the other hand, I also outline initial efforts to define the effects of conformation selective Src kinase inhibitors on its PPIs with substrate proteins in Chapter 4. However, these interactions are typically weak and difficult to detect with co-immunoprecipitation techniques.¹⁶⁶ In this case, it might be advantageous to examine how protein phosphorylation patterns change upon Src inhibition using SILAC phosphoproteomics. In this method, phosphopeptides are enriched in the MS analysis using specific antibodies or another affinity chromatography method.^{322,323}

In order to successfully define how protein networks change in response to chemical inhibitors, three considerations are important: 1) what are the PPIs that converge on the target protein?, 2) what conformation of the target is captured by the chemical tool?, and 3) what robust detection method will be used to either measure changes in bound interacting partners (or functional outcomes)? I propose that protein systems that have clearly defined answers to these questions will be the most tractable. In other words, one should pick systems with clearly defined protein interactions (*e.g.* measured affinity, available structures, *etc.*), a panel of potent inhibitors with distinct MoAs (*e.g.* agonists, antagonists, *etc.*), and readily available analytical tools (*e.g.* good antibody for pull downs, high protein expression level, *etc.*). As illustrated in Figure 5.1, several different multi-protein complexes fulfill the first requirement, including Hsp70 (Figure 5.1A) and Src kinase (Figure 5.1B), as discussed earlier. In addition, co-activator proteins, such as CBP/p300 GACGIX, mediate transcription of a large array of target genes by binding to different activators (Figure 5.1C),^{50,114,118} and 14-3-3 adaptor proteins bind to hundreds of different partners to regulate their signaling cascades (Figure 5.1D).^{324,325} However, none of these systems have the combination of all three requirements that would seem to allow for full characterization of the global effects of PPI inhibitors. While there are many Hsp70 and Src ligands, interactions between these proteins and their binding partners can be difficult to detect. Conversely, there are successful methods to detect changes in target gene expression for specific transcriptional activators and to capture 14-3-3 interacting

partners, but discovery methods for conformation selective ligands of co-activators and 14-3-3 proteins are still being developed.^{47,326,327} Nonetheless, advances in PPI inhibitor discovery and methods for in cell capture of protein networks will help make this ambitious goal a reality.

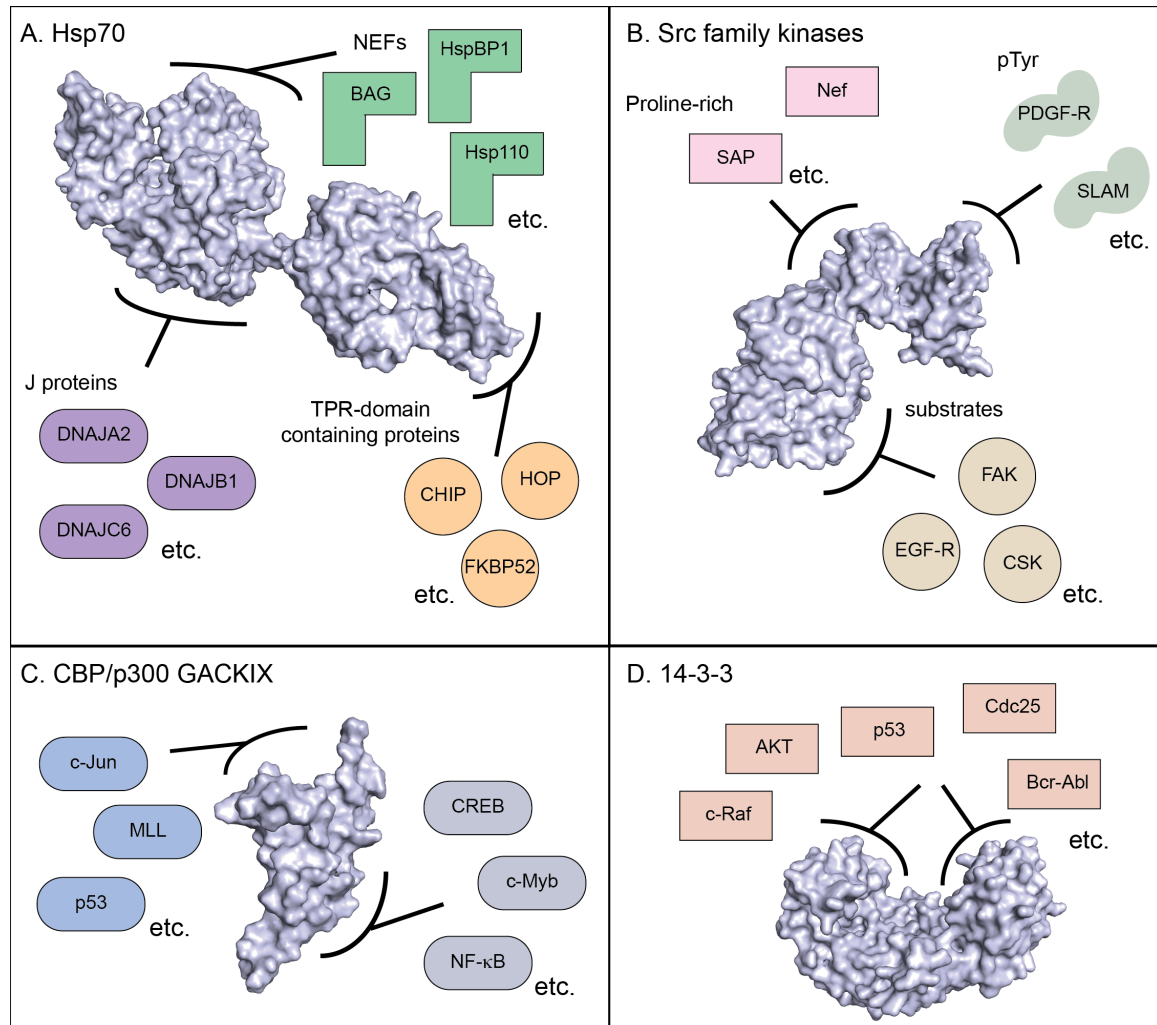


Figure 5.1 Interactions of a central protein with diverse binding partners mediate the assembly of multi-protein complexes. (A) The Hsp70 molecular chaperone complex consists of a central ATPase (Hsp70, PDB id = 2KHO), which interacts with J proteins, NEFs, and TPR domain containing proteins at distinct binding sites. Each family of co-chaperones alters Hsp70 function in a unique way. (B) Src family kinases (PDB id = 1Y57) phosphorylate client proteins through interactions with the kinase domain. N-terminal SH2 and SH3 domains mediate interactions with phospho-tyrosine residues and proline-rich binding partners, respectively. (C) The CBP/p300 GACKIX domain (PDB id = 2LXS) interacts with an array of transcriptional activation domains at two distinct, allosterically coupled binding sites. (D) 14-3-3 proteins (PDB id = 1QJA) are a versatile class of adaptor proteins that bind to hundreds of different partners at two conserved binding sites in order to regulate their activity.

5.4 Broader implications

It is now accepted that PPIs are important drug targets for the treatment of myriad human diseases; however, small molecules capable of modulating these interactions could also have utility beyond the clinic. Given the importance of PPIs in virtually all cellular processes from transcriptional regulation and protein folding to cell signaling and cell death, PPI inhibitors have already been shown, both in this work and by other research groups, to be powerful chemical probes in uncovering how interactions with specific binding partners translate to differences in the biology of a single protein target.²⁰²

To this end, there is significant need to develop new methods for the discovery of PPI inhibitors, especially for more “challenging” interactions, as discussed in Chapter 1. In particular, the “gray-box” screening method described in Chapter 2 has the potential to be a powerful tool to identify selective inhibitors of individual PPIs within a larger multi-protein complex. The strength of this assay is two-fold: 1) it measures changes in enzymatic activity resulting from individual PPIs, rather than the biophysical interaction between two protein partners itself, and 2) it is modular, meaning that many different binary and even ternary complexes can be screened in parallel. The use of enzymatic activity as a functional readout HTS means that some information on how small molecule “hits” modulate the biology of a system will be learned before any further biochemical characterization or analysis is undertaken. Furthermore, by screening multiple complexes in parallel, one can rapidly assemble a series of inhibitors of a single target, which is essential for future studies on how these inhibitors are able to alter binding across large protein networks, as discussed above. Finally, this technique is especially useful for multi-protein complexes assembled around a core enzyme and has already been applied by other research groups for the discovery of inhibitors of G protein signaling and Hsp90-mediated protein folding.^{134,135}

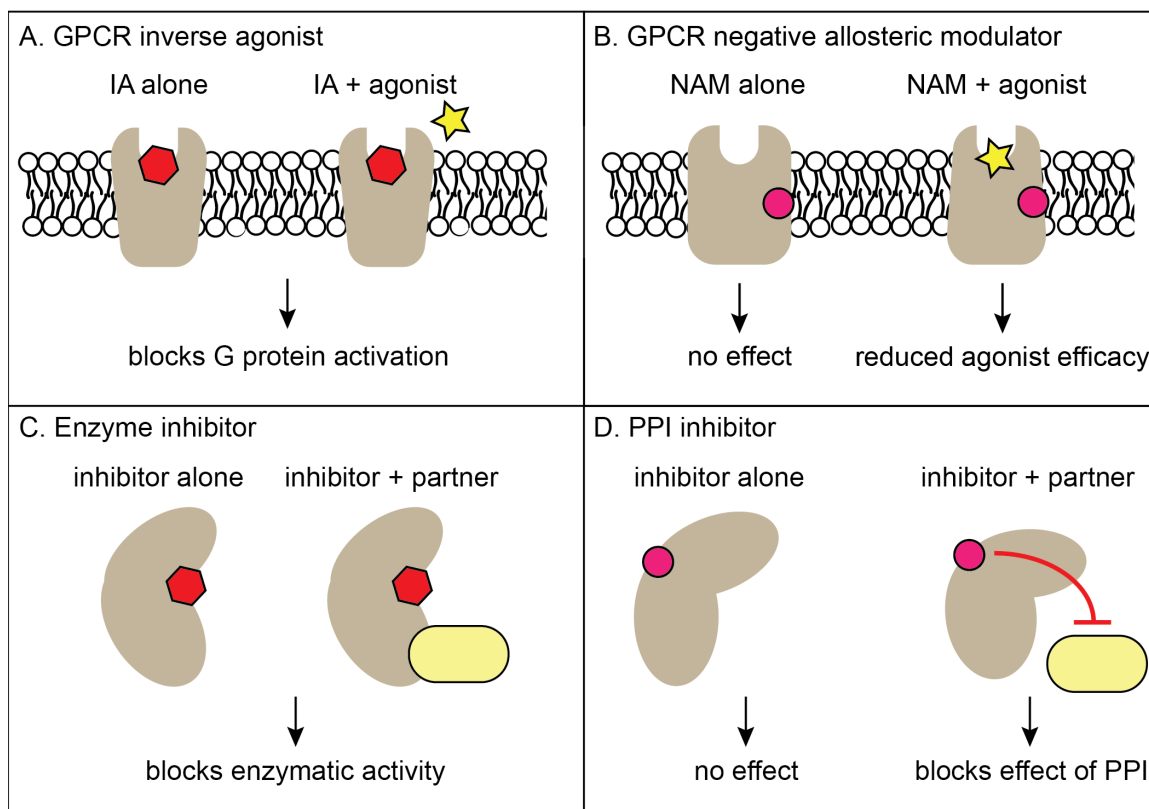
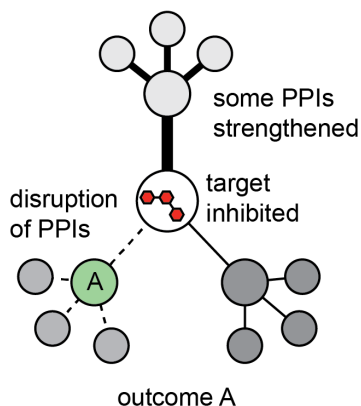


Figure 5.2 Comparison of GPCR ligands and PPI inhibitors. (A) An inverse agonist of a GPCR binds at the orthosteric site and blocks its activity in the presence or absence of native ligands. (B) Negative allosteric modulators (NAMs) only have an effect on activity in the presence of an agonist. NAMs prevent GPCR activation by reducing agonist efficacy. (C) An orthosteric enzyme inhibitor completely prevents activity in the presence or absence of binding partners. (D) An inhibitor of a specific PPI has no effect on enzymatic activity of its target alone, but abrogates binding of the regulatory partner, blocking the effect of the PPI on enzyme activity.

PPI inhibitors identified from these types of screening campaigns can be utilized to uncover new biological roles of a given multi-protein complex and to inform future efforts in the development of PPI inhibitors as new therapeutics. The strength of these small molecules lies in their ability to provide nuance in inhibition; that is, they do not completely block all activity of their protein target, but rather “tune” the functional output of the whole multi-protein system.¹⁴ It is therefore useful to compare PPI modulators to ligands of G-protein coupled receptors (GPCRs) (Figure 5.2). For instance, inverse agonists interact with GPCRs and reduce activity, analogous to the effect of orthosteric enzyme inhibitors. By contrast, allosteric modulators alter the signaling output of the receptor only in the presence of the endogenous ligand or another agonist.²⁷ Because interactions with regulatory proteins are essential for modulating the activity of a core

enzyme in a multi-protein complex, inhibitors of these PPIs would only block activity in the presence of a specific binding partner. Furthermore, just as allosteric modulators of GPCRs can either potentiate or inhibit downstream signaling, PPI modulators can also enhance or prevent binding interactions. This analogy also highlights how the field struggles with the lack of holistic terms to describe the effects of small molecules on enzymes, PPIs, and protein networks. Just as GPCR ligands have discrete effects on their targets, different “inhibitors” (even closely related ones) have unique effects on PPI networks.

A. Propagation of PPI network disruption after treatment with inhibitor A



B. Propagation of PPI network disruption after treatment with inhibitor B

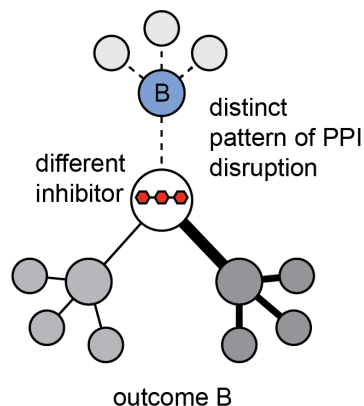


Figure 5.3 Inhibition of interactions between a single protein target and different binding partners can elicit different outcomes. A theoretical drug target (white) interacts with multiple binding partners, linking it to different “arms” of a larger PPI network that governs its biology. (A) Treatment with one inhibitor might inhibit interactions with a given binding partner A (green), directing it to a distinct outcome. The inhibitor not directly impacts the target and perturbs the global network. (B) Treatment with a different inhibitor blocks the interaction of the target with a binding partner B (blue). Even by acting on the same target, a different inhibitor generates a non-overlapping outcome by perturbing the network in a distinct way. Figure adapted from Cesa *et al.* (2015).²⁰²

Finally, by understanding the specific roles of individual PPIs in affecting the overall biology of the multi-protein system, we can build a roadmap for the development of future inhibitors that alter downstream signaling events in a particular way. This concept was introduced in Chapter 1, that binding of protein A, for example, to an enzyme produces a given outcome A, while binding of protein B yields a different outcome B. If it is known that prevention of outcome A is therapeutically advantageous, then inhibitor discovery should focus on small molecules capable of inhibiting the interaction between protein A and the target enzyme (Figure 5.3). Therefore, preliminary studies, such as

those described in Chapters 3 and 4, of how tool compounds block specific PPIs to propagate changes in protein networks and elicit distinct functional outcomes are especially useful in guiding the development of future therapeutics.

5.5 Concluding remarks

In this chapter, I summarized my thoughts on a new way of thinking about PPI inhibitors. I outlined how they might best be identified and characterized, as well as how these small molecules can be used as tool compounds. The theme of this analysis is that inhibition of a single node of a protein network might have profound implications, even on binding events that are downstream from the target. However, we often lack the full set of tools for understanding this aspect of chemical biology. We need better methods to enable small molecule discovery, study protein conformation and dynamics, and measure PPIs with adaptor and regulatory proteins. Throughout the course of my thesis work, I have used a multidisciplinary approach, applying the tools of chemical screening and drug discovery to identify new inhibitors of Hsp70's interactions with co-chaperones, biochemistry and cell biology to characterize how Hsp70 recognizes a previously unexplored class of client proteins to ensure their stability, and mass spectrometry and proteomics to explore how inhibition of Hsp70 leads to changes in global protein expression levels. In the future, the application of tools from diverse fields will be essential for understanding how best to exploit dynamic PPIs in order to achieve a desired functional outcome.

References

- (1) Höhfeld, J., Cyr, D. M., and Patterson, C. (2001) From the cradle to the grave: molecular chaperones that may choose between folding and degradation. *EMBO Rep.* 2, 885–890.
- (2) Young, A., Lyons, J., Miller, A. L., Phan, V. T., Alarcón, I. R., and McCormick, F. (2009) Ras signaling and therapies. *Adv. Cancer Res.* 102, 1–17.
- (3) Romero, G., von Zastrow, M., and Friedman, P. A. (2011) Role of PDZ protein in regulating trafficking, signaling, and function of GPCRs: means, motif, and opportunity. *Adv. Pharmacol.* 62, 279–314.
- (4) Perkins, J. R., Diboun, I., Dessailly, B. H., Lees, J. G., and Orengo, C. (2010) Transient protein-protein interactions: structural, functional, and network properties. *Structure* 18, 1233–1243.
- (5) Vidal, M., Cusick, M. E., and Barabási, A.-L. (2011) Interactome networks and human disease. *Cell* 144, 986–998.
- (6) Conn, P. J., Christopoulos, A., and Lindsley, C. W. (2009) Allosteric modulators of GPCRs: a novel approach for the treatment of CNS disorders. *Nat. Rev. Drug Discov.* 8, 41–54.
- (7) Chari, A., and Fischer, U. (2010) Cellular strategies for the assembly of molecular machines. *Trends Biochem. Sci.* 35, 676–683.
- (8) Good, M. C., Zalatan, J. G., and Lim, W. A. (2011) Scaffold proteins: Hubs for controlling the flow of cellular information. *Science* (80-.). 332, 680–686.
- (9) Liu, H., Cheng, E. H. Y., and Hsieh, J. J. D. (2009) MLL fusions: Pathways to leukemia. *Cancer Biol. Ther.* 8, 1204–1211.
- (10) Muller, P. A. J., and Vousden, K. H. (2013) p53 mutations in cancer. *Nat. Cell Biol.* 15, 2–8.
- (11) Hopkins, A. L., and Groom, C. R. (2002) The druggable genome. *Nat. Rev. Drug Discov.* 1, 727–730.

- (12) Wells, J. A., and McClendon, C. L. (2007) Reaching for high-hanging fruit in drug discovery at protein-protein interfaces. *Nature* 450, 1001–1009.
- (13) Gordo, S., and Giralt, E. (2009) Knitting and untying the protein network: Modulation of protein ensembles as a therapeutic strategy. *Protein Sci.* 18, 481–493.
- (14) Arkin, M. R., and Whitty, A. (2009) The road less traveled: Modulating signal transduction enzymes by inhibiting their protein-protein interactions. *Curr. Opin. Chem. Biol.* 13, 284–290.
- (15) Bolanos-Garcia, V. M., Wu, Q., Ochi, T., Chirgadze, D. Y., Sibanda, B. L., and Blundell, T. L. (2012) Spatial and temporal organization of multi-protein assemblies: achieving sensitive control in information-rich cell-regulatory systems. *Philos. Transactions Ser. A Math. Phys. Eng. Sci.* 370, 3023–3039.
- (16) Frye, S. V. (2010) The art of the chemical probe. *Nat. Chem. Biol.* 6, 159–161.
- (17) Arkin, M. R., Tang, Y., and Wells, J. A. (2014) Small-molecule inhibitors of protein-protein interactions: Progressing toward the reality. *Chem. Biol.* 21, 1102–1114.
- (18) Overington, J. P., Al-Lazikani, B., and Hopkins, A. L. (2006) How many drug targets are there? *Nat. Rev. Drug Discov.* 5, 993–996.
- (19) Meireles, L. M. C., and Mustata, G. (2011) Discovery of modulators of protein-protein interactions: Current approaches and limitations. *Curr. Top. Med. Chem.* 11, 248–257.
- (20) Jubb, H., Higuero, A. P., Winter, A., and Blundell, T. L. (2012) Structural biology and drug discovery for protein-protein interactions. *Trends Pharmacol. Sci.* 33, 241–248.
- (21) Smith, M. C., and Gestwicki, J. E. (2012) Features of protein-protein interactions that translate into potent inhibitors: Topology, surface area and affinity. *Expert Rev. Mol. Med.* 14, e16.
- (22) Wang, R., Fang, X., Lu, Y., and Wang, S. (2004) The PDBbind database: Collection of binding affinities for protein-ligand complexes with known three-dimensional structures. *J. Med. Chem.* 47, 2977–2980.
- (23) Negi, S. S., Schein, C. H., Oezguen, N., Power, T. D., and Braun, W. (2007) InterProSurf: a web server for predicting interacting sites on protein surfaces. *Bioinformatics* 23, 3397–3399.

- (24) Thompson, A. D., Dugan, A., Gestwicki, J. E., and Mapp, A. K. (2012) Fine-tuning multiprotein complexes using small molecules. *ACS Chem. Biol.* 7, 1311–1320.
- (25) Keov, P., Sexton, P. M., and Christopoulos, A. (2011) Allosteric modulation of G protein-coupled receptors: A pharmacological perspective. *Neuropharmacology* 60, 24–35.
- (26) Luttrell, L. M. (2008) Reviews in molecular biology and biotechnology: Transmembrane signaling by G protein coupled receptors. *Mol. Biotechnol.* 39, 239–264.
- (27) Christopoulos, A. (2014) Advances in G protein-coupled receptor allostery: From function to structure. *Mol. Pharmacol.* 86, 463–478.
- (28) Galandrin, S., and Bouvier, M. (2006) Distinct signaling profiles of beta1 and beta2 adrenergic receptor ligands toward adenylyl cyclase and mitogen-activated protein kinase reveals the pluridimensionality of efficacy. *Mol. Pharmacol.* 70, 1575–1584.
- (29) Liu, Y., and Gray, N. S. (2006) Rational design of inhibitors that bind to inactive kinase conformations. *Nat. Chem. Biol.* 2, 358–364.
- (30) Lindsley, J. E., and Rutter, J. (2006) Whence cometh the allosterome. *Proc. Natl. Acad. Sci. USA* 103, 10533–10535.
- (31) Weinkam, P., Pons, J., and Sali, A. (2012) Structure-based model of allostery predicts coupling between distant sites. *Proc. Natl. Acad. Sci. USA* 109, 4875–4880.
- (32) Monod, J., Wyman, J., and Changeux, J.-P. (1965) On the nature of allosteric transitions: A plausible model. *J. Mol. Biol.* 12, 88–118.
- (33) Li, J., Wang, J., Wang, J., Nawaz, Z., Liu, J. M., Qin, J., and Wong, J. (2000) Both corepressor proteins SMRT and N-CoR exist in large protein complexes containing HDAC3. *EMBO J.* 19, 4342–4350.
- (34) Guenther, M. G., Barak, O., and Lazar, M. A. (2001) The SMRT and N-CoR corepressors are activating cofactors for histone deacetylase 3. *Mol. Cell. Biol.* 21, 6091–6101.
- (35) Guenther, M. G., Yu, J., Kao, G. D., Yen, T. J., and Lazar, M. A. (2002) Assembly of the SMRT-histone deacetylase 3 repression complex requires the TCP-1 ring complex. *Genes Dev.* 16, 3130–3135.
- (36) Watson, P. J., Fairall, L., Santos, G. M., and Schwabe, J. W. R. (2012) Structure of HDAC3 bound to co-repressor and inositol tetrakisphosphate. *Nature* 481, 335–340.

- (37) Gronemeyer, H., Gustafsson, J.-Å., and Laudet, V. (2004) Principles for modulation of the nuclear receptor superfamily. *Nat. Rev. Drug Discov.* 3, 950–964.
- (38) le Maire, A., Teyssier, C., Erb, C., Grimaldi, M., Alvarez, S., de Lera, A. R., Balaguer, P., Gronemeyer, H., Royer, C. A., Germain, P., and Bourguet, W. (2010) A unique secondary-structure switch controls constitutive gene repression by retinoic acid receptor. *Nat. Struct. Mol. Biol.* 17, 801–807.
- (39) Perissi, V., and Rosenfeld, M. G. (2005) Controlling nuclear receptors: the circular logic of cofactor cycles. *Nat. Rev. Mol. Cell Biol.* 6, 542–554.
- (40) Germain, P., Gaudon, C., Pogenberg, V., Sanglier, S., Van Dorsselaer, A., Royer, C. A., Lazar, M. A., Bourguet, W., and Gronemeyer, H. (2009) Differential action on coregulator interaction defines inverse retinoid agonists and neutral antagonists. *Chem. Biol.* 16, 479–489.
- (41) Yaffe, M. B., Rittinger, K., Volinia, S., Caron, P. R., Aitken, A., Leffers, H., Gamblin, S. J., Smerdon, S. J., and Cantley, L. C. (1997) The structural basis for 14-3-3:phosphopeptide binding specificity. *Cell* 91, 961–971.
- (42) Hermeking, H., and Benzinger, A. (2006) 14-3-3 proteins in cell cycle regulation. *Semin. Cancer Biol.* 16, 183–192.
- (43) Johnson, C., Crowther, S., Stafford, M. J., Campbell, D. G., Toth, R., and MacKintosh, C. (2010) Bioinformatic and experimental survey of 14-3-3 binding sites. *Biochem. J.* 427, 69–78.
- (44) Würtele, M., Jelich-Ottmann, C., Wittinghofer, A., and Oecking, C. (2003) Structural view of a fungal toxin acting on a 14-3-3 regulatory complex. *EMBO J.* 22, 987–994.
- (45) Ottmann, C., Marco, S., Jaspert, N., Marcon, C., Schauer, N., Weyand, M., Vandermeeren, C., Duby, G., Boutry, M., Wittinghofer, A., Rigaud, J.-L., and Oecking, C. (2007) Structure of a 14-3-3 coordinated hexamer of the plant plasma membrane H⁺-ATPase by combining X-ray crystallography and electron cryomicroscopy. *Mol. Cell* 25, 427–440.
- (46) Zhao, J., Du, Y., Horton, J. R., Upadhyay, A. K., Lou, B., Bai, Y., Zhang, X., Du, L., Li, M., Wang, B., Zhang, L., Barbieri, J. T., Khuri, F. R., Cheng, X., and Fu, H. (2011) Discovery and structural characterization of a small molecule 14-3-3 protein-protein

interaction inhibitor. *Proc. Natl. Acad. Sci. USA* 108, 16212–16216.

(47) Milroy, L.-G., Brunsveld, L., and Ottman, C. (2013) Stabilization and inhibition of protein-protein interactions: The 14-3-3 case study. *ACS Chem. Biol.* 8, 27–35.

(48) Wisén, S., Bertelsen, E. B., Thompson, A. D., Patury, S., Ung, P., Chang, L., Evans, C. G., Walter, G. M., Wipf, P., Carlson, H. A., Brodsky, J. L., Zuiderweg, E. R. P., and Gestwicki, J. E. (2010) Binding of a small molecule at a protein-protein interface regulates the chaperone activity of Hsp70-Hsp40. *ACS Chem. Biol.* 5, 611–622.

(49) Novatchkova, M., and Eisenhaber, F. (2004) Linking transcriptional mediators via the GACKIX domain super family. *Curr. Biol.* 14, R54–R55.

(50) De Guzman, R. N., Goto, Natalie, K., Dyson, H. J., and Wright, P. E. (2006) Structural basis for cooperative transcription factor binding to the CBP coactivator. *J. Mol. Biol.* 355, 1005–1013.

(51) Vojnic, E., Mourão, A., Seizl, M., Simon, B., Wenzel, L., Lariviere, L., Baumli, S., Baumgart, K., Meisterernst, M., Sattler, M., and Cramer, P. (2011) Structure and VP16 binding of the Mediator Med25 activator interaction domain. *Nat. Struct. Mol. Biol.* 18, 404–409.

(52) Vassilev, L. T., Vu, B. T., Graves, B., Carvajal, D., Podlaski, F., Filipovic, Z., Kong, N., Kammlott, U., Lukacs, C., Klein, C., Fotouhi, N., and Liu, E. A. (2004) In vivo activation of the p53 pathway by small-molecule antagonists of MDM2. *Science* (80-.). 303, 844–848.

(53) Oltersdorf, T., Elmore, S. W., Shoemaker, A. R., Armstrong, R. C., Augeri, D. J., Belli, B. A., Bruncko, M., Deckwerth, T. L., Dinges, J., Hajduk, P. J., Joseph, M. K., Kitada, S., Korsmeyer, S. J., Kunzer, A. R., Letai, A., Li, C., Mitten, M. J., Nettesheim, D. G., Ng, S., Nimmer, P. M., O'Connor, J. M., Oleksijew, A., Petros, A. M., Reed, J. C., Shen, W., Tahir, S. K., Thompson, C. B., Tomaselli, K. J., Wang, B., Wendt, M. D., Zhang, H., Fesik, S. W., and Rosenberg, S. H. (2005) An inhibitor of Bcl-2 family proteins induces regression of solid tumours. *Nature* 435, 677–681.

(54) Cai, Q., Sun, H., Peng, Y., Lu, J., Nikolovska-Coleska, Z., McEachern, D., Liu, L., Qiu, S., Yang, C.-Y., Miller, R., Yi, H., Zhang, T., Sun, D., Kang, S., Guo, M., Leopold, L., Yang, D., and Wang, S. (2011) A potent and orally active antagonist (SM-406/AT-406) of multiple inhibitor of apoptosis proteins (IAPs) in clinical development for cancer

treatment. *J. Med. Chem.* **54**, 2714–2726.

(55) Tilley, J. W., Chen, L., Fry, D. C., Emerson, S. D., Powers, G. D., Biondi, D., Varnell, T., Trilles, R., Guthrie, R., Mennona, F., Kaplan, G., LeMahieu, R. A., Carson, M., Han, R.-J., Liu, C.-M., Palermo, R., and Ju, G. (1997) Identification of a small molecule inhibitor of the IL-2/IL-2R α receptor interaction which binds to IL-2. *J. Am. Chem. Soc.* **119**, 7589–7590.

(56) Arkin, M. R., Randal, M., DeLano, W. L., Hyde, J., Luong, T. N., Oslob, J. D., Raphael, D. R., Taylor, L., Wang, J., McDowell, R. S., Wells, J. A., and Braisted, A. C. (2003) Binding of small molecules to an adaptive protein-protein interface. *Proc. Natl. Acad. Sci. USA* **100**, 1603–1608.

(57) Brown, S. P., and Hajduk, P. J. (2006) Effects of conformational dynamics on predicted protein druggability. *ChemMedChem* **1**, 70–72.

(58) Wilson, C. G., and Arkin, M. R. (2013) Probing structural adaptivity at PPI interfaces with small molecules. *Drug Discov. Today Technol.* **10**, e501–e508.

(59) Speck, N. A., Stacy, T., Wang, Q., North, T., Gu, T.-L., Miller, J., Binder, M., and Marín-Padilla, M. (1999) Core-binding factor: A central player in hematopoiesis and leukemia. *Cancer Res.* **59**, 1789s–1793s.

(60) Liu, P., Tarlé, S. A., Hajra, A., Claxton, D. F., Marlton, P., Freedman, M., Siciliano, M. J., and Collins, F. S. (1993) Fusion between transcription factor CBF β /PEBP2 β and a myosin heavy chain in acute myeloid leukemia. *Science* (80-.). **261**, 1041–1044.

(61) Castilla, L. H., Wijmenga, C., Wang, Q., Stacy, T., Speck, N. A., Eckhaus, M., Marín-Padilla, M., Collins, F. S., Wynshaw-Boris, A., and Liu, P. P. (1996) Failure of embryonic hematopoiesis and lethal hemorrhages in mouse embryos heterozygous for a knocked-in leukemia gene CBFB-MYH11. *Cell* **87**, 687–696.

(62) Lukasik, S. M., Zhang, L., Corpora, T., Tomanicek, S., Li, Y., Kundu, M., Hartmann, K., Liu, P. P., Laue, T. M., Biltonen, R. L., Speck, N. A., and Bushweller, J. H. (2002) Altered affinity of CBF β -SMMHC for Runx1 explains its role in leukemogenesis. *Nat. Struct. Biol.* **9**, 674–679.

(63) Gorczynski, M. J., Grembecka, J., Zhou, Y., Kong, Y., Roudaia, L., Douvas, M. G., Newman, M., Bielnicka, I., Baber, G., Corpora, T., Shi, J., Sridharan, M., Lilien, R., Donald, B. R., Speck, N. A., Brown, M. L., and Bushweller, J. H. (2007) Allosteric

inhibition of the protein-protein interaction between the leukemia-associated proteins Runx1 and CBFbeta. *Chem. Biol.* 14, 1186–1197.

(64) Roman, D. L., Blazer, L. L., Monroy, C. A., and Neubig, R. R. (2010) Allosteric inhibition of the regulator of G protein signaling-Galpha protein-protein interaction by CCG-4986. *Mol. Pharmacol.* 78, 360–365.

(65) Vashisth, H., Storaska, A. J., Neubig, R. R., and Brooks, C. L. 3rd. (2013) Conformational dynamics of a regulator of G-protein signaling protein reveals a mechanism of allosteric inhibition by a small molecule. *ACS Chem. Biol.* 8, 2778–2784.

(66) Giordanetto, F., Schäfer, A., and Ottmann, C. (2014) Stabilization of protein-protein interactions by small molecules. *Drug Discov. Today* 19, 1812–1821.

(67) Huai, Q., Kim, H.-Y., Liu, Y., Zhao, Y., Mondragon, A., Liu, J. O., and Ke, H. (2002) Crystal structure of calcineurin-cyclophilin-cyclosporin shows common but distinct recognition of immunophilin-drug complexes. *Proc. Natl. Acad. Sci. USA* 99, 12037–12042.

(68) Griffith, J. P., Kim, J. L., Kim, E. E., Sintchak, M. D., Thomson, J. A., Fitzgibbon, M. J., Fleming, M. A., Caron, P. R., Hsiao, K., and Navia, M. A. (1995) X-ray structure of calcineurin inhibited by the immunophilin-immunosuppressant FKBP12-FK506 complex. *Cell* 82, 507–522.

(69) Brown, E. J., Albers, M. W., Shin, T. B., Ichikawa, K., Keith, C. T., Lane, W. S., and Schreiber, S. L. (1994) A mammalian protein targeted by G1-arresting rapamycin-receptor complex. *Nature* 369, 756–758.

(70) Delker, C., Raschke, A., and Quint, M. (2008) Auxin dynamics: the dazzling complexity of a small molecule's message. *Planta* 227, 929–941.

(71) Geske, G. D., O'Neill, J. C., and Blackwell, H. E. (2008) Expanding dialogues: from natural autoinducers to non-natural analogues that modulate quorum sensing in Gram-negative bacteria. *Chem. Soc. Rev.* 37, 1432–1447.

(72) Churchill, M. E. A., and Chen, L. (2011) Structural basis of acyl-homoserine lactone-dependent signaling. *Chem. Rev.* 111, 68–85.

(73) Marine, J.-C., Francoz, S., Maetens, M., Wahl, G., Toledo, F., and Lozano, G. (2006) Keeping p53 in check: essential and synergistic functions of Mdm2 and Mdm4. *Cell Death Differ.* 13, 927–934.

- (74) Toledo, F., and Wahl, G. M. (2006) Regulation of the p53 pathway: in vitro hypotheses, in vivo veritas. *Nat. Rev. Cancer* 6, 909–923.
- (75) Wade, M., and Wahl, G. M. (2009) Targeting Mdm2 and Mdmx in cancer therapy: Better living through medicinal chemistry? *Mol. Cancer Res.* 7, 1–11.
- (76) Tovar, C., Rosinski, J., Filipovic, Z., Higgins, B., Kolinsky, K., Hilton, H., Zhao, X., Vu, B. T., Qing, W., Packman, K., Myklebost, O., Heimbros, D. C., and Vassilev, L. T. (2006) Small-molecule MDM2 antagonists reveal aberrant p53 signaling in cancer: Implications for therapy. *Proc. Natl. Acad. Sci. USA* 103, 1888–1893.
- (77) Brown, C. J., Lain, S., Verma, C. S., Fersht, A. R., and Lane, D. P. (2009) Awakening guardian angels: drugging the p53 pathway. *Nat. Rev. Cancer* 9, 862–873.
- (78) Vassilev, L. T. (2005) p53 activation by small molecules: Application in oncology. *J. Med. Chem.* 48, 4491–4499.
- (79) Graves, B., Thompson, T., Xia, M., Janson, C., Lukacs, C., Deo, D., Di Lello, P., Fry, D., Garvie, C., Huang, K.-S., Gao, L., Tovar, C., Lovey, A., Wanner, J., and Vassilev, L. T. (2012) Activation of the p53 pathway by small-molecule-induced MDM2 and MDMX dimerization. *Proc. Natl. Acad. Sci. USA* 109, 11788–11793.
- (80) Higuera, A. P., Jubb, H., and Blundell, T. L. (2013) Protein-protein interactions as druggable targets: recent technological advances. *Curr. Opin. Pharmacol.* 13, 791–796.
- (81) Kenakin, T. P. (2010) Ligand detection in the allosteric world. *J. Biomol. Screen.* 15, 119–130.
- (82) Holdgate, G. A., Anderson, M., Edfeldt, F., and Geschwindner, S. (2010) Affinity-based, biophysical methods to detect and analyze ligand binding to recombinant proteins: matching high information content with high throughput. *J. Struct. Biol.* 172, 142–157.
- (83) Makley, L. N., and Gestwicki, J. E. (2012) Expanding the number of “druggable” targets: non-enzymes and protein-protein interactions. *Chem. Biol. Drug Des.* 81, 22–32.
- (84) Nikolovska-Coleska, Z., Wang, R., Fang, X., Pan, H., Tomita, Y., Li, P., Roller, P. P., Krajewski, K., Saito, N. G., Stuckey, J. A., and Wang, S. (2004) Development and optimization of a binding assay for the XIAP BIR3 domain using fluorescence polarization. *Anal. Biochem.* 332, 261–273.
- (85) Sarvazyan, N. A., Remmers, A. E., and Neubig, R. R. (1998) Determinants of

gila and beta gamma binding. Measuring high affinity interactions in a lipid environment using flow cytometry. *J. Biol. Chem.* 273, 7934–7940.

(86) Sklar, L. A., Edwards, B. S., Graves, S. W., Nolan, J. P., and Prossnitz, E. (2002) Flow cytometric analysis of ligand-receptor interactions and molecular assemblies. *Annu. Rev. Biophys. Biomol. Struct.* 31, 97–119.

(87) Simons, P. C., Shi, M., Foutz, T., Cimino, D. F., Lewis, J., Buranda, T., Lim, W. K., Neubig, R. R., McIntire, W. E., Garrison, J., Prossnitz, E., and Sklar, L. A. (2003) Ligand-receptor-G-protein molecular assemblies on beads for mechanistic studies and screening by flow cytometry. *Mol. Pharmacol.* 64, 1227–1238.

(88) Roman, D. L., Talbot, J. N., Roof, R. A., Sunahara, R. K., Traynor, J. R., and Neubig, R. R. (2007) Identification of small-molecule inhibitors of RGS4 using a high-throughput flow cytometry protein interaction assay. *Mol. Pharmacol.* 71, 169–175.

(89) Rauch, J. N., Nie, J., Buchholz, T. J., Gestwicki, J. E., and Kennedy, R. T. (2013) Development of a capillary electrophoresis platform for identifying inhibitors of protein-protein interactions. *Anal. Chem.* 85, 9824–9831.

(90) Rauch, J. N., and Gestwicki, J. E. (2014) Binding of human nucleotide exchange factors to heat shock protein 70 (Hsp70) generates functionally distinct complexes in vitro. *J. Biol. Chem.* 289, 1402–1414.

(91) Schultz, N. M., and Kennedy, R. T. (1993) Rapid immunoassays using capillary electrophoresis with fluorescence detection. *Anal. Chem.* 65, 3161–3165.

(92) Chu, Y.-H., Avila, L. Z., Gao, J., and Whitesides, G. M. (1995) Affinity capillary electrophoresis. *Acc. Chem. Res.* 28, 461–468.

(93) Yang, P., Whelan, R. J., Mao, Y., Lee, A. W.-M., Carter-Su, C., and Kennedy, R. T. (2007) Multiplexed detection of protein-peptide interaction and inhibition using capillary electrophoresis. *Anal. Chem.* 79, 1690–1695.

(94) Wendt, M. D., Sun, C., Kunzer, A., Sauer, D., Sarris, K., Hoff, E., Yu, L., Nettesheim, D. G., Chen, J., Jin, S., Comess, K. M., Fan, Y., Anderson, S. N., Isaac, B., Olejniczak, E. T., Hajduk, P. J., Rosenberg, S. H., and Elmore, S. W. (2007) Discovery of a novel small molecule binding site of human survivin. *Bioorg. Med. Chem. Lett.* 17, 3122–3129.

(95) Renaud, J.-P., and Delsuc, M.-A. (2009) Biophysical techniques for ligand screening

- and drug design. *Curr. Opin. Pharmacol.* 9, 622–628.
- (96) Kitevski-LeBlanc, J. L., and Prosser, R. S. (2012) Current applications of ^{19}F NMR studies of protein structure and dynamics. *Prog. Nucl. Magn. Reson. Spectrosc.* 62, 1–33.
- (97) Pomerantz, W. C., Wang, N., Lipinski, A. K., Wang, R., Cierpicki, T., and Mapp, A. K. (2012) Profiling the dynamic interfaces of fluorinated transcription complexes for ligand discovery and characterization. *ACS Chem. Biol.* 7, 1345–1350.
- (98) Mishra, N. K., Urick, A. K., Ember, S. W. J., Schönbrunn, E., and Pomerantz, W. C. (2014) Fluorinated aromatic amino acids are sensitive ^{19}F NMR probes for bromodomain-ligand interactions. *ACS Chem. Biol.* 9, 2755–2760.
- (99) Cellitti, S. E., Jones, D. H., Lagpacan, L., Hao, X., Zhang, Q., Hu, H., Brittain, S. M., Brinker, A., Caldwell, J., Bursulaya, B., Spraggon, G., Ansgar, B., Ryu, Y., Uno, T., Schultz, P. G., and Geierstanger, B. H. (2008) In vivo incorporation of unnatural amino acids to probe structure, dynamics, and ligand binding in a large protein by nuclear magnetic resonance spectroscopy. *J. Am. Chem. Soc.* 130, 9268–9281.
- (100) Gee, C. T., Koleski, E. J., and Pomerantz, W. C. K. (2015) Fragment screening and druggability assessment for the CBP/p300 KIX domain through protein-observed ^{19}F NMR spectroscopy. *Angew. Chemie Int. Ed.* 54, 3735–3739.
- (101) Janin, J., Miller, S., and Chothia, C. (1988) Surface, subunit interfaces and interior of oligomeric proteins. *J. Mol. Biol.* 204, 155–164.
- (102) Rosen, M. K., Gardner, K. H., Willis, R. C., Parris, W. E., Pawson, T., and Kay, L. E. (1996) Selective methyl group protonation of perdeuterated proteins. *J. Mol. Biol.* 263, 627–636.
- (103) Gardner, K. H., Rosen, M. K., and Kay, L. E. (1997) Global folds of highly deuterated, methyl-protonated proteins by multidimensional NMR. *Biochemistry* 36, 1389–1401.
- (104) Nicholson, L. K., Kay, L. E., Baldisseri, D. M., Arango, J., Young, P. E., Bax, A., and Torchia, D. A. (1992) Dynamics of methyl groups in proteins as studied by proton-detected carbon-13 NMR spectroscopy. Application to the leucine residues of staphylococcal nuclease. *Biochemistry* 31, 5253–5263.
- (105) Tugarinov, V., and Kay, L. E. (2005) Methyl groups as probes of structure and dynamics in NMR studies of high-molecular-weight proteins. *ChemBioChem* 6, 1567–

1577.

(106) Hajduk, P. J., Augeri, D. J., Mack, J., Mendoza, R., Yang, J., Betz, S. F., and Fesik, S. W. (2000) NMR-based screening of proteins containing ^{13}C -labeled methyl groups. *J. Am. Chem. Soc.* **122**, 7898–7904.

(107) Erlanson, D. A., Braisted, A. C., Raphael, D. R., Randal, M., Stroud, R. M., Gordon, E. M., and Wells, J. A. (2000) Site-directed ligand discovery. *Proc. Natl. Acad. Sci. USA* **97**, 9367–9372.

(108) Erlanson, D. A., Wells, J. A., and Braisted, A. C. (2004) Tethering: Fragment-based drug discovery. *Annu. Rev. Biophys. Biomol. Struct.* **33**, 199–223.

(109) Buck, E., and Wells, J. A. (2005) Disulfide trapping to localize small-molecule agonists and antagonists for a G protein-coupled receptor. *Proc. Natl. Acad. Sci. USA* **102**, 2719–2724.

(110) Buck, E., Bourne, H., and Wells, J. A. (2005) Site-specific disulfide capture of agonist and antagonist peptides on the C5a receptor. *J. Biol. Chem.* **280**, 4009–4012.

(111) Scheer, J. M., Romanowski, M. J., and Wells, J. A. (2006) A common allosteric site and mechanism in caspases. *Proc. Natl. Acad. Sci. USA* **103**, 7595–7600.

(112) Sadowsky, J. D., Burlingame, M. A., Wolan, D. W., McClendon, C. L., Jacobson, M. P., and Wells, J. A. (2011) Turning a protein kinase on or off from a single allosteric site via disulfide trapping. *Proc. Natl. Acad. Sci. USA* **108**, 6056–6061.

(113) Ostrem, J. M., Peters, U., Sos, M. L., Wells, J. A., and Shokat, K. M. (2013) K-Ras(G12C) inhibitors allosterically control GTP affinity and effector interactions. *Nature* **503**, 548–551.

(114) Thakur, J. K., Yadav, A., and Yadav, G. (2014) Molecular recognition by the KIX domain and its role in gene regulation. *Nucleic Acids Res.* **42**, 2112–2125.

(115) Wang, N., Majmudar, C. Y., Pomerantz, W. C., Gagnon, J. K., Sadowsky, J. D., Meagher, J. L., Johnson, T. K., Stuckey, J. A., Brooks, C. L. 3rd, Wells, J. A., and Mapp, A. K. (2013) Ordering a dynamic protein via a small-molecule stabilizer. *J. Am. Chem. Soc.* **135**, 3363–3366.

(116) Wang, N., Lodge, J. M., Fierke, C. A., and Mapp, A. K. (2014) Dissecting allosteric effects of activator-coactivator complexes using a covalent small molecule ligand. *Proc. Natl. Acad. Sci. USA* **111**, 12061–12066.

- (117) Law, S. M., Gagnon, J. K., Mapp, A. K., and Brooks, C. L. 3rd. (2014) Prepaying the entropic cost for allosteric regulation in KIX. *Proc. Natl. Acad. Sci. USA* *111*, 12067–12072.
- (118) Brüscheiler, S., Schanda, P., Klobner, K., Brutscher, B., Kontaxis, G., Konrat, R., and Tollinger, M. (2009) Direct observation of the dynamic process underlying allosteric signal transmission. *J. Am. Chem. Soc.* *131*, 3063–3068.
- (119) Majmudar, C. Y., Højfeldt, J. W., Arevang, C. J., Pomerantz, W. C., Gagnon, J. K., Schultz, P. J., Cesa, L. C., Doss, C. H., Rowe, S. P., Vásquez, V., Tamayo-Castillo, G., Cierpicki, T., Brooks, C. L. 3rd, Sherman, D. H., and Mapp, A. K. (2012) Sekikaic acid and lobaric acid target a dynamic interface of the coactivator CBP/p300. *Angew. Chemie Int. Ed.* *51*, 11258–11262.
- (120) Wurtz, J.-M., Bourguet, W., Renaud, J.-P., Vivat, V., Chambon, P., Moras, D., and Gronemeyer, H. (1996) A canonical structure for the ligand-binding domain of nuclear receptors. *Nat. Struct. Biol.* *3*, 87–94.
- (121) Huang, P., Chandra, V., and Rastinejad, F. (2010) Structural overview of the nuclear receptor superfamily: Insights into physiology and therapeutics. *Annu. Rev. Physiol.* *72*, 247–272.
- (122) Sheepstra, M., Nieto, L., Hirsch, A. K. H., Fuchs, S., Leysen, S., Vinh Lam, C., in het Panhuis, L., van Boeckel, C. A. A., Wienk, H., Boelens, R., Ottman, C., Milroy, L.-G., and Brunsveld, L. (2014) A natural-product switch for a dynamic protein interface. *Angew. Chemie Int. Ed.* *53*, 6443–6448.
- (123) Rose, R., Erdmann, S., Bovens, S., Wolf, A., Rose, M., Hennig, S., Waldmann, H., and Ottman, C. (2010) Identification and structure of small-molecule stabilizers of 14-3-3 protein-protein interactions. *Angew. Chemie Int. Ed.* *49*, 4129–4132.
- (124) Richter, A., Rose, R., Hedberg, C., Waldmann, H., and Ottman, C. (2012) An optimised small-molecule stabiliser of the 14-3-3-PMA2 protein-protein interaction. *Chemistry (Easton)*. *18*, 6520–6527.
- (125) Wong, V. (2011) Biology in a gray box: Targeting the emergent properties of protein complexes. *Yale J. Biol. Med.* *84*, 491–495.
- (126) Harrison, C. J., Hayer-Hartl, M., Di Liberto, M., Hartl, F. U., and Kuriyan, J. (1997) Crystal structure of the nucleotide exchange factor GrpE bound to the ATPase

domain of the molecular chaperone DnaK. *Science* (80-.). 276, 431–435.

(127) Wittung-Stafshede, P., Guidry, J., Horne, B. E., and Landry, S. J. (2003) The J-domain of Hsp40 couples ATP hydrolysis to substrate capture in Hsp70. *Biochemistry* 42, 4937–4944.

(128) Ahmad, A., Bhattacharya, A., McDonald, R. A., Cordes, M., Ellington, B., Bertelsen, E. B., and Zuiderweg, E. R. P. (2011) Heat Shock Protein 70 kDa chaperone/DnaJ cochaperone complex employs an unusual dynamic interface. *Proc. Natl. Acad. Sci. USA* 108, 18966–18971.

(129) Chang, L., Bertelsen, E. B., Wisén, S., Larsen, E. M., Zuiderweg, E. R. P., and Gestwicki, J. E. (2008) High-throughput screen for small molecules that modulate ATPase activity of the molecular chaperone DnaK. *Anal. Biochem.* 372, 167–176.

(130) Miyata, Y., Chang, L., Bainor, A., McQuade, T. J., Walczak, C. P., Zhang, Y., Larsen, M. J., Kirchhoff, P., and Gestwicki, J. E. (2010) High-throughput screen for Escherichia coli Heat Shock Protein 70 (Hsp70/DnaK): ATPase assay in low volume by exploiting energy transfer. *J. Biomol. Screen.* 15, 1211–1219.

(131) Wisén, S., and Gestwicki, J. E. (2008) Identification of small molecules that modify the protein folding activity of heat shock protein 70. *Anal. Biochem.* 374, 371–377.

(132) Chang, L., Miyata, Y., Ung, P. M. U., Bertelsen, E. B., McQuade, T. J., Carlson, H. A., Zuiderweg, E. R. P., and Gestwicki, J. E. (2011) Chemical screens against a reconstituted multiprotein complex: Myricetin blocks DnaJ regulation of DnaK through an allosteric mechanism. *Chem. Biol.* 18, 210–221.

(133) Cesa, L. C., Patury, S., Komiyama, T., Ahmad, A., Zuiderweg, E. R. P., and Gestwicki, J. E. (2013) Inhibitors of difficult protein-protein interactions identified by high-throughput screening of multiprotein complexes. *ACS Chem. Biol.* 8, 1988–1997.

(134) Monroy, C. A., Mackie, D. I., and Roman, D. L. (2013) A high throughput screen for RGS proteins using steady state monitoring of free phosphate formation. *PLoS One* 8, e62247.

(135) Patwardhan, C. A., Alfa, E., Lu, S., and Chadli, A. (2015) Progesterone receptor chaperone complex-based high-throughput screening assay: Identification of capsaicin as an inhibitor of the Hsp90 machine. *J. Biomol. Screen.* 20, 223–229.

- (136) Shekhawat, S. S., and Ghosh, I. (2011) Split-protein systems: beyond binary protein-protein interactions. *Curr. Opin. Chem. Biol.* 15, 789–797.
- (137) Luker, K. E., Smith, M. C. P., Luker, G. D., Gammon, S. T., Piwnica-Worms, H., and Piwnica-Worms, D. (2004) Kinetics of regulated protein-protein interactions revealed with firefly luciferase complementation imaging in cells and living animals. *Proc. Natl. Acad. Sci. USA* 101, 12288–12293.
- (138) Wong, E. T., Kolman, J. L., Li, Y.-C., Mesner, L. D., Hillen, W., Berens, C., and Wahl, G. M. (2005) Reproducible doxycycline-inducible transgene expression at specific loci generated by Cre-recombinase mediated cassette exchange. *Nucleic Acids Res.* 33, e147.
- (139) Li, Y.-C., Rodewald, L. W., Hoppmann, C., Wong, E. T., Lebreton, S., Safar, P., Patek, M., Wang, L., Wertman, K. F., and Wahl, G. M. (2014) A versatile platform to analyze low-affinity and transient protein-protein interactions in living cells in real time. *Cell Rep.* 9, 1946–1958.
- (140) Hodson, C., Cole, A. R., Lewis, L. P. C., Miles, J. A., Purkiss, A., and Walden, H. (2011) Structural analysis of human FANCL, the E3 ligase in the Fanconi anemia pathway. *J. Biol. Chem.* 286, 32628–32637.
- (141) Hodson, C., Purkiss, A., Miles, J. A., and Walden, H. (2014) Structure of the human FANCL RING-Ube2T complex reveals determinants of cognate E3-E2 selection. *Structure* 22, 337–344.
- (142) Vidal, M. (2005) Interactome modeling. *FEBS Lett.* 579, 1834–1838.
- (143) Boehr, D. D., McElheny, D., Dyson, H. J., and Wright, P. E. (2006) The dynamic energy landscape of dihydrofolate reductase catalysis. *Science* (80-.). 313, 1638–1642.
- (144) Henzler-Wildman, K. A., Thai, V., Lei, M., Ott, M., Wolf-Watz, M., Fenn, T., Pozharski, E., Wilson, M. A., Petsko, G. A., Karplus, M., Hübner, C. G., and Kern, D. (2007) Intrinsic motions along an enzymatic reaction trajectory. *Nature* 450, 838–844.
- (145) Tang, C., Iwahara, J., and Clore, G. M. (2006) Visualization of transient encounter complexes in protein-protein association. *Nature* 444, 383–386.
- (146) Jubb, H., Blundell, T. L., and Ascher, D. B. (2015) Flexibility and small pockets at protein-protein interfaces: New insights into druggability. *Prog. Biophys. Mol. Biol.* 119, 2–9.

- (147) Henzler-Wildman, K., and Kern, D. (2007) Dynamic personalities of proteins. *Nature* 450, 964–972.
- (148) van dem Bedem, H., and Fraser, J. S. (2015) Integrative, dynamic structural biology at atomic resolution - it's about time. *Nat. Methods* 12, 307–318.
- (149) Hopper, J. T. S., Rawlings, A., Afonso, J. P., Channing, D., Layfield, R., and Oldham, N. J. (2012) Evidence for the preservation of native inter- and intra-molecular hydrogen bonds in the desolvated FK-Binding Protein-FK506 complex produced by electrospray ionization. *J. Am. Soc. Mass Spectrom.* 23, 1757–1767.
- (150) Hopper, J. T. S., and Robinson, C. V. (2014) Mass spectrometry quantifies protein interactions - From molecular chaperones to membrane proteins. *Angew. Chemie Int. Ed.* 53, 14002–14015.
- (151) Ebong, I., Morgner, N., Zhou, M., Saraiva, M. A., Daturpalli, S., Jackson, S. E., and Robinson, C. V. (2011) Heterogeneity and dynamics in the assembly of the Heat Shock Protein 90 chaperone complexes. *Proc. Natl. Acad. Sci. USA* 108, 17939–17944.
- (152) Aquilina, J. A., Benesch, J. L. P., Ding, L. L., Yaron, O., Horwitz, J., and Robinson, C. V. (2005) Subunit exchange of polydisperse proteins: Mass spectrometry reveals consequences of alphaA-crystallin truncation. *J. Biol. Chem.* 280, 14485–14491.
- (153) Niu, S., Rabuck, J. N., and Ruotolo, B. T. (2013) Ion mobility-mass spectrometry of intact protein-ligand complexes for pharmaceutical drug discovery and development. *Curr. Opin. Chem. Biol.* 17, 809–817.
- (154) Hopper, J. T. S., and Oldham, N. J. (2009) Collision induced unfolding of protein ions in the gas phase studied by ion mobility-mass spectrometry: The effect of ligand binding on conformational stability. *J. Am. Soc. Mass Spectrom.* 20, 1851–1858.
- (155) Hyung, S.-J., Robinson, C. V., and Ruotolo, B. T. (2009) Gas-phase unfolding and disassembly reveals stability differences in ligand-bound multiprotein complexes. *Chem. Biol.* 16, 382–390.
- (156) Rabuck, J. N., Hyung, S.-J., Ko, K. S., Fox, C. C., Soellner, M. B., and Ruotolo, B. T. (2013) Activation state-selective kinase inhibitor assay based on ion mobility-mass spectrometry. *Anal. Chem.* 85, 6995–7002.
- (157) Patury, S., Miyata, Y., and Gestwicki, J. E. (2009) Pharmacological targeting of the Hsp70 chaperone. *Curr. Top. Med. Chem.* 9, 1337–1351.

- (158) Evans, C. G., Chang, L., and Gestwicki, J. E. (2010) Heat Shock Protein 70 (Hsp70) as an emerging drug target. *J. Med. Chem.* *53*, 4585–4602.
- (159) Schlecht, R., Scholz, S. R., Dahmen, H., Wegener, A., Sirrenberg, C., Musil, D., Bomke, J., Eggenweiler, H.-M., Mayer, M. P., and Bukau, B. (2013) Functional analysis of Hsp70 inhibitors. *PLoS One* *8*, e78443.
- (160) Li, X., Colvin, T., Rauch, J. N., Acosta-Alvear, D., Kampmann, M., Dunyak, B., Hann, B., Aftab, B. T., Murnane, M., Cho, M., Walter, P., Weissman, J. S., Sherman, M. Y., and Gestwicki, J. E. (2015) Validation of the Hsp70-Bag3 protein-protein interaction as a potential therapeutic target in cancer. *Mol. Cancer Ther.* *14*, 642–648.
- (161) Wang, A. M., Miyata, Y., Klinedinst, S., Peng, H.-M., Chua, J. C., Komiyama, T., Pratt, W. B., Osawa, Y., Collins, C. A., Gestwicki, J. E., and Lieberman, A. P. (2013) Activation of Hsp70 reduces neurotoxicity by promoting polyglutamine protein degradation. *Nat. Chem. Biol.* *9*, 112–118.
- (162) Miyata, Y., Rauch, J. N., Jinwal, U. K., Thompson, A. D., Srinivasan, S., Dickey, C. A., and Gestwicki, J. E. (2012) Cysteine reactivity distinguishes redox sensing by the heat-inducible and constitutive forms of heat shock protein 70. *Chem. Biol.* *19*, 1391–1399.
- (163) Wang, A. M., Morishima, Y., Clapp, K. M., Peng, H.-M., Pratt, W. B., Gestwicki, J. E., Osawa, Y., and Lieberman, A. P. (2010) Inhibition of Hsp70 by methylene blue affects signaling protein function and ubiquitination and modulates polyglutamine protein degradation. *J. Biol. Chem.* *285*, 15714–15723.
- (164) Rual, J.-F., Venkatesan, K., Hao, T., Hirozane-Kishikawa, T., Dricot, A., Li, N., Berriz, G. F., Gibbons, F. D., Dreze, M., Ayivi-Guedehoussou, N., Klitgord, N., Simon, C., Boxem, M., Miltstein, S., Rosenberg, J., Goldberg, D. S., Zhang, L. V., Wong, S. L., Franklin, G., Li, S., Albala, J. S., Lim, J., Fraughton, C., Llamasas, E., Cevik, S., Bex, C., Lamesch, P., Sikorski, R. S., Vandenhaute, J., Zoghbi, H. Y., Smolyar, A., Bosak, S., Sequerra, R., Doucette-Stamm, L., Cusick, M. E., Hill, D. E., Roth, F. P., and Vidal, M. (2005) Towards a proteome-scale map of the human protein-protein interaction network. *Nature* *437*, 1173–1178.
- (165) Parrish, J. R., Gulyas, K. D., and Finley, R. L. J. (2006) Yeast two-hybrid contributions to interactome mapping. *Curr. Opin. Biotechnol.* *17*, 387–393.

- (166) Gingras, A.-C., Gstaiger, M., Raught, B., and Aebersold, R. (2007) Analysis of protein complexes using mass spectrometry. *Nat. Rev. Mol. Cell Biol.* 8, 645–654.
- (167) Dunham, W. H., Mullin, M., Gingras, and Anne-Claude. (2012) Affinity-purification coupled to mass spectrometry: Basic principles and strategies. *Proteomics* 12, 1576–1590.
- (168) Gavin, A.-C., Aloy, P., Grandi, P., Krause, R., Boesche, M., Marzioch, M., Rau, C., Jensen, L. J., Bastuck, S., Dümpelfeld, B., Edelmann, A., Heurtier, M.-A., Hoffman, V., Hoefert, C., Klein, K., Hudak, M., Michon, A.-M., Schelder, M., Schirle, M., Remor, M., Rudi, T., Hooper, S., Bauer, A., Bouwmeester, T., Casari, G., Drewes, G., Neubauer, G., Rick, J. M., Kuster, B., Bork, P., Russell, R. B., and Superti-Furga, G. (2006) Proteome survey reveals modularity of the yeast cell machinery. *Nature* 440, 631–636.
- (169) Aebersold, R., and Mann, M. (2003) Mass spectrometry-based proteomics. *Nature* 422, 198–207.
- (170) Nesvizhskii, A. I. (2007) Protein identification by tandem mass spectrometry and sequence database searching. *Methods Mol. Biol.* 367, 87–119.
- (171) Ong, S.-E., Foster, L. J., and Mann, M. (2003) Mass spectrometric-based approaches in quantitative proteomics. *Methods* 29, 124–130.
- (172) Rikhvanov, E. G., Romanova, N., and Chernoff, Y. O. (2007) Chaperone effects on prion an nonprion aggregates. *Prion* 1, 217–222.
- (173) Walter, G. M., Smith, M. C., Wisén, S., Basrur, V., Elenitoba-johnson, K. S. J., Duennwald, M. L., Kumar, A., and Gestwicki, J. E. (2011) Ordered assembly of heat shock proteins, Hsp26, Hsp70, Hsp90, and Hsp104, on expanded polyglutamine fragments revealed by chemical probes. *J. Biol. Chem.* 286, 40486–40493.
- (174) Thompson, A. D., Scaglione, K. M., Prensner, J., Gillies, A. T., Chinnaiyan, A., Paulson, H. L., Jinwal, U. K., Dickey, C. A., and Gestwicki, J. E. (2012) Analysis of the tau-associated proteome reveals that exchange of Hsp70 for Hsp90 is involved in tau degradation. *ACS Chem. Biol.* 7, 1677–1686.
- (175) Clifford-Nunn, B., Showalter, H. D. H., and Andrews, P. C. (2011) Quaternary diamines as mass spectrometry cleavable crosslinkers for protein interactions. *J. Am. Soc. Mass Spectrom.* 23, 201–212.
- (176) Chin, J. W., and Schultz, P. G. (2002) In vivo photocrosslinking with unnatural

- amino acid mutagenesis. *ChemBioChem* 11, 1135–1137.
- (177) Hino, N., Okazaki, Y., Kobayashi, T., Hayashi, A., Sakamoto, K., and Yokoyama, S. (2005) Protein photo-cross-linking in mammalian cells by site-specific incorporation of a photoreactive amino acid. *Nat. Methods* 2, 201–206.
- (178) Majmudar, C. Y., Lee, L. W., Lancia, J. K., Nwokoye, A., Wang, Q., Wands, A. M., Wang, L., and Mapp, A. K. (2009) Impact of nonnatural amino acid mutagenesis on the in vivo function and binding modes of a transcriptional activator. *J. Am. Chem. Soc.* 131, 14240–14242.
- (179) Fuxreiter, M., Tompa, P., Simon, I., Uversky, V. N., Hansen, J. C., and Asturias, F. J. (2008) Malleable machines take shape in eukaryotic transcriptional regulation. *Nat. Chem. Biol.* 4, 728–737.
- (180) Neely, K. E., Hassan, A. H., Brown, C. E., Howe, L., and Workman, J. L. (2002) Transcription activator interactions with multiple SWI/SNF subunits. *Mol. Cell. Biol.* 22, 1615–1625.
- (181) Krishnamurthy, M., Dugan, A., Nwokoye, A., Fung, Y.-H., Lancia, J. K., Majmudar, C. Y., and Mapp, A. K. (2011) Caught in the act: Covalent crosslinking captures activator-coactivator interactions in vivo. *ACS Chem. Biol.* 6, 1321–1326.
- (182) Majmudar, C. Y., Wang, B., Lum, J. K., Håkansson, K., and Mapp, A. K. (2009) A high resolution map of three transcriptional activation domains with an essential co-activator from photocross-linking and multiplexed mass spectrometry. *Angew. Chemie Int. Ed.* 48, 7021–7024.
- (183) Roux, K. J., Kim, D. I., Raida, M., and Burke, B. (2012) A promiscuous biotin ligase fusion protein identifies proximal and interacting proteins in mammalian cells. *J. Cell Biol.* 196, 801–810.
- (184) Kwon, K., and Beckett, D. (2000) Function of a conserved sequence motif in biotin holoenzyme synthetases. *Protein Sci.* 9, 1530–1539.
- (185) Fernández-Suárez, M., Chen, T. S., and Ting, A. Y. (2008) Protein-protein interaction detection in vitro and in cells by proximity biotinylation. *J. Am. Chem. Soc.* 130, 9251–9253.
- (186) Lambert, J.-P., Tucholska, M., Go, C., Knight, J. D. R., and Gingras, A.-C. (2014) Proximity biotinylation and affinity purification are complementary approaches for the

interactome mapping of chromatin-associated protein complexes. *J. Proteomics* 118, 81–94.

(187) Kim, D. I., KC, B., Zhu, W., Motamedchaboki, K., Doye, V., and Roux, K. J. (2014) Probing nuclear pore complex architecture with proximity-dependent biotinylation. *Proc. Natl. Acad. Sci. USA* 111, E2453–E2461.

(188) Chen, A. L., Kim, E. W., Toh, J. Y., Vashisht, A. A., Rashoff, A. Q., Van, C., Huang, A. S., Moon, A. S., Bell, H. N., Bentolila, L. A., Wohlschlegel, J. A., and Bradley, P. J. (2015) Novel components of the Toxoplasma inner membrane complex revealed by BioID. *MBio* 6, e02357–14.

(189) Alber, F., Dokudovskaya, S., Veenhoff, L. M., Zhang, W., Kipper, J., Devos, D., Suprpto, A., Karni-Schmidt, O., Williams, R., Chait, B. T., Rout, M. P., and Sali, A. (2007) Determining the architectures of macromolecular assemblies. *Nature* 450, 683–694.

(190) Peterson-Kaufman, K. J., Carlson, C. D., Rodriguez-Martinez, J. A., and Ansari, A. Z. (2010) Nucleating the assembly of macromolecular complexes. *ChemBioChem* 11, 1955–1962.

(191) Jochim, A. L., and Arora, P. S. (2009) Assessment of helical interfaces in protein-protein interactions. *Mol. Biosyst.* 5, 924–926.

(192) Lindquist, S., and Craig, E. A. (1988) The heat-shock proteins. *Annu. Rev. Genet.* 22, 631–677.

(193) Dugaard, M., Rohde, M., and Jäättelä, M. (2007) The Heat Shock Protein 70 Family: Highly Homologous Proteins with Overlapping and Distinct Functions. *FEBS Lett.* 581, 3702–3710.

(194) Mayer, M. P., and Bukau, B. (2005) Hsp70 chaperones: Cellular functions and molecular mechanism. *Cell. Mol. Life Sci.* 62, 670–684.

(195) Rüdiger, S., Buchberger, A., and Bukau, B. (1997) Interaction of Hsp70 chaperones with substrates. *Nat. Struct. Biol.* 4, 342–349.

(196) Mayer, M. P., Schröder, H., Rüdiger, S., Paal, K., Laufen, T., and Bukau, B. (2000) Multistep mechanism of substrate binding determines chaperone activity of Hsp70. *Nat. Struct. Biol.* 7, 586–593.

(197) Zudierweg, E. R. P., Bertelsen, E. B., Rousaki, A., Mayer, M. P., Gestwicki, J. E.,

- and Ahmad, A. (2013) Allostery in the Hsp70 chaperone proteins. *Top. Curr. Chem.* 328, 99–153.
- (198) Swain, J. F., Dinler, G., Sivendran, R., Montgomery, D. L., Stotz, M., and Gierasch, L. M. (2007) Hsp70 chaperone ligands control domain association via an allosteric mechanism mediated by the interdomain linker. *Mol. Cell* 26, 27–39.
- (199) Gässler, C. S., Buchberger, A., Laufen, T., Mayer, M. P., Schröder, H., Valencia, A., and Bukau, B. (1998) Mutations in the DnaK chaperone affecting interaction with the DnaJ cochaperone. *Proc. Natl. Acad. Sci. USA* 95, 15229–15234.
- (200) Slepnev, S. V., and Witt, S. N. (2002) Kinetic analysis of interdomain coupling in a lidless variant of the molecular chaperone DnaK: DnaK's lid inhibits transition to the low affinity state. *Biochemistry* 41, 12224–12235.
- (201) Pierpaoli, E. V., Sandmeier, E., Schönfeld, H.-J., and Christen, P. (1998) Control of the DnaK chaperone cycle by substoichiometric concentrations of the co-chaperones DnaJ and GrpE. *J. Biol. Chem.* 273, 6643–6649.
- (202) Cesa, L. C., Mapp, A. K., and Gestwicki, J. E. (2015) Direct and propagated effects of small molecules on protein-protein interaction networks. *Front. Bioeng. Biotechnol.* 3, 119.
- (203) Packschies, L., Theyssen, H., Buchberger, A., Bukau, B., Goody, R. S., and Reinstein, J. (1997) GrpE accelerates nucleotide exchange of the molecular chaperone DnaK with an associative displacement mechanism. *Biochemistry* 36, 3417–3422.
- (204) Berggård, T., Linse, S., and James, P. (2007) Methods for the detection and analysis of protein-protein interactions. *Proteomics* 7, 2833–2842.
- (205) Pellicchia, M., Montgomery, D. L., Stevens, S. Y., Vander Kooi, C. W., Feng, H., Gierasch, L. M., and Zinder, E. R. P. (2000) Structural insights into substrate binding by the molecular chaperon DnaK. *Nat. Struct. Biol.* 7, 298–303.
- (206) Geladopoulos, T. P., Sotiropoulos, T. G., and Evangelopoulos, A. E. (1991) A malachite green colorimetric assay for protein phosphatase activity. *Anal. Biochem.* 192, 112–116.
- (207) Laufen, T., Mayer, M. P., Beisel, C., Klostermeier, D., Mogk, A., Reinstein, J., and Bukau, B. (1999) Mechanism of regulation of Hsp70 chaperones by DnaJ cochaperones. *Proc. Natl. Acad. Sci. USA* 96, 5452–5457.

- (208) McCarty, J. S., Buchberger, A., Reinstein, J., and Bukau, B. (1995) The role of ATP in the functional cycle of the DnaK chaperone system. *J. Mol. Biol.* 249, 126–137.
- (209) Zuck, P., O'Donnell, G. T., Cassaday, J., Chase, P., Hodder, P., Strulovici, B., and Ferrer, M. (2005) Miniaturization of absorbance assays using the fluorescent properties of white microplates. *Anal. Biochem.* 342, 254–259.
- (210) Buchberger, A., Theyssen, H., Schröder, H., McCarty, J. S., Virgallita, G., Milkereit, P., Reinstein, J., and Bukau, B. (1995) Nucleotide-induced conformational changes in the ATPase and substrate binding domains of the DnaK chaperone provide evidence for interdomain communication. *J. Biol. Chem.* 270, 16903–16910.
- (211) Ricci, L., and Williams, K. P. (2008) Development of fluorescence polarization assays for the molecular chaperone Hsp70 family members: Hsp72 and DnaK. *Curr. Chem. Genomics* 2, 90–95.
- (212) Chang, L., Thompson, A. D., Ung, P., Carlson, H. A., and Gestwicki, J. E. (2010) Mutagenesis reveals the complex relationships between ATPase rate and the chaperone activities of Escherichia coli Heat Shock Protein 70 (Hsp70/DnaK). *J. Biol. Chem.* 285, 21282–21291.
- (213) Abisambra, J. F., Jinwal, U. K., Miyata, Y., Rogers, J., Blair, L., Li, X., Sequin, S. P., Wang, L., Jin, Y., Bacon, J., Brady, S., Cockman, M., Guidi, C., Zhang, J., Koren, J. 3rd, Young, Z. T., Atkins, C. A., Zhang, B., Lawson, L. Y., Weeber, E. J., Brodsky, J. L., Gestwicki, J. E., and Dickey, C. A. (2013) Allosteric heat shock protein 70 inhibitors rapidly rescue synaptic plasticity deficits by reducing aberrant tau. *Biol. Psychiatry* 74, 367–374.
- (214) Zhuravleva, A., and Gierasch, L. M. (2011) Allosteric signal transmission in the nucleotide-binding domain of 70-kDa heat shock protein (Hsp70) molecular chaperones. *Proc. Natl. Acad. Sci. USA* 108, 6987–6992.
- (215) Scow, D. T., Luttermoser, G. K., and Dickerson, K. S. (2007) Leukotriene inhibitors in the treatment of allergy and asthma. *Am. Fam. Physician* 75, 65–70.
- (216) Benson, S. C., Pershadsingh, H. A., Ho, C. I., Chittiboyina, A., Desai, P., Pravenec, M., Qi, N., Wang, J., Avery, M. A., and Kurtz, T. W. (2004) Identification of telmisartan as a unique angiotensin II receptor antagonist with selective PPARgamma-modulating activity. *Hypertension* 43, 993–1002.

- (217) Berg, T. (2009) Allosteric switches: Remote controls for proteins. *Angew. Chemie Int. Ed.* 48, 3218–3220.
- (218) Rousaki, A., Miyata, Y., Jinwal, U. K., Dickey, C. A., Gestwicki, J. E., and Zuiderweg, E. R. P. (2011) Allosteric drugs: The interaction of antitumor compound MKT-077 with human Hsp70 chaperones. *J. Mol. Biol.* 411, 614–632.
- (219) Nanbu, K., Konishi, I., Mandai, M., Kuroda, H., Hamid, A. A., Komatsu, T., and Mori, T. (1998) Prognostic significance of heat shock proteins HSP70 and HSP90 in endometrial carcinomas. *Cancer Detect Prev* 22, 549–555.
- (220) Ciocca, D. R., and Calderwood, S. K. (2005) Heat shock proteins in cancer: diagnostic, prognostic, predictive, and treatment implications. *Cell Stress Chaperones* 10, 86–103.
- (221) Neckers, L. (2007) Heat shock protein 90: the cancer chaperone. *J. Biosci.* 32, 517–530.
- (222) Trepel, J., Mollapour, M., Giaccone, G., and Neckers, L. (2010) Targeting the dynamic HSP90 complex in cancer. *Nat. Rev. Cancer* 10, 537–549.
- (223) Sherman, M. Y., and Gabai, V. L. (2014) Hsp70 in cancer: back to the future. *Oncogene* 34, 4153–4161.
- (224) Rüdiger, S., Germeroth, L., Schneider-Mergener, J., and Bukau, B. (1997) Substrate specificity of the DnaK chaperone determined by screening cellulose-bound peptide libraries. *EMBO J.* 16, 1501–1507.
- (225) Rodriguez, F., Arsène-Ploetze, F., Rist, W., Rüdiger, S., Schneider-Mergener, J., Mayer, M. P., and Bukau, B. (2008) Molecular basis for regulation of the heat shock transcription factor sigma32 by the DnaK and DnaJ chaperones. *Mol. Cell* 32, 347–358.
- (226) Sekhar, A., Rosenzweig, R., Bouvignies, G., and Kay, L. E. (2015) Mapping the conformation of a client protein through the Hsp70 functional cycle. *Proc. Natl. Acad. Sci. USA* 112, 10395–10400.
- (227) Nunes, J. M., Hayer-Hartl, M., Hartl, F. U., and Müller, D. J. (2015) Action of the Hsp70 chaperone system observed with single proteins. *Nat. Commun.* 6, 6307.
- (228) Sonderrmann, H., Scheufler, C., Scheider, C., Höhfeld, J., Hartl, F. U., and Moarefi, I. (2001) Structure of a Bag/Hsc70 complex: Convergent functional evolution of Hsp70 nucleotide exchange factors. *Science (80-.)*. 291, 1553–1557.

- (229) Liu, F.-H., Wu, S.-J., Hu, S.-M., Hsiao, C.-D., and Wang, C. (1999) Specific interaction of the 70-kDa heat shock cognate protein with the tetratricopeptide repeats. *J. Biol. Chem.* 274, 4425–4432.
- (230) Colvin, T. A., Gabai, V. L., Gong, J., Calderwood, S. K., Li, H., Gummuluru, S., Matchuk, O. N., Smirnova, S. G., Orlova, N. V, Zamulaeva, I. A., Garcia, Marcos, M., Li, X., Young, Z. T., Rauch, J. N., Gestwicki, J. E., Takayama, S., and Sherman, M. Y. (2014) Hsp70-Bag3 interactions regulate cancer-related signaling networks. *Cancer Res.* 74, 4731–4740.
- (231) Hunter, A. M., LaCasse, E. C., and Korneluk, R. G. (2008) The inhibitors of apoptosis (IAPs) as cancer targets. *Apoptosis* 12, 1543–1568.
- (232) Birnbaum, M. J., Clem, R. J., and Miller, L. K. (1994) An apoptosis-inhibiting gene from a nuclear polyhedrosis virus encoding a polypeptide with Cys/His sequence motifs. *J. Virol.* 68, 2521–2528.
- (233) Hinds, M. G., Norton, R. S., Vaux, D. L., and Day, C. L. (1999) Solution structure of a baculoviral inhibitor of apoptosis (IAP) repeat. *Nat. Struct. Biol.* 6, 648–651.
- (234) Sun, C., Cai, M., Gunasekera, A. H., Meadows, R. P., Wang, H., Chen, J., Zhang, H., Wu, W., Xu, N., Ng, S.-C., and Fesik, S. W. (1999) NMR structure and mutagenesis of the inhibitor-of-apoptosis protein XIAP. *Nature* 401, 818–822.
- (235) Eckelman, B. P., Salvesen, G. S., and Scott, F. L. (2006) Human inhibitor of apoptosis proteins: why XIAP is the black sheep of the family. *EMBO Rep.* 7, 953–1059.
- (236) Vaux, D. L., and Silke, J. (2005) IAPs, RINGs and ubiquitylation. *Nat. Rev. Mol. Cell Biol.* 6, 287–297.
- (237) Galbán, S., and Duckett, C. S. (2010) XIAP as a ubiquitin ligase in cellular signaling. *Cell Death Differ.* 17, 54–60.
- (238) Darding, M., and Meier, P. (2012) IAPs: Guardians of RIPK1. *Cell Death Differ.* 19, 58–66.
- (239) Davenport, E. L., Zeisig, A., Aronson, L. I., Moore, H. E., Hockley, S., Gonzalez, D., Smith, E. M., Powers, M. V, Sharp, S. Y., Workman, P., Morgan, G. J., and Davies, F. E. (2010) Targeting heat shock protein 72 enhances Hsp90 inhibitor-induced apoptosis in myeloma. *Leukemia* 24, 1804–1807.
- (240) Powers, M. V, Clarke, P. A., and Workman, P. (2008) Dual targeting of HSC70

and HSP72 inhibits HSP90 function and induces tumor-specific apoptosis. *Cancer Cell* 14, 250–262.

(241) Williamson, D. S., Borgognoni, J., Clay, A., Daniels, Z., Dokurno, P., Drysdale, M. J., Foloppe, N., Francis, G. L., Graham, C. J., Howes, R., Macias, A. T., Murray, J. B., Parsons, R., Shaw, T., Surgenor, A. E., Terry, L., Wang, Y., Wood, M., and Massey, A. J. (2009) Novel adenosine-derived inhibitors of 70 kDa heat shock protein, discovered through structure-based design. *J. Med. Chem.* 52, 1510–1513.

(242) Nylandsted, J., Brand, K., and Jäättelä, M. (2000) Heat shock protein 70 is required for the survival of cancer cells. *Ann. N. Y. Acad. Sci.* 926, 122–125.

(243) da Silva, V. C. H., and Ramos, C. H. I. (2012) The network interaction of the human cytosolic 90 kDa heat shock protein Hsp90: A target for cancer therapeutics. *J. Proteomics* 75, 2790–2802.

(244) Jolly, C., and Morimoto, R. I. (2000) Role of the heat shock response and molecular chaperones in oncogenesis and cell death. *J. Natl. Cancer Inst.* 92, 1564–1572.

(245) Matts, R. L., Brandt, G. E. L., Lu, Y., Dixit, A., Mollapour, M., Wang, S., Donnelly, A. C., Neckers, L., Verkhivker, G., and Blagg, B. S. J. (2011) A systematic protocol for the characterization of Hsp90 modulators. *Bioorg. Med. Chem.* 19, 684–692.

(246) Whitesell, L., and Lindquist, S. L. (2005) HSP90 and the chaperoning of cancer. *Nat. Rev. Cancer* 5, 761–772.

(247) Porter, J. R., Fritz, C. C., and Depew, K. M. (2010) Discovery and development of Hsp90 inhibitors: a promising pathways for cancer therapy. *Curr. Opin. Chem. Biol.* 14, 412–420.

(248) Chandarlapaty, S., Sawai, A., Ye, Q., Scott, A., Silinski, M., Huang, K., Fadden, P., Partridge, J., Hall, S., Steed, P., Norton, L., Rosen, N., and Solit, D. B. (2008) SNX2112, a synthetic heat shock protein 90 inhibitor, has potent antitumor activity against HER kinase-dependent cancers. *Clin. Cancer Res.* 14, 240–248.

(249) Caldas-Lopes, E., Cerchietti, L., Ahn, J. H., Clement, C. C., Robles, A. I., Rodina, A., Moulick, K., Taldone, T., Gozman, A., Guo, Y., Wu, N., de Stanchina, E., White, J., Gross, S. S., Ma, Y., Varticovski, L., Melnick, A., and Chiosis, G. (2009) Hsp90 inhibitor PU-H71, a multimodal inhibitor of malignancy, induces complete responses in triple-negative breast cancer models. *Proc. Natl. Acad. Sci. USA* 106, 8368–8373.

- (250) Kirkegaard, T., Roth, A. G., Petersen, N. H. T., Mahalka, A. K., Olsen, O. D., Moilanen, I., Zylitz, A., Knudsen, J., Sandhoff, K., Arenz, C., Kinnunen, P. K. J., Nylandsted, J., and Jäättelä, M. (2010) Hsp70 stabilizes lysosomes and reverts Niemann-Pick disease-associated lysosomal pathology. *Nature* 463, 549–543.
- (251) Christofferson, D. E., Li, Y., and Yuan, J. (2014) Control of life-or-death decisions by RIP1 kinase. *Annu. Rev. Physiol.* 76, 129–150.
- (252) Tenev, T., Bianchi, K., Darding, M., Broemer, M., Langlais, C., Wallberg, F., Zachariou, A., Lopez, J., MacFarlane, M., Cain, K., and Meier, P. (2011) The Ripoptosome, a signaling platform that assembles in response to genotoxic stress and loss of IAPs. *Mol. Cell* 43, 432–448.
- (253) Galluzzi, L., Kepp, O., and Kroemer, G. (2009) RIP kinases initiate programmed necrosis. *J. Mol. Cell Biol.* 1, 8–10.
- (254) Feoktistova, M., Geserick, P., Kellert, B., Dimitrova, D. P., Langlais, C., Hupe, M., Cain, K., MacFarlane, M., Häcker, G., and Leverkus, M. (2011) cIAPs block ripoptosome formation, a RIP1/caspase 8 containing intracellular cell death complex differentially regulated by cFLIP isoforms. *Mol. Cell* 43, 449–463.
- (255) Wertz, I. E., and Dixit, V. M. (2010) Signaling to NF-kappaB: regulation by ubiquitination. *Cold Spring Harb. Perspect. Biol.* 2, a003350.
- (256) Moquin, D. M., McQuade, T., and Chan, F. K.-M. (2013) CYLD deubiquitinates RIP1 in the TNFalpha-induced necrosome to facilitate kinase activation and programmed necrosis. *PLoS One* 8, e76841.
- (257) Palacios, C., López-Pérez, A. I., and López-Rivas, A. (2010) Down-regulation of RIP expression by 17-dimethylaminoethylamino-17-demethoxygeldanamycin promotes TRAIL-induced apoptosis in breast tumor cells. *Cancer Lett.* 287, 207–215.
- (258) Li, J., McQuade, T., Siemer, A. B., Napetschnig, J., Moriwaki, K., Hsiao, Y.-S., Damko, E., Moquin, D., Walz, T., McDermott, A., Chan, F. K.-M., and Wu, H. (2012) The RIP1/RIP3 necrosome forms a functional amyloid signaling complex required for programmed necrosis. *Cell* 150, 339–350.
- (259) Li, X., Srinivasan, S. R., Connarn, J., Ahmad, A., Young, Z. T., Kabza, A. M., Zuiderweg, E. R. P., Sun, D., and Gestwicki, J. E. (2013) Analogues of the allosteric heat shock protein 70 (Hsp70) inhibitor, MKT-077, as anti-cancer agents. *ACS Med. Chem.*

Lett. 4, 1042–1047.

- (260) Brough, P. A., Aherne, W., Barril, X., Borgognoni, J., Boxall, K., Cansfield, J. E., Cheung, K.-M. J., Collins, I., Davies, N. G. M., Drysdale, M. J., Dymock, B., Eccles, S. A., Finch, H., Fink, A., Hayes, A., Howes, R., Hubbard, R. E., James, K., Jordan, A. M., Lockie, A., Martins, V., Massey, A., Matthews, T. P., McDonald, E., Northfield, C. J., Pearl, L. H., Prodromou, C., Ray, S., Raynaud, F. I., Roughley, S. D., Sharp, S. Y., Surgenor, A., Walmsley, D. L., Webb, P., Wood, M., Workman, P., and Wright, L. (2008) 4,5-Diarylisoazole Hsp90 chaperone inhibitors: potential therapeutic agents for the treatment of cancer. *J. Med. Chem.* 51, 196–218.
- (261) Schnur, R. C., Corman, M. L., Gallaschun, R. J., Cooper, B. A., Dee, M. F., Doty, J. L., Muzzi, M. L., Moyer, J. D., and DiOrio, C. I. (1995) Inhibition of the oncogene product p185erbB-2 in vitro and in vivo by geldanamycin and dihydrogeldanamycin derivatives. *J. Med. Chem.* 38, 3806–3812.
- (262) Stebbins, C. E., Russo, A. A., Schneider, C., Rosen, N., Hartl, F. U., and Pavletich, N. P. (1997) Crystal structure of an Hsp90-geldanamycin complex: targeting of a protein chaperone by an antitumor agent. *Cell* 89, 239–250.
- (263) Fenteany, G., Standaert, R. F., Lane, W. S., Choi, S., Corey, E. J., and Schreiber, S. L. (1995) Inhibition of proteasome activities and subunit-specific amino-terminal threonine modification by lactacystin. *Science* (80-.). 268, 726–731.
- (264) Nakatani, Y., Kleffmann, T., Linke, K., Condon, S. M., Hinds, M. G., and Day, C. L. (2013) Regulation of ubiquitin transfer by XIAP, a dimeric RING E3 ligase. *Biochem. J.* 450, 629–638.
- (265) Gyrð-Hansen, M., Darding, M., Miasari, M., Santoro, M. M., Zender, L., Xue, W., Tenev, T., da Fonseca, P. C. A., Zvelebil, M., Bujnicki, J. M., Lowe, S., Silke, J., and Meier, P. (2008) IAPs contain an evolutionary conserved ubiquitin-binding domain that regulates NF-kappaB as well as cell survival and oncogenesis. *Nat. Cell Biol.* 10, 1309–1317.
- (266) Lewis, J., Burstein, E., Reffey, S. B., Bratton, S. B., Roberts, A. B., and Duckett, C. S. (2004) Uncoupling of the signaling and caspase-inhibitory properties of X-linked inhibitor of apoptosis. *J. Biol. Chem.* 279, 9023–9029.
- (267) Sun, H., Nikolovska-Coleska, Z., Lu, J., Meagher, J. L., Yang, C.-Y., Qiu, S.,

- Tomita, Y., Ueda, Y., Jiang, S., Krajewski, K., Roller, P. P., Stuckey, J. A., and Wang, S. (2007) Design, synthesis, and characterization of a potent, nonpeptide, cell-permeable, bivalent Smac mimetic that concurrently targets both the BIR2 and BIR3 domains in XIAP. *J. Am. Chem. Soc.* *129*, 15279–15294.
- (268) Zhu, X., Zhao, X., Burkholder, W. F., Gragerov, A., Ogata, C. M., Gottesman, M. E., and Hendrickson, W. A. (1996) Structural analysis of substrate binding by the molecular chaperone DnaK. *Science* (80-.). *272*, 1606–1614.
- (269) Bertelsen, E. B., Chang, L., Gestwicki, J. E., and Zuiderweg, E. R. P. (2009) Solution conformation of wild-type E. coli Hsp70 (DnaK) chaperone complexed with ADP and substrate. *Proc. Natl. Acad. Sci. USA* *106*, 8471–8476.
- (270) Rohrer, K. M., Haug, M., Schwörer, D., Kalbacher, H., and Holzer, U. (2014) Mutations in the substrate binding site of human heat-shock protein 70 indicate specific interaction with HLA-DR outside the peptide binding groove. *Immunology* *142*, 237–247.
- (271) Zhang, P., Leu, J. I.-J., Murphy, M. E., George, D. L., and Marmorstein, R. (2014) Crystal structure of the stress-inducible human heat shock protein 70 substrate-binding domain in complex with peptide substrate. *PLoS One* *9*, e103518.
- (272) Goloudina, A. R., Demidov, O. N., and Garrido, C. (2012) Inhibition of HSP70: A challenging anti-cancer strategy. *Cancer Lett.* *325*, 117–124.
- (273) Brodsky, J. L., and Chiosis, G. (2006) Hsp70 molecular chaperones: emerging roles in human disease and identification of small molecule modulators. *Curr. Top. Med. Chem.* *6*, 1215–1225.
- (274) Shrestha, L., Patel, H. J., and Chiosis, G. (2016) Chemical tools to investigate mechanisms associated with HSP90 and HSP70 in disease. *Cell Chem. Biol.* *23*, 158–172.
- (275) Silke, J., Kratina, T., Chu, D., Ekert, P. G., Day, C. L., Pakusch, M., Huang, D. C. S., and Vaux, D. L. (2005) Determination of cell survival by RING-mediated regulation of inhibitor of apoptosis (IAP) protein abundance. *Proc. Natl. Acad. Sci. USA* *102*, 16182–16187.
- (276) Varfolomeev, E., Blankenship, J. W., Wayson, S. M., Fedorova, A. V., Kayagaki, N., Garg, P., Zobel, K., Dynek, J. N., Elliott, L. O., Wallweber, H. J. A., Flygare, J. A., Fairbrother, W. J., Deshayes, K., Dixit, V. M., and Vucic, D. (2007) IAP antagonists

induce autoubiquitination of c-IAPs, NF-kappaB activation, and TNFalpha-dependent apoptosis. *Cell* 131, 669–681.

(277) Wang, N., Feng, Y., Zhu, M., Siu, F.-M., Ng, K.-M., and Che, C.-M. (2013) A novel mechanism of XIAP degradation induced by timosaponin AIII in hepatocellular carcinoma. *Biochim. Biophys. Acta* 1833, 2890–2899.

(278) Schlecht, R., Erbse, A. H., Bukau, B., and Mayer, M. P. (2011) Mechanics of Hsp70 chaperones enables differential interaction with client proteins. *Nat. Struct. Mol. Biol.* 18, 345–351.

(279) Banerjee, R., Jayaraj, G. G., Peter, J. J., Kumar, V., and Mapa, K. (2016) Monitoring conformational heterogeneity of the lid of DnaK substrate binding domain during its chaperone cycle. *FEBS J.* 283, 2853–2868.

(280) Kellner, R., Hofmann, H., Barducci, A., Wunderlich, B., Nettels, D., and Schuler, B. (2014) Single-molecule spectroscopy reveals chaperone-mediated expansion of substrate protein. *Proc. Natl. Acad. Sci. USA* 111, 13355–13360.

(281) Höhfeld, J., Minami, Y., and Hartl, F.-U. (1995) Hip, a novel cochaperone involved in the eukaryotic Hsc70/Hsp40 reaction cycle. *Cell* 83, 589–598.

(282) Meacham, G. C., Patterson, C., Zhang, W., Younger, J. M., and Cyr, D. M. (2001) The Hsc70 co-chaperone CHIP targets immature CFTR for proteasomal degradation. *Nat. Cell Biol.* 3, 100–105.

(283) Zhang, H., Amick, J., Chakravarti, R., Santarriaga, S., Schlanger, S., McGlone, C., Dare, M., Nix, J. C., Scaglione, K. M., Stuehr, D. J., Misra, S., and Page, R. C. (2015) A bipartite interaction between Hsp70 and CHIP regulates ubiquitination of chaperoned client proteins. *Structure* 23, 472–482.

(284) Young, Z. T., Rauch, J. N., Assimon, V. A., Jinwal, U. K., Ahn, M., Li, X., Dunyak, B. M., Ahmad, A., Carlson, G. A., Srinivasan, S. R., Zuiderweg, E. R. P., Dickey, C. A., and Gestwicki, J. E. (2016) Stabilizing the Hsp70-tau complex promotes turnover in models of tauopathy. *Cell Chem. Biol.* 23, 992–1001.

(285) Cailleau, R., Young, R., Olivé, M., and Reeves, W. J. (1974) Breast tumor cell lines from pleural effusions. *J. Natl. Cancer Inst.* 53, 661–674.

(286) Levenson, A. S., and Jordan, V. C. (1997) MCF-7: the first hormone-responsive breast cancer cell line. *Cancer Res.* 57, 3071–3078.

- (287) Pratt, W. B., Morishima, Y., Murphy, M., and Harrell, M. (2006) Chaperoning of glucocorticoid receptors. *Handb. Exp. Pharmacol.* 172, 111–138.
- (288) Echeverria, P. C., and Picard, D. (2010) Molecular chaperones, essential partners of steroid hormone receptors for activity and mobility. *Biochim. Biophys. Acta* 1803, 641–649.
- (289) Alvira, S., Cuéllar, J., Röhl, A., Yamamoto, S., Itoh, H., Alfonso, C., Rivas, G., Buchner, J., and Valpuesta, J. M. (2014) Structural characterization of the substrate transfer mechanism in Hsp70/Hsp90 folding machinery mediated by Hop. *Nat. Commun.* 5, 5484.
- (290) Kirschke, E., Goswami, D., Southworth, D., Griffin, P. R., and Agard, D. A. (2014) Glucocorticoid receptor function regulated by coordinated action of the Hsp90 and Hsp70 chaperone cycles. *Cell* 157, 1685–1697.
- (291) Mann, M. (2006) Functional and quantitative proteomics using SILAC. *Nat. Rev. Mol. Cell Biol.* 7, 952–958.
- (292) Harsha, H. C., Molina, H., and Pandey, A. (2008) Quantitative proteomics using stable isotope labeling with amino acids in cell culture. *Nat. Protoc.* 3, 505–516.
- (293) Wu, Z., Gholami, A. M., and Kuster, B. (2012) Systematic identification of the HSP90 regulated proteome. *Mol. Cell. Proteomics* 11, M111.016675.
- (294) Szklarczyk, D., Franceschini, A., Wyder, S., Forslund, K., Heller, D., Huerta-Cepas, J., Simonovic, M., Roth, A., Santos, A., Tsafou, K. P., Kuhn, M., Bork, P., Jensen, L. J., and von Mering, C. (2015) STRING v10: protein-protein interaction networks, integrated over the tree of life. *Nucleic Acids Res.* 43, D447–D452.
- (295) Huang da, W., Sherman, B. T., and Lempicki, R. A. (2009) Systematic and integrative analysis of large gene lists using DAVID bioinformatics resources. *Nat. Protoc.* 4, 44–57.
- (296) Huang da, W., Sherman, B. T., and Lempicki, R. A. (2009) Bioinformatics enrichment tools: paths toward the comprehensive functional analysis of large gene lists. *Nucleic Acids Res.* 37, 1–13.
- (297) Verhagen, A. M., and Vaux, D. L. (2002) Cell death regulation by the mammalian IAP antagonist Diablo/Smac. *Apoptosis* 7, 163–166.
- (298) Shiozaki, E. N., and Shi, Y. (2004) Caspases, IAPs and Smac/DIABLO: mechanisms from structural biology. *Trends Biochem. Sci.* 29, 486–494.

- (299) Erbse, A. H., Mayer, M. P., and Bukau, B. (2004) Mechanism of substrate recognition by Hsp70 chaperones. *Biochem. Soc. Trans.* 32, 617–621.
- (300) Hartl, F. U., and Hayer-Hartl, M. (2009) Converging concepts of protein folding in vitro and in vivo. *Nat. Struct. Mol. Biol.* 16, 574–581.
- (301) Kabani, M., and Martineau, C. N. (2008) Multiple Hsp70 isoforms in the eukaryotic cytosol: Mere redundancy or functional specificity? *Curr. Genomics* 9, 338–348.
- (302) Kampinga, H. H., and Craig, E. A. (2010) The Hsp70 chaperone machinery: J proteins as drivers of functional specificity. *Nat. Rev. Mol. Cell Biol.* 11, 579–592.
- (303) Ungewickell, E., Ungewickell, H., Holstein, S. E. H., Lindner, R., Prasad, K., Barouch, W., Martini, B., Greene, L. E., and Eisenberg, E. (1995) Role of auxilin in uncoating clathrin-coated vesicles. *Nature* 378, 632–635.
- (304) Rothnie, A., Clarke, A. R., Kuzmic, P., Cameron, A., and Smith, C. J. (2011) A sequential mechanism for clathrin cage disassembly by 70-kDa heat-shock cognate protein (Hsc70) and auxilin. *Proc. Natl. Acad. Sci. USA* 108, 6927–6932.
- (305) Pratt, W. B., Gestwicki, J. E., Osawa, Y., and Lieberman, A. P. (2014) Targeting Hsp90/Hsp70-based protein quality control for treatment of adult onset neurodegenerative diseases. *Annu. Rev. Pharmacol. Toxicol.* 55, 353–371.
- (306) Bantscheff, M., Lemeer, S., Savitski, M. M., and Kuster, B. (2012) Quantitative mass spectrometry in proteomics: Critical review update from 2007 to present. *Anal. Bioanal. Chem.* 404, 939–965.
- (307) Manning, G., Whyte, D. B., Martinez, R., Hunter, T., and Sudarsanam, S. (2002) The protein kinase complement of the human genome. *Science* (80-.). 298, 1912–1934.
- (308) Wang, Q., Zorn, J. A., and Kuriyan, J. (2014) A structural atlas of kinases inhibited by clinically approved drugs. *Methods Enzymol.* 548, 23–67.
- (309) Bromann, P. A., Korkaya, H., and Courtneidge, S. A. (2004) The interplay between Src family kinases and receptor tyrosine kinases. *Oncogene* 23, 7957–7968.
- (310) Frame, M. C. (2004) Newest findings on the oldest oncogene; how activated src does it. *J. Cell Sci.* 117, 989–998.
- (311) Kwarcinski, F. E., Brandvold, K. R., Phadke, S., Beleh, O. M., Johnson, T. K., Meagher, J. L., Seeliger, M. A., Stuckey, J. A., and Soellner, M. B. (2016) Conformation-

selective analogues of dasatinib reveal insight into kinase inhibitor binding and selectivity. *ACS Chem. Biol.* **11**, 1296–1304.

(312) Parsons, J. T. (2003) Focal adhesion kinase: the first ten years. *J. Cell Sci.* **116**, 1409–1416.

(313) Moroco, J. A., Baumgartner, M. P., Rust, H. L., Choi, H. G., Hur, W., Gray, N. S., Camacho, C. J., and Smithgall, T. E. (2015) A discovery strategy for selective inhibitors of c-Src in complex with the focal adhesion kinase SH3/SH2-binding region. *Chem. Biol. Drug Des.* **86**, 144–155.

(314) Gillies, A. T., Taylor, R., and Gestwicki, J. E. (2012) Synthetic lethal interactions in yeast reveal functional roles of J protein co-chaperones. *Mol. Biosyst.* **8**, 2901–2908.

(315) Assimon, V. A., Southworth, D. R., and Gestwicki, J. E. (2015) Specific binding of tetratricopeptide repeat proteins to heat shock protein 70 (Hsp70) and heat shock protein 90 (Hsp90) is regulated by affinity and phosphorylation. *Biochemistry* **54**, 7120–7131.

(316) Wadhwa, R., Sugihara, T., Yoshida, A., Nomura, H., Reddel, R. R., Simpson, R., Maruta, H., and Kaul, S. C. (2000) Selective toxicity of MKT-077 to cancer cells is mediated by its binding to the Hsp70 family protein mot-2 and reactivation of p53 function. *Cancer Res.* **60**, 6818–6821.

(317) Koya, K., Li, Y., Wang, H., Ukai, T., Tatsuta, N., Kawakami, M., Shishido, and Chen, L. B. (1996) MKT-077, a novel rhodacyanine dye in clinical trials, exhibits anticarcinoma activity in preclinical studies based on selective mitochondrial accumulation. *Cancer Res.* **56**, 538–543.

(318) Chiba, Y., Kubota, T., Watanabe, M., Matsuzaki, S. W., Otani, Y., Teramoto, T., Matsumoto, Y., Koya, K., and Kitajima, M. (1998) MKT-077, localized lipophilic cation: antitumor activity against human tumor xenografts serially transplanted into nude mice. *Anticancer Res.* **18**, 1047–1052.

(319) Miyata, Y., Li, X., Lee, H.-F., Jinwal, U., Srinivasan, S. R., Seguin, S. P., Young, Z. T., Brodsky, J. L., Dickey, C. A., Sun, D., and Gestwicki, J. E. (2013) Synthesis and initial evaluation of YM-08, a blood-brain barrier permeable derivative of the heat shock protein 70 (Hsp70) inhibitor MKT-077, which reduces tau levels. *ACS Chem. Neurosci.* **4**, 930–939.

(320) Matallanas, D., and Crespo, P. (2010) New druggable targets in the Ras pathway?

Curr. Opin. Mol. Ther. 12, 674–683.

(321) Singh, J., and Udgaonkar, J. B. (2015) Molecular mechanism of the misfolding and oligomerization of the prion protein: Current understanding and its implications. *Biochemistry* 54, 4431–4442.

(322) Kosako, H., and Nagano, K. (2011) Quantitative phosphoproteomics strategies for understanding protein kinase-mediated signal transduction pathways. *Expert Rev. Proteomics* 8, 81–94.

(323) Rigbolt, K. T. G., and Blagoev, B. (2012) Quantitative phosphoproteomics to characterize signaling networks. *Semin. Cell Dev. Biol.* 23, 863–871.

(324) Yang, X., Lee, W. H., Sobott, F., Papagrigoriou, E., Robinson, C. V, Grossmann, J. G., Sundström, M., Doyle, D. A., and Elkins, J. M. (2006) Structural basis for protein-protein interactions in the 14-3-3 protein family. *Proc. Natl. Acad. Sci. USA* 103, 17237–17242.

(325) Pozuelo Rubio, M., Geraghty, K. M., Wong, B. H. C., Wood, N. T., Campbell, D. G., Morrice, N., and MacKintosh, C. (2004) 14-3-3 affinity purification of over 200 human phosphoproteins reveals new links to regulation of cellular metabolism, proliferation and trafficking. *Biochem. J.* 379, 395–408.

(326) Mapp, A. K., Pricer, R., and Sturlis, S. (2015) Targeting transcription is no longer a quixotic quest. *Nat. Chem. Biol.* 11, 891–894.

(327) Bartel, M., Schäfer, A., Stevers, L. M., and Ottmann, C. (2014) Small molecules, peptides and natural products: getting a grip on 14-3-3 protein-protein modulation. *Future Med. Chem.* 6, 903–921.